THE UNIVERSITY OF MICHIGAN

INDUSTRY PROGRAM OF THE COLLEGE OF ENGINEERING

EARTHQUAKE FORCES IN TALL BUILDINGS WITH SETBACKS

Dilip P. Jhaveri

A dissertation submitted in partial fulfillment
of the requirements for the degree of
Doctor of Philosophy in the
University of Michigan
Department of Civil Engineering
1967

March, 1967

IP-771

Doctoral Committee:

Professor G. V. Berg, Chairman
Professor R. C. F. Bartels
Professor B. G. Johnston
Associate Professor W. S. Rumman

ACKNOWLEDGEMENTS

The author is sincerely grateful to Professor G. V. Berg, chairman of his doctoral committee, for suggesting the problem and for providing continuous guidance and encouragement in the course of research and preparation of the dissertation. He also wishes to thank all other members of his doctoral committee for their helpful suggestions. The research reported herein forms a part of a project supported by the National Science Foundation, Grant No. GP-42. Several fellowships and scholarships were provided by the University of Michigan. The author wishes to express his appreciation for the financial support received from both institutions. Thanks are also due to the Computing Center of the University of Michigan and its staff for the use of its electronic digital computer for the numerical computations. Miss Reta Teachout typed part of the first draft. The final typing, drafting and reproduction was done by the staff of the Industry Program of the College of Engineering. The author wishes to thank all the individuals who have helped in the production of this dissertation.

TABLE OF CONTENTS

LIST OF TABLES

LIST OF FIGURES

LIST OF FIGURES (CONT'D)

LIST OF FIGURES (CONT'D)

NOMENCLATURE

Symbols are defined when they first appear in the text; those which appear frequently are listed below for reference.

A_B	cross-sectional area, base portion.
A_T	cross-sectional area, tower portion.
B	subscript to denote base or base portion.
[C]	damping matrix.
C_B, C_{1B}	base shear coefficient.
C_{3B}	base torque coefficient.
C_T	tower-base shear coefficient.
C_{ijk}	coefficients in expression for mode shapes of shear beam.
G	rigidity per unit area along the x direction in shear beam.
[I]	identity matrix.
[K]	stiffness matrix.
[M]	inertia matrix
N	number of stories.
P	story at which setback occurs.
R:k	kth torsional mode.
T_i	torque in ith story.
T_j	natural period of jth mode.
T:k	kth translational mode, x direction.
T	subscript to denote tower portion.
V_1, V_2	resultant shear force on horizontal cross-section, shear beam.
V_3	resultant torque on horizontal cross-section, shear beam.

V_i	shear force in ith story.
a_1, a_2	width in x and y directions, tower portion.
b_1, b_2	width in x and y directions, base portion.
b	subscript to denote base portion.
c	degree of setback.
e_1, e_2	offset between tower and base centroids in x and y directions.
f	frequency expression, shear beam.
f, $\{f\}$	external force per unit length; external force vector.
g	acceleration due to gravity.
h	height of beam to step.
i	story or floor number.
k	mode number.
i, j, k	indices
k_1, k_2, k_3	stiffness per unit length in x and y directions and torsional stiffness per unit length.
kx_i	ith story stiffness in x direction.
ky_i	ith story stiffness in y direction.
$k\Theta_i$	ith story torsional stiffness.
ℓ	total height of beam.
m, m_1, m_2	mass per unit length.
m_3	mass moment of inertia per unit length.
m_i	ith mass.
$m\Theta_i$	mass moment of inertia of ith mass.
p	level of setback.
q, s	stiffness to inertia ratio in base and tower portions.
$\{r\}$	displacement vector.

t	subscript to denote tower portion.
t	time coordinate.
u, v x_1, x_2	displacement along x and y directions.
x, y	principal directions beam and building cross-sections.
$\ddot{x}_{01}, \ddot{x}_{02}$	ground accelerations in x and y directions.
x_3	rotation of cross section about vertical axis, shear beam.
z	vertical coordinate axis, shear beam.
α_b, α_t	ratios $(b_2/b_1, a_2/a_1)$ of widths in base and tower portions.
β	fraction of critical damping.
γ^2	ratio of rigidity per unit area in y direction to that in x direction.
η	modal displacement coordinate
Θ	rotation of cross-section about vertical axis through centroid, shear beam.
Θ_i	rotation of ith mass about vertical axis through centroid.
λ	modal participation factor.
μ	distribution factor for stiffness.
ξ	displacement co-ordinate of a one-degree-of-freedom system.
ρ	mass per unit volume of shear beam.
σ^2	the ratio $(k_3/m_3)/(k_1/m_1)$ (shear beam) or $(k\Theta_i/m\Theta_i)/(kx_i/m_i)$ (shear building).
ϕ	mode shape.
$\{\phi\}$	mode shape vector.
ω	circular frequency.
$\lvert\ \rvert$	absolute value.
$\lVert\ \rVert$	determinant.

CHAPTER 1

INTRODUCTION

THE PROBLEM

A troublesome problem in earthquake engineering is evaluating the effect of a setback on the dynamic stresses induced in a tall building by earthquake ground motion. Two difficulties arise. First, there are stress concentrations in the vicinity of the setback. The method of dealing with this problem in some of the current seismic building codes[1,2,3] is to ignore the setback if the plan area of tower is more than a certain percentage (25% in the case of one code[1] and approximately 50% in the case of some others[2,3]) of the base area; for other conditions of setbacks the tower is considered as a separate building for its own height[1] or as a part of the overall structure, whichever gives the larger force at the base of tower[2,3]. The separate tower concept does not take into account the fact that the ground motion is modified greatly by the base portion of the structure before it affects the tower. The tower is subjected essentially to a harmonic forced vibration[4] instead of the nearly random motion of the ground.

A second difficulty arises with unsymmetrical setbacks. It is well known that if dynamic symmetry is not preserved the ground motion induces torsional oscillations in the structure. In the dynamically symmetric case the translational vibrations in the two principal directions and the torsional vibrations are uncoupled from each other. Torsional oscillations due to earthquake are negligible in this case because the torsional component of earthquake ground motion is small. Unsymmetrical

setbacks will in general destroy the dynamic symmetry of a structure in one or both principal directions. If dynamic symmetry is absent in one or both of the principal directions torsional motion is coupled with the translations in one or both of the principal directions, and in the latter case the translations in the two directions are mutually coupled.

Dynamic symmetry in a uniform building (i.e. one without a setback) may also be lacking due to the unsymmetrical distribution of inertia or stiffness. The dynamic effect of such lack of symmetry is usually ignored by the current seismic building codes[1,2,3]. The design forces are computed on the implicit assumption of absence of coupling between the torsional and translational motions, and the torque resulting from the static application of such design forces is provided for in design.

PRIOR RELATED STUDIES

Very little work has been done on the problem of the effect of setbacks on seismic forces in buildings. Berg[5] made an exploratory study of this problem using a rectangular stepped cantilever shear beam as a model for the building with setback. He considered the general case of coupled lateral-torsional vibrations of the beam with unsymmetric setback.

Multi-story buildings with appendages or very light towers on their top may be considered as extreme cases of buildings with setback. Penzien and Chopra[6] gave an approximate method of computing the seismic forces in the appendages. When one of the lower mode periods

of the building is very close to or equal to the period of the appendage (or tower) very high seismic forces may be expected in the appendages. This problem was considered by Skinner et al[7] as well as by Penzien and Chopra.[6]

There have been several studies of the problem of coupled lateral-torsional vibrations in buildings.[8-15] Ayre[8] set forth the theory of torsion coupling in building vibrations in a paper in 1938 in which he reported the results of analytical and experimental research on symmetric and unsymmetric models of one and two story buildings. In a later paper[9] he reported an experimental study of the response of an unsymmetric single story building to a damped sinusoidal one-directional translation of the base. An excellent brief summary on the theory of torsional coupling was included in a paper presented by Ayre at the First World Conference on Earthquake Engineering.[10]

In 1958, Housner and Outinen[11] analysed the stresses and energy input for symmetrical and unsymmetrical buildings and compared them with the customary design results obtained by static procedures. Bustamante and Rosenbleuth[12] examined the effect of eccentricity between centers of mass and stiffness in one principal direction in one or more stories of a large number of four and eigth-story idealized structures using three different simplified acceleration spectra. Bustamante[13] also investigated the torsional behavior of four-story buildings subjected to earthquakes.

Skinner et al[7], in their paper referred to earlier in connection with the problem of a building with periods close to that of a light tower situated on its top, also dealt with a similar problem

arising out of the introduction of small unbalance (i.e. lack of dynamic symmetry) in a building having close translational and torsional mode periods. Shiga[14] examined the coupled lateral-torsional vibrations of multi-story buildings with certain properties that lead to a considerable simplification in the modal analysis of the system. He also examined the response of such buildings to sinusoidal ground motions. Medearis[15] analysed the coupled lateral-torsional vibrations of a geometrically (as well as dynamically) unsymmetric sky-scraper and presented its coupled mode shapes and frequencies in a recent paper.

Among other related studies are the investigations of torsional coupling in unsymmetric uniform thin walled beams of open cross-section by Gere and Lin[16], Lin[17], and Tso.[18] Less directly related work has been done on the vibration of twisted blades and the coupled longitudinal-torsional vibrations of bars and shafts.

SCOPE OF PRESENT STUDY

The purpose of the present study is to gain information about the effects of setbacks on the dynamic behavior of multistory buildings, which may eventually lead to improved methods of treating setbacks in seismic building codes. The study is restricted to buildings having setback at only one level along their height and having a rectangular cross-section both above and below the level of setback (the tower and the base portions, respectively).

Further, the structure is assumed to be linearly elastic, and damping is assumed to be of the viscous type. It is also assumed that the damping has negligible effect on the mode shapes and frequencies of

the undamped structure. Only the horizontal motions of the building are considered and these are assumed to be independent of the vertical motions.

The multi-story building with setback is represented by two models: one, a cantilever shear beam stepped at one location along its height and having a uniform rectangular cross-section in each part of the structure; and the other, a multi-mass model obtained by assuming that all the mass in the building is lumped at the floor levels and the interconnecting stiffness elements (springs) are weightless. The structure is assumed to be simply coupled in stiffness, i.e. springs connect only the adjacent masses to each other and only one mass to the ground. This is the so-called "shear building" assumption and is equivalent to the assumption of infinitely rigid girders in moment resisting space frames.

The stepped cantilever shear beam was used as a model of the building with setback by Berg.(5) The formulation of the equations of motion of the coupled vibrations of a shear beam with unsymmetric setback and their solution as developed in Reference 5 is given in Appendix A with minor changes.

The equations of motion for the coupled vibrations of the lumped mass model are developed in Chapter II. Conditions under which the translational and the torsional vibrations uncouple are also discussed. The solution of the equations of motion in the usual modal superposition form and a method of finding the mode shapes and frequencies are also described in Chapter II.

The study of the effect of setbacks on building vibrations is divided into two parts. First it is assumed that the setback is symmetric about one principal direction and the translational vibrations in that direction are uncoupled from torsional vibrations. Two parameters represent the setback insofar as the uncoupled translational vibrations of the shear beam are concerned. They are the ratio of the height of base portion to the total height, termed the level of setback, and the ratio of plan area of tower portion to that of base portion, termed the "degree" of setback. The stiffness and mass properties of the lumped mass model are idealized so as to permit the representation of setback by two similar parameters.

The effects on various modal quantities (periods, mode shapes etc.) of the two models of the variations in the two parameters of setback are examined in Chapter III. Also in this chapter the computed responses of the lumped mass model to recorded earthquakes and the approximate responses of the shear beam model are compared with the specifications of seismic building codes in regards to the effect of setback.

Second, the coupled torsional-lateral vibrations in buildings having unsymmetric setbacks are examined in Chapter IV. For the present study it is assumed that stiffness and mass are symmetrically distributed about the geometrical planes of symmetry in each of the two portions of the structure. The tower and the base portions of the buildings are then dynamically symmetric structures by themselves.

The lack of dynamic symmetry in the structure is due to its lack of geometric symmetry and it is represented by the offsets in two mutually perpendicular directions between the tower and the base centroids.

Results are obtained for the case of buildings with setback unsymmetric about only one principal direction for which case the translational vibrations in that direction alone are coupled with the torsional vibrations. Variation of the eccentricity of the setback along one of the principal directions and its effect on the modal properties is examined in Chapter IV for the two models of a building with given level and degree of setback. The responses of the lumped mass model of the building to recorded earthquakes are also computed and examined for the effect of variation in the eccentricity of the setback.

CHAPTER II

DIFFERENTIAL EQUATIONS OF MOTION OF MULTI-STORY BUILDINGS SUBJECTED TO EARTHQUAKES

EQUATIONS OF MOTION

Multistory buildings are very complex structures and their dynamic analyses are impossible without introducing simplifying assumptions. During earthquakes the ground shakes in all directions and induces motion in buildings in all six components of motion. Buildings are designed to carry static vertical dead and live loads with a reasonable factor of safety. Due to this reserve strength in the vertical direction it is customary to neglect the vertical components of vibration.

Mass is distributed throughout the building. However, since in most buildings much of the mass is indeed concentrated at floor levels, it will be assumed here, for mathematical convenience, that all mass in the structure is concentrated at floor levels (Figure 2.1). The error introduced by this approximation is expected to be small in the lower modes of vibration[19] which are the modes of primary importance in structural response to earthquakes. Ignoring the vertical translatory inertia and the rotatory inertia about the horizontal axes, one is left with three degrees of freedom per floor in the building. Thus 3N coordinates will describe completely the motion of interest, viz. the motion of each floor in its horizontal plane, in an N-story building. It is also assumed that the effect of vertical motions on the horizontal vibrations in the structure is negligible.

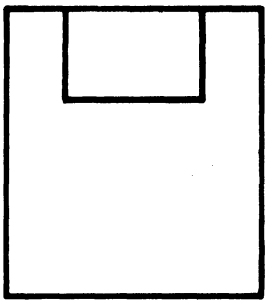

a. Plan

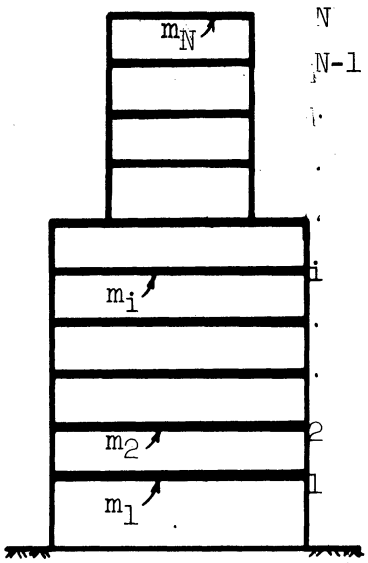

b. Elevation

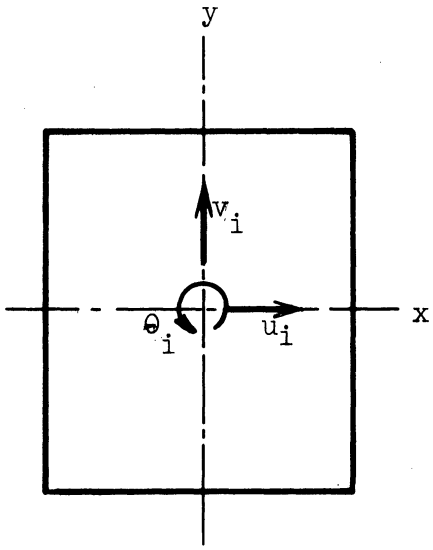

c. Plan of a Typical floor

Figure 2.1. An N-Story Building.

If we further assume that,

a. stiffness is linearly elastic,

b. damping is of the viscous type,

and

c. there is no foundation yielding,

the differential equation of motion for an N-story building (Figure 2.1) may be written in the matrix form as

$$[M]\ \{\ddot{r}\} + [C]\ \{\dot{r}\} + [K]\ \{r\} = \{f(t)\} \qquad (2.1)$$

In Equation (2.1) $\{r\}$ is the displacement vector of order $3N$

$$r = \begin{Bmatrix} r_1 \\ r_2 \\ \cdot \\ \cdot \\ \cdot \\ r_{3N} \end{Bmatrix}; \qquad (2.2)$$

$[M]$ is $3N \times 3N$ inertia matrix

$$[M] = \begin{bmatrix} m_{1,1} & \cdots & & & & m_{1,3N} \\ \vdots & & & & & \vdots \\ \vdots & & & & & \vdots \\ \vdots & & & & & \vdots \\ m_{3N,1} & \cdots & & & & m_{3N,3N} \end{bmatrix} \qquad (2.3)$$

where m_{ij} is the inertia force acting along the i-th coordinate of displacement when the configuration of the structure is such that the acceleration along the j-th coordinate is unity and zero along the rest, i.e. $\ddot{r}_j = 1$, $\ddot{r}_i = 0$ for all $i \neq j$.

[C] is the 3N x 3N damping matrix

$$[C] = \begin{bmatrix} c_{1,1} & \cdots & & & & c_{1,3N} \\ \vdots & & & & & \vdots \\ \vdots & & & & & \vdots \\ c_{3N,1} & \cdots & & & & c_{3N,3N} \end{bmatrix} \tag{2.4}$$

where c_{ij} is the force exerted by dampers on the mass along the i-th coordinate when the configuration of the structure is such that the velocity along the j-th coordinate is unity and zero along the rest, i.e. $\dot{r}_j = 1$, $\dot{r}_i = 0$ for all $i \neq j$;

[K] is the 3N x 3N stiffness matrix

$$[K] = \begin{bmatrix} k_{1,1} & \cdots & & & & k_{1,3N} \\ \vdots & & & & & \vdots \\ \vdots & & & & & \vdots \\ k_{3N,1} & \cdots & & & & k_{3N,3N} \end{bmatrix} \tag{2.5}$$

where k_{ij} is the force exerted by the springs on the mass along the i-th coordinate when the configuration of the structure is such that the displacement along the j-th coordinate is unity and zero along the rest, i.e. $r_j = 1$, $r_i = 0$ for all $i = j$; and

$\{f(t)\}$ is the 3N-order driving force vector

$$\{f(t)\} = \begin{Bmatrix} f_1(t) \\ f_2(t) \\ \vdots \\ f_{3N}(t) \end{Bmatrix} \tag{2.6}$$

where $f_i(t)$ is the driving force acting on the mass along the i-th coordinate at time t; dots above letters denote differentiation with respect to time.

The terms "displacement" and "force" are used in a general sense to include, respectively, translation and rotation, and linear force and torque. The terms "velocity" and "acceleration" are used in the similar generalized sense. It may also be noted that the vectors and matrices involved are not necessarily homogenious dimensionally. The matrices [M], [C] and [K] are symmetric, [M] and[K] positive definite and [C] non-negative definite, for stable structures.

The displacements of each mass will be measured as the translations of its center of gravity (c.g.) along any set of two mutually perpendicular directions, x and y, and its rotation about the vertical axis through its c.g. as shown in Figure 2.1c, which also indicates the positive sense of these displacements. All displacements are measured relative to the ground. The elements of the vector $\{r\}$ will be ordered such that

$$\{r\} = \begin{Bmatrix} u \\ \hline v \\ \hline \theta \end{Bmatrix} \tag{2.7}$$

where

$$\{u\} = \begin{Bmatrix} u_1 \\ u_2 \\ \cdot \\ \cdot \\ \cdot \\ u_N \end{Bmatrix} \qquad \{v\} = \begin{Bmatrix} v_1 \\ v_2 \\ \cdot \\ \cdot \\ \cdot \\ v_N \end{Bmatrix} \qquad \{\theta\} = \begin{Bmatrix} \theta_1 \\ \theta_2 \\ \cdot \\ \cdot \\ \cdot \\ \theta_N \end{Bmatrix} \tag{2.8}$$

are sub-vectors of $\{r\}$ and u_i, v_i, θ_i are, respectively, the translations in the x and y directions and rotation about the vertical axis of the i-th mass.

The above choice of the system of coordinates makes the inertia matrix, [M], diagonal. The matrices [M], [C] and [K] can be partitioned into nine N x N sub-matrices following the partitioning of vector $\{r\}$ into subvectors $\{u\}$, $\{v\}$ and $\{\theta\}$, Equation (2.7). Thus one may write

$$[M] = \begin{bmatrix} [M_u] & [0] & [0] \\ [0] & [M_v] & [0] \\ [0] & [0] & [M_\theta] \end{bmatrix} \tag{2.9}$$

$$[C] = \begin{bmatrix} [C_u] & [C_{uv}] & [C_{u\theta}] \\ [C_{vu}] & [C_v] & [C_{v\theta}] \\ [C_{\theta u}] & [C_{\theta v}] & [C_\theta] \end{bmatrix} \tag{2.10}$$

$$[K] = \begin{bmatrix} [K_u] & [K_{uv}] & [K_{u\theta}] \\ [K_{vu}] & [K_v] & [K_{v\theta}] \\ [K_{\theta u}] & [K_{\theta v}] & [K_\theta] \end{bmatrix} \tag{2.11}$$

with all the submatrices being of size N x N. In Equation (2.9) [0] is the null matrix. Since [M] is diagonal all its off-diagonal submatrices are null matrices and $[M_u]$, $[M_v]$ and $[M_\theta]$ are diagonal matrices. Also,

$$[M_u] = [M_v] = \begin{bmatrix} m_1 & 0 & \cdots & 0 \\ 0 & m_2 & & \vdots \\ \vdots & & \ddots & \vdots \\ 0 & \cdots & 0 & m_N \end{bmatrix} \tag{2.12}$$

where m_i is the value of i-th mass;

and

$$[M_\theta] = \begin{bmatrix} m\theta_1 & 0 & \cdots & 0 \\ 0 & m\theta_2 & & \vdots \\ \vdots & & \ddots & \vdots \\ 0 & \cdots & 0 & m\theta_N \end{bmatrix} \tag{2.13}$$

where $m\theta_i$ is the rotational inertia of the i-th mass about the vertical axis through its centroid.

The matrices [C] and [K] are symmetric; therefore

$$[C_{uv}] = [C_{vu}]^T, \quad [C_{u\theta}] = [C_{\theta u}]^T, \quad [C_{v\theta}] = [C_{\theta v}]^T \tag{2.14}$$

and

$$[K_{uv}] = [K_{vu}]^T, \quad [K_{u\theta}] = [K_{\theta u}]^T, \quad [K_{v\theta}] = [K_{\theta v}]^T \tag{2.15}$$

The driving force vector $\{f(t)\}$ may also be partitioned into three subvectors

$$\{f(t)\} = \begin{Bmatrix} f_u(t) \\ \hline f_v(t) \\ \hline f_\theta(t) \end{Bmatrix} \tag{2.16}$$

CONDITIONS FOR UNCOUPLING

The motion of a building under dynamic forces has been divided into three components: (1) translation of all masses parallel to x direction, $\{u\}$; (2) translation of all masses parrallel to y direction, $\{v\}$; and (3) rotation of all masses in the horizontal plane, $\{\theta\}$. From Equations (2.7), (2.9), (2.11) and (2.16), Equation

(2.1) may be seen as three sets of equations, one for each component of motion. If the off-diagonal submatrices of [K] and [C] are zero matrices, the set of 3N simultaneous equations, Equation (2.1), degenerates into three sets of N simultaneous equations independent from each other, viz.

$$[M_u]\{\ddot{u}\} + [C_u]\{\dot{u}\} + [K_u]\{u\} = \{f_u(t)\} \qquad (2.17)$$

$$[M_v]\{\ddot{v}\} + [C_v]\{\dot{v}\} + [K_v]\{v\} = \{f_v(t)\} \qquad (2.18)$$

$$[M_\theta]\{\ddot{\theta}\} + [C_\theta]\{\dot{\theta}\} + [K_\theta]\{\theta\} = \{f_\theta(t)\} \qquad (2.19)$$

Accordingly the three components of motion will also be uncoupled from each other. It should be noted here that by the choice of the particular system of coordinates that has been made to describe the motion of structure, the off-diagonal submatrices of the inertia matrix [M] are zero matrices.

When some or all of the off-diagonal submatrices of the matrices [K] and [C] are non-zero, any two or all three sets of equations will be coupled and the corresponding components of motion therefore will also be coupled. In such a case a single component of driving forces (i.e. either $\{f_u\}$, or $\{f_v\}$, or $\{f_\theta\}$) may induce motions not only of its own type ($\{u\}$, $\{v\}$, or $\{\theta\}$, respectively) but also in one or both of the other types. Whether or not such coupleing will exist in a structure depends on the distribution of stiffness and damping in the structure and on the orientation of the x, y axes.

Not much is known about the nature and extent of damping in buildings. The assumption made here that it is of the viscous type is essentially for mathematical convenience. In any case, damping is not expected to affect significantly the modes of vibration of the structure. For these reasons the conditions for decoupling of the three components of motions are discussed only with regard to the distribution of stiffness. It may be noted, however, that conditions of decoupling similar to those derived for stiffness distribution may also be obtained in exactly the same manner for viscous damping.

The equation for undamped vibration, from Equation (2.1), is

$$[M]\{\ddot{r}\} + [K]\{r\} = \{f(t)\} \qquad (2.20)$$

Using Equations (2.7), (2.9), (2.11) and (2.16), Equation (2.20) may be written in the following form

$$[M_u]\{\ddot{u}\} + [K_u]\{u\} + [K_{uv}]\{v\} + [K_{u\theta}]\{\theta\} = \{f_u(t)\} \qquad (2.21)$$

$$[M_v]\{\ddot{v}\} + [K_{vu}]\{u\} + [K_v]\{v\} + [K_{v\theta}]\{\theta\} = \{f_v(t)\} \qquad (2.22)$$

$$[M_\theta]\{\ddot{\theta}\} + [K_{\theta u}]\{u\} + [K_{\theta v}]\{v\} + [K_\theta]\{\theta\} = \{f_\theta(t)\}. \qquad (2.23)$$

The lateral stiffness in a building may be represented by springs acting laterally, interconnecting, in general, every pair of masses as well as all masses and the ground. This is shown schematically in Figure 2.2 for a two-story building. For buildings where the "shear building" assumption can be made, the stiffness may be represented by springs connecting only adjacent masses and only one mass to the ground. (The set of springs connecting m_2 and ground would then be absent in

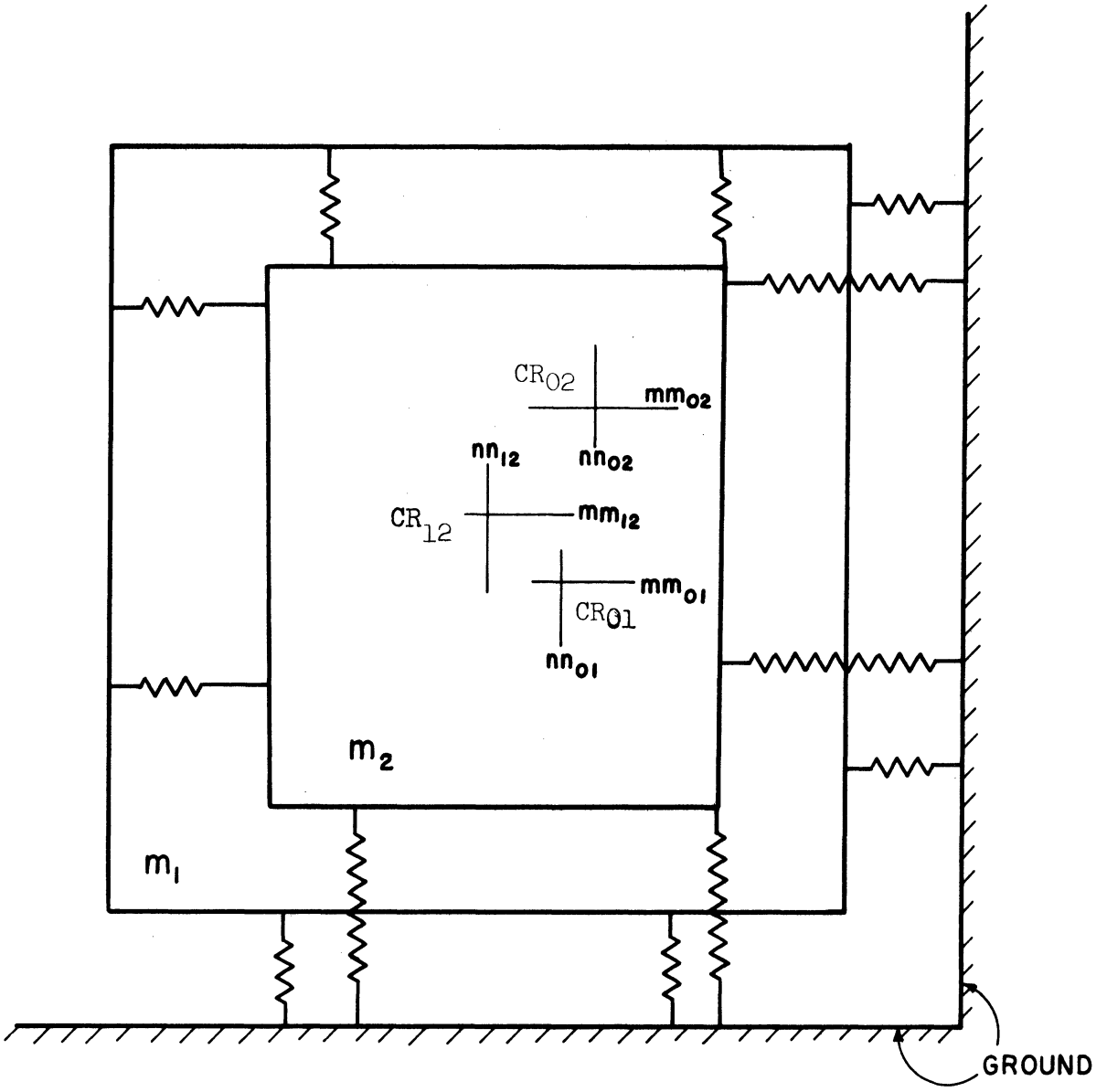

Figure 2.2. Schematic Representation (in Plan) of Stiffness in a Two-Story Building.

Figure 2.2.) Ayre examined the nature of coupling in one-and two-story shear buildings[8]. The ideas used there can be readily extended to the general case. For each set of springs connecting a pair of masses or a mass to the ground, there may be defined two principal elastic axes perpendicular to each other (mm_{01}, nn_{01} etc., in Figure 2.2.) Any force applied along a principal elastic axis will, by definition of principal elastic axis, produce deflection only along that axis and vice versa. The point of intersection of the two principal elastic axes for a set of springs may be called the center of rigidity (c.r.) for that set of springs (CR_{01}, CR_{02}, CR_{12} in Figure 2.2); and the springs may be equivalently represented by two resultant stiffnesses acting along the principal elastic axes and a torsional stiffness about the vertical through the c.r. The principal elastic axes are unique except for the case of equal stiffness in all directions, in which case any set of perpendicular lines through the c.r. may be called the principal axes.

There will be a pair of principal elastic axes and a center of rigidity for each set of springs connecting each pair of masses or mass and ground.

In most regular shaped buildings all the stiffness elements such as walls and moment resisting frames will in general, have their principal axes oriented in two fixed perpendicular directions over the entire height of the structure. In the mathematical model of all such structures the principal elastic axes of all the sets of springs will also be oriented along two fixed perpendicular directions. These may then be called the principal directions of the structure. If the x and y directions are taken parallel to these principal directions, direct

coupling between the translation components in x and y directions will be eliminated and

$$[K_{uv}] = [K_{vu}]^T = [0] \tag{2.24}$$

This will be assumed to be the case throughout this work.

However, unless certain other conditions are also satisfied, the rotational component of motion will still be coupled with the two translational components, since the three equations, (2.21) through (2.23), still remain coupled.

In addition to the above condition, if the lateral stiffness in one of the principal directions is distributed symmetrically about one vertical plane of symmetry over the entire height of the structure, the principal elastic axes of all the sets of springs in that direction will be on the same vertical plane. The c.r.'s of each set of springs will then lie in this plane. Further, if the mass in the structure is so distributed as to have one plane of symmetry valid for the entire height of the building, and if this plane coincides with the plane of symmetry of stiffness, then the c.g.'s of all the masses will also lie in that plane. This plane is then a plane of dynamic symmetry. Translations in these directions will then be uncoupled from rotations.

If the plane of symmetry is parallel to x then

$$[K_{u\theta}] = [K_{\theta u}]^T = [0] \tag{2.25}$$

and Equation (2.21) will be independent from Equations (2.22) and (2.23). They may be rewritten as

$$[M_u] \{\ddot{u}\} + [K_u] \{u\} = \{f_u(t)\} \tag{2.26}$$

and

$$[M_v]\{\ddot{v}\} + [K_v]\{v\} + [K_{v\theta}]\{\theta\} = \{f_v(t)\} \qquad (2.27)$$

$$[M_\theta]\{\ddot{\theta}\} + [K_{\theta v}]\{v\} + [K_\theta]\{\theta\} = \{f_\theta(t)\} \qquad (2.28)$$

If the plane of dynamic symmetry were parallel to y, then

$$[K_{v\theta}] = [K_{\theta v}]^T = [0] \qquad (2.29)$$

and Equations (2.21) - (2.23) may be rewritten as

$$[M_v]\{\ddot{v}\} + [K_v]\{v\} = \{f_v(t)\} \qquad (2.30)$$

and

$$[M_u]\{\ddot{u}\} + [K_u]\{u\} + [K_{u\theta}]\{\theta\} = \{f_u(t)\} \qquad (2.31)$$

$$[M_\theta]\{\ddot{\theta}\} + [K_{\theta u}]\{u\} + [K_\theta]\{\theta\} = \{f_\theta(t)\} \qquad (2.32)$$

If the mass and stiffness distributions were such as to have planes of dynamic symmetry in both x and y directions, the principal elastic axes in each direction would all lie in a plane of symmetry and all the c.r.'s, and the c.g.'s, would lie on the same vertical. Under these conditions Equations (2.25) and (2.29) will hold simultaneously resulting in decoupling of all three components of motion, since Equations (2.21) - (2.23) would reduce to

$$[M_u]\{\ddot{u}\} + [K_u]\{u\} = \{f_u(t)\} \qquad (2.33)$$

$$[M_v]\{\ddot{v}\} + [K_v]\{v\} = \{f_v(t)\} \qquad (2.34)$$

$$[M_\theta]\{\ddot{\theta}\} + [K_\theta]\{\theta\} = \{f_\theta(t)\} \qquad (2.35)$$

A case of no real practical interest occurs when the c.r.'s and the c.g.'s all lie on the same vertical, but not all the principal elastic axes are oriented in the same directions. Here rotation is decoupled from translations since

$$[K_{u\theta}] = [K_{\theta u}]^T = [0] \tag{2.36}$$

and

$$[K_{v\theta}] = [K_{\theta v}]^T = [0] \tag{2.37}$$

but the translations themselves cannot be decoupled for any orientation of the x and y directions. For this condition, Equations (2.21) - (2.23) may be rewritten as

$$[M_\theta]\{\ddot{\theta}\} + [K_\theta]\{\theta\} = \{f_\theta(t)\} \tag{2.38}$$

$$[M_u]\{\ddot{u}\} + [K_u]\{u\} + [K_{uv}]\{v\} = \{f_u(t)\} \tag{2.39}$$

$$[M_v]\{\ddot{v}\} + [K_{vu}]\{u\} + [K_v]\{v\} = \{f_v(t)\} \tag{2.40}$$

It may again be noted that a similar discussion can be made with regard to the damping distribution in the structure replacing it by equivalent dashpots, etc.

SOLUTION

As seen earlier, the differential equations of motion (2.1) of a building are a set of 3N simultaneous second-order equations. The movement of a building may be divided into three components and the 3N Equations (2.1) may be seen as three sets of N equations, one set corresponding to each component of motion. The three sets of equations are in general coupled but, as shown in the foregoing section, under certain conditions some of the three sets may become independent of the other sets. In the latter case two or three sets of N or 2N simultaneous

equations will have to be solved separately. However, whether one, two, or three components are involved in the set of Q (Q=N, 2N or 3N) equations to be solved simultaneously, in all cases the form of the equations remains the same, viz.

$$[M]\{\ddot{r}\} + [C]\{\dot{r}\} + [K]\{r\} = \{f(t)\} \qquad (2.41)$$

with the definition of various matrices and vectors depending on the case considered.

In the previous section the effect that damping might have on the nature of coupling was ignored. In writing Equation (2.41) as valid for one, two or all three components of motion, it is implicity assumed that the nature of damping in the structure is also such as to satisfy the requirements for the uncoupling of the components of motion assumed in the equation.

First consider the undamped system

$$[M]\{\ddot{r}\} + [K]\{r\} = \{f(t)\} \qquad (2.42)$$

The natural frequencies and modes of free vibration of the undamped system (2.42) may be obtained by considering the related homogeneous equations

$$[M]\{\ddot{r}\} + [K]\{r\} = \{0\} \qquad (2.43)$$

Let

$$\{r\} = \{\phi\} e^{i\omega t} \qquad (2.44)$$

be a solution of Equation (2.43) where ω is a constant scalar of dimension T^{-1}, $\{\phi\}$ is a constant vector with the dimension of its

elements being consistent with the dimension of the corresponding elements of the vector $\{r\}$, t is the independent time variable, and $i = \sqrt{-1}$.

Differentiating (2.44) twice, one gets

$$\ddot{r} = -\omega^2 e^{i\omega t} \{\phi\} \tag{2.45}$$

Using relations (2.44) and (2.45), Equation (2.43) becomes

$$e^{i\omega t} (-\omega^2 [M] \{\phi\} + [K] \{\phi\}) = \{0\} \tag{2.46}$$

or

$$([K] - \omega^2 [M]) \{\phi\} = \{0\} \tag{2.47}$$

For nontrivial solution, $\{\phi\} \neq \{0\}$, hence

$$\| [K] - \omega^2 [M] \| = 0 \tag{2.48}$$

where the symbol $\| \ \|$ stands for determinant. Equation (2.48) is a Q^{th}-order polynomial in ω^2. If the matrices [M] and [K] are symmetric and positive definite, then the Q roots, ω_1^2, ω_2^2,...ω_Q^2, of Equation (2.48) are real and positive, but not necessarily distinct. These conditions on [M] and [K] are always satisfied for stable structural systems. For each root ω_k^2, $k = 1, 2, \ldots, Q$, Equation (2.47) can be solved for the vector $\{\phi\} = \{\phi^k\}$, which contains an arbitrary constant factor. The positive values ω_1 ω_2,..., ω_Q, and the corresponding vectors $\{\phi^1\}$, $\{\phi^2\}$, ..., $\{\phi^Q\}$ are termed the natural frequencies and the natural modes of system (2.43). The roots ω_k^2 and corresponding vectors $\{\phi^k\}$ are also called the latent roots or eigenvalues and eigenvectors, respectively, of the matrix $[M]^{-1}$ [K], since by premultiplying Equation (2.47) by $[M]^{-1}$ it may be seen that

$$[M]^{-1} [K] \{\phi\} = \omega^2 [I] \{\phi\} \tag{2.49}$$

The inverse $[M]^{-1}$ of the matrix $[M]$ exists because $[M]$ is positive definite.

Let ω_j and ω_k be any two of the natural frequencies and $\{\phi^j\}$ and $\{\phi^k\}$ the corresponding natural modes of system (2.43). Then

$$\{r\} = e^{i\omega_j t} \{\phi^j\} \tag{2.50}$$

and

$$\{r\} = e^{i\omega_k t} \{\phi^k\} \tag{2.51}$$

are both solutions of system (2.43).

Hence, applying relations (2.50) and (2.51) to Equation (2.43) one gets

$$-\omega_j^2 [M] \{\phi^j\} + [K] \{\phi^j\} = \{0\} \tag{2.52}$$

$$-\omega_k^2 [M] \{\phi^k\} + [K] \{\phi^k\} = \{0\} \tag{2.53}$$

On premultiplying (2.52) by $\{\phi^k\}^T$ and transposing Equation (2.53) and postmultiplying it by $\{\phi^j\}$, it follows that

$$-\omega_j^2 \{\phi^k\}^T [M] \{\phi^j\} + \{\phi^k\}^T [K] \{\phi^j\} = 0 \tag{2.54}$$

$$-\omega_k^2 \{\phi^k\}^T [M]^T \{\phi^j\} + \{\phi^k\}^T [K]^T \{\phi^j\} = 0 \tag{2.55}$$

Since $[M]$ is diagonal and $[K]$ is symmetric

$$[M]^T = [M] \tag{2.56}$$

$$[K]^T = [K] \tag{2.57}$$

Subtracting (2.55) from (2.54) and using (2.56) and (2.57), one finds that

$$(\omega_k^2 - \omega_j^2) \{\phi^k\}^T [M] \{\phi^j\} = 0 \tag{2.58}$$

Hence if $\omega_k^2 \neq \omega_j^2$,

$$\{\phi^k\}^T [M] \{\phi^j\} = 0 \tag{2.59}$$

From (2.54) it also follows that

$$\{\phi^k\}^T [K] \{\phi^j\} = 0 \tag{2.60}$$

Relations (2.59) and (2.60) are known as the orthogonality relations of the natural modes of the undamped system (2.42).

In case of repeated eigenvalues (of the matrix $[M]^{-1} [K]$) also, it can be shown that if $[M]$ and $[K]$ are positive definite then there are as many associated linearly independent eigenvectors as the multiplicity of the eigenvalue. These eigenvectors are orthogonal to eigenvectors associated with other eigenvalues of $[M]^{-1} [K]$ as shown above. Furthermore, the set of linearly independent eigenvectors associated with the repeated eigenvalue may, by suitable linear combination, be transformed to a mutually orthogonal set of eigenvectors.

The vectors $\{\phi^k\}$, $(k = 1,2,\ldots,Q)$ form a linearly independent set of Q vectors. Hence any displacement configuration of the system can be expressed in terms of its modes, i.e.

$$\{r\} = [\Phi] \{\zeta\} \tag{2.61}$$

where the columns of matrix $[\Phi]$ are the modes $\{\phi^j\}$ $(j = 1,2,\ldots,Q)$ and ζ_j are the so-called generalized coordinates. It was noted earlier that the modes $\{\phi^j\}$ are arbitrary to a constant factor. But in whatever suitable way the modes are normalized, there will exist an appropriate $\{\zeta\}$ so that Equation (2.61) holds. It may also be noted that $[\Phi]^{-1}$ exists and

$$\{\zeta\} = [\Phi]^{-1} \{r\}$$

Considering now the general case of forced vibration, Equation (2.61) put in Equation (2.42) gives

$$[M]\,[\Phi]\,\{\ddot{\eta}\} + [K]\,[\Phi]\,\{\eta\} = \{f(t)\} \quad . \tag{2.63}$$

Premultiplying by $\{\phi^k\}^T$, we get

$$\{\phi^k\}^T\,[M]\,[\Phi]\,\{\ddot{\eta}\} + \{\phi^k\}^T\,[K]\,[\Phi]\,\{\eta\} = \{\phi^k\}^T\,\{f(t)\}, \tag{2.64}$$

and using Equations (2.59) and (2.60), this reduces to

$$\{\phi^k\}^T\,[M]\,\{\phi^k\}\,\ddot{\eta}_k + \{\phi^k\}^T\,[K]\,\{\phi^k\}\,\eta_k = \{\phi^k\}^T\,\{f(t)\}. \tag{2.65}$$

From Equation (2.53) it is clear that

$$\{\phi^k\}^T\,[K]\,\{\phi^k\} = \omega_k^2\,\{\phi^k\}^T\,[M]\,\{\phi^k\} > 0 \tag{2.66}$$

since [M] and [K] are positive definite. Therefore, Equation (2.65) may be written as

$$\ddot{\eta}_k + \omega_k^2\,\eta_k = g_k(t) \qquad k = 1,2,\ldots,Q \tag{2.67}$$

where

$$g_k(t) = \frac{\{\phi^k\}^T\,\{f(t)\}}{\{\phi^k\}^T\,[M]\,\{\phi^k\}} \tag{2.68}$$

A simple way customarily used to take account of damping in a structure is to introduce a damping term in the uncoupled equations (2.67) in generalized coordinates:

$$\ddot{\eta}_k + 2\beta_k\,\omega_k\,\dot{\eta}_k + \omega_k^2\,\eta_k = g_k(t) \qquad (k = 1,2,\ldots,Q) \tag{2.69}$$

where β_k is the fraction of critical damping in the k-th mode. This is based on the assumption that the damping does not affect the natural

modes and frequencies of the structure. The modes are indeed unaffected if the damping matrix is expressible as a linear sum of the mass and stiffness matrices. For if

$$[C] = \alpha[M] + \gamma[K] \tag{2.70}$$

where α and γ are constants of dimension $[T^{-1}]$ and $[T]$, respectively, then the equation for damped vibration (2.41) becomes

$$[M]\{\ddot{r}\} + (\alpha[M] + \gamma[K])\{\dot{r}\} + [K]\{r\} = \{f(t)\}. \tag{2.71}$$

Using (2.61) and premultiplying by $\{\phi^k\}^T$ we get

$$\{\phi^k\}^T [M] \{\phi^k\} \ddot{\eta}_k + (\alpha\{\phi^k\}^T [M] \{\phi^k\} + \gamma\{\phi^k\}^T [K] \{\phi^k\}) \dot{\eta}_k + \{\phi^k\}^T [K] \{\phi^k\} \eta_k = \{\phi^k\}^T \{f(t)\} \quad k = 1,2,\ldots,Q, \tag{2.72}$$

also utilizing Equations (2.59) and (2.60). Using Equation (2.55) for the case $j = k$ and dividing through by $\{\phi^k\}^T [M] \{\phi^k\}$, Equation (2.72) reduces to

$$\ddot{\eta}_k + (\alpha + \omega_k^2 \gamma) \dot{\eta}_k + \omega_k^2 \eta_k = g_k(t) \tag{2.73}$$

which in comparison with Equation (2.69) gives

$$\beta_k = \frac{\alpha + \omega_k^2 \gamma}{2\omega_k} \tag{2.74}$$

The relation (2.70) between the damping matrix and the mass and stiffness matrices is a sufficient condition for the modes of the undamped system (2.42), the so-called classical modes, to be valid for

the damped system (2.41). Caughey[20] showed that the necessary and sufficient condition is that the transformation that diagonalizes the mass and stiffness matrix also diagonalizes the damping matrix. For symmetric mass and stiffness matrices and distinct eigenvalues, it was shown that the above condition reduces to the following restriction on the damping matrix[21],

$$[M]^{-1}[C] = \sum_{j=0}^{j=Q-1} a_j \left([M]^{-1}[K] \right)^j \qquad (2.75)$$

where a_j are constants.

Equation (2.70) is a special case of this for which $a_0 = \alpha$, $a_1 = \gamma$, and $a_2 = a_3 = \ldots a_Q = 0$.

For the general linear viscous damped system the solution may be obtained by changing the problem of solving Q equations of second order to 2Q equations of first order[22,23]. Unless the damping matrix [C] satisfies relation (2.75), the resulting modes will be complex so that, although in any one mode different parts of the system will oscillate at the same frequency, they may not necessarily be in phase.

Since, as mentioned earlier, not much is known about the nature of damping in structures, it is assumed for the purpose of present investigation that the damping is viscous and that it does not affect the undamped modes, i.e., the damping matrix does satisfy the condition (2.75).

GIVENS' METHOD

The problem of determining the frequencies and modes of the system

$$[M]\{\ddot{r}\} + [K]\{r\} = \{0\} \qquad (2.76)$$

is equivalent to the problem of determining the eigenvalues and eigenvectors of the matrix $[M]^{-1}[K]$. There are several methods available to solve this problem. Prominent among these are Jacobi's Method, Givens' Method, Matrix Iteration (Stodola-Vianello) Method, Power Method, and Lanczos' (pq algorithm) Method. All these methods are described in Reference 24. Givens' Method was originally presented in Reference 25. It was decided to use Givens' Method because of its advantages over other methods of accuracy, possibility of determining any or all eigenvalues with equal ease, less time-consumption, and suitability to the present problem. It was, of course, necessary to use a digital computer to solve the large systems encountered in this investigation.

Givens' Method is applicable to real symmetric matrices. The matrix $[M]^{-1}[K]$ is, in general, not symmetric but can be easily transformed into one by means of a similarity transformation. The eigenvalue problem is

$$[M]^{-1}\,[K]\,\{\phi\} = \omega^2\,\{\phi\} \quad . \tag{2.77}$$

Let

$$\{\phi\} = [M]^{-\frac{1}{2}}\,\{\psi\} \quad , \tag{2.78}$$

then substituting for $\{\phi\}$ into Equation (2.77) and premultiplying by $[M]^{+\frac{1}{2}}$, we get

$$[M]^{+\frac{1}{2}}\,[M]^{-1}\,[K]\,[M]^{-\frac{1}{2}}\,\{\psi\} = \omega^2\,[M]^{\frac{1}{2}}\,[M]^{-\frac{1}{2}}\,\{\psi\} \tag{2.79}$$

or

$$[A]\,\{\psi\} = \omega^2\,\{\psi\} \tag{2.80}$$

where

$$[A] = [M]^{-\frac{1}{2}} [K] [M]^{-\frac{1}{2}} \tag{2.81}$$

is symmetric since

$$[A]^T = \left([M]^{-\frac{1}{2}} [K] [M]^{-\frac{1}{2}} \right)^T = \left([M]^{-\frac{1}{2}} \right)^T [K]^T \left([M]^{-\frac{1}{2}} \right)^T$$

$$= [M]^{-\frac{1}{2}} [K] [M]^{-\frac{1}{2}} = [A] \tag{2.82}$$

noting that $[M]$ and $[M]^{-\frac{1}{2}}$ and $[K]$ are symmetric.

A word of explanation about the matrices $[M]^{\frac{1}{2}}$ and $[M]^{-\frac{1}{2}}$. $[M]^{\frac{1}{2}}$ is a square root of the matrix $[M]$, i.e.

$$[M]^{\frac{1}{2}} [M]^{\frac{1}{2}} = [M] \quad . \tag{2.83}$$

Similarly, $[M]^{-\frac{1}{2}}$ is a square root of the matrix $[M]^{-1}$, i.e.

$$[M]^{-\frac{1}{2}} [M]^{-\frac{1}{2}} = [M]^{-1} \quad . \tag{2.84}$$

The number of square roots, and in general the m-th roots, of a square matrix are dependent upon the nature of the matrix[22]. The matrices $[M]$ and $[M]^{-1}$ are diagonal matrices. For such matrices, matrices having diagonal elements equal to one of the two square roots of the corresponding elements of the original matrix are the obvious, among other, square roots.

The matrix $[M]$, and hence also $[M]^{-1}$, is real and positive definite; therefore, their diagonal elements are real and positive. The square roots of such elements are real. Here the square root matrix is restricted to the one having its elements equal to the positive square roots. Thus the matrix $[M]^{\frac{1}{2}}$ is diagonal and its diagonal elements are $\sqrt{m_i}$ $(i = 1,2,\ldots,Q)$ where $[M]$ is a diagonal matrix with elements $m_i > 0$ $(i = 1,2,\ldots,Q)$. $[M]^{-1}$ is also diagonal having

elements $\frac{1}{m_i}$ $(i = 1,2,\ldots,Q)$ and $[M]^{-\frac{1}{2}}$ is diagonal having elements $\sqrt{\frac{1}{m_i}}$, $i = 1,2,\ldots,Q$.

Comparing Equations (2.80) and (2.77) it is seen that the eigenvalues of the matrices $[A]$ and $[M]^{-1}[K]$ are the same, and their eigenvectors are related by Equation (2.78).

Givens[25] showed that it is possible to construct an orthogonal transformation T

$$\{\psi\} = [T]\{\rho\} \tag{2.85}$$

$$[T]^T[T] = [I] \quad , \tag{2.86}$$

where $[I]$ is an identity matrix, which would transform a real symmetric matrix $[A]$ into a tridiagonal matrix $[S]$

$$[S] = [T]^T[A][T] \tag{2.87}$$

Since (2.87) is also a similarity transformation (noting the property of $[T]$ given by (2.86)), the eigenvalues of $[S]$ and $[A]$ are identical and their eigenvectors are related by Equation (2.85).

The transformation T is made up of a finite number of successive orthogonal transformations $T_{2,3}$, $T_{2,4}$,....., $T_{2,Q}$, $T_{3,4}$....., $T_{Q-2,Q}$, formed so as to eliminate successively the (2,3), (2,4),...., (2,Q), (3,4),....,(Q-2,Q) elements, respectively, (and also the corresponding transposed elements by symmetry) of $[A]$. Q is the order of matrix $[A]$. Thus,

$$[T] = [T_{23}[\,[T_{24}] \cdots\cdots [T_{2Q}]\,][T_{34}] \cdots\cdots [T_{Q-2,Q}] \quad . \tag{2.88}$$

In all, at most $\frac{1}{2}(Q-1)(Q-2)$ transformations are needed to reduce a

symmetric matrix [A] into a tridiagonal matrix [S]. See Reference (25) for details of construction of matrix [T].

The eigenvalues of matrix [S] are the roots of the determinantal equation

$$\| \omega^2 [I] - [S] \| = 0 \quad . \tag{2.89}$$

The successive principal minors of the matrix $[\omega^2 [I] - [S]]$, $f_i(\omega^2)$, are given by

$$f_i(\omega^2) = (\omega^2 - s_{i,i}) f_{i-1}(\omega^2) - (s_{i-1,i})^2 f_{i-2}(\omega^2) \quad i = 1,2,\ldots,Q$$
$$f_0(\omega^2) = 1, \quad s_{0,1} = 0 \quad ; \tag{2.90}$$

$f_Q(\omega^2)$ is the determinant in Equation (2.89). It may be noted that if $s_{i-1,i} = 0$ for one or more i, the matrix [S] can be split up into two or more smaller tridiagonal submatrices; each may be treated separately in the same way as [S] with $s_{i-1,i} \neq 0$ for all i, as described here. The zeros of Equation (2.90) can then be found by linear interpolation.

A property of the sequence of the principal minors $f_Q(\omega^2)$, $f_{Q-1}(\omega^2)$, ..., $f_0 = 1$ (Equations 2.90), known as Sturm sequence, corresponding to the matrix [S] is that the number of eigenvalues of [S] greater than α is equal to the number of the variations in the algebraic signs in the sequence, $f_Q(\alpha)$, $f_{Q-1}(\alpha)$, ..., 1. This property can be used, among other things, to check against slipping over a set of two or more close eigenvalues, while searching for them by the method of interpolation.

The eigenvector corresponding to a eigenvalue, ω_j^2, of [S] is found by solving the equations

$$[\omega_j^2\,[I] - [S]]\,\{\rho^j\} = 0 \quad . \tag{2.91}$$

Since [S] is tridiagonal, (2.91) may be solved by a simple recursion formula

$$\rho_{i+1}^j = \left[(\omega_j^2 - s_{i,i})\,\rho_i^j - s_{i-1,i}\,\rho_{i-1}^j\right] \Big/ s_{i,i+1}$$

$$i = 1,2,\ldots,Q \tag{2.92}$$

in terms of ρ_1^j; $\rho_0^j = 0$. $\rho_{Q+1}^j = 0$ is a check on the computation.

The eigenvalues of [S], [A] and $[M]^{-1}$ [K] are identical. The eigenvectors $\{\phi\}$ of $[M]^{-1}$ [K] are obtained from Equations (2.78) and (2.85):

$$\{\phi\} = [M]^{-\frac{1}{2}}\,[T]\,\{\rho\} \quad . \tag{2.93}$$

CHAPTER III

BUILDINGS WITH SYMMETRIC SETBACKS

INTRODUCTION

The effect of a symmetric setback in a building upon its uncoupled translational vibration is examined in this chapter. Conditions for the uncoupling of the translational vibrations in the direction considered from other components of vibration are assumed to exist. Two models are used: (a) a rectangular cantilever shear beam stepped at one location along its height, and (b) a lumped mass model based on the assumption that mass is lumped at floor levels in buildings. Simple coupling in stiffness is assumed in the latter model, i.e., the massless springs are assumed to connect only the adjacent masses and only one mass to the ground. This assumption is often termed as the "shear building" assumption.

The setback is represented by two parameters, the level of setback and the degree of setback. In the case of the shear beam the degree of setback is defined as the ratio of plan area in the tower portion to that in the base portion. In the case of lumped mass model the mass lumped at all floor levels in each part of the structure is assumed to be constant; the ratio of the mass value of the tower portion to that in the base portion is then termed the degree of setback.

The effect of changes in these parameters on the modal properties of the two models are examined. Approximate reponses of the shear beam are computed and the effect of setback on the responses is studied. Actual maximum responses of the lumped mass model to two strong-motion earthquake records (El Centro 1940, S, and Taft 1952, N69°W) are also computed and examined for the effect of setback. Finally, the effect of

setback on shear coefficients as obtained from these responses are compared with that obtained from the specifications for buildings with setbacks in one of the seismic building codes currently (1966) in effect.

SHEAR BEAM

The uncoupled translational vibration of a vertical cantilever shear beam of rectangular section stepped at one location along its height is considered here. A general description of such a beam is given in the Appendix. Here it is assumed that the step is such that the translational vibration in the direction considered is uncoupled from other vibrations,(i.e., e_1 and/or e_2 equal to zero).

Equation of Motion and Solution

In Figure 3.1 is shown a stepped shear beam with setback symmetric about x axis. Notations used here are the same as those defined in the Appendix. The equation of motion for vibration in the x direction may be written as

$$mu_{,tt} - ku_{,zz} = f(z,t) \qquad (3.1)$$

where $u(x,t)$ is the displacement of centroid in the x direction, m is the mass per unit length, k the stiffness per unit length and f is the external force per unit length acting on the beam in the z direction; t is the time coordinate. Subscripts after a comma denote differentiation with respect to that variable.

Equation (3.1) is the first ($i = 1$) of the three equations derived in the Appendix, Equation (A.7); here the subscripts have been dropped and x_1 is replaced by u .

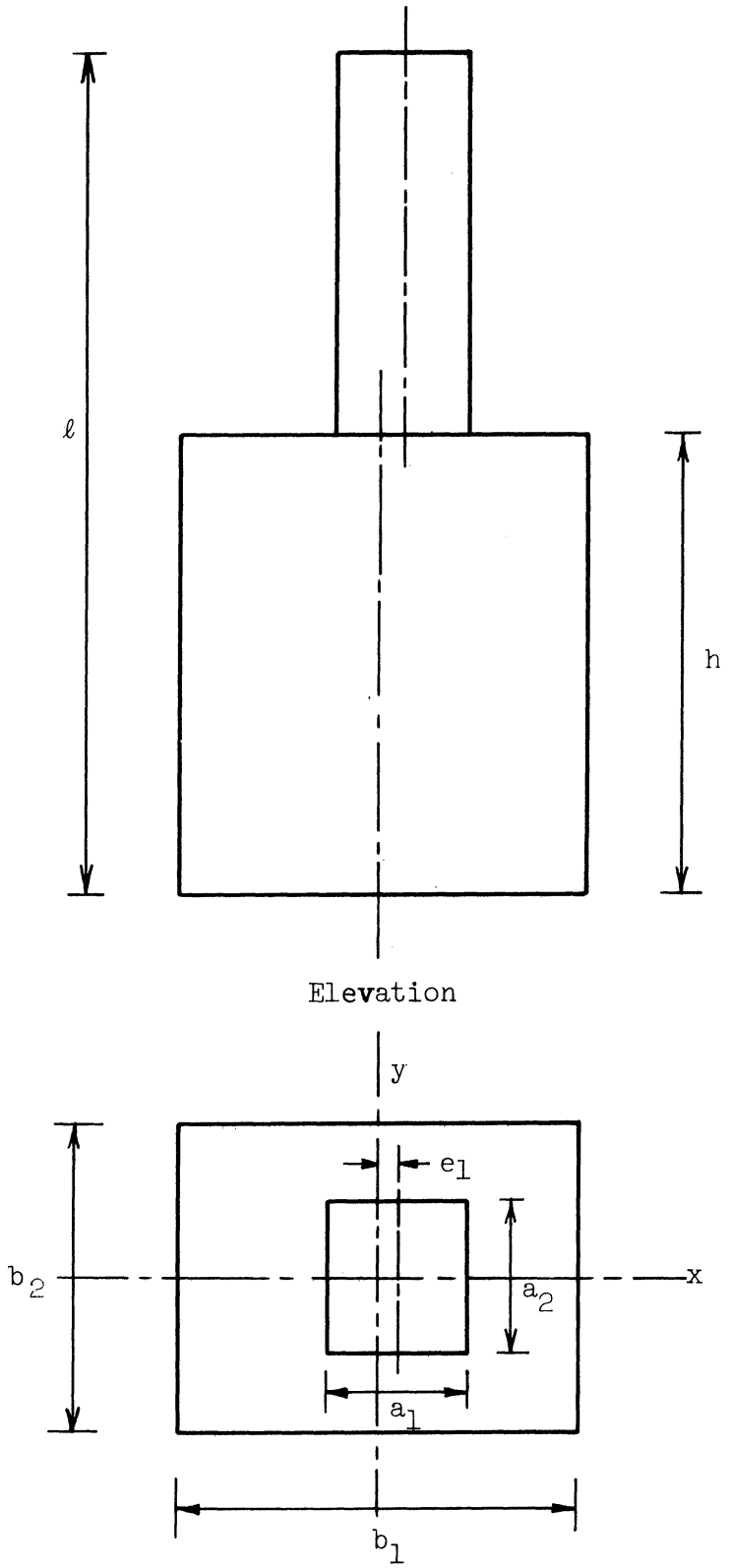

Figure 3.1. Stepped Shear Beam with Setback Symmetric About x-axis.

The inertia coefficient m and stiffness coefficient k in Equation (3.1) have different values in the base portion ($0 < z < h$) and the tower portion ($h < z < \ell$) of the beam. From Equations (A.5) and (A.6), (with i = 1)

$$\text{(in } 0 < z < h\text{)}$$

$$\begin{aligned} m &= \rho\, b_1 b_2 \\ k &= G\, b_1 b_2 \end{aligned} \tag{3.2}$$

and

$$\text{(in } h < z < \ell\text{)}$$

$$\begin{aligned} m &= \rho\, a_1 a_2 \\ k &= G\, a_1 a_2 \end{aligned} \tag{3.3}$$

The boundary conditions are

$$u(0, t) = 0 \tag{3.4}$$

$$V(\ell, t) = 0 \tag{3.5}$$

and the conditions at the step are

$$u(h - 0, t) = u(h + 0, t) \tag{3.6}$$

and

$$V(h - 0, t) = V(h + 0, t) \tag{3.7}$$

where V is the resultant shear force on horizontal cross section and is given by

$$V(z, t) = GAu_{,z} \tag{3.8}$$

where A is the area of cross section.

Equations (3.4) and (3.5) are first (i = 1) of Equations (A.9) and (A.10); Equations (3.6) and (3.7) are first of Equations (A.11) and (A.12), the latter with $e_2 = 0$.

Equation (3.1) can be solved by the method of separation of variables used for the set of three simultaneous equations (A.7) for the general unsymmetric ($e_1 \neq 0$, $e_2 \neq 0$) shear beam in Appendix A. The solution may be written in the form

$$u(z, t) = \sum_{k=1}^{\infty} \phi_k (z) \cdot \eta_k (t) \tag{3.9}$$

where $\phi_k (z)$ is the kth mode shape and $\eta_k (t)$ is the kth modal displacement. $\eta_k (t)$ is given by the equation

$$\ddot{\eta}_k + 2\beta_k \omega_k \dot{\eta}_k + \omega_k^2 \eta_k = g_k(t) \ , \ k = 1,2,... \tag{3.10}$$

where ω_k is the frequency of the kth mode and $g_k(t)$ is given by

$$g_k(t) = \frac{\int_0^{\ell} f(z,t)\, \phi_k dz}{\int_0^{\ell} m\, \phi_k^{\,2}\, dz} \ . \tag{3.11}$$

When the beam is subjected to earthquake acceleration $\ddot{x}_o$,

$$f(z, t) = - m\, \ddot{x}_o(t) \tag{3.12}$$

and

$$g_k(t) = - \lambda_k \cdot \ddot{x}_o(t) \tag{3.13}$$

where

$$\lambda_k = \frac{\int_0^{\ell} m\, \phi_k\, dz}{\int_0^{\ell} m\, \phi_k^{\,2} dz} \tag{3.14}$$

λ_k is known as the modal participation factor of the kth mode.

In Equation (3.10) β_k is the fraction of critical damping in the kth mode. The term in Equation (3.10) containing β_k has been added on the assumption that viscous damping exists and that the undamped modes remain valid for the damped case as well.

The mode shapes ϕ_k are given by (see Equations (A.20) and (A.21))

$$\begin{aligned} \phi_k &= C_{1k} \sin \frac{\omega_k z}{q} && 0 < z < h \\ &= C_{2k} \cos \frac{\omega_k z}{s} + C_{3k} \sin \frac{\omega_k z}{s} && h < z < \ell \end{aligned} \tag{3.15}$$

in which

$$\begin{aligned} q^2 &= \frac{m}{k} && 0 < z < h \\ s^2 &= \frac{m}{k} && h < z < \ell \end{aligned} \tag{3.16}$$

From Equations (3.2) and (3.3) it is seen that

$$q = s = \sqrt{\frac{G}{\rho}} \tag{3.17}$$

In the Appendix it is shown that the boundary conditions and conditions at the step, when applied to Equation (A.20), lead to Equations (A.21) and (A.22). The matrix Equation (A.22) can be solved for C_{ij}'s for those values of ω for which the determinant of the coefficient matrix is zero. Such values of ω are the frequencies and the corresponding C_{ij} give the corresponding mode shapes of the general unsymmetric shear beam. Here it has been assumed that $e_2 = 0$, and the first three equations are then equations in C_{11}, C_{12}, and C_{13}, and are uncoupled from the remaining six equations. Dropping the first subscript, 1, from the C_{ij}'s these equations are

$$\begin{bmatrix} 0 & \sin \frac{\omega \ell}{s} & \cos \frac{\omega \ell}{s} \\ -\sin \frac{\omega h}{q} & \cos \frac{\omega h}{s} & \sin \frac{\omega h}{s} \\ b_1 b_2 \cos \frac{\omega h}{s} & a_1 a_2 \sin \frac{\omega h}{s} & -a_1 a_2 \cos \frac{\omega h}{s} \end{bmatrix} \begin{Bmatrix} C_1 \\ C_2 \\ C_3 \end{Bmatrix} = \begin{Bmatrix} 0 \\ 0 \\ 0 \end{Bmatrix} \tag{3.18}$$

Equation (3.18) may be derived directly by considering vibration in the x direction alone of the shear beam symmetric about the x axis (i.e. $e_2 = 0$), which is under consideration here. For such a shear beam, the values of ω for which the determinant of the coefficient matrix in (3.18) is zero are the natural frequencies of vibration, ω_k, and the values of C_1, C_2, and C_3 determined from (3.18) for these values of ω give the coresponding mode shapes ϕ_k, k = 1, 2, 3, ...

Let

$$c = \frac{a_1 a_2}{b_1 b_2} \tag{3.19}$$

$$p = \frac{h}{\ell} \tag{3.20}$$

and

$$\omega' = \frac{\omega \ell}{q} = \frac{\omega \ell}{s} \tag{3.21}$$

noting that $q = s$ (Equation (3.17)). Expanding the determinant of the matrix in Equation (3.18) and using the notations introduced in Equations (3.19), (3.20) and (3.21), one gets the frequency equation

$$\begin{aligned} f(\omega') \equiv\ & c \sin \omega' p \sin \omega' (1-p) \\ & - \cos \omega' p \cos \omega' (1-p) = 0 \end{aligned} \tag{3.22}$$

The zeros of $f(\omega')$, the frequencies of the system, were found by simple interpolation. Only the few smallest positive frequencies are of interest since the lower modes of vibration are the modes of primary importance in structural response.

Since Equations (3.18) is a linear homogeneous set of equations they cannot be solved uniquely for C_j's for a given frequency. To assign numerical values to C_j's some normalization is therefore necessary. If the mode shapes are normalized by making $\phi(\ell) = 1$, the following solution may be obtained for the C_j's from Equation (3.18)

$$
\begin{aligned}
C_{1k} &= \frac{\cos \omega'_k(1-p)}{\sin \omega'_k p} \quad \text{if} \quad \sin \omega'_k p \neq 0 \\
&= \frac{c \sin \omega'_k(1-p)}{\cos \omega'_k p} \quad \text{if } \cos \omega'_k p \neq 0 \\
C_{2k} &= \cos \omega'_k \\
C_{3k} &= \sin \omega'_k
\end{aligned}
\tag{3.23}
$$

where $f(\omega'_k) = 0$. From Equation (3.15) it can be checked that

$$
\begin{aligned}
\phi_k(\ell) &= C_{2k} \cos \frac{\omega'_k \ell}{s} + C_{3k} \sin \frac{\omega'_k \ell}{s} \\
&= \cos^2 \omega'_k + \sin^2 \omega'_k \\
&= 1
\end{aligned}
$$

Parameters Representing the Setback

Two assumptions that have been made implicitly in the shear beam model of a building with setback that is used here should be pointed out:

a. Values of the mass per unit length and stiffness per unit length in each part of the structure (the base portion and the tower portion) are assumed to be constant.

b. The mass and stiffness of the tower are both in the same proportion to the mass and stiffness in the base, i.e.

$$\frac{m_t}{m_b} = \frac{k_t}{k_b} \frac{a_1 a_2}{b_1 b_2} = c \qquad (3.24)$$

where m_t , k_t are the mass per unit length and stiffness per unit length in the tower and m_b , k_b are corresponding values in the base. This is seen from Equations (3.2), (3.3), and (3.19).

With these assumptions only two parameters (see Equations (3.22) and (3.23)) represent the setback insofar as the uncoupled translational vibrations are concerned. These are:

a. The level of setback which may be represented by p as defined in Equation (3.20);

and

b. what may be termed as the "degree" of setback represented by c as defined in Equation (3.19); the significance of c as seen in Equation (3.24) is also important.

The ranges of possible variation of the two parameters are $0 \leq p \leq 1$ and $0 \leq c \leq 1$. The values $p = 1$ and $c = 1$, each by themselves, represent a uniform beam regardless of the value of the other parameter. The value $p = 0$ also represents a uniform shear beam, the cross section depending on the value of c . The value $c = 0$ represents no real physical beam. However, it is taken here to represent the extreme case of beam with a tower section infinitely small compared to its base section. The value $c = 0$ should not be interpreted as representing a uniform beam of height h .

Periods

Periods for the first four modes are plotted (Figure 3.2) as functions of c for various values of p. From Equation (3.22) it is obvious that frequencies are equal for beams with $p = p'$ and $p = 1-p'$. The values $p = 0$ and $p = 1$ represent uniform beams and so does $c = 1$. The periods have been non-dimensionalized,

$$T' = \frac{2\pi}{\omega'} = \frac{2\pi}{\omega} \cdot \frac{s}{\ell} = T \frac{\ell^2 p}{G} \tag{3.25}$$

The periods for the case $c = 0$ were obtained by letting $c = 0$ in Equation (3.22), i.e. from

$$\cos \omega' p \cos \omega' (1-p) = 0 \tag{3.26}$$

which requires that

$$\cos \omega' p = \cos \frac{\omega h}{q} = 0$$

or

$$\cos \omega' (1-p) = 0 = \cos \frac{\omega(\ell-h)}{s} = 0 \tag{3.27}$$

Equations (3.27) are the frequency equations of uniform cantilever shear beams of height h and $(\ell-h)$ i.e. of the base portion and the tower portion acting separately as cantilever beams. Frequencies of these two beams are combined together and numbered in the usual ascending order of their magnitude. It is this combined set of frequencies that is used for the periods plotted in Figure 3.2 of case $c = 0$. Two modes with equal frequencies are possible for certain values of p when $c = 0$ (e.g., for modes 1 and 2,3 and 4 etc., for $p = .5$).

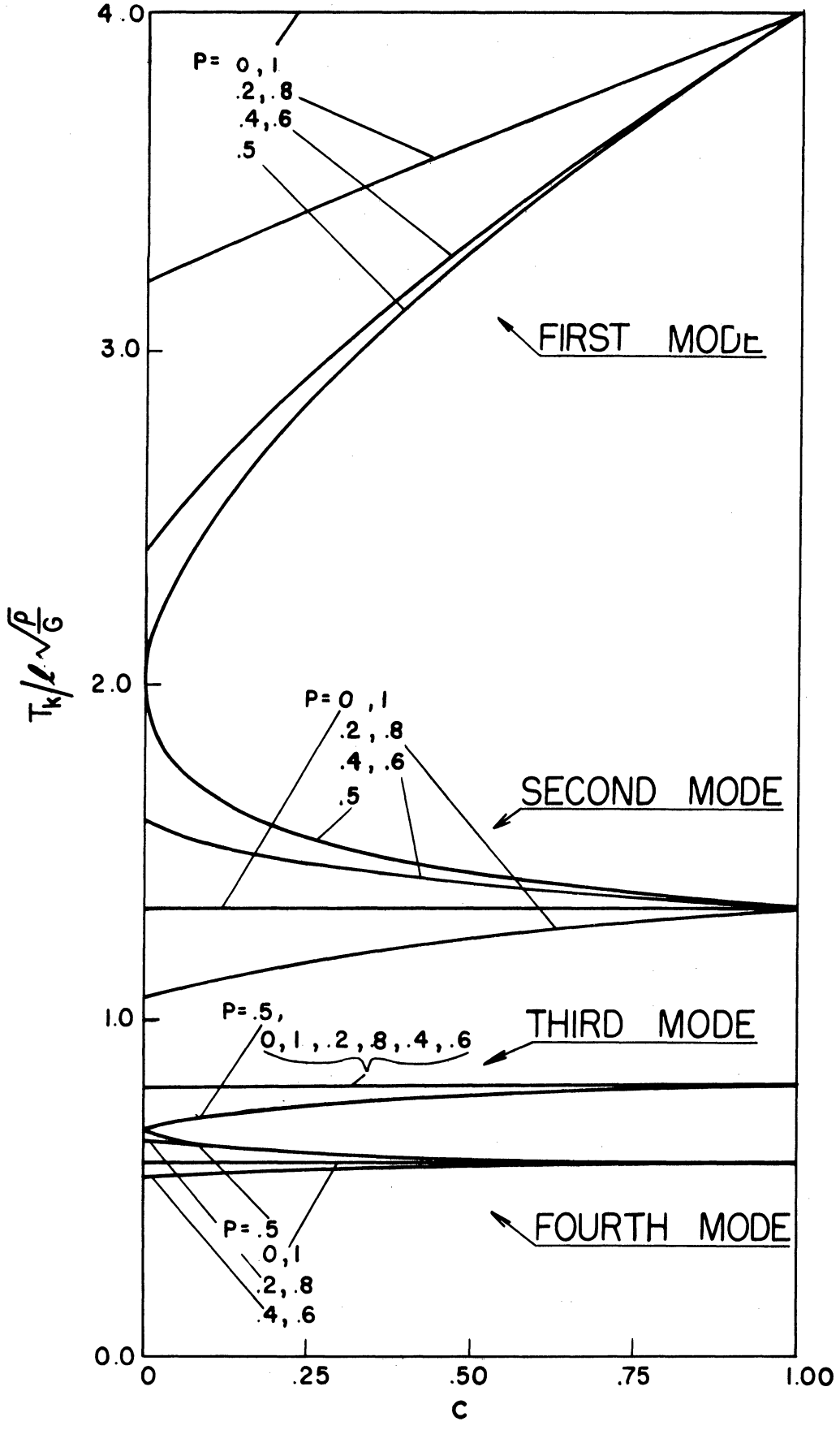

Figure 3.2. Fundamental and Higher Mode Periods, Shear Beam.

The following observations may be made from Figure 3.2. The first mode period decreases monotonically as the tower cross section decreases relative to the base cross section, i.e. as c decreases from 1 to 0. The influence of a variation in c is maximum when the setback level is exactly at midheight, i.e. when $p = .5$, and diminishes as the setback level is moved towards either end.

For any fixed value of p, the higher mode periods are monotonic functions of c. Whether they increase or decrease with c, or remain constant, depends upon the value of p. The influence of a variation of c on the higher mode periods is smaller than its influence on the first mode period.

The third mode period remains constant with varying c for shear beam with setback levels at $p = .2, .4, .6$, and $.8$ (and also for the trivial cases $p = 0$ and 1), see Figure 3.2. For other modes there are other values of p for which the period will remain independent of c. It is easy to see that these setback levels p should be such that the natural frequency of the particular mode for the uniform ($c = 1$) shear beam ($\omega' = (2k-1)\pi/2$, $k = 1,2,3,....$) will satisfy either

$$\sin \omega' p = \cos \omega'(1-p) = 0 \tag{3.28}$$

or

$$\cos \omega' p = \sin \omega'(1-p) = 0 \tag{3.29}$$

so that the frequency equation, Equation (3.22), is satisfied regardless of the value of c. That the particular values (viz. $p = .2, .4, .6$, and $.8$) chosen for study satisfy this condition for the third mode, which has a frequency $\omega'_3 = 5\pi/2$, is coincidental.

In Figure 3.3 the first four periods are given as functions of p for beams with $c = .25$. For each mode the horizontal line is drawn to represent the corresponding mode period of the uniform beam ($c = 1$). It was noted from Figure 3.2 earlier that the change in periods with c for a beam with a given level of setback p is monotonic. Hence Figure 3.3 provides information about the range of levels of setback for which the period of a stepped beam ($c < 1$) in a given mode will be always greater than or always smaller than the corresponding mode period of the uniform beam. Thus, for example, the second mode periods of stepped beams with a level of setback p such that $0 < p < 1/3$ or $2/3 < p < 1$ will always be smaller than that of the second mode of the uniform beam. Further, the points at which the graph of T'_k ($c = .25$) cuts the horizontal line representing the uniform beam period are the values of p in the particular mode for which the periods are independent of c.

In the above discussion the stiffness to mass ratio (G/ρ) has been assumed to remain constant as p and c change. However, even if this assumption is not made, the plots in Figure 3.2 indicate, in general, a significant reduction in the ratios of fundamental period to higher mode periods for buildings with slender towers ($c \ll 1$) compare with those of the uniform beam. In fact it can be shown that these ratios will always either decrease or remain constant as c decreases.

Mode Shapes

The first four natural mode shapes of beams with varying levels of setback, p, and degrees of setback, c, are given in Figure 3.4. Corresponding modes of beams with degrees of setback, $c = 1, .5, .25,$ and 0 ($.00625$ for $p = .5$) but having the same setback level, are drawn

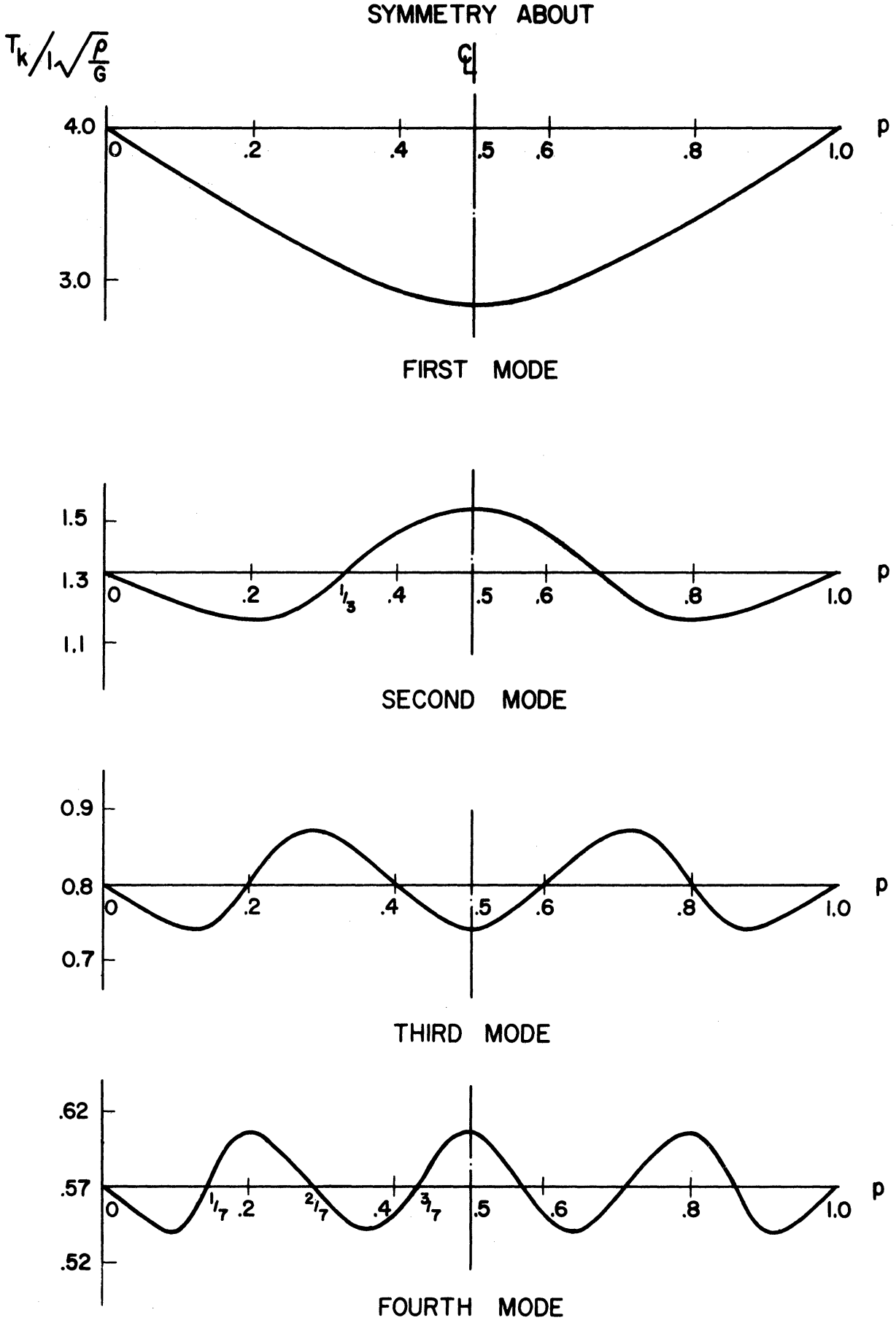

Figure 3.3. Periods Vs. Setback Level. (c = 0.25)

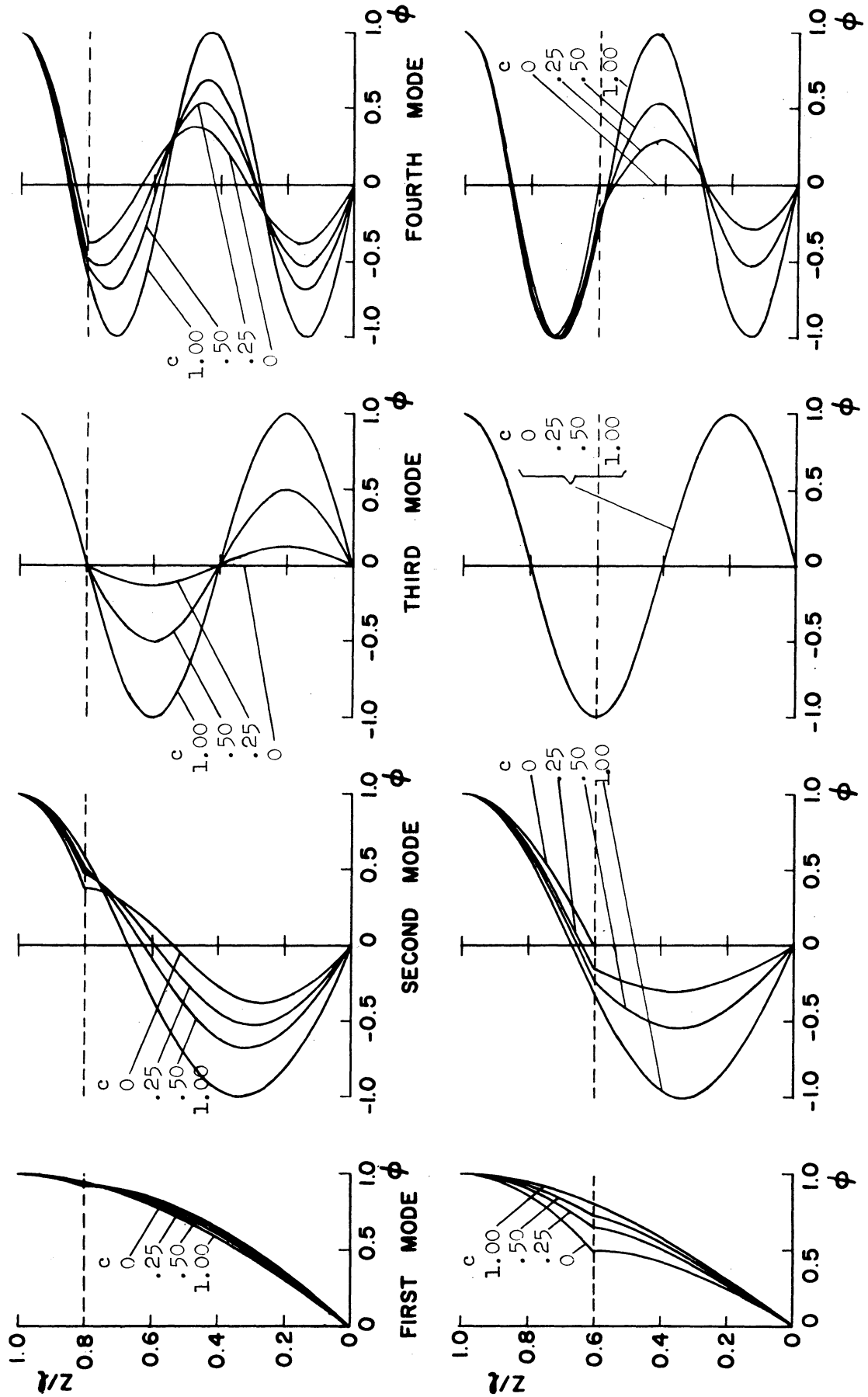

Figure 3.4. Mode Shapes, Shear Beam. Above: p=.8, Below: p=.6.

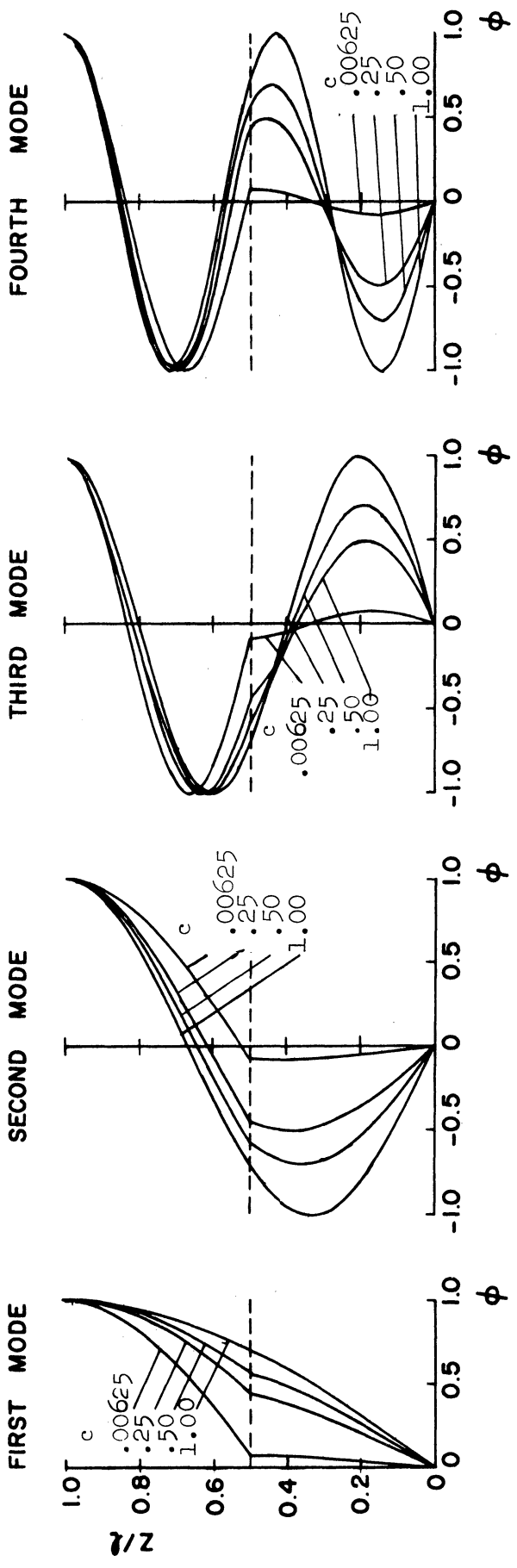

Figure 3.4. (Cont'd.) Mode Shapes, Shear Beam. p=.5

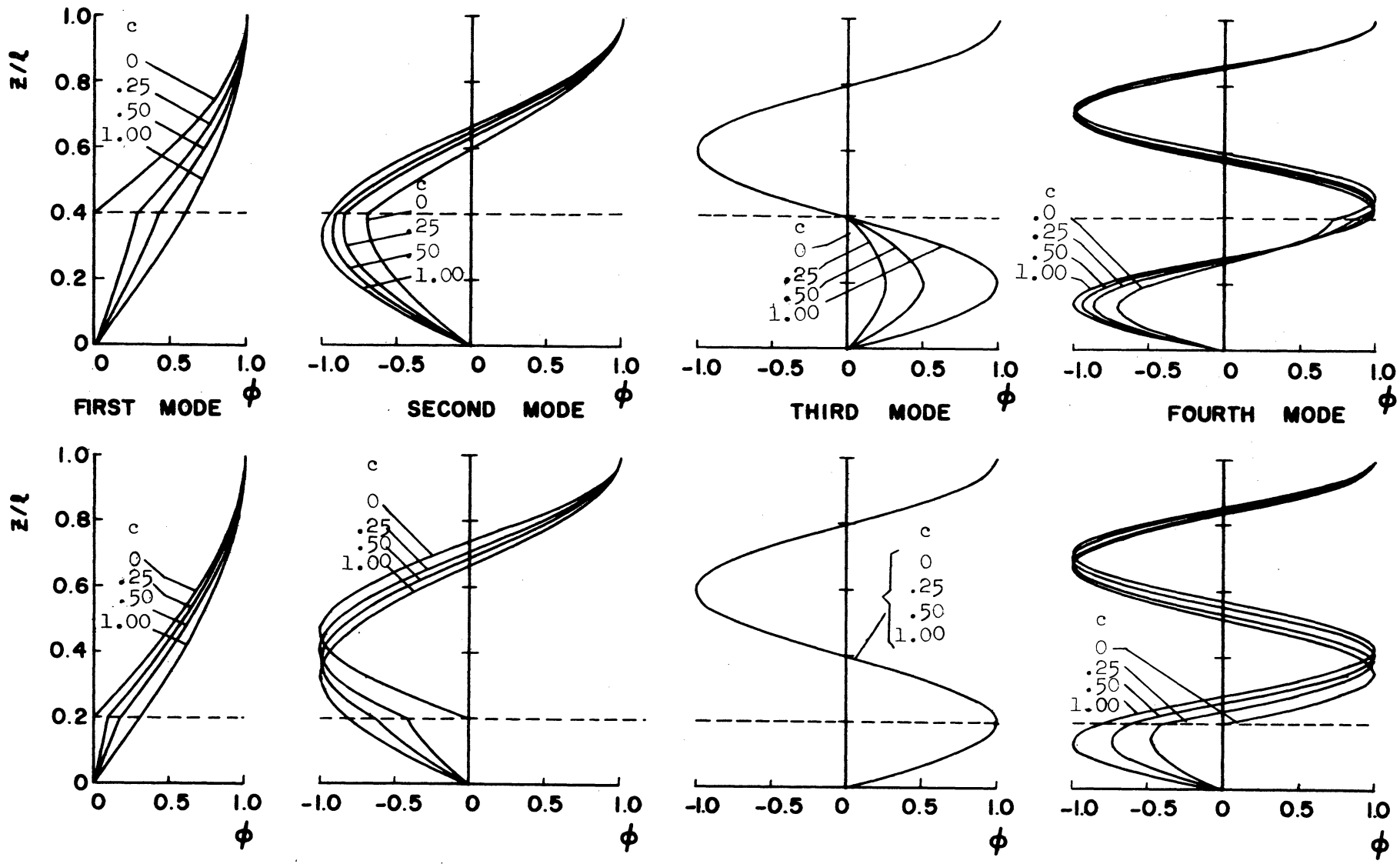

Figure 3.4. (Cont'd.) Mode Shapes, Shear Beam. Above: p=.4, Below: p=.2.

on the same plot; this is done for five values of p, viz.,.8, .6, .5, .4, and .2. The mode shapes have been normalized by fixing the displacement at the top of the beam, $(z = \ell)$, equal to 1.

For any value of p, the case $c = 0$ may be looked upon as representing the extreme case of beam with a tower section infinitely small relative to its base section. The frequencies for such a case are computed by using Equation (3.27) as explained earlier. The corresponding mode shapes are computed by using Equations (3.23) with $c = 0$ and Equation (3.15).

It was shown earlier that the natural frequency of any mode of a beam with setback at $c = 0$ is equal to a frequency of either the tower portion or the base portion, or both in special cases like $p = .5$, each acting alone as a uniform cantilever shear beam. It is possible to make the following interpretation of the mode shapes for the case $c = 0$. As $c \to 0$ if the kth frequency of the entire beam approaches the jth frequency of the tower (acting alone), then the tower portion of the kth mode shape is identical to the jth mode shape of the tower and there is no motion in the base portion. However, if, as $c \to 0$, the kth frequency of the beam approaches the jth frequency of the base (acting alone), then the base portion of the kth mode shape is identical to the jth mode shape of the base; and the tower portion of the kth mode shape is the steady state response amplitude (absolute displacement) of the tower to a periodic base motion of period $(2\pi / \omega'_k)$ and amplitude $\phi_k(p)$, neglecting damping. (The latter statement is true of course regardless of the value of c.).

Except for the third mode shapes of beams with setback level $p = .6$ and $.2$, an abrupt change in slope is apparent in all the four mode shapes of all beams with $c \neq 1$. This can be explained by recalling the condition that the shear force just above the setback level, $V(h+0)$, must be equal to the shear force just below the setback level, $V(h-0)$. This is the equilibrium condition at the step, Equation (3.7), which also holds for each mode individually. This condition requires that, for any natural mode shape ϕ,

$$\frac{\phi_{,z}(h-0)}{\phi_{,z}(h+0)} = \frac{a_1 a_2 G}{b_1 b_2 G} = c \qquad (3.32)$$

Thus the ratio of slopes of mode shapes just above and just below the setback is equal to the degree of setback c and is different from 1 whenever $c \neq 1$. However, for some cases the slope in the mode shape at the setback may be equal to zero and remain unaffected by c. This is what happens for the third mode shapes of beams with setback level $p = .6, .2$.

Earlier it was shown that if either of Equations (3.28) and (3.29) is satisfied for some frequency of a beam with a given level of setback p, then that frequency will be independent of the degree of setback c. When such is the case it can be seen from Equation (3.23) that C_2 and C_3, and hence the mode shape in the tower part ($h < z < \ell$) given by Equation (3.15), would also be independent of c. This is indeed the case for the third mode shapes for beams with $p = .2, .4, .6$, and $.8$ for which one of the Equations (3.28) and (3.29) is satisfied. Further,

from the first of Equation (3.15)

$$\phi_{,z}(h\text{-}0) = \omega' C_1 \cos \omega' p \qquad (3.33)$$

where $\omega' = \omega\ell/q$ and $p = h/\ell$. If Equation (3.29) is satisfied for some ω' and p , then $\cos \omega' p = 0$ or

$$\phi_{,z}(h\text{-}0) = 0 .$$

For $p = .6$ and $.2$, Equation (3.29) holds for the third mode frequency $\omega' = (5\pi)/2$. For these cases the entire mode shapes remain unaffected by changes in c , see Figure 3.4.

Modal Shear Coefficients

An important quantity used in the design of buildings for earthquake resistance is the shear at the base of buildings, generally known as the base shear. In buildings with setback the shear at the base of towers will also be of importance. The base shear and the tower-base shear in the first four modes of the stepped beam, when subjected to earthquake ground acceleration $\ddot{x}_o$, will therefore be examined.

From Equations (3.8) and (3.9) the base shear in the kth mode is:

$$V_k(0, t) = GA \phi_{k,z} (0) \eta_k(t) \qquad (3.34)$$

It may also be written as the summation of inertia forces over the height of beam,

$$V_k(0, t) = \left(\int_0^{\ell} m\phi_k dz \right)\left(\ddot{\eta}_k(t) + \lambda_k \ddot{x}_o (t)\right) \qquad (3.35)$$

although this is an approximation when damping exists. The kth modal displacement η_k is given by Equation (3.10) with Equation (3.13) used for $g_k(t)$:

$$\ddot{\eta}_k + 2\beta_k\omega_k\dot{\eta}_k + \omega_k^2\eta_k = - \lambda_k \ddot{x}_o(t) \tag{3.36}$$

Since Equation (3.36) is linear and λ_k is independent of time, t , one can write

$$\eta_k = \lambda_k \xi_k \tag{3.37}$$

where ξ_k is the response of a one degree of freedom oscillator with frequency ω_k and fraction of critical damping β_k subjected to base acceleration $\ddot{x}_o(t)$:

$$\ddot{\xi}_k + 2\beta_k\omega_k\dot{\xi}_k + \omega_k^2 \xi_k = - \ddot{x}_o(t) \tag{3.38}$$

Equation (3.35) then becomes

$$V_k(0, t) = \lambda_k \left(\int_o^\ell m \phi_k dz\right) (\ddot{\xi}_k(t) + \ddot{x}_o(t))$$

and the base shear per unit weight or the base shear coefficient is given by

$$\begin{aligned} C_{Bk}(t) &= \frac{V_k(0, t)}{g \int_o^\ell m \, dz} \\ &= \lambda_k \frac{\int_o^\ell m \phi_k dz}{\int_o^\ell m \, dz} \; (\ddot{\xi}_k(t) + \ddot{x}_o(t))/g \end{aligned} \tag{3.39}$$

in which g is the acceleration due to gravity.

Similarly it can be shown that the ratio of tower-base shear to the weight of tower, i.e., the tower-base shear coefficient, in the kth mode is given by

$$C_{Tk} = \lambda_k \frac{\int_h^\ell m \phi_k dz}{\int_h^\ell m \, dz} (\ddot{\xi}_k(t) + \ddot{x}_o(t))/g \qquad (3.40)$$

The term $(\ddot{\xi}_k(t) + \ddot{x}_o(t))$ in the above equations is the absolute acceleration of the oscillator described by Equation (3.38). It varies with time, t , and is dependent on the earthquake ground acceleration $\ddot{x}_o(t)$ to which the oscillator is subjected.

In Equations (3.39) and (3.40), the terms

$$C'_{Bk} = \lambda_k \frac{\int_o^\ell m \phi_k dz}{\int_o^\ell m \, dz} \qquad (3.41)$$

and

$$C'_{Tk} = \lambda_k \frac{\int_h^\ell m \phi_k dz}{\int_h^\ell m \, dz} \qquad (3.42)$$

are independent of the earthquake ground motion. They are the base shear and tower-base shear coefficients in the kth mode of a beam subjected to a one g static acceleration[26] , (i.e. of a beam subjected to a static force per unit length equal to its weight per unit length over the entire height along the centroidal axis). The term λ_k in the above equations is the modal participation factor defined in Equation (3.14).

By substituting Equation (3.15) for ϕ_k in Equations (3.14), (3.41), and (3.42), and using Equation (3.22) for the coefficients C_2 and C_3, one may derive the following relations after integration and proper use of the boundary and other conditions:

$$\lambda_k = \frac{1}{\omega'_k} \cdot \frac{2C_{1k}}{C_{1k}^2\, p + c(1-p)} \tag{3.43}$$

$$C'_{Bk} = \lambda_k \cdot \frac{1}{\omega'_k} \cdot \frac{C_{1k}}{p + c(1-p)} \tag{3.44}$$

$$C'_{Tk} = \lambda_k \cdot \frac{1}{\omega'_k} \cdot \frac{C_{1k}\cos \omega'_k p}{c(1-p)} \tag{3.45}$$

Thus C'_{Bk} and C'_{Tk} and therefore the modal base shear and tower-base shear coefficients are, like other modal quantities such as periods, functions of level and degree of setback. C'_{Bk} and C'_{Tk} are plotted in Figures 3.5 and 3.6 as functions of the degree of setback, c, for several levels of setback p.

In Equations (3.43) - (3.45) either of the formulae for C_{1k} in Equation (3.23), whichever is applicable, is used. Values of C'_{Bk} and C'_{Tk} at $c = 0$ in Figures 3.5 and 3.6 were derived by substituting $c = 0$ or taking the limits as $c \to 0$ in Equations (3.43) - (3.45) and (3.23). The values $p = 0$ and $p = 1$ represent uniform beams regardless of the value of c. Hence C'_{Bk} does not change with c for these values of p. C'_{Tk} for beams with $p = 0$ is the same as C'_{Bk}, and for beams with $p = 1$, C'_{Tk} is always equal to zero.

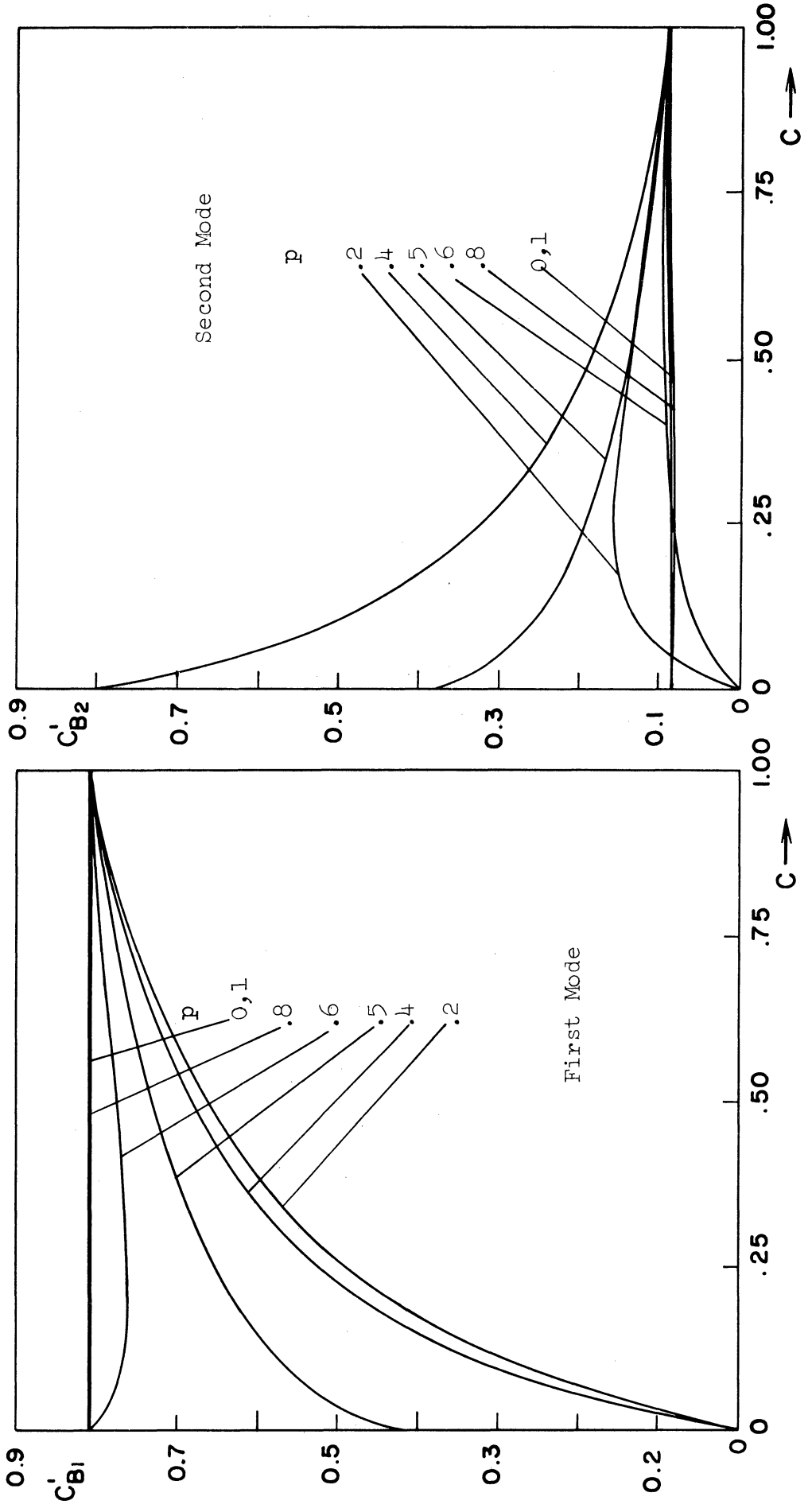

Figure 3.5. Modal Base Shear Coefficients, Shear Beam.

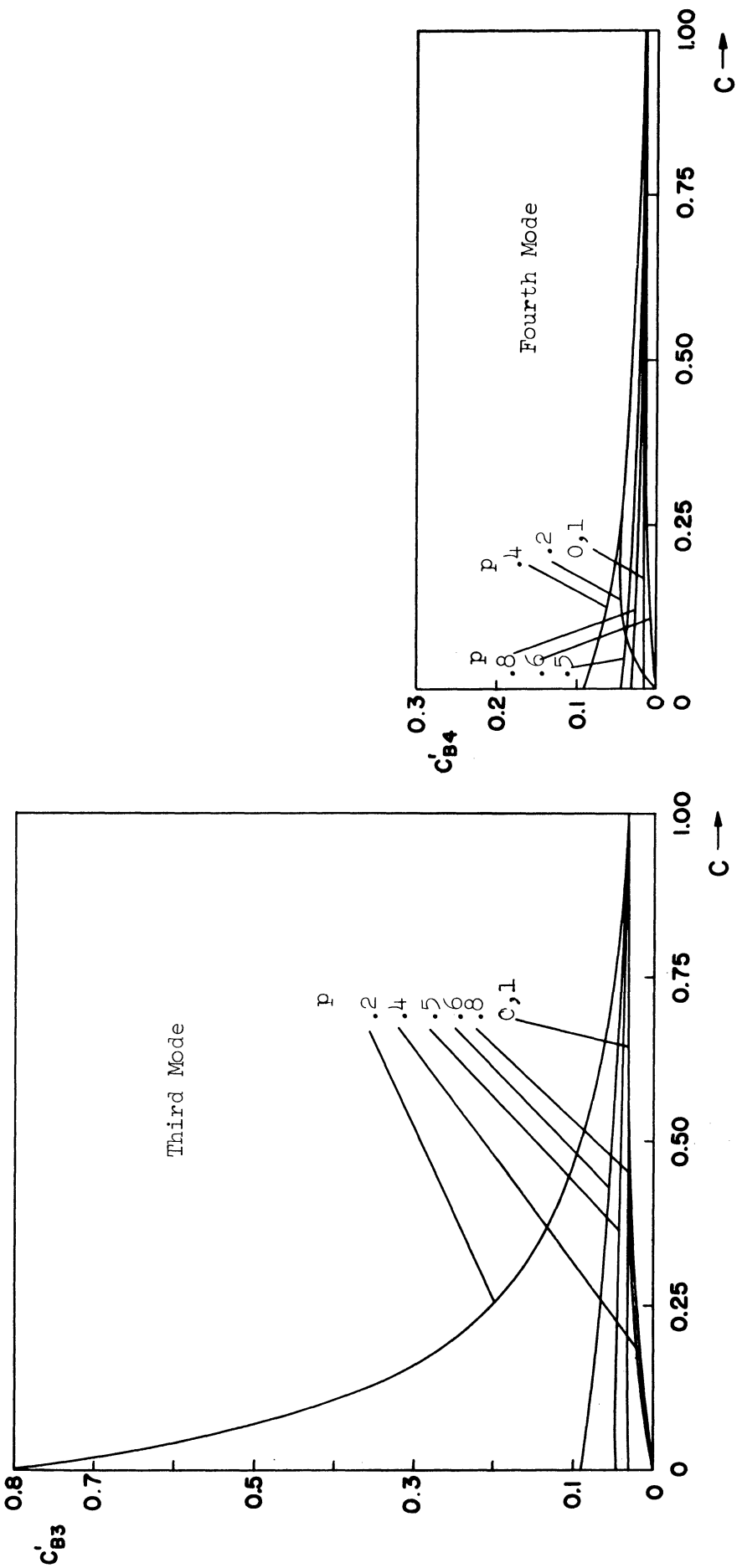

Figure 3.5(Cont'd). Modal Base Shear Coefficients, Shear Beam.

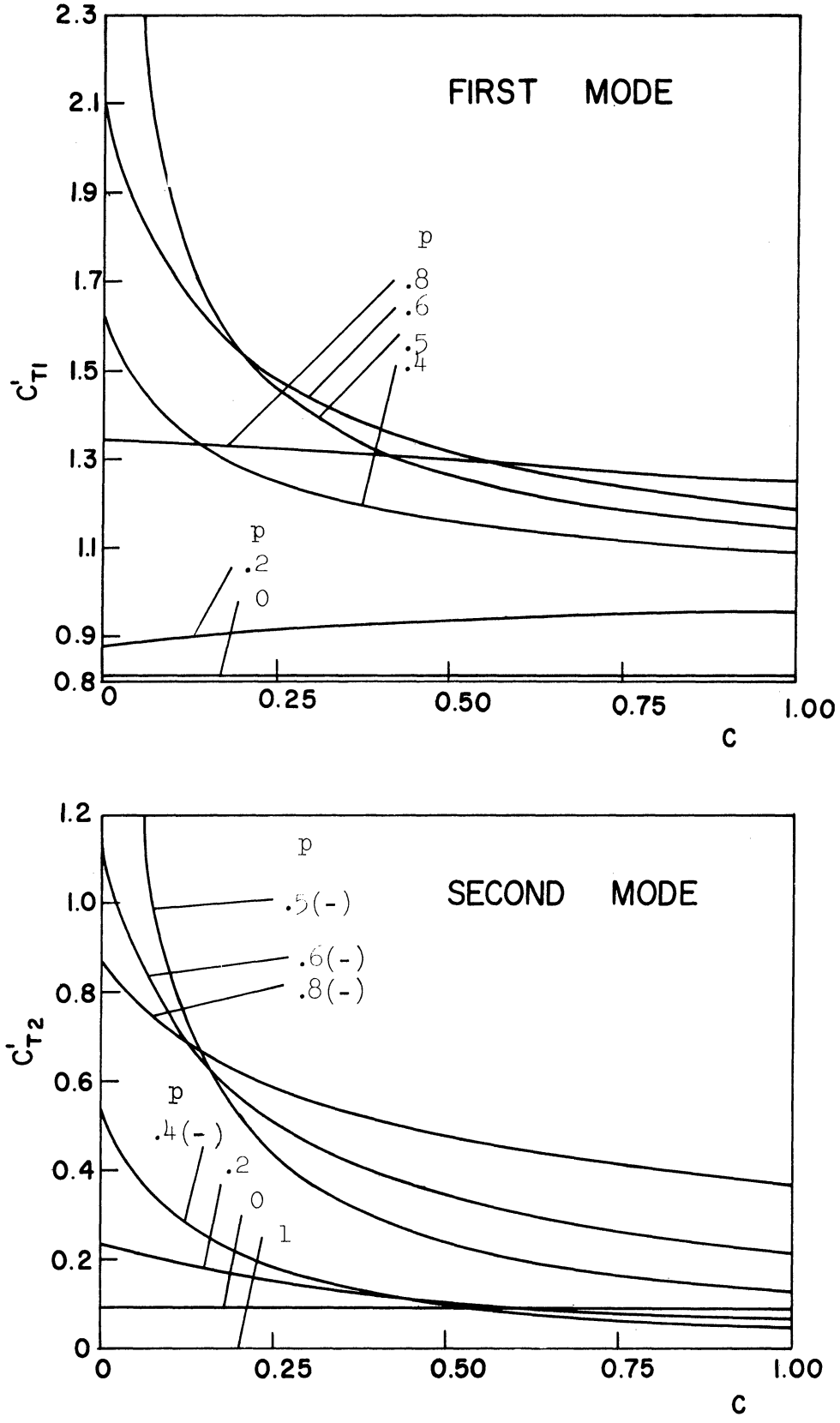

Figure 3.6. Modal Tower-base Shear Coefficients, Shear Beam.

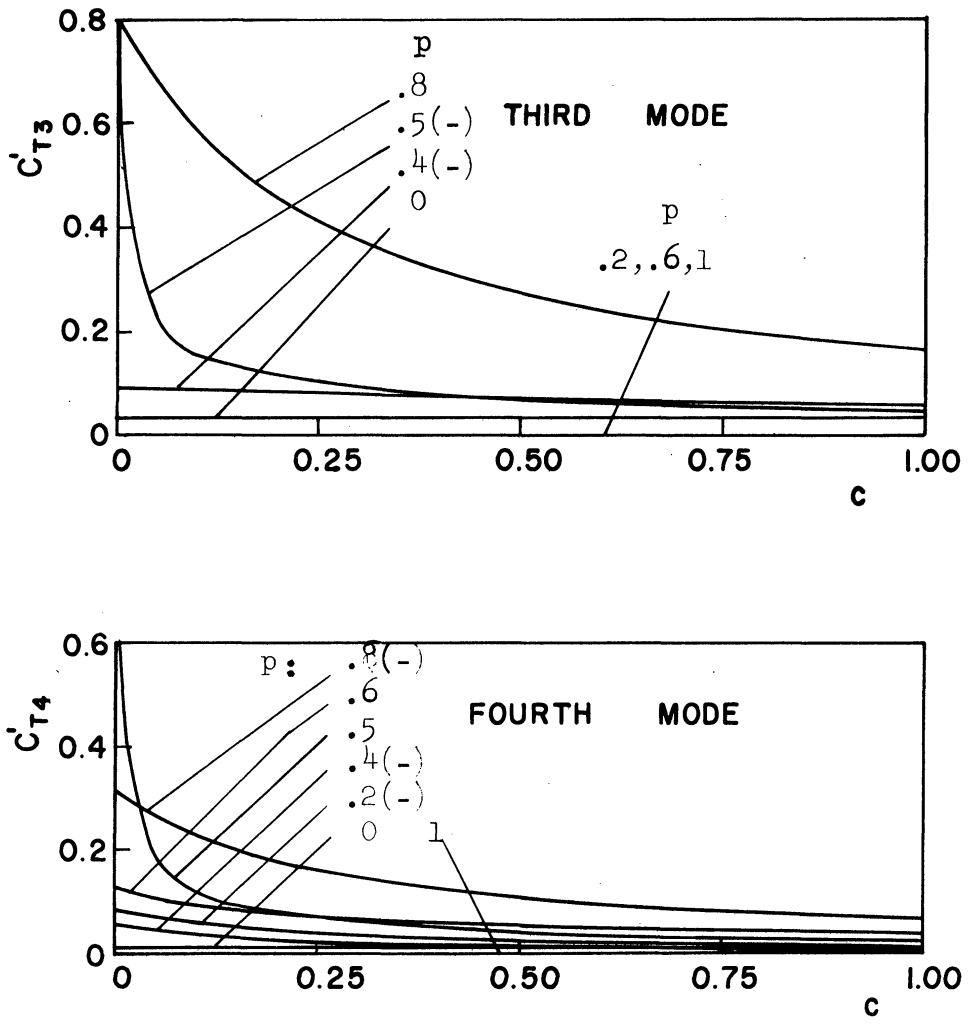

Figure 3.6. Cont'd.) Tower-base Shear Coefficients.

It was shown earlier that at $c = 0$ the frequencies of the stepped beam were equal to a frequency of either the tower portion or the base portion acting alone as a uniform cantilever shear beam. Further, if the kth frequency of the entire beam is equal to the jth frequency of the base portion acting alone, then the base portion of the mode shape of the entire beam is identical to the jth mode shape of the base; and the tower portion of the mode shape of the entire beam is identical to the response of the tower subjected to sinusoidal base motion of amplitude $\phi_k(p)$ and frequency ω_k. In this case the C'_{Bk} value of the whole beam is identical to C'_{Bj} value of the base acting alone, whereas the C'_{Tk} of the whole beam is the amplitude of base-shear coefficient response of the tower subjected to a sinusoidal base acceleration of amplitude $\lambda_k\phi_k(p)$ and frequency ω_k.

However, if the kth frequency of the entire beam is equal to the jth frequency of the tower, then the tower portion of the mode shape of the entire beam is identical to the jth mode shape of the tower; and there is no motion in the base portion (or if finite motion is assumed in the base portion then the amplitude of the motion in the tower portion tends to infinity). In this case C'_{Bk} is equal to zero whereas C'_{Tk} is in indeterminate $(\frac{0}{0})$ form. The limiting value of C'_{Tk} as $c \to 0$ can, however, be evaluated, and it is found to be always equal to or greater than the C'_{Bj} value of the tower, though no significance of such value is apparent.

For a beam with setback exactly at mid-height ($p = .5$) the frequencies of the base and the tower (each acting alone) are identical. Thus at $c = 0$ such a beam will have pairs of modes with identical frequencies, and the mode shapes will involve finite motions in the

tower portion and zero motion in the base portion or finite motion in the base portion and unbounded motion in the tower. The C'_B and C'_T values for such cases are indeterminate. When the limiting process is applied to Equations (3.44) and (3.45) it turns out that in each of the pair of modes with equal frequencies $C'_T \to \infty$ and C'_B values (in both modes) are equal to half the C'_B value of the corresponding mode of the base (or the tower). The unbounded increase in C'_{Tk} as $c \to 0$ can be considered as the effect of resonance since the frequencies of the base and the tower are identical, and the tower is subjected to sinusoidal base motions of frequencies equal to its natural frequencies.

There are other values of p (i.e. other than $p = .5$) for which some (but not all) frequencies of the base and the tower are identical. Such cases are not encountered in the results presented here. For such cases too, there are pairs of modes whose frequencies tend toward identical values as $c \to 0$. The observation made in the preceding paragraph hold for these pairs of modes also.

From Equations (3.38) - (3.42) it can be easily verified that C'_{Bk} and C'_{Tk} values are independent of the actual length and the cross-sectional area of the beam and the manner in which the mode shape is normalized. Thus the C'_{Bk} value of a uniform beam is the same regardless of its length, cross-sectional area, etc. Therefore the C'_{Bj} value of the base acting alone for a given j will be the same no matter what its height and will equal the C'_{Bj} value of the stepped beam with $c = 1$. Also, it may be observed from Figure 3.5 that for uniform beams ($c = 1$) $C'_{B1} > C'_{B2} > C'_{B3} > C'_{B4}$.

For a stepped beam with setback level below mid-height ($p < .5$) the base is smaller in height than the tower. The frequencies of a uniform beam are inversely proportional to its height. Thus when $p < .5$ the first mode frequency of the base is larger than at least the first mode frequency of the tower; and for sufficiently small p the first mode frequency of the base will be larger than the second or higher mode frequency of the tower. Keeping in mind that the modes are numbered so that $\omega_1 < \omega_2 < \omega_3 < .... < \omega_{n-1} < \omega_n ...$, for stepped beams with $p < .5$ it will be the second or higher mode frequency (of the whole beam) that will equal the first mode frequency of the base as $c \to 0$. Thus for such stepped beams (i.e. with $p < .5$) the C'_{Bk} value for one of the higher modes (i.e. for $k > 1$) will, in general, increase as c decreases and will equal C'_{B1} value of the uniform beam as $c \to 0$. (It may be noted again that C'_{Bk} values for a given k are the same for all uniform cantilever shear beams regardless of their height.) In Figure 3.5 it is seen that for beam with setback level $p = .4$ it is in the second mode and for beam with $p = .2$ it is in the third mode that C'_{Bk} ($k = 2$ and 3, respectively) increases, as $c \to 0$, to C'_{B1} value of the uniform beam; for smaller values of p it will be in still higher modes that this will happen.

For uniform beams ($c = 1$) C'_{B1} is much greater than C'_{Bk} in the higher modes and usually the first mode base shear will make up a large portion of the total base shear. However, as seen above as well as in Figure 3.5, for stepped beams with setback level below mid-height and $c \ll 1$ the C'_{Bk} value in one of the higher modes will be much larger than in the first mode, and this higher mode will therefore be the most significant one for base shear computation. Thus, if the base

shear for structures corresponding to such shear beams is computed by the method of modal analysis of the structure as a whole, higher modes must be taken into account. However, for such structures with tower very small in cross section compared to the base, the method of treating the base portion as a separate structure (that is used in the present day building codes) removes this problem and, as can be deduced from the observations made above for the shear beam, has a rational basis.

In the case of beams with setback above mid-height ($p > .5$) since the first mode frequency of the beam at $c = 0$ will be equal to the first mode frequency of the base portion the C'_{B1} value at $c = 0$ will remain the same as for the uniform beam. This is the case for $p = .6$ and $p = .8$ in Figure 3.5 although there is a small decrease in C'_{B1} for intermediate values of c. In the second or higher modes the C'_{Bk} values will either decrease to zero or tend to C'_{Bk} values of second or higher modes of uniform beams as $c \to 0$. C'_{Bk} values in second and higher modes are much less than that in the first mode for the uniform beam as moted earlier. Thus in the second or higher modes of beams with $p > .5$ C'_{Bk} will not increase much (if at all) as c decreases and consequently will not increase the importance of higher modes as far as base shear is concerned.

The C'_{Tk} values as computed by Equation (3.45) are negative for one or more higher modes for all beams with various levels of setback. However, the sign of C'_{Tk} does not change in any mode as c changes, the level of setback remaining fixed. In Figure 6 the minus sign is placed along with the values of p to indicate that C'_{Tk} values are negative for those cases.

The shear at the base of tower of beams with $p = .2$ and $.6$ happens to be zero in the third mode for all values of c.

As is seen in Figure 3.6, for all levels of setback, C'_{Tk} increases as c decreases in almost all modes. The increase is more for those beams with setback levels above mid-height than those with setback levels below mid-height. For a beam with setback level exactly at mid-height the increase in C'_{Tk} is unbounded in all modes as $c \to 0$. This was noted earlier as a resonance effect. The sign of C'_{Tk} alternates in successive modes for this case.

The maximum tower-base shear coefficient in the kth mode is a function of C'_{Tk} as well as the maximum absolute acceleration $(|\ddot{\xi}_k(t) + \ddot{x}_o(t)|_{max})$, which itself is a function of the kth natural period. The increase in C'_{Tk} for all levels of setback in almost all modes, therefore, suggests a possible increase in the tower-base shear coefficient response as c decreases for a given ground acceleration.

For almost all cases (of p), the increase in C'_{Tk} as c decreases seems to be confined at the left ($c = 0$) end of the plot in all four modes studied. This suggests that the possible increase in tower-base shear coefficient may be significant only for sturctures with very small tower section as compared to the base section, say with $c < .25$ approximately. Due to the nature of variation in C'_{Bk} with decreasing c in the four modes studied (Figure 3.5), the possible effects of decreasing c on base shear coefficient are not at all obvious.

Approximate Combined Maximum Responses

The response of a structure subjected to earthquake excitation varies with time. For design purposes only the absolute maximum values

of the response are of interest. In Equations (3.39) and (3.40) for the base shear coefficient and tower-base shear coefficient, the term $(\ddot{\xi} + \ddot{x}_o)$ is the one that varies with time. The maximum value that this term will take on for a given earthquake excitation $\ddot{x}_o(t)$, is dependent on the frequency ω_k and the fraction of critical damping β_k ; this is obvious from Equation (3.38). They symbol $S_a(\beta, \omega)$ is commonly used to denote the maximum value of the absolute acceleration $(\ddot{\xi} + \ddot{x}_o)$ of an oscillator with frequency ω and fraction of critical damping β subjected to earthquake ground acceleration $\ddot{x}_o$, i.e.

$$S_a(\beta, \omega) = \left| \ddot{\xi}(t) + \ddot{x}_o(t) \right|_{max} \qquad (3.46a)$$

The plot of S_a vs. ω or S_a vs. T , where $T = 2\pi/\omega$, for several values of β , for a given earthquake excitation is known as the absolute acceleration response spectrum. Similar plots of the maximum values of other response quantities.

$$S_v(\beta, \omega) = \left| \dot{\xi} \right|_{max} \qquad (3.46b)$$

and

$$S_d(\beta, \omega) = \left| \xi \right|_{max} \qquad (3.46c)$$

are known as the relative velocity response spectrum and the relative displacement response spectrum, respectively. The following relations have been shown to hold approximately between the various spectra values:[27]

$$\omega S_d \simeq S_v \simeq \frac{1}{\omega} S_a \qquad (3.47)$$

Advantage may be taken of this relation by plotting the spectra (S_V vs. T) on a log-log plot so that all the three spectrum values may be read off the same plot.[28] Figure 3.7 is an example of such a plot for the response spectra of the S component of El Centro, 1940, earthquake record. The plots are given for four different values of β.

Alternative definitions of the response spectra S_d, S_V, and S_a are possible.[27] They are slightly different from the definitions used here and lead to an exact relationship between the three spectrum values instead of the approximate relationship (3.47). The results obtained from various definitions are substantially the same for low damping.

The maximum values of the base shear and the tower-base shear coefficients in the kth mode

$$C_{Bk} = C'_{Bk} \cdot S_a/g \tag{3.48a}$$

and

$$C_{Tk} = C'_{Tk} \cdot S_a/g \tag{3.48b}$$

(from Equations (3.39) - (3.42)) for a beam with given level and degree of setback (responding to the N-S component of the El Centro, 1940, earthquake) can be computed by reading off C'_{Bk} and C'_{Tk} values from Figures 3.5 and 3.6 and the S_a value from Figure 3.7. The period T_k can be obtained from Figure 3.2 (for $k \leq 4$) with the knowledge of the ℓ, G and ρ values of the beam.

The actual total base shear response V_B and tower-base shear response V_T, or the corresponding coefficients C_B and C_T, in a beam subjected to external dynamic forces are, at any instant, the sum of the

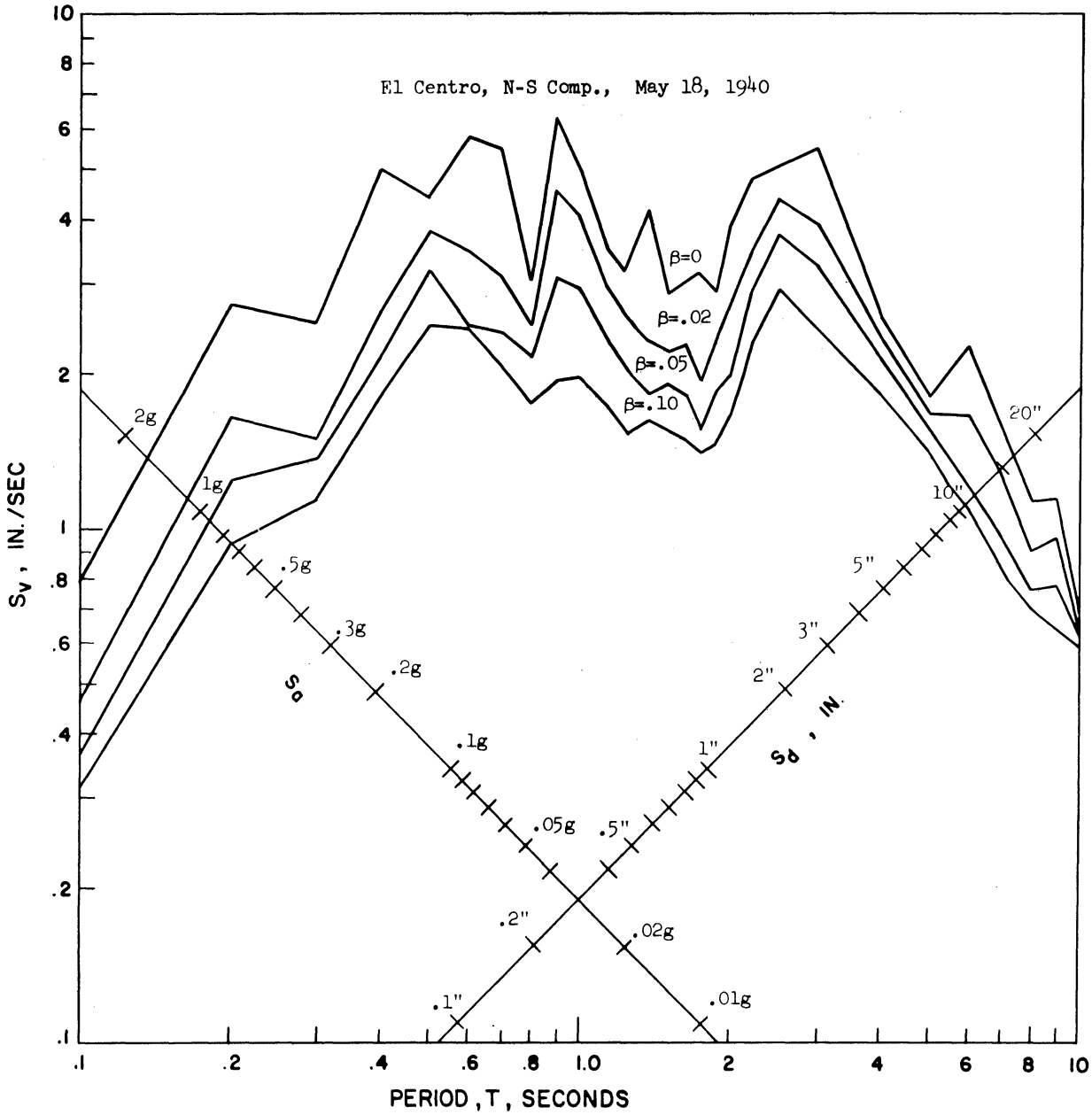

Figure 3.7. Response Spectrum.

corresponding values in each mode at that instant. Thus

$$C_B(t) = \sum_{k=1}^{\infty} C'_{Bk} \cdot (\ddot{\xi}_k(t) + \ddot{x}_o(t))$$

and (3.49)

$$C_T(t) = \sum_{k=1}^{\infty} C'_{Tk} (\ddot{\xi}_k(t) + \ddot{x}_o(t))$$

when the beam is subjected to ground acceleration $\ddot{x}_o$. The maximum values that $C_B(t)$ and $C_T(t)$ take on are the maximum values that the corresponding sums on the right hand side reach during the response. Generally, the terms of the sum on the right hand side will reach their maximum values at different times so that the knowledge of such maximum values will not enable one to know the maximum value that the sum might attain. The sum of the maximum absolute values of each term will provide only an upper bound to the actual maximum of the sum. Several other methods of superimposing the individual modal maxima to obtain approximate total maximum responses have been suggested and investigated.[29,30] It has been suggested[31] that the "probable" value of the maximum response is approximately the square root of the sum of the squares (RSS) of the modal maxima. This is based on the assumption that the modal components are random variables, which is consistent with the random nature of the earthquake ground accelerations $\ddot{x}_o(t)$. This method of superposition has been found to give as good or better approximation to the actual maximum response than most other methods of superposition.[29, 30]

The response spectrum for the S component of El Centro, 1940, earthquake is given in Figure 3.7. For a given fraction of critical damping β , the maximum response, for example, the maximum velocity response S_V , is an irregular function of period T . The same is true

of the response spectra of other recorded earthquake ground motion. Moreover, the overall magnitude of the various maximum responses is different for different recorded ground accelerations. The plots of the average maximum velocity and acceleration responses of the various recorded ground acceleration (of strong-motion earthquakes), normalized in a suitable manner, have been found to be reasonably smooth functions of period T.[32] Further, it has been observed that for a given β the average maximum velocity response remains almost constant with change in period, T, over a wide range of periods.[32]

To obtain a rough idea as to the effect of setback on the maximum base shear and tower-base shear coefficients of a stepped shear beam subjected to earthquake acceleration, the method of RSS (square root of sum of squares) superposition of modal maxima to obtain the total maximum will be used. The modal maxima will be obtained from the average spectrum assuming that fraction of critical damping remains constant in all modes for all beams with various levels and degrees of setback. Further, it will be assumed that the range of period encountered is within the range of period for which the average maximum velocity response is almost constant. Only the first four modes will be used, the contribution of the higher modes to the significant response parameters being negligible in comparison to that of first two or three modes in the cases considered here. Then using Equation (3.48),

$$C_B \simeq \sqrt{\sum_{k=1}^{4} (C'_{Bk}\ \omega'_k)^2}\cdot \frac{S_V}{g}\ \frac{s}{\ell}$$

$$\simeq C'_B\ \frac{S_V}{g}\cdot\sqrt{\frac{G}{\rho \ell^2}} \qquad (3.50)$$

and

$$C_T \simeq \sqrt{\sum_{k=1}^{4} (C'_{Tk} \quad \omega'_k)^2} \cdot \frac{S_v}{g} \cdot \frac{s}{\ell}$$

$$\simeq C'_T \cdot \frac{S_v}{g} \cdot \sqrt{\frac{G}{\rho \ell^2}} \qquad (3.51)$$

where C_B and C_T are the maximum base shear coefficient (BSC) and the tower-base shear coefficient (TBSC) respectively. Advantage is also taken of the approximate relation (3.47)

$$S_a \simeq \omega S_v$$

in writing Equations (3.50) and (3.51), and ω is replaced by ω' (see Equations (3.21) and (3.17)) so that C'_B and C'_T are dimensionless.

The variation in C'_B and C'_T with c for various levels of setback p is shown in Figures 3.8 and 3.9, respectively. The base shear coefficient increases with decreasing c for all levels of setback. This increase becomes larger and larger as the level of setback gets lower (i.e. as p decreases) when $c < .375$ (approximately); the case of setback level exactly at mid-height is an exception.

The tower-base shear coefficient also increases with decreasing c for all levels of setbacks. The C_T values at $c = 1$ for different values of p are nothing but the seismic coefficients at various levels of a uniform beam. From Figure 3.9 it is clear that the seismic coefficient increases from bottom to top of the uniform shear beam. The seismic coefficient at a given level is defined identically as the tower-base shear coefficient, i.e. as the ratio of shear at that level to the weight of structure above that level.

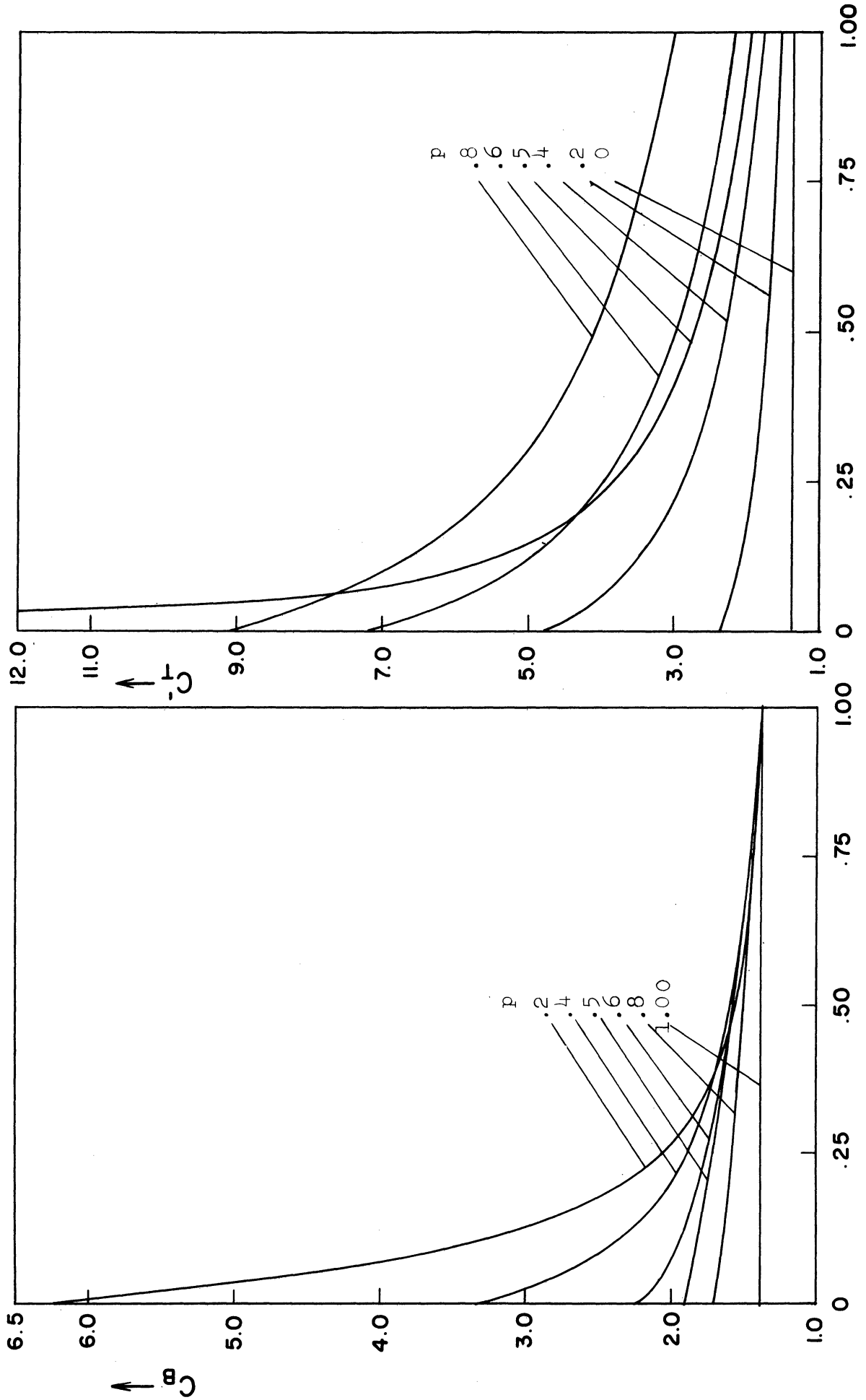

Figure 3.8. RSS Response, BSC.

Figure 3.9. RSS Response, TBSC.

The increase in tower-base shear coefficient with decreasing c is most for setback level $p = .8$ and becomes smaller as the setback level is lowered, (i.e. as p decreases), the case $p = .5$ being an exception. For setback level exactly at mid-height, the increase in C'_T is unbounded as $c \to 0$ since C'_{Tk} in each of the four modes increase indefinitely as $c \to 0$ (as was observed earlier) due to resonance effects. There will also be an unbounded increase in C'_T value for those values of p for which at $c = 0$, there is at least a pair of modes whose frequencies are equal.

The RSS combination of the maximum modal responses will give a reasonable approximation of the actual combined maximum response only if the periods of the modes involved are well separated.(31) If the periods of any two of the lower modes involved are very close or equal, as in the case of shear beam with setback at midheight ($p = .5$) and very slender tower (i.e. very small c), the RSS combination will not, in general, give a good approximation. Besides $p = .5$, there are other values of p for which two lower mode periods will be close when the tower portion of the shear beam is very slender, e.g. the second and third modes for $p = .75$.

When two modes have close periods, the algebraic sum of the two modal maximum responses may, under certain conditions, be a good approximation of the true combined response of the two modes. This depends on several factors such as the ratio of the periods involved, the ratio of the amplitudes of the responses in the two modes, and damping. Skinner *et al*(7) have investigated this problem. They find that if the algebraic sum is not too small in comparison with the individual modal responses (i.e., if the ratio of amplitudes of the two modal responses is

sufficiently different from -1), it will be a good approximation of the actual combined response for a small range of period ratios around 1, and that this range of period ratio would increase to some extent with increase in damping. The algebraic sum combination will of course give exact results when the periods of the modes involved are exactly equal.

In the case of shear beam with setback at midheight and very small c ,the ratios of the modal base shear coefficient (BSC) responses in successive pair of modes (viz. first and second modes, third and fourth modes, etc., each pair having close periods, see Figure 3.2) is very nearly equal to one, see Figure 3.5. The algebraic combination of the maximum modal BSC responses of successive pair of modes will in this case, therefore, give good results. Further, at $c = 0$ such algebraic sums hold exactly since the periods of each successive pair of modes are equal. The RSS combination of the algebraic sums of first and second, and third and fourth mode BSC responses for this case ($c = 0$) gives $C_B' = 2.68$ instead of 1.9 as shown in Figure 3.8, a value obtained by the RSS combination of all four individual modal responses.

The ratio of the modal tower-base shear coefficient (TBSC) responses in successive pair of modes of the shear beam with setback at midheight and extremely slender tower is more nearly equal to -1, see Figure 3.6. Algebraic sum of the modal responses in such pairs of modes will be small and therefore will not give a good approximation of the actual combined response. The actual combined responses in such cases have been found to be very high although not as high as would be suggested by the RSS combination of the modal responses.[6,7]

SHEAR BUILDING

In the previous section, the effects of step size and levels on the uncoupled translational vibrations of the stepped shear beam were examined. The shear beam is a highly idealized model of multi-story buildings. However, the simplicity of this model made it possible to obtain some information about the effect of setbacks that would not be easily apparent otherwise.

In Chapter II, equations of motions of a multi-story building have been developed using a multi-mass model. The mass of the building is assumed to be concentrated at floor levels in such a model. This is much closer to reality than the assumption of uniform mass and stiffness distribution made in the case of shear beam.

Conditions were established in Chapter II under which the lateral vibrations in one or both principal directions (assuming the existence of such principal directions, see Chapter II) are uncoupled from the torsional vibration. As with the shear beam, the uncoupled translational vibrations in one of the principal directions of the multi-mass model of the multi-story building will be studied next in this chapter, assuming that conditions for such uncoupling exist.

Equations of Motion and Solution

In Figure 3.10a is shown a N-story building with a setback above the Pth story. The setback is geometrically symmetric about the x axis and it is assumed that dynamic symmetry also exists about this axis. If we assume linear elastic stiffness and viscous damping, the equations of motion for uncoupled translational vibration in the

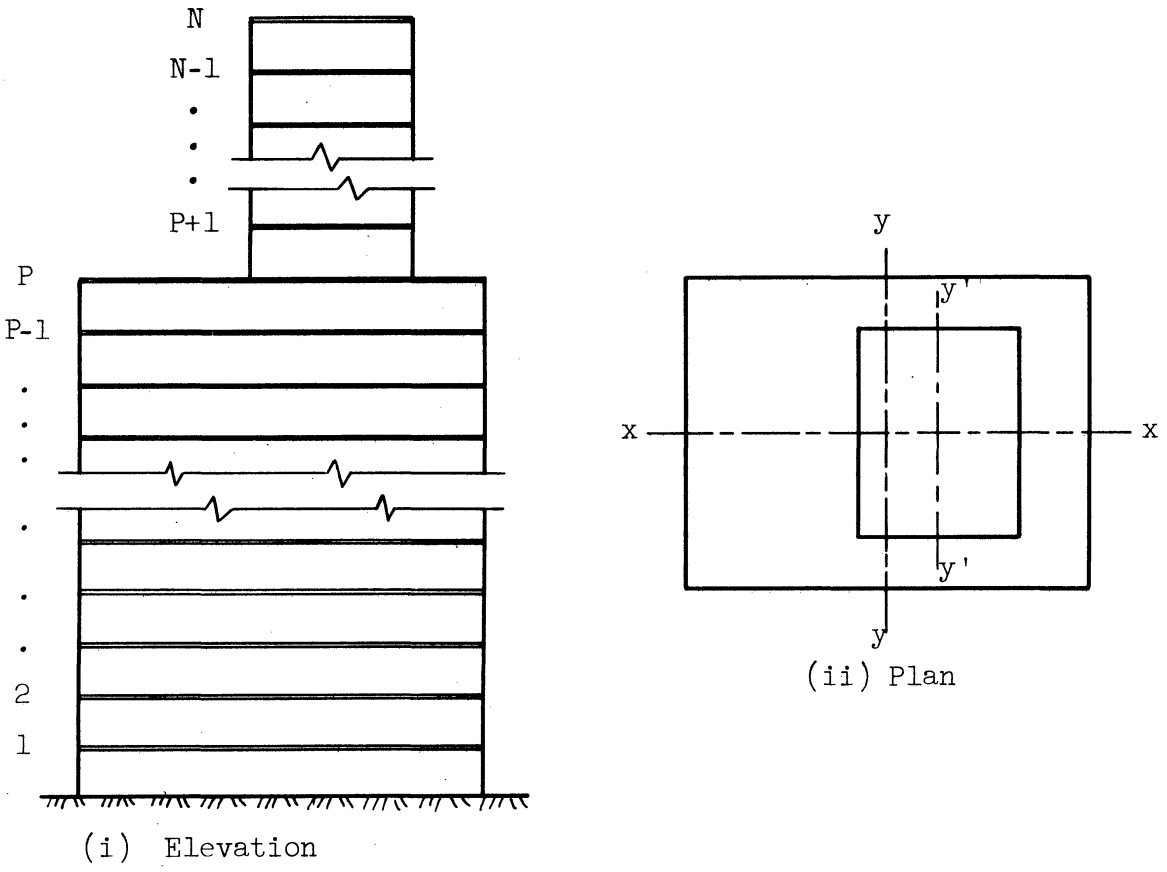

Figure 3.10a. N-Story Structure with Setback at Pth Story.

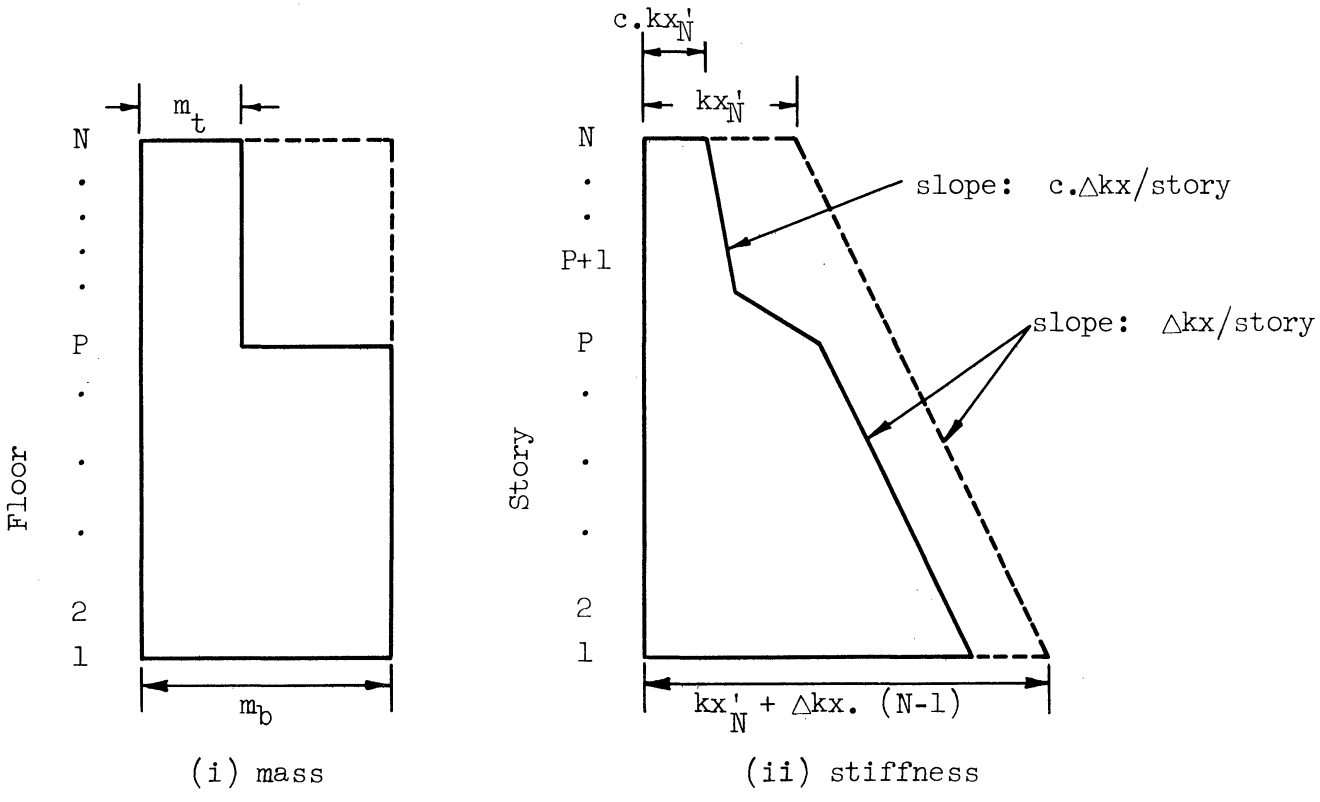

Figure 3.10b. Assumed Mass and Stiffness Distribution.

x direction of a N-story structure is given by Equation (2.17). Dropping the subscript u , Equation (2.17) may be written as

$$[M]\{\ddot{u}\} + [C]\{\dot{u}\} + [K]\{u\} = \{f(t)\} \tag{3.52}$$

The usual normal mode solution of the equations of type (3.52) was outlined in Chapter II. The solution of the system of Equation (3.52) with no damping,

$$[M]\{\ddot{u}\} + [K]\{u\} = \{f(t)\} \tag{3.53}$$

may be written as

$$\{u\} = [\Phi]\{\eta\} \tag{3.54}$$

where $[\Phi]$ is NxN modal matrix,each column of $[\Phi]$ being a mode shape of the system (3.53),and $\{\eta\}$ is the Nxl modal displacement vector. The kth element of $\{\eta\}$ corresponding to the kth mode is given by

$$\ddot{\eta}_k + \omega_k^2 \eta_k = g_k(t) \tag{3.55}$$

where ω_k is the kth mode frequency of system (3.53) and

$$g_k(t) = \frac{\{\phi^k\}^T\{f(t)\}}{\{\phi^k\}^T [M]\{\phi^k\}} \tag{3.56}$$

where $\{\phi^k\}$ is the kth mode shape of system (3.52) i.e. the kth column of matrix $[\Phi]$.

Assuming that the damping in the system is viscous and that it does not affect the normal modes and frequencies of the corresponding undamped system,the term $2\beta_k\omega_k\dot{\eta}_k$ may be added on the left side in

Equation (3.55)

$$\ddot{\eta}_k + 2\beta_k \omega_k \dot{\eta}_k + \omega_k^2 \eta_k = g_k(t) \qquad (3.57)$$

to represent the damping in the structures, where β_k is the fraction of critical damping in the kth mode. With elements of vector $\{\eta\}$ given by Equation (3.57), Equation (3.54) is then the solution of Equation (3.52).

When the structure is subjected to ground acceleration, the force vector $\{f(t)\}$ is

$$\{f(t)\} = - [M] \{\underset{\sim}{1}\} \ddot{x}_o(t) \qquad (3.58)$$

where $\{\underset{\sim}{1}\}$ is a Nxl vector with all elements equal to unity. Substituting for $\{f(t)\}$ in Equation (3.56)

$$g_k(t) = - \lambda_k \cdot \ddot{x}_o(t) \qquad (3.59)$$

where

$$\lambda_k = \frac{\{\phi^k\}^T [M] \{\underset{\sim}{1}\}}{\{\phi^k\}^T [M] \{\phi^k\}} \quad ; \qquad (3.60)$$

λ_k is generally known as the modal participation factor of the kth mode.

A method of obtaining the frequencies and the mode shapes of system (3.53) was described in Chapter II.

Assumption of Simple Coupling in Stiffness

It is assumed that the structure is simply coupled in stiffness, i.e., the shear force acting in a story is independent of the deformations in other stories. The stiffness of the structure may then be represented by springs connecting adjacent masses only with the first floor alone being connected to the ground. Such structures are sometimes also referred to as "shear" buildings.[10]

The deformation of buildings in which lateral forces are resisted by shear walls may be well represented by the above model if the walls are of such proportions as to have negligible bending type deformation.

In buildings where a space frame provides the resistance against lateral forces, if the floor girders are assumed to be infinitely rigid in comparison to the columns the model described above would again be adequate. However, in most buildings this is not the case, especially in the lower floors of tall buildings. Rubinstein and Hurty(33) have found that such an assumption leads to more than 50% decrease in the fundamental period of a typical 19-story steel-frame building.

On the other hand Housner and Brady(34) have found that fundamental periods of steel-frames computed by assuming infinitely rigid girders give better correlation with measured periods than periods calculated without making this assumption. This may be partly accounted for by the stiffening effect of floor slabs on girders (where adequate bond exists between them) and other effects such as the stiffness of "non-structural" elements.

It is expected that the nature of the effects of setbacks will not be affected much by the assumption of simple coupling in stiffness.

Idealized Structural Properties

Consider a N-story structure with setback above the Pth story, Figure 3.10a. Let kx_i be the stiffness of the ith story and m_i be the value of the lumped mass at ith level. The following distribution

of mass and stiffness is assumed:

in the base portion $(1 \leq i \leq P)$

$$m_i = m$$

$$kx_i = kx'_N + \Delta kx \cdot (P - i + 1) + c \cdot \Delta kx \quad (N-P+1) \qquad (3.61)$$

and in the tower portion $(P + 1 \leq i \leq N)$

$$\begin{aligned} m_i &= c \cdot m \\ kx_i &= c \cdot kx'_N + c \cdot \Delta kx \cdot (N-i) \end{aligned} \qquad (3.62)$$

In Equations (3.61) and (3.62) kx'_N, Δkx and m are constants; c is the degree of setback. The distribution of mass and stiffness described by Equations (3.61) and (3.62) is shown graphically in Figure 3.10b. The range of c is restricted to $0 < c \leq 1$. The case $c = 1$ represents a uniform building and the mass and stiffness distribution for this case is shown by dotted lines in Figure 3.10b.

Whenever the behavior of a building with setback is compared with that of a uniform building, it is a uniform building with the same number of stories and whose properties are given by Equations (3.61) and (3.62) with $c = 1$ and the values of the constants kx'_N, Δkx and m the same as those of the building with setback. Such a uniform building will be termed "comparable" uniform building.

The value of the lumped masses in each part of the structure is assumed to be constant: $m_B = m$ in the base portion and $m_t = cm$ in the tower portion. The ratio m_t/m_b then defines the degree of setback c,

$$c = \frac{m_t}{m_b} \qquad (3.63)$$

This definition is similar to the one made in the case of shear beam, see Equation (3.24).

Stiffness at any level is assumed to be equal to a constant (kx'_N or $c \cdot kx'_N$) plus a quantity $\Delta kx/m_b$ times the total mass above that level. Thus, the increment in stiffness per story is Δkx in the base portion and $c \cdot \Delta kx$ in the tower portion, see Figure 3.10. Also the constant parts in the stiffness at any level are kx'_N in the base portion and $c \cdot kx'_N$ in the tower portion.

The multi-mass model of buildings with setback being considered here can also be seen as a discrete mass approximation of a stepped shear beam. In the case of shear beam model used in the previous section both the stiffness and mass values per unit length were assumed to be constant in each part of the structure. In the discrete-mass model considered here the value of lumped mass is constant in each part of the structure; the same is not necessarily true (unless $\Delta kx = 0$) with regard to the stiffness.

In the tower portion the ratio of the mass or stiffness at a given level of a building with respect to the corresponding values at the same level in a comparable uniform ($c = 1$) building (having identical values for Δkx, kx'_N and m) is equal to c in the discrete mass model as well as in the shear beam model. In the base portion such ratios for mass as well as stiffness are equal to 1 for shear beam model. This is also the case for mass in the multi-mass model; but not for stiffness, (see Figure 3.10b) unless $\Delta kx = 0$.

The mass and stiffness distribution used by Housner and Brady[34] for space frames with infinitely rigid girders in their investigation of fundamental periods of structures is of the same form as assumed here for uniform structures. The value of the ratio $\Delta kx/kx'_N$ is 1/3 for the results presented in this chapter, which is the same value that was used by Housner and Brady. This seems to be a reasonable value for space-frame buildings where columns are the main lateral resistance elements.

Results were also obtained using $\Delta kx/kx'_N = 0$, i.e. constant story stiffness in each part of the structure, which along with the assumed constant mass distribution in each part of the structure, leads to a lumped mass approximation of the stepped shear beam of the previous section. As should be expected, the results for this case were not very much different from those presented in the previous section. For example, the effects of decreasing c on the fundamental period and mode shape of a 15 story building with $\Delta kx/kx'_N = 0$ are compared with similar effects in the case of shear beam in Figure 3.11. No further results for this case will be presented.

The ratio kx'_N/m was chosen so as to give a fundamental period of approximately one second for a uniform structure of 10 stories satisfying the code[3] formula, $T = 0.1N$ (for $N = 10$), for space-frame buildings. This value is $kx'_N/m = 579.132\ sec^{-2}$, which gave a period of 1.03 seconds for such a building.

The level of setback p, defined here by

$$p = P/N \tag{3.64}$$

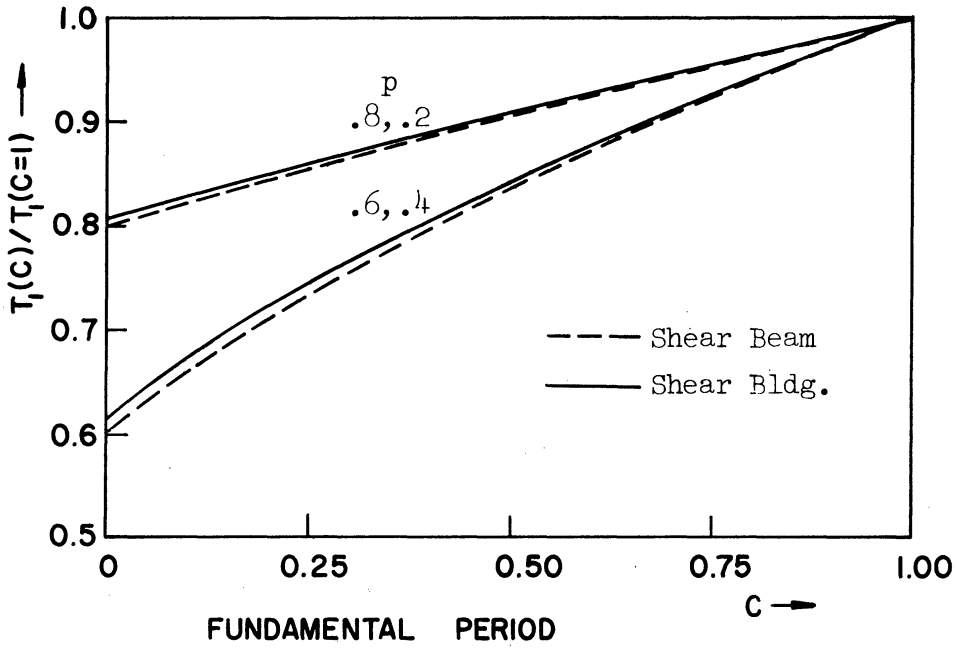

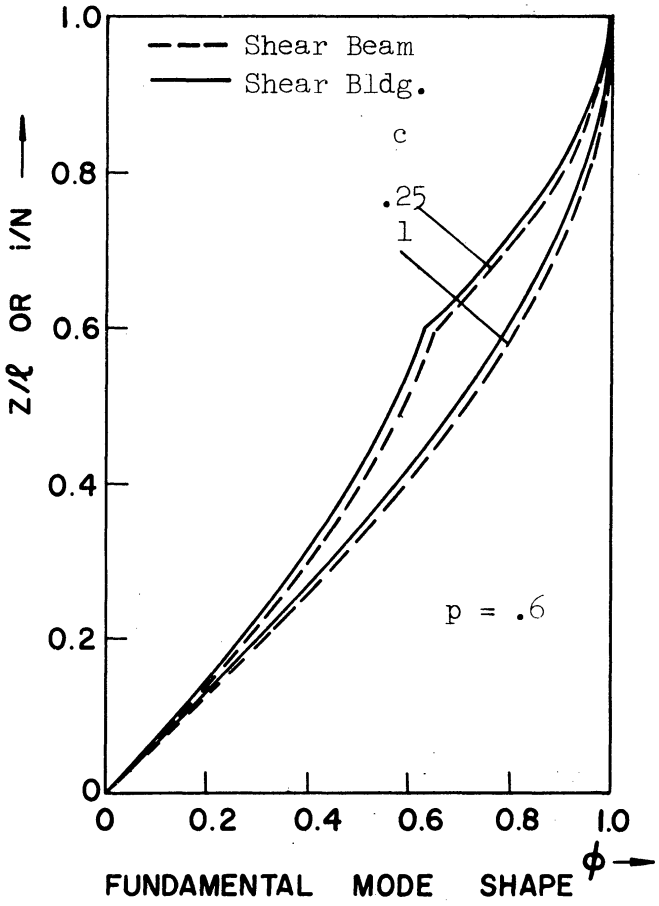

Figure 3.11. Comparison of Effect of Setback on Fundamental Period and Mode Shape of Shear Beam and Shear Building with $\Delta k x = 0$.

and the degree of setback c are now left as parameters as in the case of shear beam. The range of possible values that the parameters p and c can assume are $0 \leq p \leq 1$ and $0 < c \leq 1$, again just as in the case of shear beam. However, p can take on only a few discrete values in this range noting that P and N in Equation (3.64) are integers.

Having chosen the values of the two quantities kx'_N/m and $\Delta kx/kx'_N$ one can evaluate m_i and kx_i $(i = 1,..,N)$ for an N-story structure given P and c, by using Equations (3.61) and (3.62). The construction of matrices [M] and [K] of Equation (3.52) is then a simple matter. For the inertia matrix [M], which is diagonal,

$$\begin{aligned} m_{ij} &= 0 \qquad i \neq j \\ & \qquad\qquad i,j = 1, 2, \ldots, N. \\ m_{ii} &= m_i \end{aligned} \tag{3.65}$$

and for the stiffness matrix which for the shear building assumption is tridiagonal

$$\begin{aligned} k_{i,\,i-1} &= -kx_i \\ k_{i,\,i} &= kx_i + kx_{i+1} \\ & \qquad\qquad i,j = 1, 2, \ldots, N \\ k_{i,\,i+1} &= -kx_{i+1} \\ k_{i,j} &= 0 \qquad \begin{cases} j > i+1 \\ \text{or} \quad j < i-1 \end{cases} \end{aligned} \tag{3.66}$$

The mode shapes and frequencies were obtained by using Givens' method described in Chapter II. Computations for these and other modal quantities presented here were made on a digital computer. Results were obtained for a 15 story building with different levels (P/N) and degrees

of setback (c) . Similar results were also obtained for 5-, 10-, and 20-story structures. Since these results show a similar trend as far as the effect of level and degree of setback is concerned, results are presented here only for the 15-story structures.

Periods

In Figure 3.12 the first four mode periods are plotted as functions of c for values of p = 0, .2, .4, .6, .8, and 1 (i.e. P = 0, 3, 6, 9, 12 and 15). The values p = 0 and p = 1 represent the uniform building (i.e. one without a setback) for all values of c as was the case with the shear beam. For these values of p , therefore, periods, and all other modal quantities discussed later, do not change with c .

Periods and other modal quantities for the extreme case c = 0 cannot be directly computed for the multi-mass model as was possible with continuous shear beam model. The smallest value of c for which the periods have been computed directly is .00625. It was shown in the case of shear beam that a frequency of the stepped shear beam with c = 0 is equal to a frequency of either the base portion acting alone or the tower portion acting alone (each as a uniform cantilever beam). Periods of uniform buildings of P and N-P stories were computed. The two sets of periods were combined together and rearranged to that for the combined set $T_n > T_{n+1}$, n = 1, 2, ..., N-1.

Periods thus obtained are given in Table III .1 for the first four modes (n = 1 through 4) for N = 15 and P = 12, 9, 6, and 3. In each case the period is identified by its origin, i.e. whether it is a period of the base portion or tower portion, and the mode number in the

TABLE III.1

PERIODS AT $c = 0$ $(N = 15)$

Mode No.	Setback Level, P			
	12	9	6	3
1	1.1485 Base, 1	0.9673 Base, 1	0.9673 Tower, 1	1.1485 Tower, 1
2	0.4904 Tower, 1	0.7551 Tower, 1	0.7551 Base, 1	0.4904 Base, 1
3	0.4493 Base, 2	0.3744 Base, 2	0.3744 Tower, 2	0.4493 Tower, 2
4	0.2781 Base, 3	0.2894 Tower, 2	0.2894 Base, 2	0.2781 Tower, 3

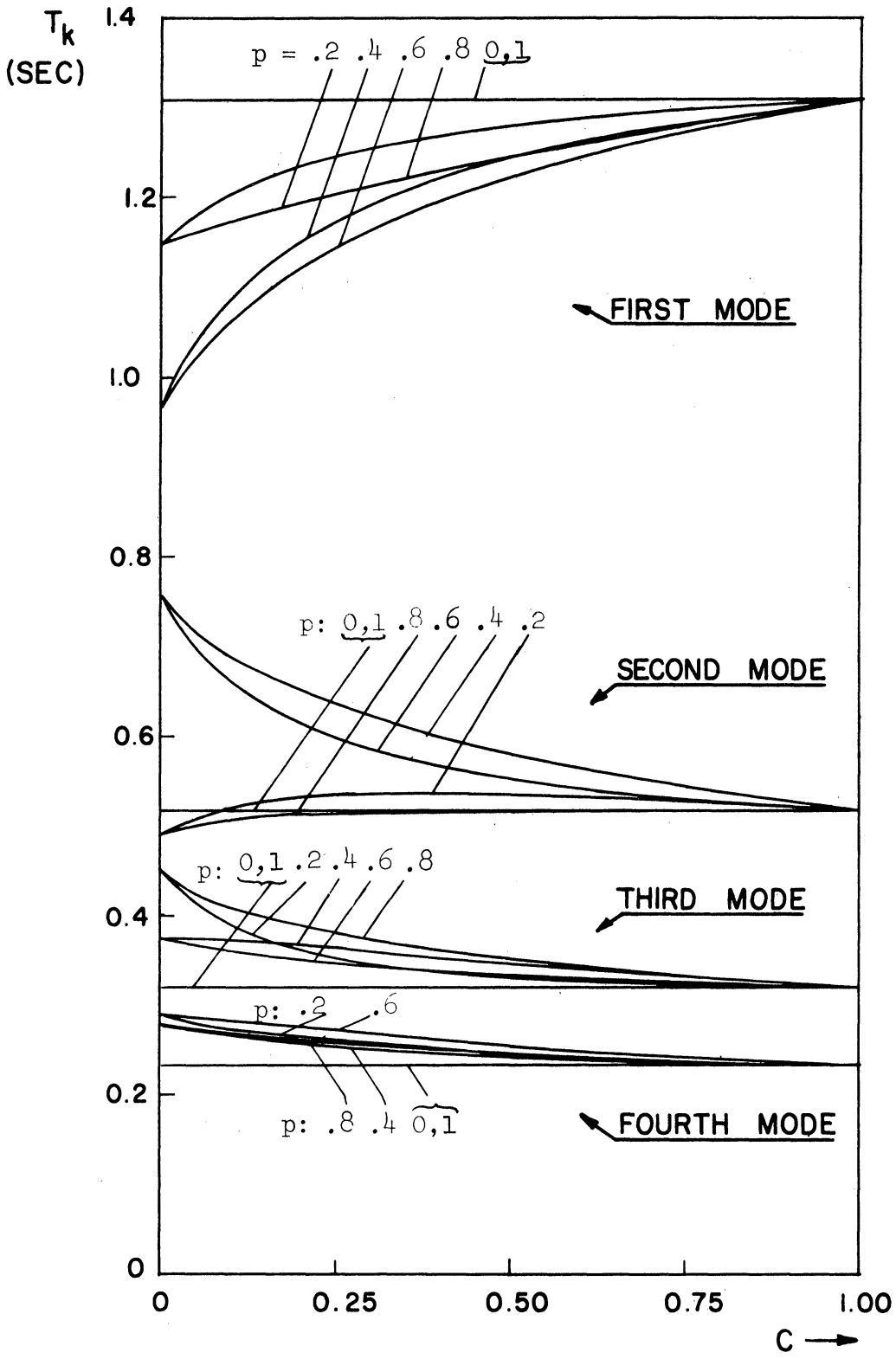

Figure 3.12. Fundamental and Higher Mode Periods, Shear Building.

original structure. Smooth extensions of the T_i vs. c plots in Figure 3.10 beyond $c = .00625$ to $c = 0$ are in excellent agreement with the corresponding periods in Table III .1.

It may be noted from Equation (3.61) that the mass and stiffness distributions in the base portion at $c = 0$ is the same as those given by Equations (3.61) and (3.62) for a uniform ($c = 1$) building of P stories. Noting that the periods are dependent only on the mass and stiffness distribution and the mass-to-stiffness ratio, the same is true for the tower portion.

Although the periods for structures with $P = P'$ and $P = N-P'$ are identical at $c = 0$ this does not hold for other values of $c < 1$. For shear beam the periods for $p = p'$ and $p = 1-p'$ were identical for all c. This difference is due to the assumed effect of c on the stiffness in the base portion as seen in Equation (3.61).

The following observations may be made from Figure 3.12. The first mode period decreases as c decreases for all levels of setback. The influence of a variation of c on the fundamental period is greater when the setback level is near mid-height ($p = .4, .6$ in Figure 3.12) and decreases as the setback level is moved towards either end. Similar behavior was observed in the first mode period of stepped shear beam though the extent of decrease in the period is much more than in the present model.

In third and fourth modes in general the periods increase as c decreases. (This was also observed in fifth through eighth modes, the results for which are not presented because they are relatively unimportant.) Also, the changes in periods with c in the higher modes are not monotonic. For the shear beam the changes in higher mode periods

with c are both ways depending on the level of setback, but for the period in a given mode changes monotonically with c . The non-monotonic variation in period observed here is due to the assumed effect of c on the stiffness in the base portion as seen in Equation(3.61).

Mode Shapes

The mode shapes have been normalized by fixing the displacement of the Nth mass (at the top), ϕ_N , equal to 1. First four mode shapes of the 15-story buildings with levels of setback p = .2, .4, .6 and .8 and degrees of setback c = 1, .5, .25 (except for third and fourth modes) and .125 are shown in Figure 3.13.

In the first and second mode shapes the effect of setback is apparent in the somewhat abrupt change in slope at the level of setback when $c \neq 0$; the smaller the value of c the sharper the kink. These kinks at the setback level, however, are not as sharp as in the case of the first and second modes of the shear beam. The reason for this lies mainly with the difference in the stiffness distributions assumed for the two models. In the shear beam the stiffness is constant in each part of the structure, whereas in the multi-mass model used here stiffness varies linearly with the height in each part of the structure. The difference in the modes shapes for the uniform structure (c = 1), especially in the fundamental mode shape, is also due to this same reason.

Sharp changes in slope occur in the third and fourth mode shapes of the uniform structure (c = 1). Hence, in these modes distinctive kinking at the level of setback is not apparent in most cases.

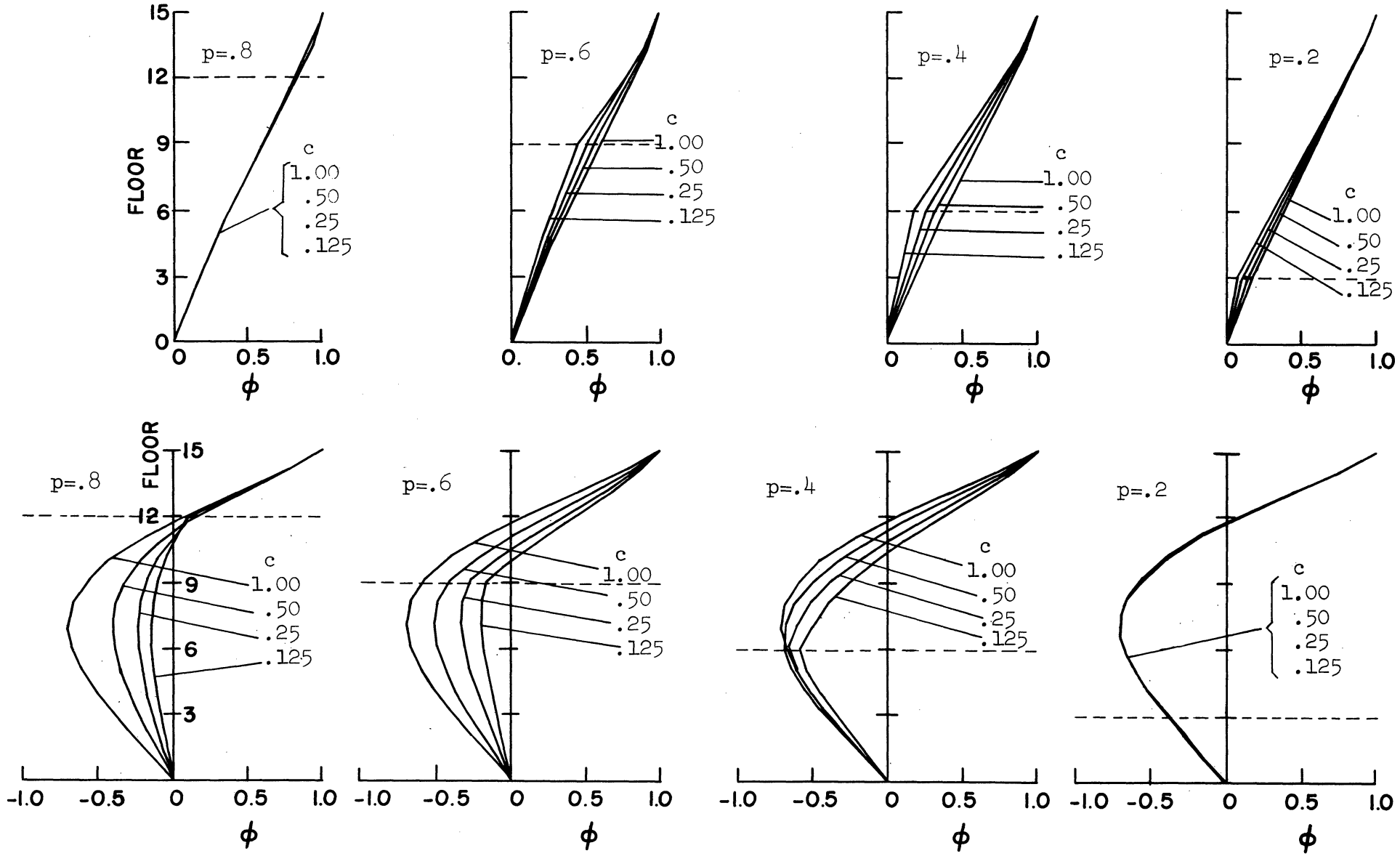

Figure 3.13. Mode Shapes, Shear Building. Above: first, Below: second.

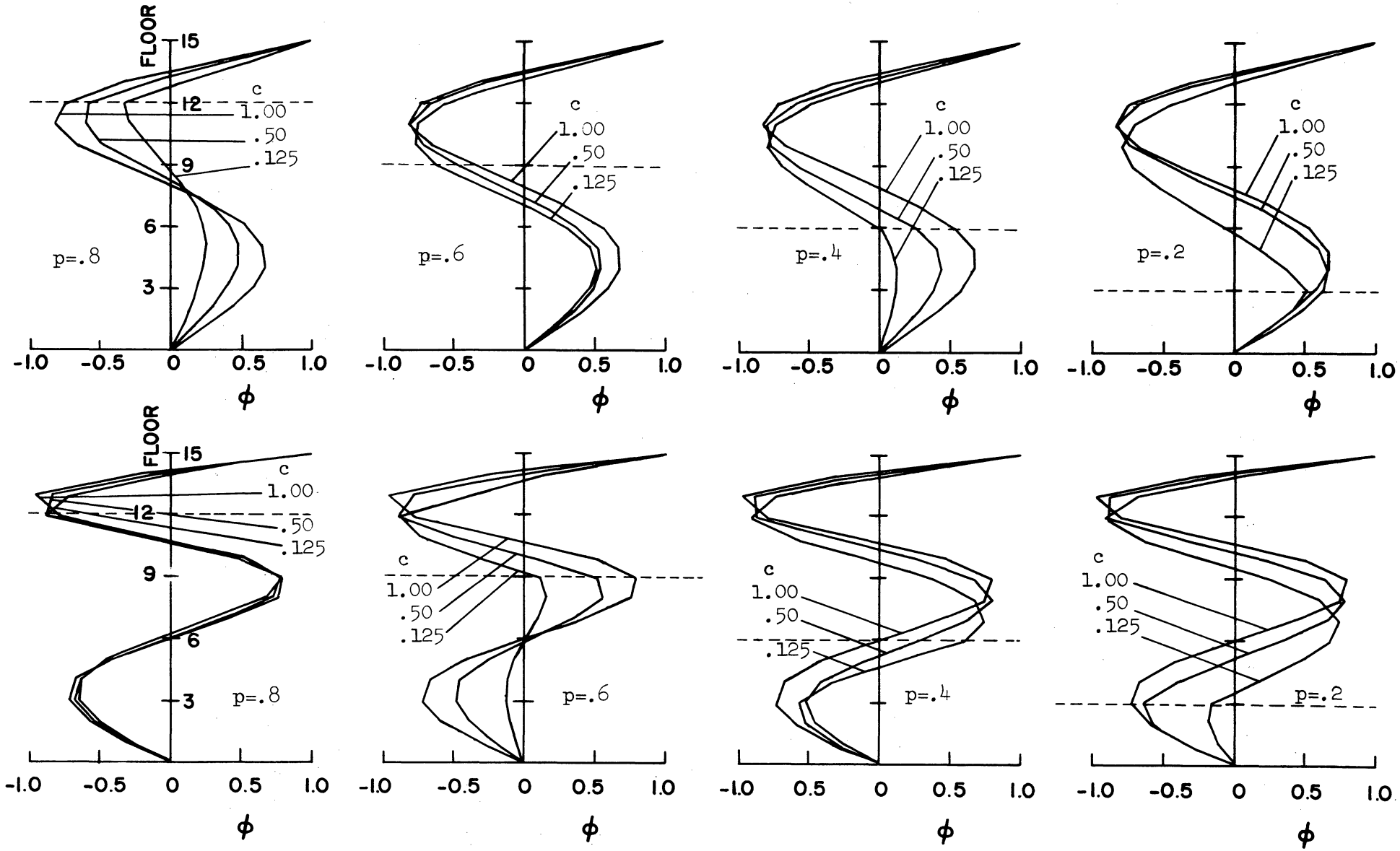

Figure 3.13. (Cont'd.) Mode Shapes, Shear Building. Above: third, Below: fourth

In the case of the shear beam, the smoothness of the mode shapes in each part of structure makes the kink at the level of setback distinctly apparent whenever $c \neq 1$. However, some consistency can be seen in the way the mode shapes change with decreasing c in each group of third and fourth mode shapes in Figure 3.13.

Exceptions were noted in the case of shear beam where for some levels of setback p there was no effect of change in c on some mode shapes, e.g. the third modes for $p = .6$ or $p = .2$. The second mode for $p = .2$ in the multi-mass model seems to be a similar exception. Also, the first mode for $p = .8$ shows very little effect of decreasing c, as was also the case with the shear beam.

In general, the effect of setback on the mode shapes is to decrease the amplitude of displacements in the base portion relative to that in the tower portion in comparison with the same mode shape of the corresponding uniform structure. This effect is amplified with decreasing c. With a few exceptions this observation is borne out in all the four mode shapes of the shear beam as well as the multi-mass model given in Figures 3.4 and 3.13, respectively.

Modal Shear Coefficients

In the section on shear beams, formulae were derived for modal base shear coefficients and tower-base shear coefficients of the stepped shear beam subjected to earthquake ground acceleration $\ddot{x}_o(t)$ (Equations (3.39) and (3.40)). Similar formulae for these coefficients can be derived for the multi-mass model. Omitting the intermediate steps, which

are similar to those in the preceding section on the shear beam, the base shear coefficient in the kth mode is given by

$$C_{Bk}(t) = \lambda_k \cdot \frac{\sum_{i=1}^{N} m_i \phi_i^k}{\sum_{i=1}^{N} m_i} \cdot (\ddot{\xi}_k(t) + \ddot{x}_o(t))/g \qquad (3.67)$$

and the tower-base shear coefficient is given by

$$C_{Tk}(t) = \lambda_k \cdot \frac{\sum_{i=P+1}^{N} m_i \phi_i^k}{\sum_{i=P+1}^{N} m_i} \cdot (\ddot{\xi}_k(t) + \ddot{x}_o(t))/g \; . \qquad (3.68)$$

In Equations (3.67) and (3.68), λ_k is the modal participation factor of the kth mode defined by Equation (3.60); m_i is the value of ith mass; ϕ_i^k is the displacement of ith mass in the kth mode; g is the acceleration due to gravity; and $(\ddot{\xi}_k(t) + \ddot{x}_o(t))$ is the absolute acceleration of a single-degree-of-freedom oscillator with frequency ω_k and damping coefficient β_k subjected to ground acceleration $\ddot{x}_o(t)$

$$\ddot{\xi}_k + 2\beta_k \omega_k \dot{\xi}_k + \omega_k^2 \xi_k = - \ddot{x}_o \qquad (3.69)$$

The kth modal displacement η_k (Equation (3.57)) is related to ξ_k by

$$\eta_k = \lambda_k \xi_k \; , \qquad (3.70)$$

which is apparent on comparing Equations (3.57) and (3.69) noting that $g_k(t)$ in Equation (3.57) is given by Equation (3.59).

From Equations (3.67) and (3.68) it is seen that C_{Bk} and C_{Tk} vary with time and are dependent on the ground acceleration $\ddot{x}_o$ The portions of the expressions for C_{Bk} and C_{Tk} given by

$$C'_{Bk} = \lambda_k \cdot \frac{\sum_{i=1}^{N} m_i \phi_i^k}{\sum_{i=1}^{N} m_i} \tag{3.71}$$

and

$$C'_{Tk} = \lambda_k \cdot \frac{\sum_{i=P+1}^{N} m_i \phi_i^k}{\sum_{i=P+1}^{N} m_i} \tag{3.72}$$

are however independent of ground acceleration and are dependent only on the structural properties of the building. C'_{Bk} and C'_{Tk} can be looked upon as the kth mode base shear and tower-base shear coefficients, respectively, in a building subjected to unit g static acceleration.[26] (i.e. in a building subjected to static lateral force at each floor equal to the weight of the floor). C'_{Bk} and C'_{Tk} were similarly defined by Equations (3.41) and (3.42) for shear beam.

In Figure 3.14 and 3.15 are given plots of C'_{Bk} vs. c and C'_{Tk} vs. c for several setback levels p , for the first four modes (k = 1 through 4). The values p = 0 and p = 1 represent uniform structure regardless of the value of c . Hence C'_{Bk} does not change with c . For p = 1 the tower-base shear coefficient is equal to zero (i.e. $C'_{Tk} = 0$) and for p = 0 it is equal to the base shear coefficient (i.e. $C'_{Tk} = C'_{Bk}$) regardless of the value of c .

As was pointed out earlier no direct computations can be made for the extreme case c = 0 . The smallest value of c for which computations were made is .00625. Smooth extensions of the C'_{Bk} vs. c plots beyond c = .00625 to c = 0 give values that are in good agreement with corresponding values obtained from uniform buildings of P

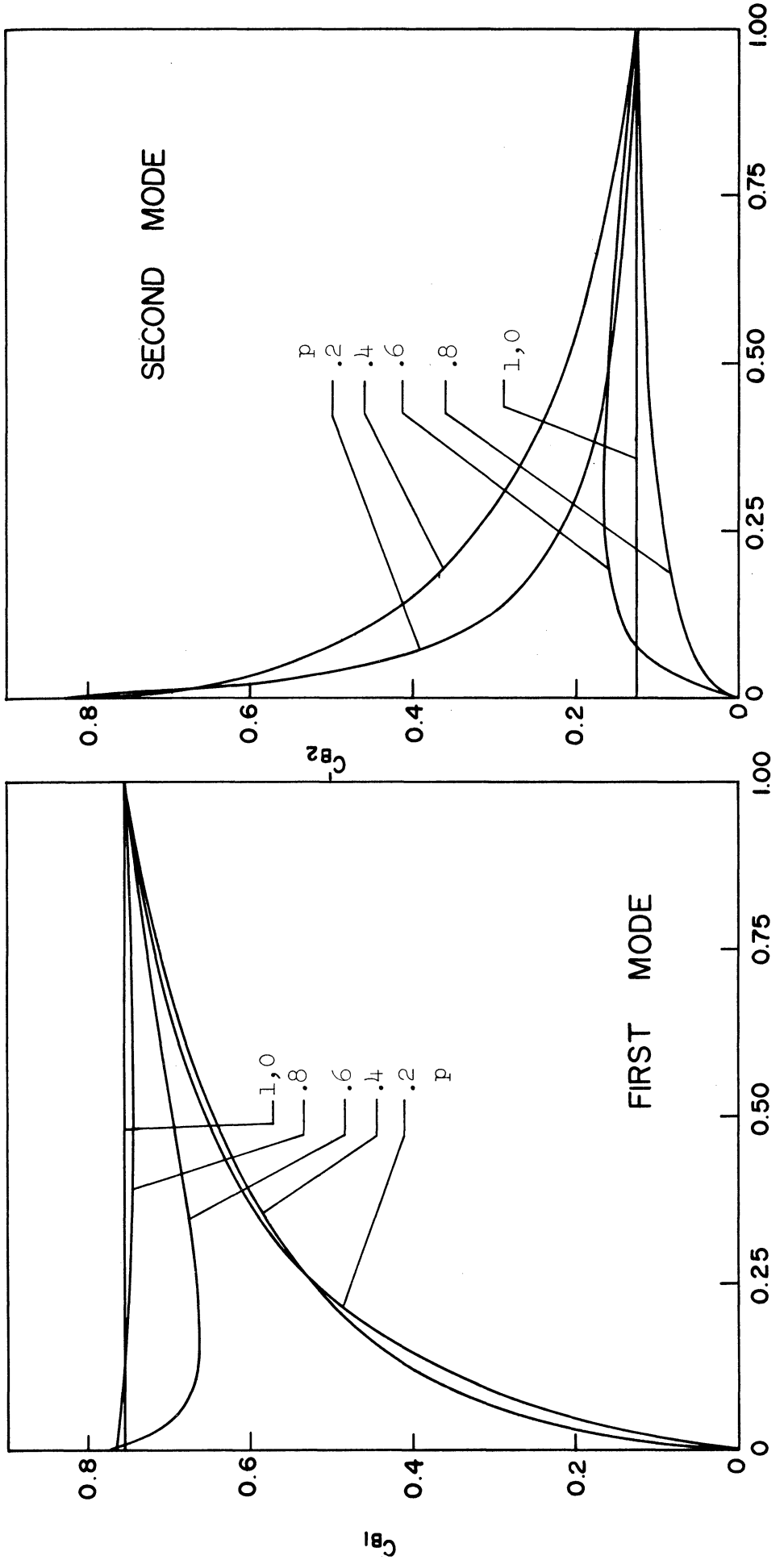

Figure 3.14. Modal Base Shear Coefficients, Shear Building

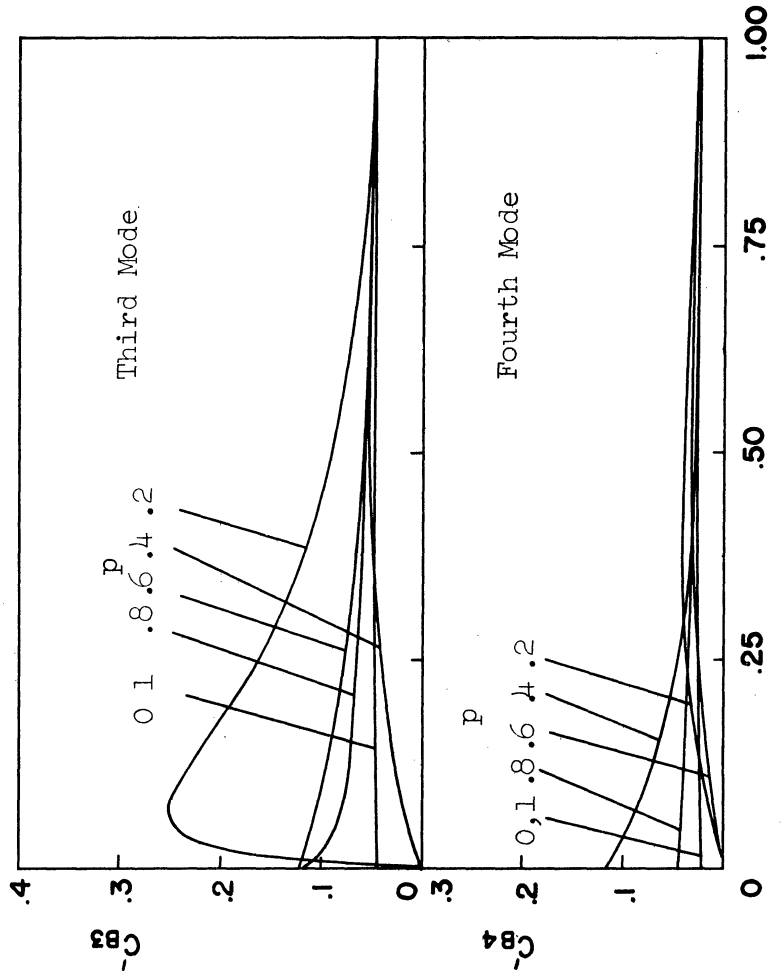

Figure 3.14(Cont'd). Modal Base Shear Coefficients, Shear Building.

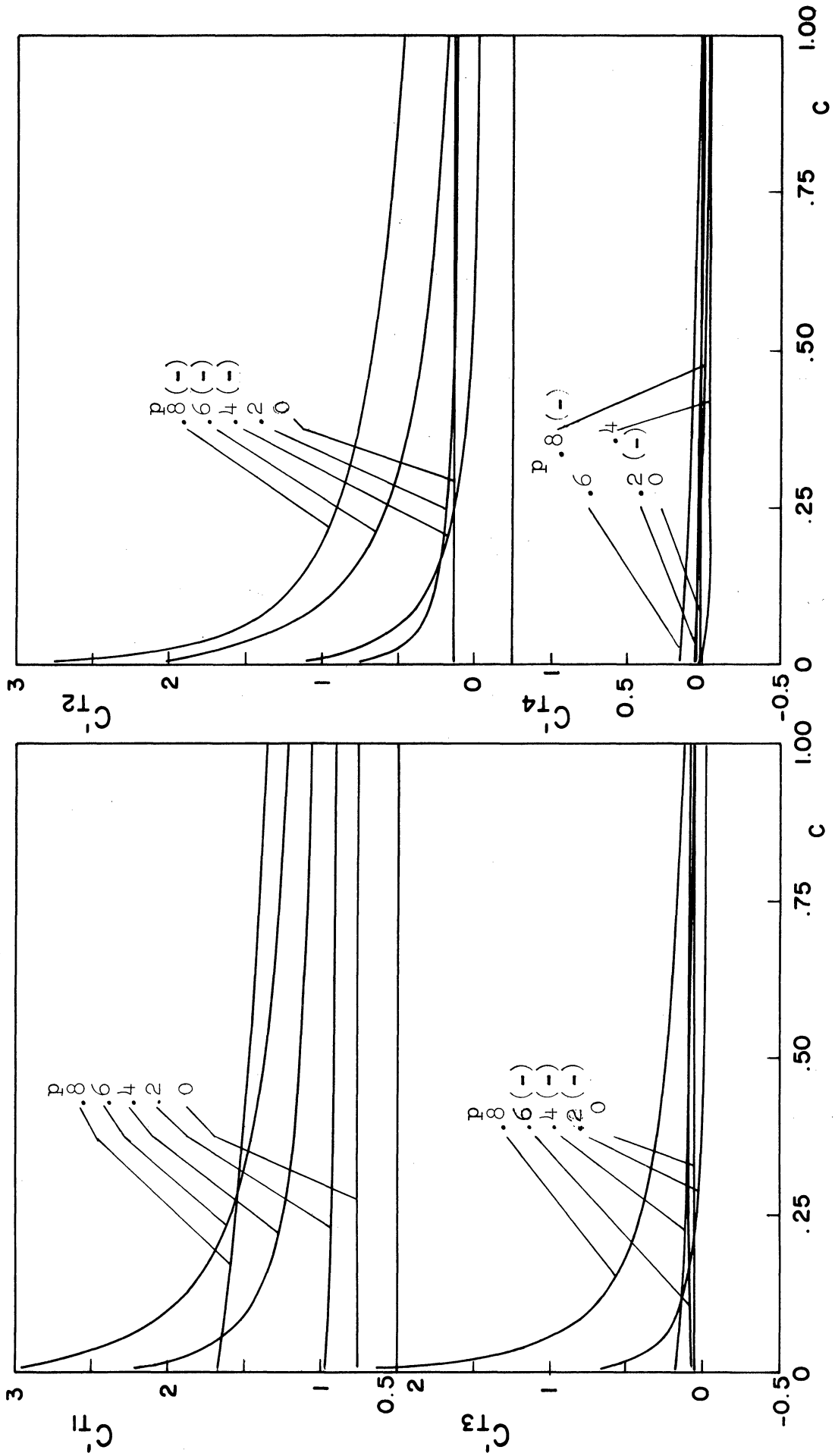

Figure 3.15. Modal Tower-base Shear Coefficients, Shear Building.

and (N-P) stories as per the interpretations made for C'_{Bk} in the case of stepped shear beam with $c = 0$. It may be recalled that for the stepped shear beam no interpretation of the C'_{Tk} value at $c = 0$ was possible in some cases.

In Figure 3.14, the first mode C'_{B1} decreases with decreasing c and tends to zero as $c \to 0$ when setback level is below midheight ($p < .5$). When the setback level is above midheight there is some decrease in C'_{B1} as c decreases; on further decrease in c C'_{Bk} begins to increase and tends to a finite value (equal to the C'_{B1} value of P-story uniform building) as $c \to 0$.

In the second mode for setback levels $p = .2$ and $p = .4$, C'_{B2} increases with decreasing c and tends to finite values (equal to the C'_{B1} value of 3- and 6-story uniform buildings, respectively). For $p = .6$ and .8 C'_{B2} decreases with c and tends to zero as $c \to 0$.

For setback level $p = .2$, C'_{B3} in the third mode increases significantly over most of the range of c and then decreases very sharply at the $c = 0$ end. No definite reason is apparent for this peculiar behavior. No other significant increase in C'_{Bk} is noted in the higher modes.

Unlike the modal base shear coefficient C'_{Bk}, the modal tower-base shear coefficient C'_{Tk} has different signs in different modes. Furthermore, shear coefficient C'_{Tk} changes in sign (but at most once) as it varies with C.

In Figure 3.15, the C'_{Tk} plots for some cases are drawn with signs that are opposite to the actual, for convenience. Such plots are identified by minus signs placed along with the values of the parameter p.

As with the shear beam, the absolute value of C'_{Tk} increases with decreasing c in almost all modes for all levels of setback as seen in Figure 3.15. The increase is more when $p > .5$, i.e. for structures with setback level above mid-height. Also, much of the increase in C'_{Tk} in all modes and for all values of p is confined to the $c = 0$ end.

The observations noted above suggests that the maximum tower-base shear coefficient of a structure with setback subjected to a given earthquake acceleration would possibly be quite high when the tower section is very small in comparison with the base section, especially when the setback level is above mid-height.

It may be noted that the mode shapes and the quantities C'_{Bk} and C'_{Tk} defined by Equations (3.71) and (3.72) are dependent only on the mass and stiffness distributions in the structure. They are independent of the actual magnitudes of the mass or stiffness and also the stiffness-to-mass ratio. The mass and stiffness distributions are governed by p and c.

The stiffness-to-mass ratio (kx'_N/m) was assumed to have a constant value, say q, in the study of the effect of p and c on the periods. For a different value of stiffness-to-mass ratio, say q' (assuming it remains constant as p and c change), the plots of period vs. c in Figure 3.72 would be valid with a different scale for the

period axis, $T' = T\ q/q'$. However, the effect of p and c on the ratios $T_1 : T_2 : T_3 : T_4$ is independent of the stiffness-to-mass ratio.

Responses to Recorded Earthquakes

Having studied the influence of setbacks on some of the important modal quantities, the maximum responses of structures with setback subjected to recorded earthquake ground motion will next be examined.

Responses are computed for the 15-story structures with the same properties as were assumed in the modal study. Computations were made for structures with setback above 12th, 9th, 6th and 3rd stories and with degree of setback $c = 1, .75, .50, .25$ and $.125$ for each setback level.

The earthquake excitations used for the response computations are the NS component of the El Centro, May 18, 1940, and the N69°W component of the Taft, July 21, 1952, earthquake records. These are two among the strongest earthquake ground motions recorded to date (1966). These records (among many others) have been reduced to digital form with appropriate base line adjustments.(35)

The total response of the system of Equation (3.52) is a linear combination of modal responses as seen in Equation (3.54). Hence, first the modal displacements η_k (or alternately ξ_k , see Equations (3.69) and (3.70)) were computed by solving Equation (3.69) by a numerical integration procedure and then using Equation (3.70). A fourth order Runge-Kutta procedure, available as a subroutine at the University of Michigan Computing Center, was used for this purpose.

At the end of each step (in time) of numerical integration the desired total responses were then computed from the knowledge of the values of ξ_k at that instant of time.

Since the contribution of higher modes to the various significant response parameters is known to be small in comparison with first two or three modes, only the first four modes were considered in computing the total response. Earlier, it was pointed out that for some cases the base shear coefficient in the higher modes may be significant. However, among the cases for which response computations were made, there was no indication of modes higher than the third contributing significantly to the total base shear coefficient.

In the past response studies of multi-story buildings damping has been assumed to be anywhere between zero and 20% of critical in one or more modes. Vibration tasts of multistory buildings indicate low values of damping,[36,37] usually less than 5% and much less in steel frame structures, at the small excitation levels produced by the vibration generators used in the tests in comparison to the earthquake generated excitations. These tests also indicate that, in general, damping in the higher modes is greater than in the first one or two modes. Here, it was decided to use 4% of critical damping in the first two modes and 6% of critical in the third and fourth modes.

Only the maximum absolute values attained by the responses of a structure during the time it vibrates when subjected to some earthquake excitation is of interest for design purposes. The maximum magnitudes of displacements (relative to ground) u_i of all floors and the relative

story displacements Δu_i of all the stories were computed. Since the structure was assumed to be simply coupled in stiffness, the shear forces in each story is proportional to the relative story displacements.

The root sum of squares (RSS) combination of the maximum modal displacements and relative story displacements in the four modes were also computed. In general, a very good agreement was found between the RSS sum of the modal maxima and the actual maximum in case of both the responses for all values of P and c for which computations were made.

Floor Displacements and Relative Story Displacements

In Figure 3.16 are given the maximum floor displacements of 15-story structures with various levels and degrees of setback subjected the N69°W component of the Taft '52 earthquake record. The maximum displacements of successive stories are joined by straight lines giving a envelope of the maximum displacement responses. It should be remembered that the maximum displacements of each floor may have occured at different times. The maximum response envelopes of structure with various degrees of setback (c) but with the same setback level (p) are given on the same plot. In each plot the case $c = 1$ represents the response of the uniform building.

Maximum relative story displacement envelopes of the same 15-story structures subjected to the same (Taft '52, N69°W) earthquake excitation are given in Figure 3.17. Similar maximum response envelopes of these same structures subjected to S component of El Centro '40 earthquake record are given in Figures 3.18 and 3.19. It may be noted

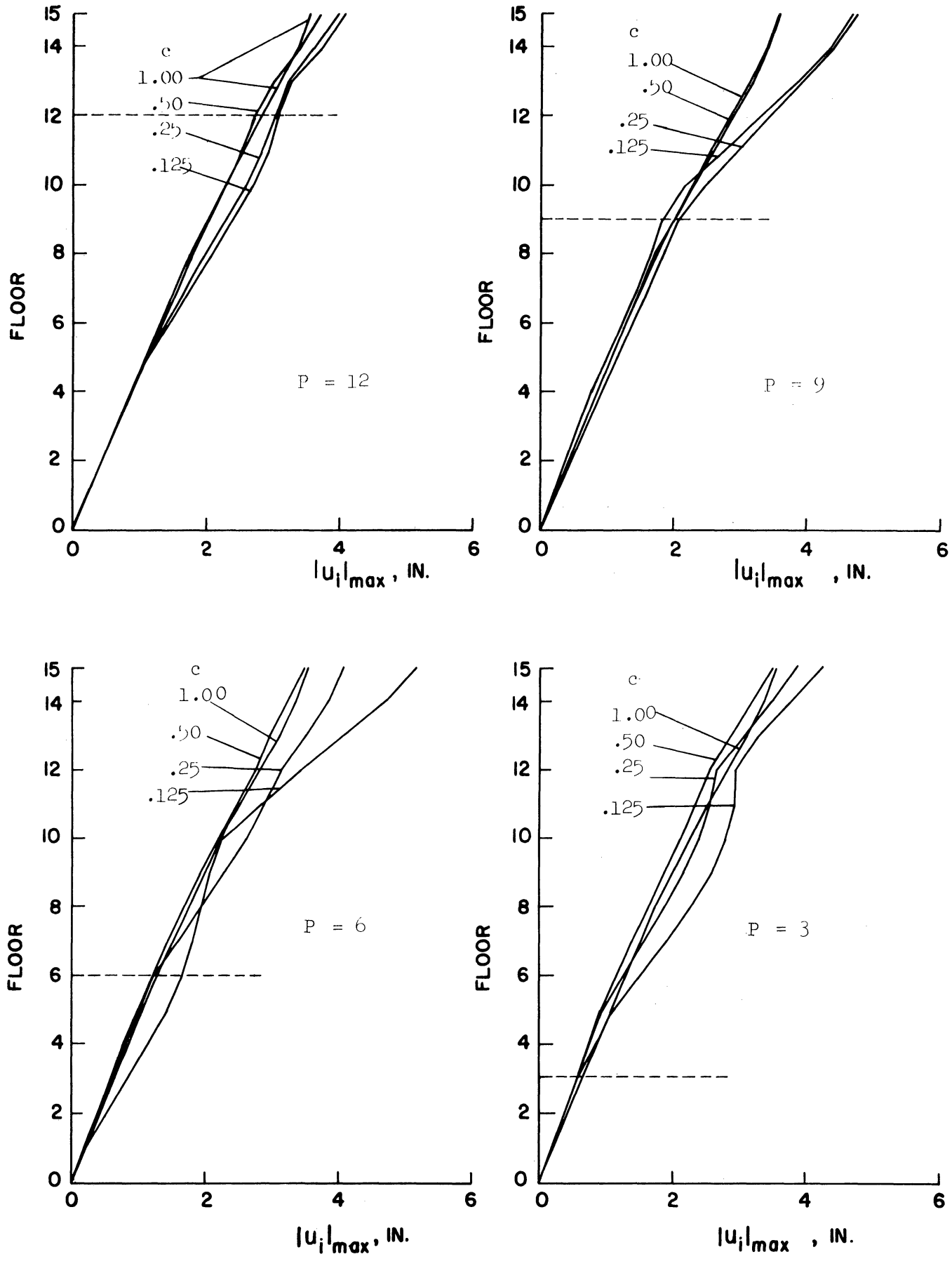

Figure 3.16. Maximum Response Envelopes, Floor Displacements. (Taft '52, N69°W)

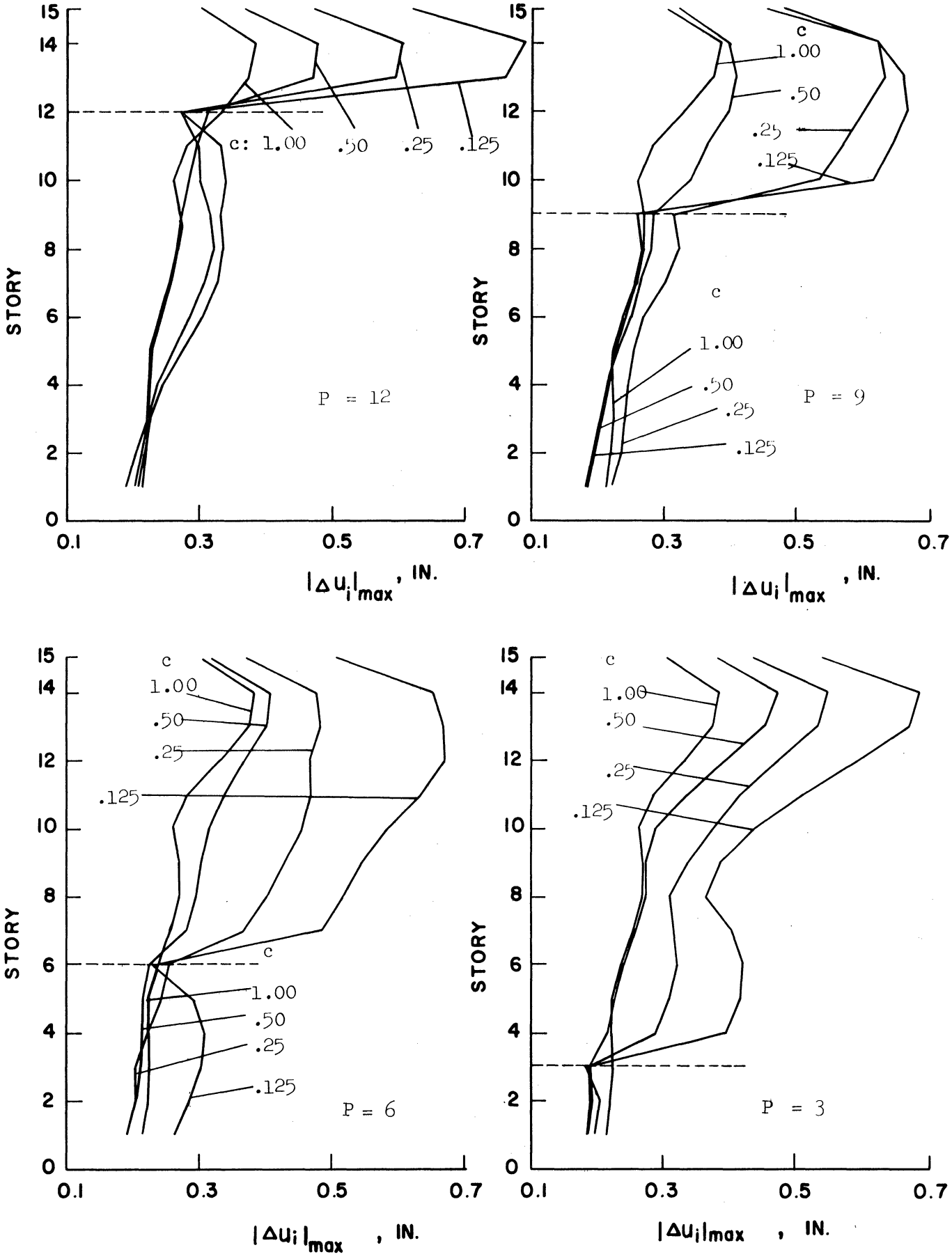

Figure 3.17. Maximum Response Envelopes, Story Displacements. (Taft '52, N69°W)

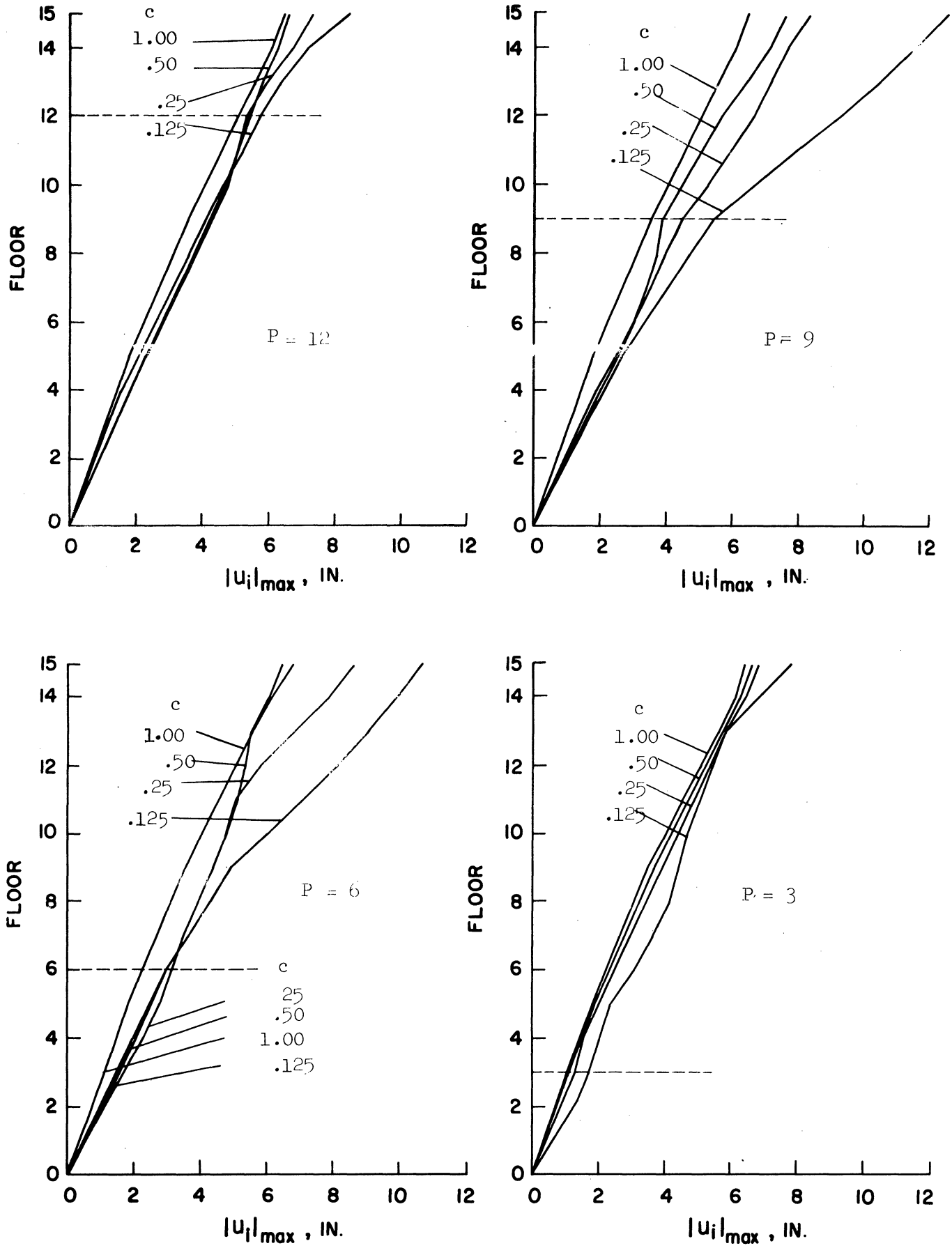

Figure 3.18. Maximum Response Envelopes, Displacements. (El Centro '40 S.)

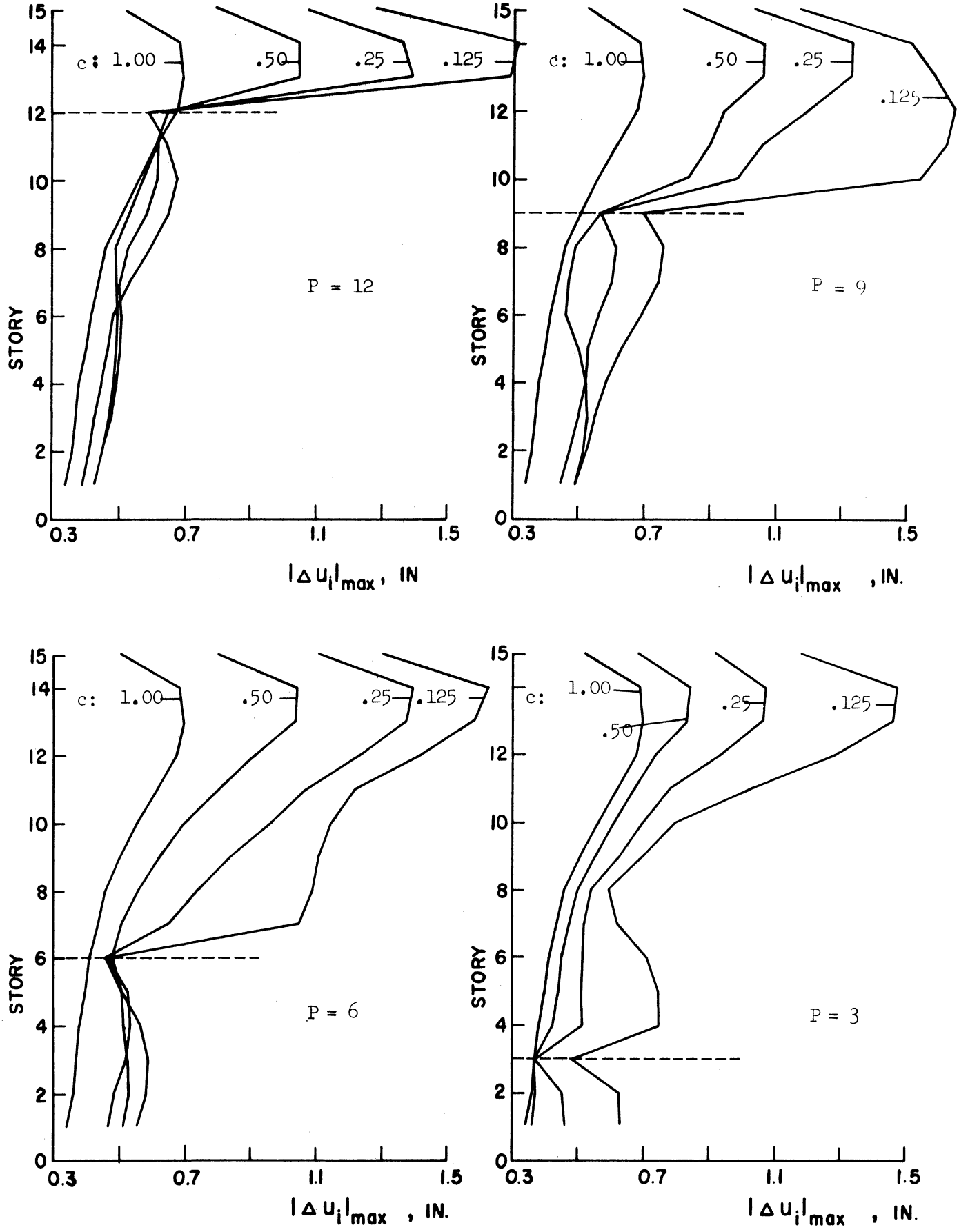

Figure 3.19. Maximum Response Envelopes, Story Displacements.
(El Centro '40 S.)

that in magnitude the El Centro responses are roughly twice as large as the Taft responses.

In structures with degrees of setback $c = .25$ and $c = .125$ (and also $c = .5$ in the case of El Centro), the maximum displacements of the floors in the tower portion are in general higher than the corresponding displacements of the uniform structure ($c = 1$). This increase in displacements is much more pronounced when the setback is at 6th or 9th stories than when the setback is at 3rd or 12th stories. This is true for both the Taft and the El Centro responses.

In the El Centro responses (Figure 3.18), the maximum displacements in the base portion are also, in general, slightly higher in buildings with setback ($c < 1$) than the corresponding displacements in the uniform building.

In the Taft responses, it is noted that maximum displacements in structures with $c = .50$ are not significantly different from, and in some cases are even less than, the corresponding displacements of the uniform structure.

The maximum relative story displacement (MRSD), Figures 3.17 and 3.19, in the tower portions of buildings with setback ($c < 1$) are also much larger than the corresponding displacements in uniform buildings ($c = 1$). The smaller the value of c, i.e, the smaller the tower section in comparison to the base section, the larger the MRSD in the tower; the MRSD's in the base portion do not vary regularly with c and also the changes are not as drastic as in tower portion.

The MRSD's for structures with $c = .25$ and $c = .125$ are extremely high, especially in the El Centro responses. In some cases drifts (story deflection/story height) greater than .01 are indicated, assuming a standard story height of 12'.

Shear Coefficients

The seismic shear coefficient at any level in a building is defined as the ratio of shear at that level to the total weight of the structure above that level. Since the structure is assumed to be simply coupled in stiffness the shear in any story is the stiffness times the relative story displacement of that story. Noting that the stiffness and mass are both assumed to be proportional to c in the tower portion (see Equation (3.62)), the MRSD's of Figures 3.17 and 3.19 also represent the effect of c on the maximum seismic coefficients on a different scale, although the change in scale is different for each story. Thus, Figures 3.17 and 3.19 also show an increase in seismic shear coefficients values in the tower portions of buildings with decreasing tower section (i.e. decreasing c). This increase is tremendous for small values of c, e.g. in the El Centro responses for the case $P = 12$ the seismic shear coefficient for the 14th story for $c = .125$ is over 250% greater than that of the uniform structure.

Next the maximum base shear coefficients and the tower-base shear coefficients of the Taft and the El Centro responses will be compared with those obtained from the 1966 Uniform Building Code.[3]

For uniform buildings the base shear coefficient according to the code is

$$C_B = \frac{.05}{(T)^{1/3}} \tag{3.73}$$

where T is the fundamental period of the building. The seismic shear coefficient at any other level is obtained from the code formula for lateral force distribution in uniform structures:

$$F_x = V_B \frac{W_x h_x}{\Sigma Wh} \tag{3.74}$$

where V_B is the base shear,

F_x is lateral force applied to a level designated as x,

W_x the portion of total deal load which is located at or is assigned to the level designated as x,

h_x height in feet to the level designated as x,

ΣWh is summation of the product of all W_x, h_x for the building.

Noting that mass is assumed to be lumped at floor level, x is replaced by i in the above formula for the ith floor level. Then seismic shear coefficient in the $(P + 1)$th story will be

$$C_T = \frac{\sum_{i=P+1}^{N} F_i}{\sum_{i=P+1}^{N} W_i} = V_B \cdot \frac{\sum_{i=P+1}^{N} W_i h_i}{\sum_{i=P+1}^{N} W_i \cdot \sum_{i=1}^{N} W_i h_i} \tag{3.75}$$

where $W_i = m_i \cdot g$, g being the acceleration due to gravity. The base shear V_B is given in terms of base shear coefficient of Equation (3.73) by

$$V_B = K C_B W \tag{3.76}$$

where $W = \sum_{i=1}^{N} W_i$ is the total dead load and K is a numerical coefficient varying between .67 and 1.50 reflecting the ability of structure to deform into the plastic range. Here K is taken equal to unity. Substituting for C_B from Equation (3.73) in Equation (3.76) and using the latter in Equation (3.75),

$$C_T = \frac{.05}{(T)^{1/3}} \frac{\sum_{i=P+1}^{N} W_i h_i}{\sum_{i=1}^{N} W_i h_i} \frac{\sum_{i=1}^{N} W_i}{\sum_{i=P+1}^{N} W_i} \qquad (3.77)$$

Equations (3.73) and (3.77) give the base shear coefficient and the seismic shear coefficient in the (P + 1)th story for uniform buildings as specified by the Uniform Building Code (UBC). For buildings with setback this code specifies the following:

> "Buildings having setbacks wherein the plan dimensions of the tower in each direction are at least 75 percent of the corresponding plan dimension of the lower part may be considered as a uniform building without setbacks for the purpose of determining seismic forces.
>
> "For other conditions of setbacks the tower shall be designed as a separate building using the larger of the seismic coefficient at the base of the tower determined by considering the tower as either a separate building for its own height or as part of the over-all structure. The resulting total shear from the tower shall be applied at the top of the lower part of the building which shall be otherwise considered separately for its own height."

Assuming that the degree of setback c is also the ratio of tower cross-sectional area to base cross-sectional area (as was the case with shear beam, see Equation (3.24)), according to the above specification

building with setbacks having $c < (3/4)^2 = .5625$ should be treated as uniform buildings. The values for the case $c = .75$ are therefore also computed from Equations (3.73) and (3.77).

The tower-base shear coefficient (C_T) for the cases $c = .5$, .25, and .125 were computed by either Equation (3.77) (tower as a part of the overall structure) or by

$$C_T = \frac{.05}{(T_T)^{1/3}} \tag{3.78}$$

(tower as a separate structure for its own height), whichever gave the greater value for C_T. In Equation (3.78) T_T is the period of the tower portion as a separate building. It turned out that for all cases ($c < .5$) Equation (3.77) gave the larger value for C_T.

The base shear coefficients C_B for the cases $c < .5625$ are given by

$$C_B = \frac{\frac{.05}{(T_B)^{1/3}} \sum_{i=1}^{P} W_i + C_T \sum_{i=P+1}^{N} W_i}{\sum_{i=1}^{N} W_i} \tag{3.79}$$

where T_B is the fundamental period of the base portion alone and C_T is the tower base shear coefficient computed as described above.

In computing the C_B and C_T values as described in the previous paragraphs, actual values of the various fundamental periods involved (viz. T, T_B, and T_T) have been used. The story height was assumed to be the same for all stories in computing h_i.

The C_B and C_T values thus obtained from the UBC specifications for 15-story buildings with setbacks at 12th, 9th, 6th and 3rd stories for various values of c (including c = 1 for the uniform building), along with the corresponding (maximum) values obtained from the Taft and El Centro responses described previously are given in Table III.2 and Table III.3.

As would be expected, the code values for both the coefficients are much smaller than the Taft and El Centro response values. For example for uniform building the base shear coefficient given by code specifications is about 1/3rd of the Taft value and about 1/4th of the El Centro value. Incidentally, the difference in the intensity of Taft and El Centro responses can also be noted from Tables III.2 and Table III.3. It would be uneconomical to design structures to remain elastic when subjected to earthquake ground motion as severe as that of the Taft and the El Centro records. The capacity of structures to deform inelastically, thus absorbing a large part of the energy imparted to it by earthquakes without collapsing, is relied upon in specifying design lateral loads smaller than would be suggested by the elastic analyses.

To measure the effectiveness of the code provisions for buildings with setback in the elastic range, the ratios of the base shear coefficient of building with setback to that of uniform building as obtained from the two responses and by application of code specifications are plotted against c in Figure 3.20. Similar plots for the ratios of tower-base shear coefficients are given in Figure 3.21.

The above mentioned ratios as obtained from approximate response values computed for the shear beam in the previous section are also plotted in Figures 3.20 and 3.21. It may be recalled that these values were

TABLE III.2

BASE SHEAR COEFFICIENTS (C_B)

P	c				
	1.00	0.75	0.50	0.25	0.125
	TAFT RESPONSES ($\beta_{1,2}$ = 4%, $\beta_{3,4}$ = 6%)				
12	.1210	.1184	.1158	.1171	.1105
9	.1210	.1075	.1068	.1321	.1117
6	.1210	.1132	.1145	.1190	.1685
3	.1210	.1188	.1134	.1256	.1416
	EL CENTRO RESPONSES ($\beta_{1,2}$ = 4%, $\beta_{3,4}$ = 6%)				
12	.1940	.2182	.2476	.2498	.2259
9	.1940	.2475	.2864	.2661	.2958
6	.1940	.2349	.3030	.3443	.2992
3	.1940	.2015	.2199	.3065	.4554
	CODE[3]				
12	.0457	.0461	.0534	.0511	.0496
9	.0457	.0461	.0614	.0587	.0558
6	.0457	.0460	.0671	.0678	.0655
3	.0457	.0458	.0668	.0731	.0775

TABLE III.3

TOWER-BASE SHEAR COEFFICIENTS (C_T)

P	c				
	1.00	0.75	0.50	0.25	0.125
	TAFT RESPONSES ($\beta_{1,2}$ = 4%, $\beta_{3,4}$ = 6%)				
12	.3124	.3578	.3937	.4983	.6366
9	.1744	.1851	.2279	.3567	.4118
6	.1576	.1537	.1719	.2262	.2985
3	.1298	.1262	.1272	.1694	.2318
	EL CENTRO RESPONSES ($\beta_{1,2}$ = 4%, $\beta_{3,4}$ = 6%)				
12	.5850	.6934	.8781	1.1672	1.4113
9	.3718	.4189	.5550	.6541	1.0254
6	.2676	.2917	.3128	.4049	.6405
3	.2230	.2388	.2521	.3007	.4365
	CODE(3)				
12	.0800	.0839	.0887	.0949	.0986
9	.0714	.0769	.0850	.0985	.1093
6	.0629	.0677	.0762	.0940	.1135
3	.0543	.0571	.0634	.0768	.0990

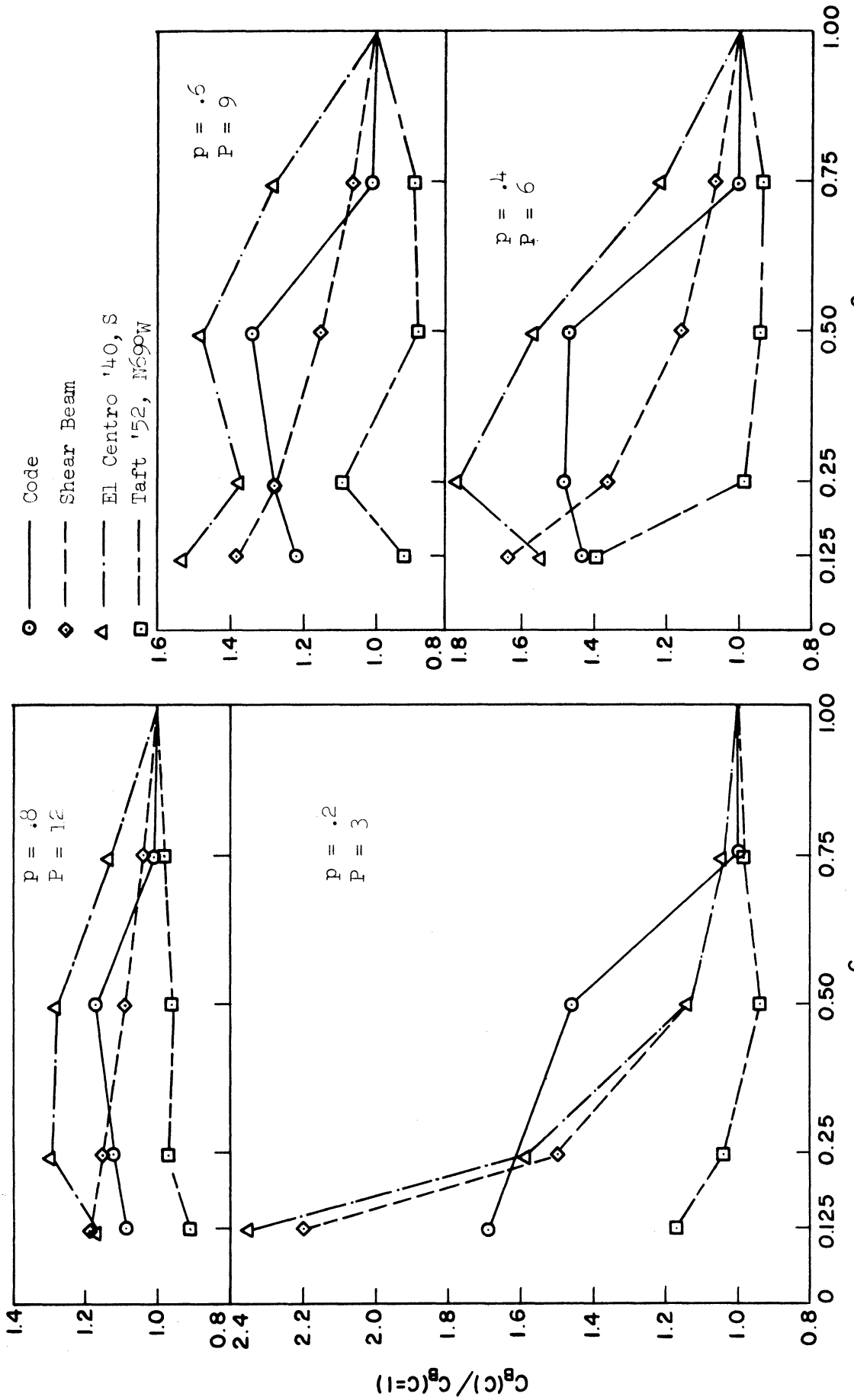

Figure 3.20. Comparison of Effect of Setback on C_B as Obtained from Responses and Code Specifications.

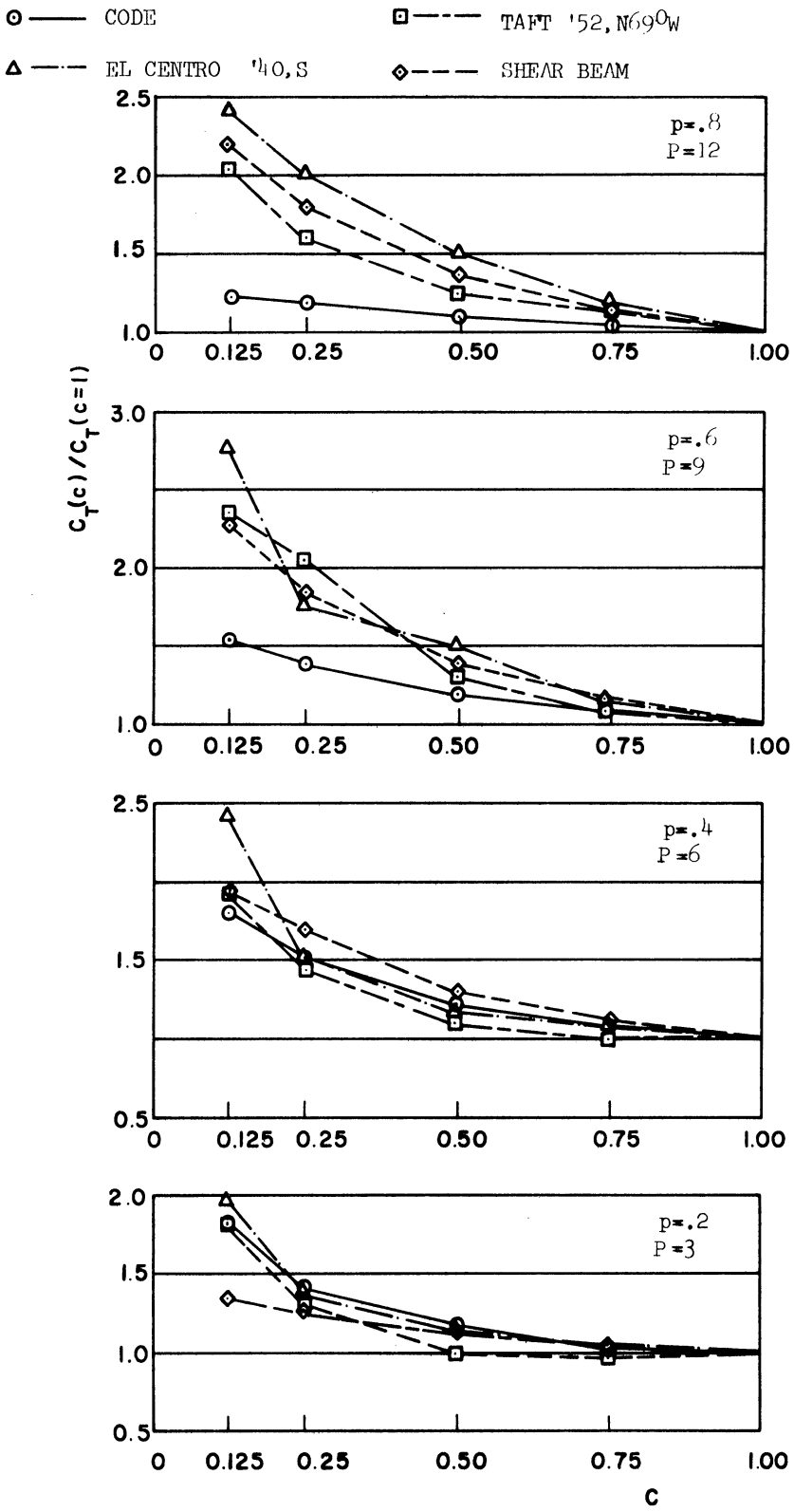

Figure 3.21. Comparison of Effect of Setback on C_T as Obtained from Responses and Code Specifications.

obtained by RSS superposition of the corresponding quantities in the first four modes and on the assumption that the velocity response spectrum S_v had the same constant value in each mode for all beams with various levels and degrees of setback.

The striking feature of Figure 3.20 is the disparity between the effect of setback on the base shear coefficients as obtained from the El Centro responses and as obtained from the Taft responses. The El Centro values in general show an increase in base shear coefficients as c decreases for all levels of setback, the increase becoming larger with lower levels of setback. The Taft values show in general a small and irregular decrease in C_B due to setbacks. The shear beam values demonstrate effects similar to the El Centro values (only more regularly) though the extent of increase in C_B is generally smaller. The code values also show an irregular increase in C_B for buildings with setback. The effect of setback on C_B' thus seems to be very much dependent on the nature (as represented roughly by the response spectra) of the earthquake excitation used to measure this effect.

Considerably more consistency is noticeable in Figure 3.21 in the effects of setback on the tower-base shear coefficient as obtained from the El Centro and the Taft responses. The tower-base shear coefficients, in general, are higher than the seismic coefficients at the corresponding levels in uniform buildings and increase as the tower cross section decreases in both responses. The same is true about the values obtained from code specifications.

There is however a significant difference in the extent of change in tower-base shear coefficients obtained from the four sets of responses when the setback level is above mid-height (p = .6, .8 or 9, 12). In general the increase is most in the El Centro responses and least in the code values, with the Taft response and the shear beam values falling somewhere in between. When the setback is below mid-height (p = .2, .4; P = 3, 6) the agreement between the four sets of values is generally good.

The above comparison of tower-base shear coefficients is based on the assumption that seismic coefficients at the various levels in the uniform structure as obtained from the code are equal to the corresponding response values. However, it is known that code specifications underestimate shears at levels near the top of structures as compared to the actual responses assuming that the code base shear is equal to the response base shear. This is clearly seen in Table III.4 wherein the ratio C_T/C_B at various levels in a uniform structure obtained from response and code values are given. The difference between the responses and code values of the tower-base shear coefficients for setback levels above midheight would thus be accentuated further if they were compared on the basis of equal base shear coefficients in uniform structures.

TABLE III.4

C_T/C_B RATIOS FOR UNIFORM STRUCTURE.

Story	Taft	El Centro	Code
12	2.58	3.02	1.75
9	1.44	1.92	1.56
6	1.30	1.38	1.38
3	1.07	1.15	1.19

Comparison of Code and Response Shear Distributions

Shear V_i in the ith story (i = 1 through N) as specified by the code may be as computed as follows. In structures which are to be treated as uniform as per the code specifications,

$$V_i = \sum_{j=i}^{N} F_j$$

$$= V_B \frac{\sum_{j=i}^{N} W_i h_i}{\sum_{k=1}^{N} W_k h_k} \qquad (3.80)$$

where V_B is given by Equation (3.76).

In structures where the tower and the base portions are to be treated as separate structures as per the code specifications:

for $N \geq i \geq P + 1$,

$$V_i = V_T \frac{\sum_{j=i}^{N} W_j h_j}{\sum_{k=P+1}^{N} W_k h_k} \qquad (3.81a)$$

and for $P \geq i \geq 1$,

$$V_i = V_T + V_B' \frac{\sum_{j=i}^{P} W_j h_j}{\sum_{k=1}^{P} W_k h_k} \qquad (3.81b)$$

In Equations (3.81a) and (3.81b) V_T is the shear at the base of tower acting alone,

$$V_T = C_T \sum_{i=P+1}^{N} W_i \qquad (3.82)$$

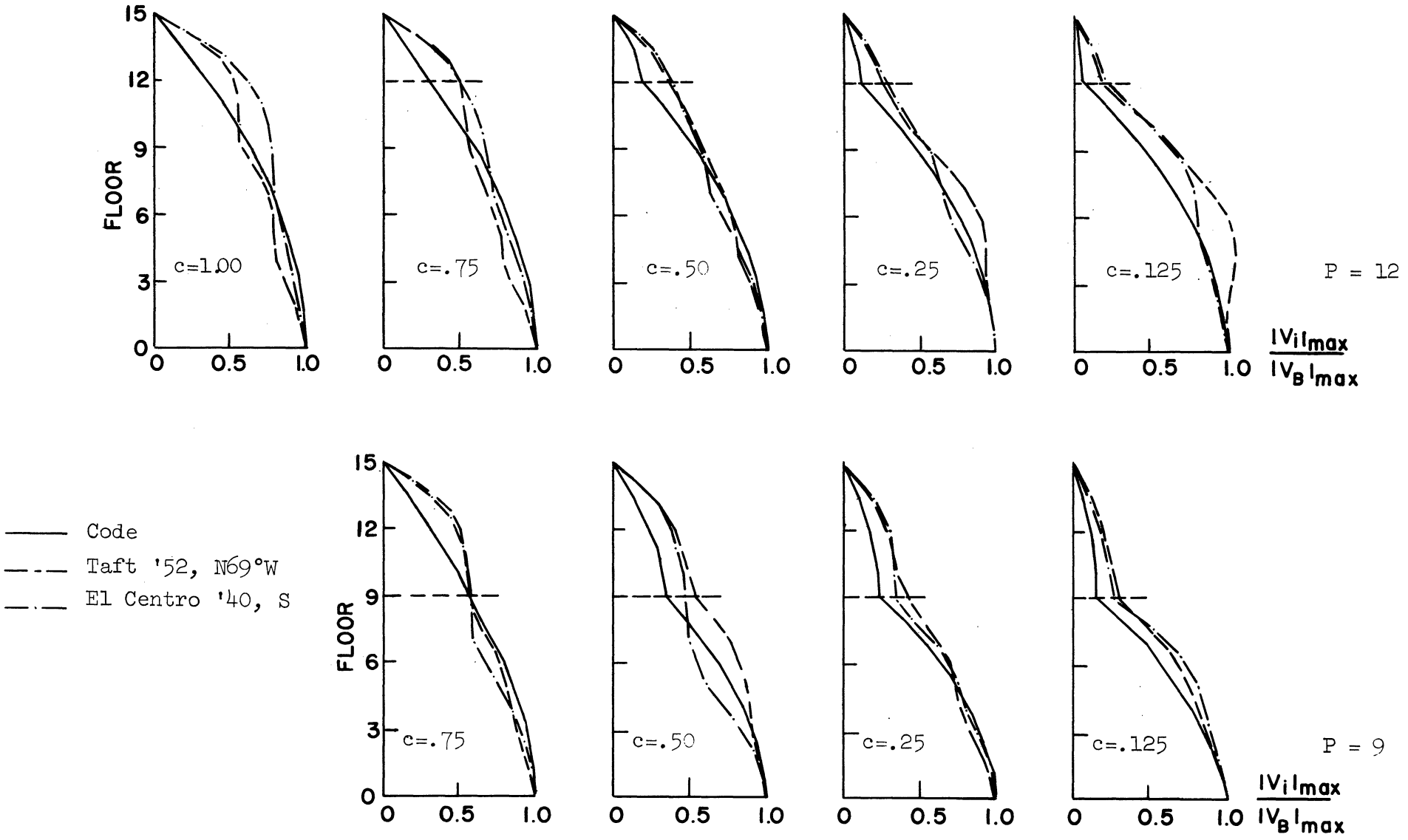

Figure 3.22. Comparison of Code and Response Shear Distributions.

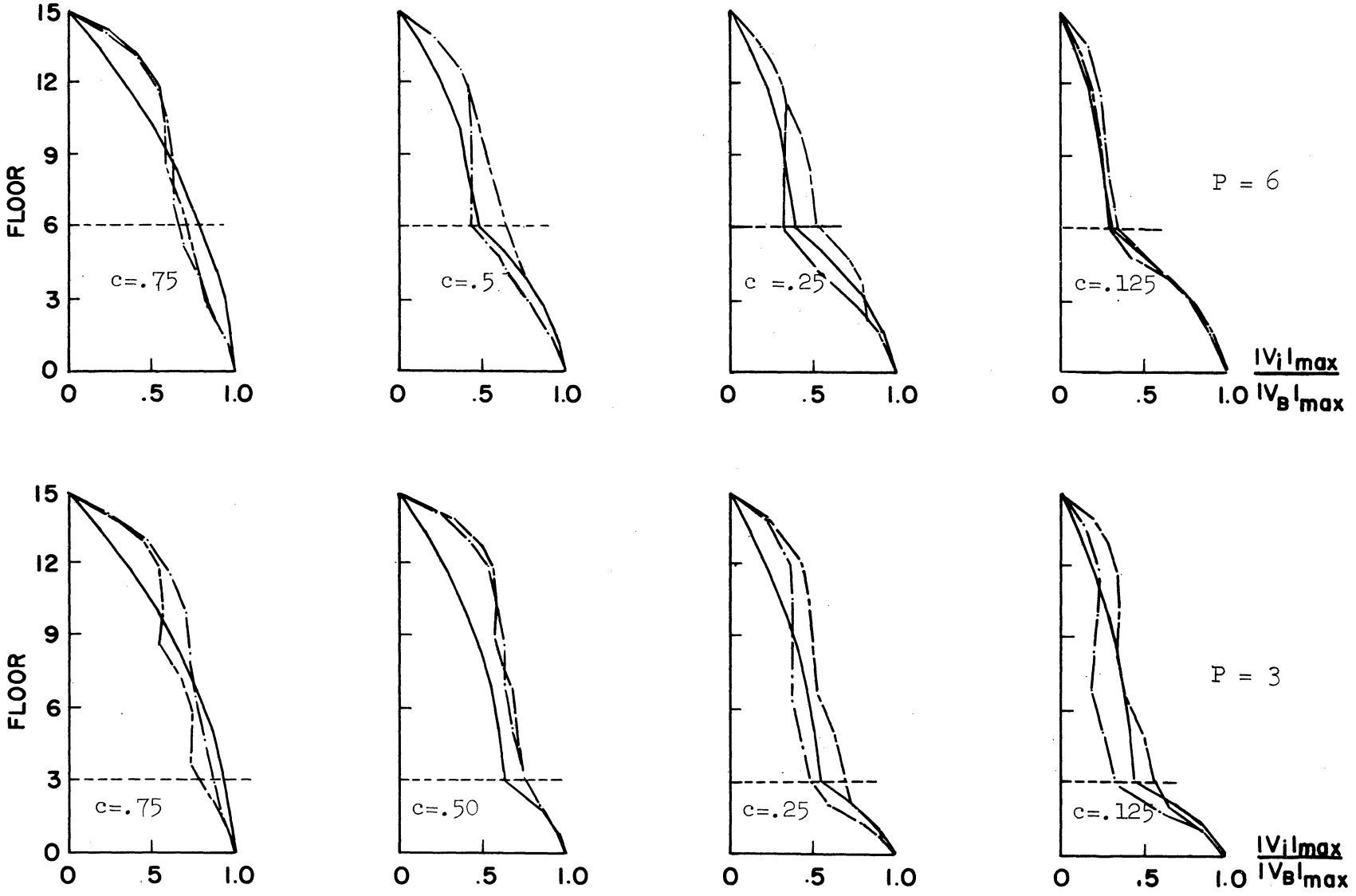

Figure 3.22. (Cont'd.) Comparison of Code and Response Shear Distributions.

where C_T is larger of the values given by Equations (3.77) or (3.78); and V_B' is the shear at the base of base portion acting alone,

$$V_B' = \frac{.05}{(T)^{1/3}} \sum_{i=1}^{P} W_i \, . \qquad (3.83)$$

Shear distributions (V_i/V_B) obtained as described above from the Uniform Building Code are compared with the response shear distributions for the uniform structure $(c = 1)$ as well as structures with various degrees and levels of setback in Figure 3.22.

As expected as c decreases the shears obtained from the responses as well as the code decrease throughout the height of the structure relative to the base shear. In the code shear distribution kinks are apparent at the setback level for structures having degrees of setback $c \leq 0.5$. Such distinct kinks at the setback level are not always apparent in the response shear distributions.

The response shear distribution values exceed those given by the code in the upper half (approximately) of the uniform structure. The same is true in the case of structures with setback $(c \neq 1)$ in the upper portion generally and in some cases almost throughout the height of the structure.

CHAPTER IV

BUILDINGS WITH UNSYMMETRIC SETBACKS

INTRODUCTION

The coupled lateral-torsional vibrations of a building with unsymmetric setback are examined in this chapter. The geometric asymmetry of the setback is assumed to be the only reason for the lack of dynamic symmetry; i.e., the tower and the base portions of the building with setback are assumed to be dynamically symmetric by themselves. Again two models of a building are used, a shear beam and a lumped mass shear building.

Results are obtained for a building with setback unsymmetric about one principal direction only, with given level and degree of setback, and having fixed and similar cross-sections in plan in both the base and the tower portions. These results are examined for the effect of variation in the eccentricity of the setback upon the modal properties of the two models and upon the response of the lumped mass model to two strong-motion earthquake records.

SHEAR BEAM

This section is concerned with the coupled lateral-torsional vibrations of a vertical cantilever shear beam of rectangular section stepped at one location along its height. The shear beam is a hypothetical ideal beam whose properties have been described in Appendix A. The coupling in the lateral and torsional vibrations of the shear beam

is assumed to be due to the asymmetry of the setback, the tower centroid being offset from the base centroid by distances e_1 and e_2 along the x and y axis, respectively, as shown in Figure A.1.

Equations of Motion and Solution

The equations of motion for the coupled vibration of the vertical cantilever shear beam with unsymmetric setback along with appropriate boundary conditions and conditions at the setback are derived in the Appendix. The solution of these equations by the method of separation of variables is also presented in Appendix A. For convenience, the equations of motion and the solution will be briefly described here. Notations used are as defined in Appendix A.

The equations of motion (Equation (A.7)) are:

$$m_i x_{i,tt} - k_i x_{i,zz} = f_i(z, t) \qquad i = 1, 2, 3 ; \tag{4.1}$$

the boundary conditions (Equations (A.9), (A.10)) are:

$$x_i(o, t) = 0 \qquad i = 1, 2, 3 \tag{4.2}$$

$$V_i(\ell, t) = 0 \qquad i = 1, 2, 3 ; \tag{4.3}$$

and the conditions at the steps (Equations (A.11), (A.12)) are:

$$\begin{aligned} V_i(h\text{-}o, t) &= V_i(h\text{+}o, t) \qquad i = 1, 2 \\ [V_3 - e_1 V_2 + e_2 V_1]_{(h\text{-}o,t)} &= V_3(h\text{+}o, t) \end{aligned} \tag{4.4}$$

$$\begin{aligned} [x_1 - e_2 x_3]_{(h\text{-}o, t)} &= x_1(h\text{+}o, t) \\ [x_2 + e_1 x_3]_{(h\text{-}o, t)} &= x_2(h\text{+}o, t) \\ x_3(h\text{-}o, t) &= x_3(h\text{+}o, t) . \end{aligned} \tag{4.5}$$

The solution of Equation (4.1) may be written as (Equation (A.29))

$$x_i = \sum_{k=1}^{\infty} \phi_{ik} \eta_k \tag{4.6}$$

where ϕ_{ik} is the ith component of the kth mode (i = 1 refers to translation along x axis, i = 2 to translation along y axis, i = 3 to rotation about the vertical); and η_k is the kth modal displacement and is given by (Equation (A.36)):

$$\ddot{\eta}_k + 2\beta_k \omega_k \dot{\eta}_k + \omega_k^2 \eta_k = g_k(t) \quad . \tag{4.7}$$

In Equation (4.7) ω_k is the kth mode frequency; β_k is thr fraction of critical damping in the kth mode and the term containing it in Equation (4.7) is added on the assumption that viscous damping exists and that the undamped modes remain valid for the damped case also; and dots above variables denote differentiation with respect to time. Finally, $g_k(t)$ in Equation (4.7) is given by (Equation (A.35)):

$$g_k(t) = \frac{\sum_{i=1}^{3} \int_0^{\ell} f_i \phi_{ik} \, dz}{\sum_{i=1}^{3} \int_0^{\ell} m_i \phi_{ik}^2 \, dz} \quad . \tag{4.8}$$

When the driving forces f_i in Equation (4.1) result from base acceleration, they are given by

$$f_i = - m_i \ddot{x}_{oi} \tag{4.9}$$

where $\ddot{x}_{oi}$ is the ith component of the base acceleration. The torsional component (i = 3) in ground motion due to earthquake is assumed to be negligible and will be taken here to be nil. Then, using Equation (4.9), $g_k(t)$ may be written as

$$g_k(t) = -(\lambda_{1k}\,\ddot{x}_{01} + \lambda_{2k}\,\ddot{x}_{02}) \tag{4.10}$$

where

$$\lambda_{ik} = \frac{\int_0^{\ell} m_i\,\phi_{ik}\,dz}{\sum_{i=1}^{3}\int_0^{\ell} m_i\,\phi_{ik}^2\,dz} \,. \tag{4.11}$$

The quantities λ_{1k} and λ_{2k} are then the x- and y-direction modal participation coefficients, respectively.

The mode shapes ϕ_{ik} (i = 1, 2, 3) are given by:

in $0 < z < h$

$$\phi_{ik} = C_{iok}\cos\frac{\omega_k z}{q_i} + C_{i1k}\sin\frac{\omega_k z}{q_i} \tag{4.12a}$$

and in $h < z < \ell$

$$\phi_{ik} = C_{i2k}\cos\frac{\omega_k z}{s_i} + C_{i3k}\sin\frac{\omega_k z}{s_i} \,. \tag{4.12b}$$

In Equation (4.12) q_i and s_i are given by (Equation (A.18))

$$\begin{aligned} q_i^2 &= \frac{k_i}{m_i} && 0 < z < h \,, \\ s_i^2 &= \frac{k_i}{m_i} && h < z < \ell \,, \end{aligned} \qquad i = 1,2,3 \tag{4.13}$$

where k_i and m_i are the stiffness and inertia (lateral or torsional) per unit length of the shear beam.

By virtue of the boundary condition (4.2)

$$C_{io} = 0 \qquad i = 1, 2, 3 \tag{4.14}$$

and the mode shapes are then given by:

in $0 < z < h$

$$\phi_{ik} = C_{ik} \sin \frac{\omega_k z}{q_i} , \tag{4.15a}$$

and in $h < z < \ell$

$$\phi_{ik} = C_{i2k} \cos \frac{\omega_k z}{s_i} + C_{i3k} \sin \frac{\omega_k z}{s_i} . \tag{4.15b}$$

The orthogonality of the modes

$$\sum_{i=1}^{3} \int_{o}^{\ell} m_i \phi_{ik} \phi_{ij} \, dz = 0 \qquad j \neq k \tag{4.16}$$

is established in Appendix A.

Application of the remaining boundary conditions, Equation (4.3), and conditions at the step, Equations (4.4) and (4.5), to Equation (4.15) leads to a set of linear homogeneous simultaneous equations in $C_{ij}(i, j = 1,2,3)$, Equation (A.22). Non-trivial solutions C_{ijk} $(k = 1,2,3,..)$ of Equation (A.22) exists for such values of $\omega = \omega_k$ $(k = 1,2,3,...)$ which make the determinant of the coefficients of C_{ij}'s equal to zero. These values ω_k are then the frequencies and the corresponding solutions C_{ijk} give the mode shapes of the shear beam.

New Notations

Before proceeding further the following notations are introduced:

$$\begin{aligned} \alpha_b &= b_2/b_1 \\ \alpha_t &= a_2/a_1 \end{aligned} \tag{4.17}$$

$$\sigma_b^2 = (\gamma^2/\alpha_b + \alpha_b)/(1/\alpha_b + \alpha_b)$$

$$\sigma_t^2 = (\gamma^2/\alpha_t + \alpha_t)/(1/\alpha_t + \alpha_t) \quad . \tag{4.18}$$

The term α is then the ratio of sides of the shear beam section. The subscripts b and t denote, respectively, the base portion and the tower portion of the shear beam. The term γ^2 is the ratio of rigidity of the shear beam in the y direction to its rigidity in the x direction. It can also be seen as the ratio (from Equations (A.5), (A.6) and (4.13)):

$$\gamma^2 = q_2^2/q_1^2 = s_2^2/s_1^2 \tag{4.19}$$

and it is assumed to have the same value in the base and tower portions of the shear beam.

From Equations (A.4), (A.5), (4.13) and (4.16), it can also be seen that

$$\sigma_b^2 = q_3^2/q_1^2$$

$$\sigma_t^2 = s_3^2/s_1^2 \quad . \tag{4.20}$$

Using Equations (4.13), (4.19) and (4.20), it may be shown that

$$\gamma^2 = \frac{k_2/m_2}{k_1/m_1}$$

and

$$\sigma^2 = \frac{k_3/m_3}{k_1/m_1} \quad .$$

The similarity in the nature of the quantities γ^2 and σ^2 is apparent from these equations. However, unlike γ^2, σ^2 has different values in the base and the tower portions of the beam unless $\alpha_b = \alpha_t$. If $\alpha_b = \alpha_t$ then, as is obvious from Equation (4.17), $\sigma_b = \sigma_t$.

The following notations are also introduced for convenience:

$$d_b = \sigma_b \cdot (1/\alpha_b + \alpha_b)/12$$

$$d_t = c^2 \cdot \sigma_t \cdot (1/\alpha_t + \alpha_t)/12 \ . \tag{4.21}$$

Further, the following definitions are recalled from Chapter III:

$$p = h/\ell \tag{4.22}$$

$$c = a_1 a_2 / b_1 b_2 \tag{4.23}$$

$$\omega' = \omega/\sqrt{\frac{G}{\rho \ell^2}} = \frac{\omega \ell}{q_1} = \frac{\omega \ell}{s_1} \ ; \tag{4.24}$$

p is termed the level of setback and c the degree of setback (in a restricted sense in this chapter) and ω' is the non-dimensionalized form of frequency.

The eccentricities e_1 and e_2 of the tower centroid with respect to the base centroid and the coefficients C_{3j} $(j = 1,2,3)$ are redefined with a slight change to make Equation (A.22) dimensionally homogeneous.

$$e'_i = e_i/\sqrt{A_B} \qquad i = 1, 2 \tag{4.25}$$

$$C'_{3j} = C_{3j}\sqrt{A_B} \qquad j = 1, 2, 3 \tag{4.26}$$

where $A_B = b_1 b_2$ is the plan area of the base portion of the beam.

$$
\begin{bmatrix}
0 & -\sin\omega' & \cos\omega' & 0 & 0 & 0 & 0 & 0 & 0 \\
-\sin\omega'p & \cos\omega'p & \sin\omega'p & 0 & 0 & 0 & 0 & 0 & 0 \\
\cos\omega'p & \csin\omega'p & -c\cos\omega'p & 0 & 0 & 0 & 0 & 0 & 0 \\
0 & 0 & 0 & 0 & \cos\frac{\omega'}{\gamma} & \sin\frac{\omega'p}{\gamma} & -c\cos\frac{\omega'p}{\gamma} & 0 & 0 \\
0 & 0 & 0 & -\sin\frac{\omega'}{\gamma} & \cos\frac{\omega'p}{\gamma} & c\sin\frac{\omega'p}{\gamma} & 0 & 0 & 0 \\
0 & 0 & 0 & -\sin\frac{\omega'p}{\gamma} & \cos\frac{\omega'p}{\gamma} & -c\sin\frac{\omega'p}{\gamma} & 0 & 0 & 0 \\
e_2'\cos\omega'p & 0 & 0 & 0 & -\gamma e_1'\cos\frac{\omega'p}{\gamma} & 0 & 0 & 0 & 0
\end{bmatrix}
\begin{bmatrix}
0 & 0 & 0 & 0 & 0 & 0 & 0 & 0 & 0 \\
0 & 0 & e_2'\sin\frac{\omega'p}{\sigma_b} & 0 & -e_1'\sin\frac{\omega'p}{\sigma_b} & 0 & 0 & -\sin\frac{\omega'p}{\sigma_b} & d_b\cos\frac{\omega'p}{\sigma_b} \\
0 & 0 & 0 & 0 & 0 & 0 & -\sin\frac{\omega'}{\sigma_t} & \cos\frac{\omega'p}{\sigma_t} & d_t\sin\frac{\omega'p}{\sigma_t} \\
0 & 0 & 0 & 0 & 0 & 0 & \cos\frac{\omega'}{\sigma_t} & \cos\frac{\omega'p}{\sigma_t} & -d_t\cos\frac{\omega'p}{\sigma_t}
\end{bmatrix}
=
\begin{bmatrix}
c_{11} & c_{12} & c_{13} & c_{21} & c_{22} & c_{23} & c'_{31} & c'_{32} & c'_{33}
\end{bmatrix}
\tag{4.27}
$$

Frequency Equation

Introducing the above changes in notation, Equation (A.22) may be re-written here as Equation (4.27). Expanding the determinant of the coefficients with the help of Laplacian expansion of a determinant(38) and equating it to zero, one gets the frequency equation

$$f(\omega') \equiv f_1 f_2 f_3 - c \sin \frac{\omega' p}{\sigma_b} \cos \frac{\omega'(1-p)}{\sigma_t} \left[e_2'^2 f_2 \cos \omega' p \sin \omega'(1-p) + \gamma \, e_1'^2 \, f_1 \cos \frac{\omega' p}{\gamma} \sin \frac{\omega'(1-p)}{\gamma} \right] = 0 \quad (4.28)$$

where

$$f_1(\omega') = c \sin \omega' p \sin \omega'(1-p) - \cos \omega' p \cos \omega'(1-p), \quad (4.29)$$

$$f_2(\omega') = c \sin \frac{\omega' p}{\gamma} \sin \frac{\omega'(1-p)}{\gamma} - \cos \frac{\omega' p}{\gamma} \cos \frac{\omega'(1-p)}{\gamma}, \quad (4.30)$$

and

$$f_3(\omega') = d_t \sin \frac{\omega' p}{\sigma_b} \sin \frac{\omega'(1-p)}{\sigma_t} - d_b \cos \frac{\omega' p}{\sigma_b} \cos \frac{\omega'(1-p)}{\sigma_t}. \quad (4.31)$$

From Equation (3.22) of Chapter III, it is evident that $f_1(\omega') = 0$ is the frequency equation of uncoupled translational vibration in the x direction of the shear beam with $e_2' = 0$. The quantity f_1 is also the determinant of the upper most 3×3 diagonal submatrix of the matrix of coefficients in Equation (4.24). This submatrix is associated with the translational vibration in x direction and when $e_2' = 0$ it will form the coefficient matrix of C_{1j} $(j = 1,2,3)$, equations in which will be uncoupled from the rest of the equations in C_{ij} $(i = 2,3,\ j = 1,2,3)$ in Equation (4.27).

Similarly, f_2 is the determinant of the central 3 x 3 diagonal submatrix in Equation (4.27) and is associated with the translational vibration in the y- direction of the shear beam. When the setback is such that $e_1' = 0$, the equation $f_2(\omega') = 0$ is the frequency equation of the uncoupled translational vibration in the y direction.

Finally, $f_3(\omega')$, which is in a slightly different form than f_1 or f_2, is the determinant of the lowermost 3 x 3 diagonal submatrix in Equation (4.27). It refers to the torsional vibration of the shear beam about a vertical axis. When both e_1' and e_2' are equal to zero, the equation $f_3(\omega') = 0$ is the frequency equation of the uncoupled torsional vibration of the shear beam.

The zeroes of $f(\omega')$, Equation (4.28), are found by linear interpolation. There are cases of repeated frequencies for specific properties of the shear beam even when e_1' and e_2' are not equal to zero. In the computer program written for locating the frequencies of the unsymmetrically stepped shear beam, provision was not made for spotting repeated frequencies. Only one case of repeated frequency, of multiplicity two, was found in the results presented in this report. The details of this case are mentioned later. Suspicion of two missing modes in results obtained from the above program led to a detailed check of this particular case, and repeated frequency was confirmed by the behavior of $f(\omega')$ at the value of ω' equal to the repeated frequency (viz. $f = 0$ and $\frac{df}{d\omega'} = 0$).

Evaluation of Coefficients C_{ijk}

Equation (4.27) can be solved for C_{ijk} $(i,j = 1,2,3)$ when $\omega' = \omega_k'$ for which the determinant of the coefficients is zero in the

following manner for the general unsymmetric case ($e_1' \neq 0$, $e_2' \neq 0$) . First of all it is noted that Equations (4.27) being a linear homogeneous set, only the relative values of C_{ijk} can be determined. The case of repeated frequency is assumed not to occur. (This case is considered later.) A normalization process is used to assign a unique numerical value to each of the C_{ijk}'s. To this end let

$$\phi'_{3k}(\ell) = C'_{32k} \cos \frac{\omega'_k \ell}{\sigma_t} + C'_{33k} \sin \frac{\omega'_k \ell}{\sigma_t} = 1 \tag{4.32}$$

assuming that $\phi'_{3k}(\ell) \neq 0$ where $\phi'_{3k} = \phi_{3k} \cdot \sqrt{A_B}$, see Equation (4.26)). Then the first of the last three equations in Equation (4.27) leads to

$$C'_{32k} = \cos \frac{\omega'_k}{\sigma_t} \tag{4.33a}$$

and

$$C'_{33k} = \sin \frac{\omega'_k}{\sigma_t} \, . \tag{4.33b}$$

The second of the last three equations in Equation (4.29) then yields

$$C'_{31k} = \frac{\cos \omega'_k(1-p)/\sigma_t}{\sin \omega'_k p/\sigma} \quad \text{if } \sin \frac{\omega'_k p}{\sigma_b} \neq 0 \, . \tag{4.33c}$$

If $\sin \frac{\omega'_k p}{\sigma_b} = 0$, then it is clear from Equation (4.27) that the mode will consist only of the rotational components the other two translational components vanishing, i.e., $C_{1jk} = C_{2jk} = 0$, $j = 1,2,3$. Thus, the last equation of Equation (4.27) would then give

$$C'_{31k} = \frac{d_t \sin \omega'_k(1-p)/\sigma_t}{d_b \cos \omega'_k \, p/\sigma_b} \tag{4.33d}$$

Assuming that $\sin \frac{\omega'_k p}{\sigma_b} \neq 0$, the first three equations and the middle three equations of Equation (4.27) can be solved, respectively, for

C_{1jk} and C_{2jk} $(j = 1,2,3)$ by means of Craemer's Rule:

$$C_{11k} = \{e'_2 \; C'_{31k} \sin \frac{\omega'_k p}{\sigma_b} \quad C \sin \omega'_k (1-p)\}/f_1$$

$$C_{12k} = \{e'_2 \; C'_{31k} \sin \frac{\omega'_k p}{\sigma_b} \quad \cos \omega'_k \cos \omega'_k p\}/f_1 \qquad (4.34)$$

$$C_{13k} = \{e'_2 \; C'_{31k} \sin \frac{\omega'_k p}{\sigma_b} \quad \sin \omega'_k \cos \omega'_k p\}/f_1 \quad ;$$

and

$$C_{21k} = -\{e'_1 \; C'_{31k} \sin \frac{\omega'_k p}{\sigma_b} \quad c \sin \frac{\omega'_k (1-p)}{\gamma}\}/f_2$$

$$C_{22k} = -\{e'_1 \; C'_{31k} \sin \frac{\omega'_k p}{\sigma_b} \cos \frac{\omega'_k}{\gamma} \cos \frac{\omega'_k p}{\gamma}\}/f_2 \qquad (4.35)$$

$$C_{23k} = -\{e'_1 \; C'_{31k} \sin \frac{\omega'_k p}{\sigma_b} \sin \frac{\omega'_k}{\gamma} \cos \frac{\omega'_k p}{\gamma}\}/f_2$$

If $f_1 = 0$, then the mode shape consists only of the x-translational component and the other two components are absent. Similarly, if $f_2 = 0$, the mode shape consists only of y-translational component. In such cases the sets of first three or the second three equations can be solved for C_{1jk} or C_{2jk} $(j = 1,2,3)$, respectively in the same manner as was done for C_{3jk} above.

In the case when $\phi'_{3k}(\ell) = 0$, it is clear from Equation (4.15b) and the boundary condition $V_3(\ell) = 0$ (which means $\phi'_{3,z}(\ell) = 0$) that

$$C'_{32k} = C'_{33k} = 0 \quad . \qquad (4.36)$$

Arbitrary value may then be assigned to C'_{31k}, and Equations (4.31) and (4.32) may be solved for this value of C'_{31k}.

The above procedure of computing C_{ijk} does not take account of all the possible special cases that may arise. For example, the case of repeated frequencies mentioned earlier is not accounted for in this procedure. The case of isotropic $(\gamma^2 = 1)$ shear beam with unsymmetric setback was mentioned in the Appendix. Since such a beam has a (vertical) plane of dynamic symmetric passing through the centroids of the tower and the base portions it can be treated as a beam with setback unsymmetric about one axis by appropiately rotating the x and y axes. This case is also not accounted for in the above procedure except when either e'_1 or e'_2 is zero.

In the case of repeated frequencies there are as many associated linearly independent modes as the multiplicity of the repeated frequency (for the type of problem under consideration). The coefficients C_{ijk} may then be evaluated as follows. A number of coefficients equal to the multiplicity of the frequency are assigned arbitrary values and Equation (4.27) is solved for the remaining coefficients. The number of linearly independent sets of arbitrary values that may be assigned to the chosen coefficients is equal to the multiplicity of the frequency. Equation (4.27) can therefore be solved for each of the set of arbitrary values of the chosen coefficients. Thus there will be as many linearly independent sets of coefficients C_{ijk} satisfying Equation (4.27) for the repeated frequency as the multiplicity of the frequency. Care is needed in choosing the coefficients to be assigned arbitrary values in that they should not be vanishing for all the modes of the repeated frequency.

Modes thus obtained will be orthogonal with respect to the modes of other frequencies of the beam, but they are not neccessarily mutually orthogonal. However, since any linear combination of the modes

belonging to a single frequency is also a mode of that frequency, a mutually orthogonal set may be easily found by appropriate linear combination of the computed modes.

The above procedure was used in evaluating C_{ijk}'s by hand computation for the particular case of repeated frequency encountered.

Parameters of the Problem

The parameters involved in the problem of coupled lateral torsional vibrations of the shear beam with unsymmetric setback then are: p, c, α_b, α_t, γ^2, e_1', and e_2' ; σ_b^2 and σ_t^2 may be considered as parameters in place of α_b and α_t, although they are also dependent on γ^2, see Equation (4.18).

The number of parameters involved in the problem makes a complete study of it unfeasible. All the same, the range of possible variation of each of the parameters is discussed below. Later on, the restricted range for which the problem is studied is outlined.

The quantities p and c are, respectively, the level and degree of setback and were first defined in Chapter III by Equations (3.20) and (3.24). Their ranges are:

$$0 \leq p \leq 1 \tag{4.37}$$

and

$$0 < c \leq 1 \tag{4.38}$$

with p = 0, p = 1, and c = 1 representing uniform beams.

The ratio of the lengths of sides of the beam cross-section, α, can take on any positive value. In reality, though, buildings (with rectangular cross-sections) are restricted to a much smaller range around

$\alpha = 1$. The subscripts t and b of α denote the tower and base portions, respectively. For a given c and α_b the range of α_t is restricted to

$$c\,\alpha_b \leq \alpha_t \leq \alpha_b/c \quad . \tag{4.39}$$

The quantities e_1 and e_2 are the offsets of the tower centroid from the base centroid along the x and y axes, respectively; e_1' , e_2' are in nondimensionalized form, see Equation (4.25). For given c , α_b, and α_t, e_1' and e_2' are restricted within the range:

$$0 \leq | e_1' | \leq 1/2 \left(\sqrt{1/\alpha_b} + \sqrt{c/\alpha_t}\right) \tag{4.40}$$

$$0 \leq | e_2' | \leq 1/2 \left(\sqrt{\alpha_b} + \sqrt{c\alpha_t}\right) \quad . \tag{4.41}$$

The frequencies of the shear beam with unsymmetric setback are dependent only on the arithmetical value of e_1' and e_2' and are independent of their signs as is apparent from Equation (4.25). Also, as can be verified from Equations (4.30), (4.31), and (4.32), a change in sign in e_1' and/or e_2' will change the signs of one or two components of the mode shapes with respect to its third component but otherwise will not affect the mode shape. Since this will not affect the numerical value of any of the maximum responses of the beam the variation of e_1' and e_2' will be restricted to positive values within the range prescribed by Equations (4.40) and (4.41).

The ratio γ^2 of the lateral stiffnesses in the y-direction to that in the x-direction can take on all positive values. Again, in real structures the value of γ^2 would be restricted to a much smaller range around the value $\gamma^2 = 1$. For example, consider a structure with steel columns providing the main lateral resistance. The commonly used sections

for columns in multi-storied buildings are 14 x 16 and 14 x $14\frac{1}{2}$ WF sections. The ratio of moment of inertia about the weak axis to that about the strong axis of such sections is around .36 to .39. If the lateral stiffness is assumed to be proportional to the moment of inertia values of the columns, then γ^2 would be around .36 to .39 if all the columns are arranged with their strong axis parallel to the x axis (of the structure); if the columns are arranged to have their weak axis parallel to the x axis, γ^2 would be around 2.56 to 2.78. If the arrangement is such that alternating columns in a row have their strong (or weak) axis parallel to a axis of the structure, the value of γ^2 would tend to be more nearly around 1.

Finally, it may be of some interest to note that for a given γ^2, the range of σ will be

$$\begin{array}{ll} 1 < \sigma < \gamma^2 & \gamma^2 < 1 \\ \sigma = 1 & \gamma^2 = 1 \\ 1 > \sigma > \gamma^2 & \gamma^2 > 1 \ . \end{array} \qquad (4.42)$$

The actual value of σ within this range depends on the value of α (viz. $\alpha \to \infty$, $\alpha \to 0$), except when $\gamma^2 = 1$.

Shear Beam With Setback Unsymmetric About One Axis

The investigation here is restricted to the study of the properties of the coupled vibrations of a shear beam with setback unsymmetric about one axis only. It is assumed for this purpose here that the setback is symmetric about the y axis, i.e. $e_1' = 0$. The translational vibrations in the x direction and the torsional vibrations will be coupled and these will be the subject of the present investigation. The

translational vibrations in the y direction will remain uncoupled. The effect of setback on uncoupled translational vibrations was examined in Chapter III.

In this section the phrase "translational vibrations", unless otherwise qualified, will hereinafter be assumed to mean the translational vibration in the x direction.

The study is further restricted to a shear beam with a fixed degree and level of setback,

$$c = .25, \quad p = .6 , \tag{4.43a}$$

and with a square cross-section in the base as well as the tower portion,

$$\alpha_b = \alpha_t = 1 , \tag{4.43b}$$

see Figure 4.1.

When $e_1' = 0$ the frequency equation of the coupled vibrations, Equation (4.28), can be separated into two independent equations:

$$f_{13}(\omega') = f_1 f_3 - ce_2'^2 \sin \frac{\omega' p}{\sigma_b} \cos \frac{\omega'(1-p)}{\sigma_t} \cos \frac{\omega' p}{\sigma_b} \sin \frac{\omega'(1-p)}{\sigma_t} = 0 \tag{4.44}$$

and

$$f_2(\omega') = 0 . \tag{4.45}$$

The latter equation refers to the translational vibrations in the y directions and is of no interest here. Equation (4.44) is the frequency equation of coupled vibrations consisting of translational vibration in the x direction and the torsional vibration.

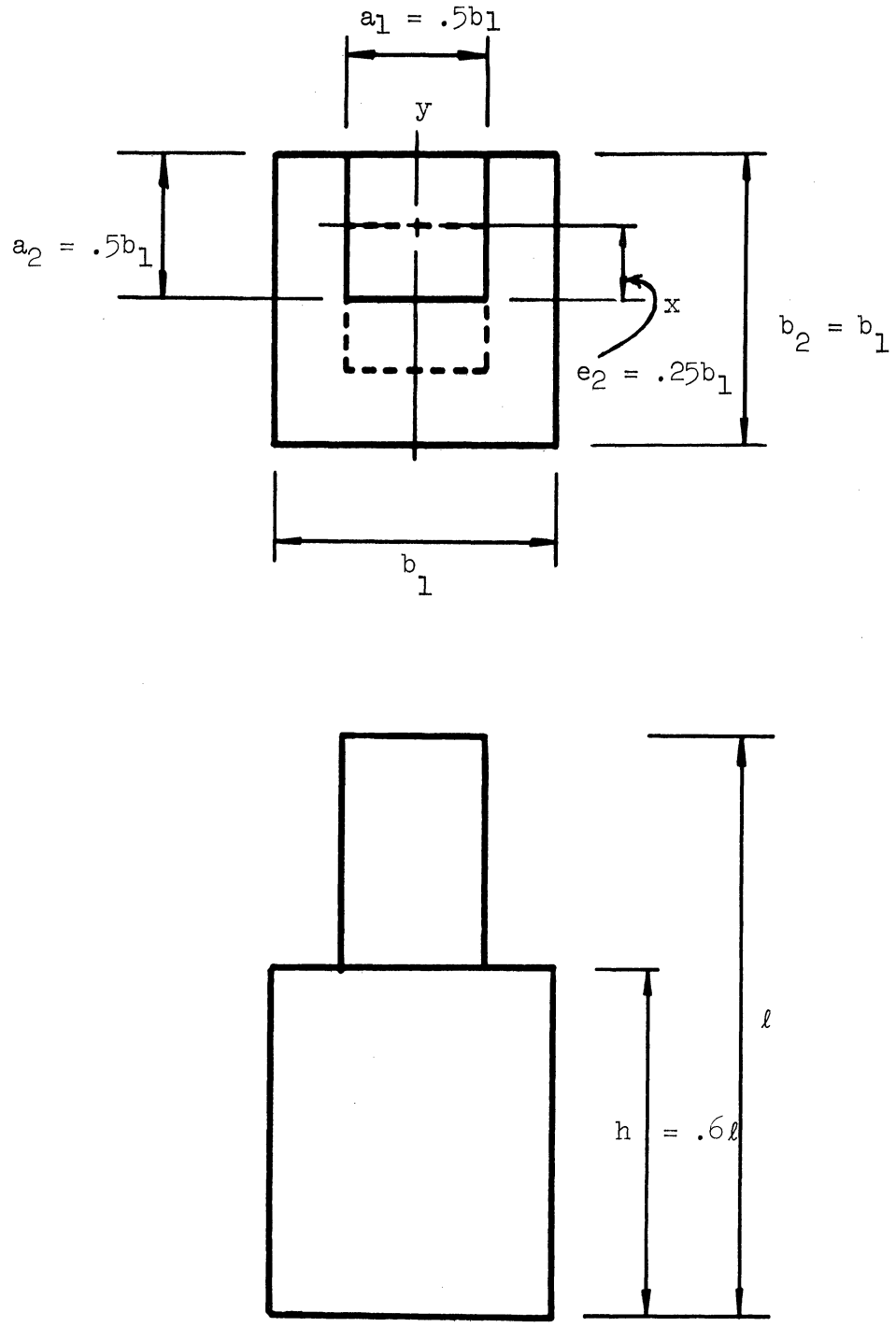

Figure 4.1. Shear Beam with Setback Unsymmetric About x-Axis and Dimensions Assumed Fixed.

The two components of the coupled mode shape are still given by Equation (4.15) with $i = 1$ and 3. The coefficients $C_{ij}(i=1,3;\ j=1,2,3)$ of the coupled mode shape are given by Equations (4.33) and (4.34).

Uncoupled Translational and Rotational Mode Periods

When e'_2 is also equal to zero the translational vibration in the x direction and the torsional vibration are uncoupled from each other and their natural frequencies are then given by Equations (4.29) and (4.31), respectively. It may be observed from Equation (4.18) that

$$\sigma_b = \sigma_t \qquad \text{when} \quad \alpha_b = \alpha_t \ . \tag{4.46}$$

Having chosen α_b and α_t such that $\alpha_b = \alpha_t$, from Equation (4.21) and (4.46) one gets

$$d_t = c^2 d_b \ . \tag{4.47}$$

The frequency equation for the torsional vibration, Equation (4.31), may then be transformed to

$$c^2 \sin \frac{\omega' p}{\sigma} \sin \frac{\omega'(1-p)}{\sigma} - \cos \frac{\omega' p}{\sigma} \cos \frac{\omega'(1-p)}{\sigma} = 0 \ . \tag{4.48}$$

The similarity between the frequency equations for the uncoupled torsional vibration when $\alpha_b = \alpha_t$ and the uncoupled translational vibration, Equation (4.29), should be noted. Figure 3.2 shows the effect of varying the degree and the level of setback on the translational mode periods. The same figure represents the variation of the torsional mode periods if the abscissa and the ordinate axis represent, respectively, c^2 and $T'\sigma$.

For fixed p and c and with $\sigma_b = \sigma_t = \sigma$, the natural periods (non-dimensionalized as in Equation (4.24)) of the torsional vibration are thus proportional to $1/\sigma$. The variation in the first five uncoupled torsional and the translational mode periods with $1/\sigma$ is shown in Figure 4.2. The translational mode periods are, of course, independent of σ.

For convenience a new notation for the modes as used in Figure 4.2 is introduced here. In this notation (viz. T:j or R:j), the letters T and R refer to the translational and the torsional modes, respectively, and the numeral j indicates the mode number in the individual group of modes.

The following observations may be made from Figure 4.2. If for a given value of σ the two groups of modes are combined together and then numbered according to the ascending order of their frequencies, then the same torsional (or translational) mode may be numbered differently for different values of σ. This is the main reason for denoting the modes by the convention described in the previous paragraph. Furthermore, thus numbered the modes are not always alternately translational and torsional. Also, there are several values of σ at which a torsional mode period is equal to a translational mode period.

For the already chosen values of c, α_b, and α_t, (Equation (4.43)), the range of variation of e_2' is given by (see Equation (4.41)):

$$0 \leq | e_2' | \leq .25 \quad . \tag{4.49}$$

As stated before, since the sign of e_2' does not affect the results numerically, the variation of e_2' will be restricted positive values within the above range, see Figure 4.1.

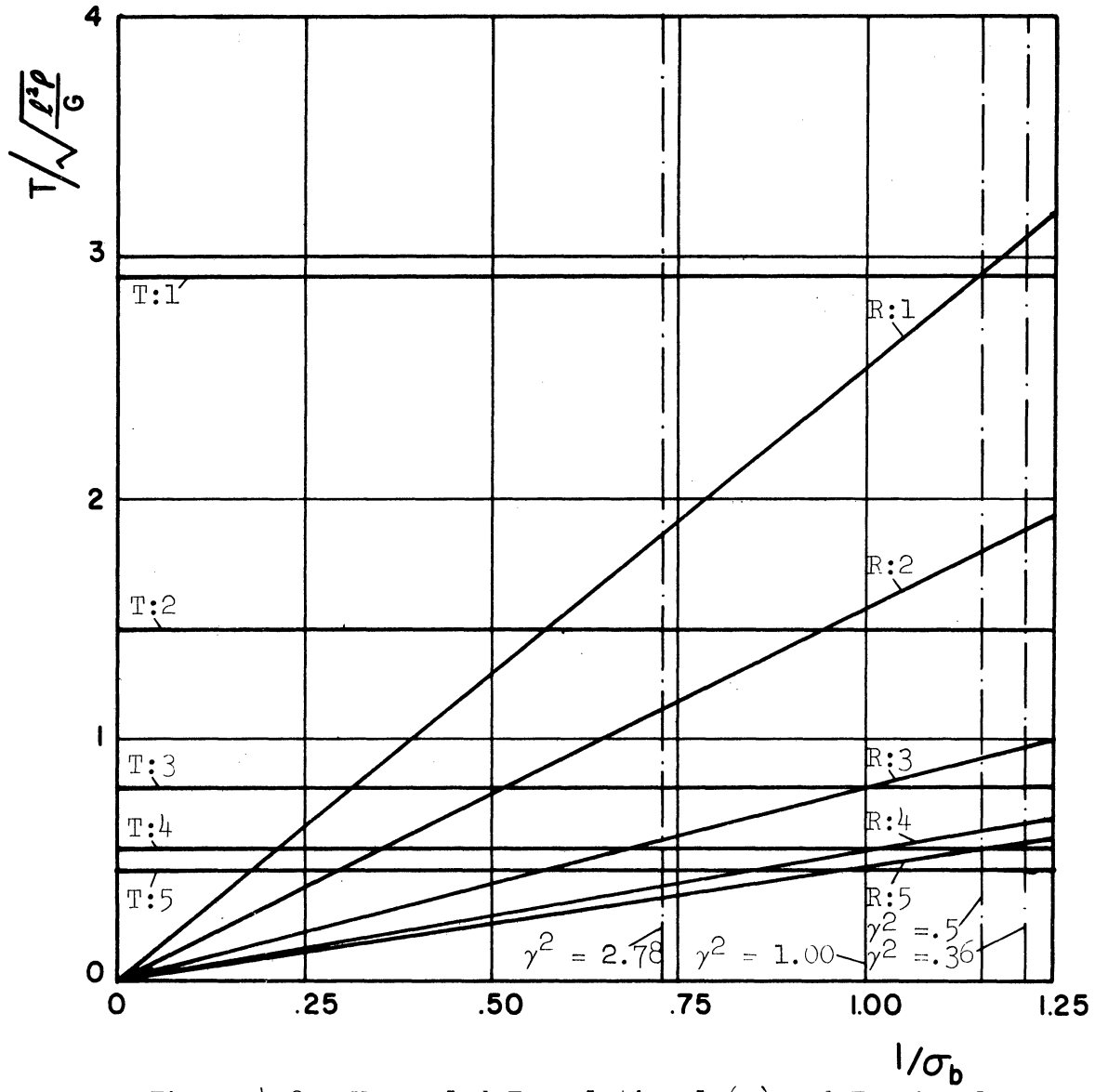

Figure 4.2. Uncoupled Translational (x) and Torsional Mode Periods, Shear Beam.

The effect of varying e_2' on the coupled mode properties of the beam chosen to be studied will be examined next. This effect will be studied for a few different values of σ^2 (i.e. the ratio $\frac{k_3}{m_3}/\frac{k_1}{m_1}$). Since α_b and α_t are already fixed, σ^2 will be varied by varying γ^2 , see Equation (4.18).

Earlier, while discussing the range of the parameter γ^2, it was mentioned that for a building using steel columns of 14 x 16 and 14 x $14\frac{1}{2}$ WF sections the value of γ^2 could possibly range between .36 and 2.78. Values of σ^2 corresponding to these two values of γ^2 , as well as that corresponding to $\gamma^2 = 1$ are chosen for study. Another value, $\gamma^2 = .5$, is also included in the study. The significance of this value of γ^2 is explained in the following paragraphs. The value of σ^2 equivalent to the chosen values of γ^2 and for fixed α_b and α_t ($\alpha_b = \alpha_t = 1$) are given in Table IV.1

TABLE IV.1

EQUIVALENT VALUES OF σ^2 AND γ^2 , SHEAR BEAM

γ^2	.36	.5	1	2.78
σ^2	.68	.75	1	1.89

An interesting problem in the case of coupled lateral torsional vibrations of buildings is the one that arises when a building has a torsional mode period equal to a translational mode period. If slight unbalance is introduced in such a building, there well be severe twisting in these two modes (which are now of the coupled type) when the building is subjected to translational ground motions. However, unless damping in the two modes is very low, the true combined rotations or torsional

forces of the two modes will not be large as would be suggested by the RSS combination of the maximum responses of the two modes or by their absolute sum.(7)

This problem has been investigated by Skinner et al(7) for buildings where dynamic asymmetry is due to eccentricity between the center of rigidity and the center of mass. Even though the asymmetry is assumed to be due to different conditions in the case of buildings with setback, a similar behavior is also observed in this case as will be seen later. To this end the value $\gamma^2 = .5$, for which, as may be observed from Figure 4.2, the first mode torsional and the first mode translational periods are almost equal, is also included in the present study.

Periods

The effect of varying e_2' on first several mode periods of a shear beam with other properties given by Equation (4.43) is shown in Figure 4.3. The modes are identified by the notation introduced in Figure 4.2 for the uncoupled (translational and torsional) modes. The kth coupled mode is identified by the same notation as used for the kth mode in the combined set of uncoupled translational and torsional modes for the beam with otherwise (i.e. other than e_2') identical properties. For example, in Figure 4.2 the first mode of the combined uncoupled modes for $\gamma^2 = 2.78$ is T:1. The first mode of the corresponding coupled modes is also called T:1. Thus the first mode is T:1 for $\gamma^2 = 2.78$ and $\gamma^2 = 1$, and R:1 for $\gamma^2 = .5$ and .36.

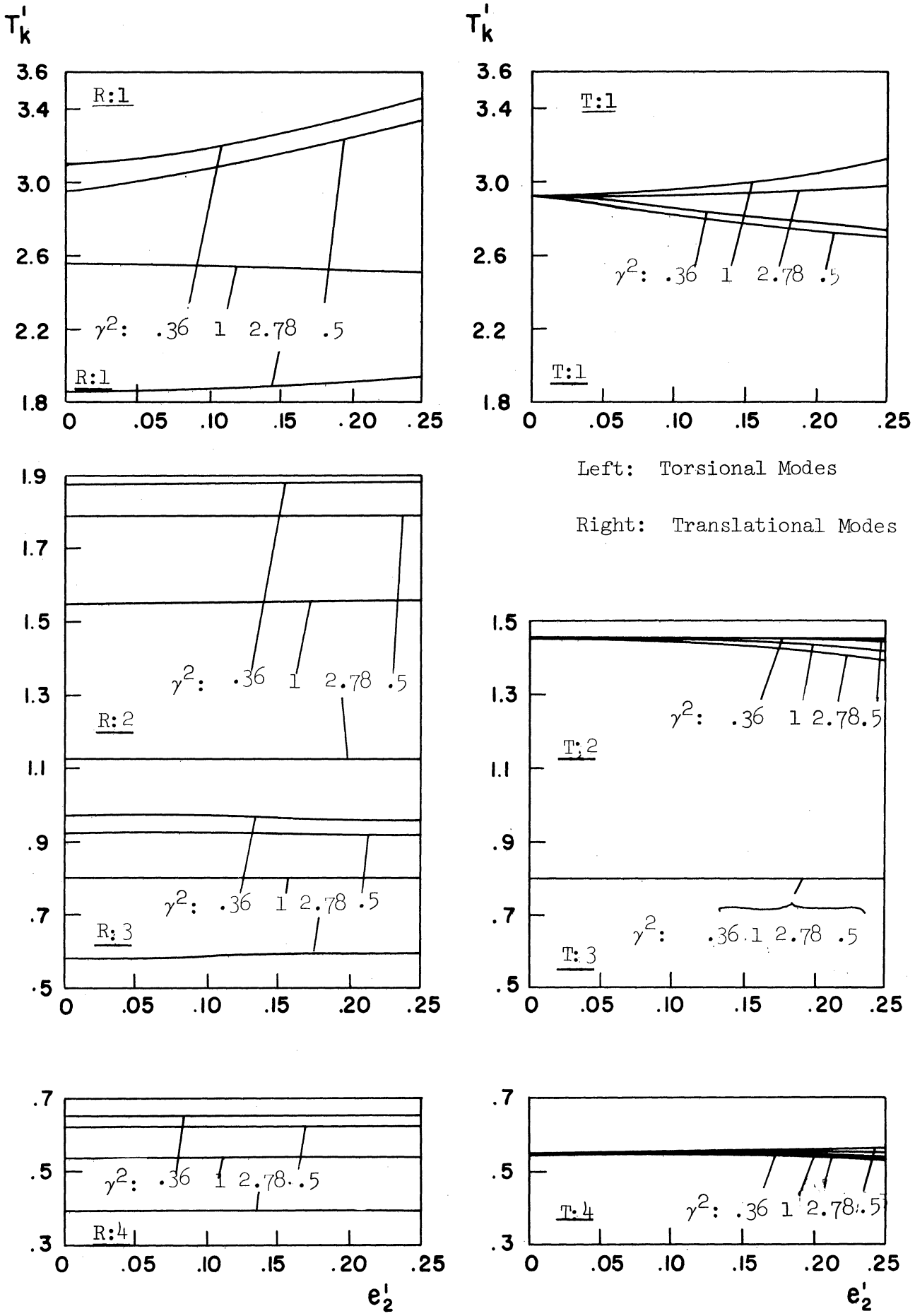

Left: Torsional Modes

Right: Translational Modes

Figure 4.3. Coupled Mode Periods, Shear Beam.

The modes R:1 through R:4 and T:1 through T:4 constitute the first eight coupled modes of the shear beam except for the T:4 and R:4 modes of $\gamma^2 = .36$ and 2.78, respectively. For $\gamma^2 = .36$, the T:4 mode is the ninth mode whereas the eighth mode is the R:5 mode. Simllarly for $\gamma^2 = 2.78$, the R:4 mode is the ninth mode and T:5 is the eighth mode.

The following observations may be made from Figure 4.3. The first mode (i.e. R:1 mode for the cases $\gamma^2 = .36$ and .5 and T:1 mode for $\gamma^2 = 1$ and 2.78, see Figure 4.2) period always increases with increasing eccentricity regardless of the value of γ^2. In the higher modes, changes (i.e. increase or decrease) in periods with increasing e_2' are monotonic.

Changes in higher mode periods (i.e. in T:j or R:j mode, $j \geq 2$) are, in general, small compared to the changes in T:1 or R:1 mode periods. However, for some cases of γ^2 (e.g. $\gamma^2 = 2.78$) the changes in periods in some of the higher translational (T) modes are equal to or greater than those in the T:1 mode on a percentage basis.

Such changes in periods as do occur over the entire range of e_2' are in general very small compared to those occuring in the uncoupled mode periods over the entire range of c (Figure 3.2) or σ (Figure 4.2).

The T:1 and R:1 mode periods for $\gamma^2 = .5$ in the uncoupled case (i.e. when $e_2' = 0$) are almost equal, see Figure 4.2. It may be observed in Figure 4.3 that the changes in T:1 and R:1 mode periods with e_2' for this case ($\gamma^2 = .5$) occur at a higher rate than for other cases especially for smaller values of e_2'. Also, the total changes in these mode periods for $\gamma^2 = .5$ are greater than the rest.

The third translational (T:3) mode period remains constant with e_2' for all values of γ^2. The third torsional (R:3) mode period for the case $\gamma^2 = 1$ which is identically equal to the T:3 mode period also remains constant with varying e_2'. Thus the T:3 and the R:3 mode frequency for the case $\gamma^2 = 1$ is a repeated frequency of multiplicity two regardless of the value e_2' for the shear beam with other properties given in Equation (4.43).

Mode Shapes

The component mode shapes of the coupled modes are given by Equation (4.15) with $i = 1,3$, and the coefficients $C_{ij}(i=1,2;\ j=1,2,3)$ are given by Equations (4.33) and (4.34). The translation component $\phi_1(z)$ is the displacement of the centroid along the x direction. The translational component $\phi_1(z)$ thus represents the displacements of two non-coincidental vertical lines in the two parts, the tower and the base portions, of the structure. This presents some difficulty in representing the translational component in two-dimensional form. Here therefore the translational component is instead represented by the displacements along a single vertical line, passing through the tower centroid, for the entire height of the beam. The torsional component ϕ_3' as modified by Equation (4.26) $(\phi_3' = \phi_3 \cdot \sqrt{A_B})$, gives A_B times the rotation of the cross-section at z and of course is constant for the section. No modification is thus needed for the torsional component.

The first two mode shapes of each type (i.e. of T:1, T:2, R:1 and R:2) of modes are given in Figure 4.4 for the case $\gamma^2 = 1$ showing the effect of e_2'. The mode shapes are normalized by making either $\phi_{1k}(\ell)$ or $\phi_{3k}'(\ell)$ equal to unity depending on whether the mode was originally

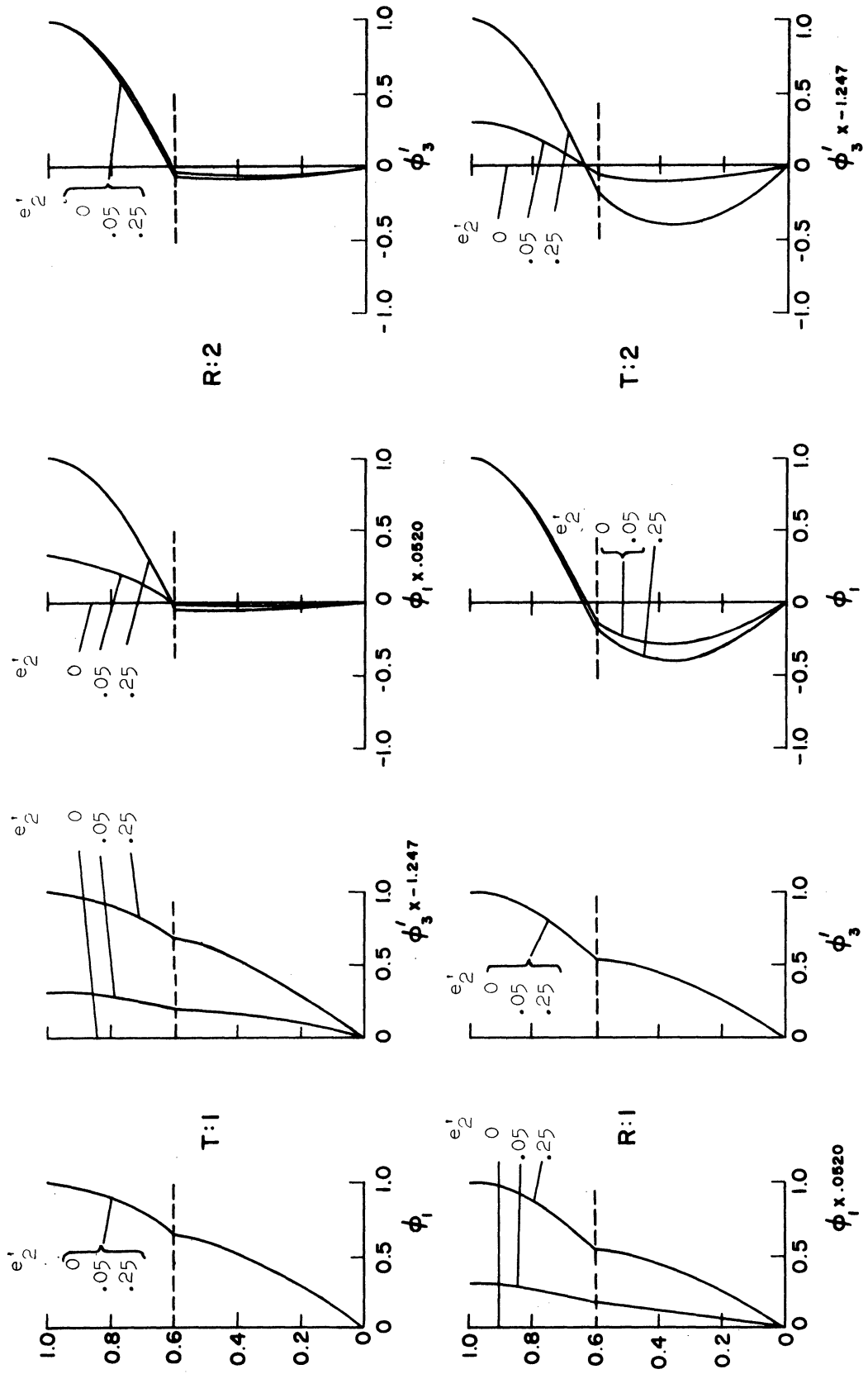

Figure 4.4. Coupled Mode Shapes, Shear Beam. (γ^2=1)

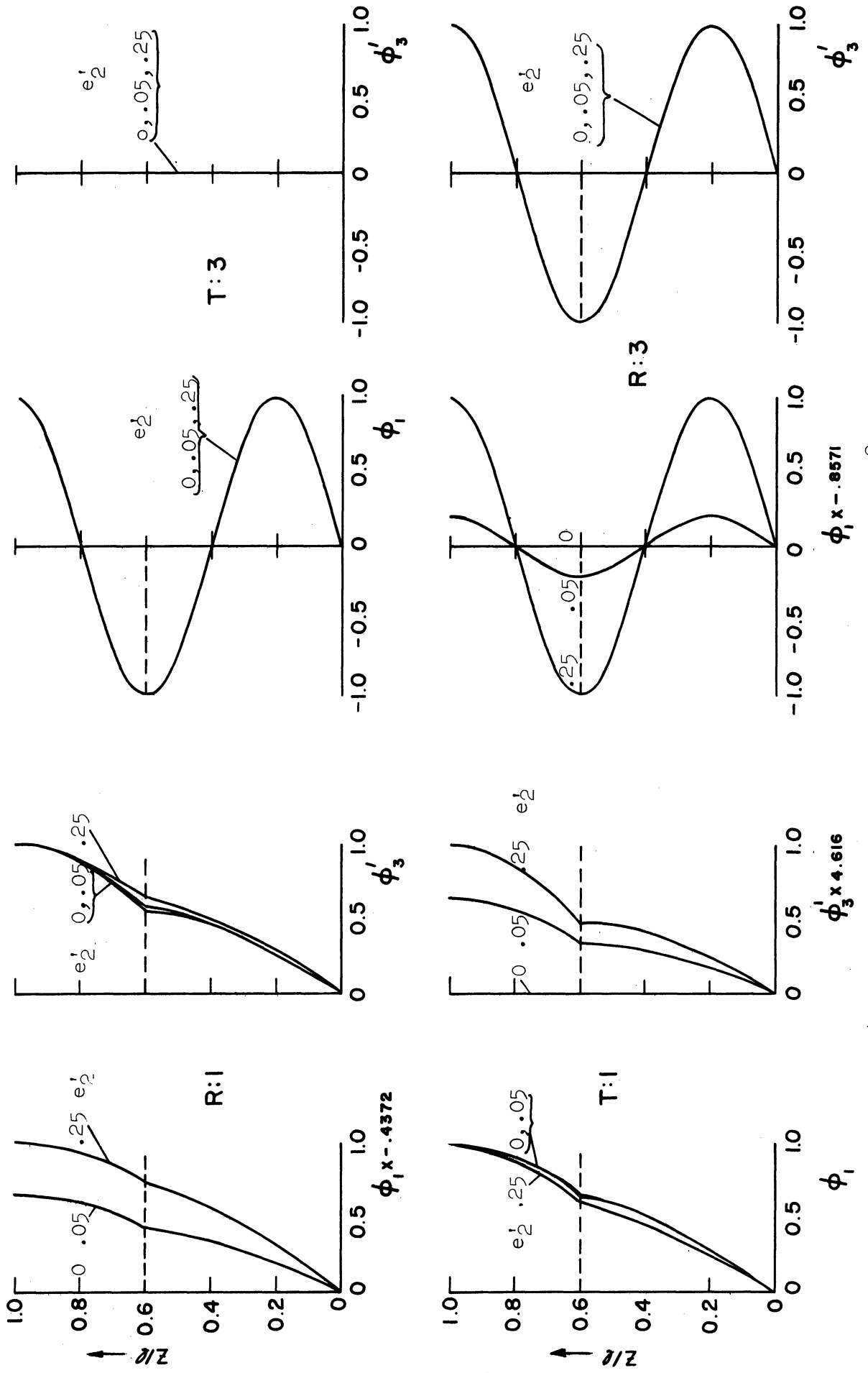

Figure 4.5. Coupled Mode Shapes, Shear Beam. Left: $\gamma^2 = .5$, Right: $\gamma^2 = 1$.

(i.e. at $e_2' = 0$) purely translational or torsional mode, respectively, i.e. in the T modes the normalization is $\phi_{1k}(\ell) = 1$, and in the R modes it is $\phi'_{3k}(\ell) = 1$.

The effect of increasing e_2' on the mode shapes is to increase that component (numerically) which is absent at $e_2' = 0$ relative to the component which constitutes the mode at $e_2' = 0$. Similar effect is observed in the higher modes and also modes of the same beam with different values of γ^2.

However, in the R:1 and T:1 modes for $\gamma^2 = .5$ having almost equal periods at $e_2' = 0$, the component originally (i.e. at $e_2' = 0$) absent increases sharply relative to the other component for small values of e_2' (upto about $e_2' = .05$) and then increases further at a much slower rate with further increase in e_2'. These modes are shown in Figure 4.5.

The T:3 and R:3 modes for the case $\gamma^2 = 1$ have identical frequencies for all values of e_2'. The method of determining the coefficients C_{ijk} for the two mode shapes for this repeated frequency has been already explained. These two mode shapes are also shown in Figure 4.5. Any linear combination of the two mode shapes will again be a mode shape corresponding to the repeated frequency. The mode shapes as given in Figure 4.5 are mutually orthogonal. One of the two modes has zero torsional component and is therefore denoted as the T:3 mode, and the other mode which has a relatively small translational component is termed the R:3 mode.

The T:3 and R:3 mode shapes for the case $\gamma^2 = 1$, computed as mentioned above show very little or no coupling even though they have equal periods. It is apparent that this is an exception to the general rule of a high degree of coupling from small values of e_2' when a pair of T and R mode periods are equal or very close at $e_2'=0$, as was observed here earlier in the case of T:1 and R:1 mode for $\gamma^2=.5$ and as has been observed by others.(7)

Kinks form in both components of the mode shapes at the setback level. The T:3 and R:3 modes for $\gamma^2 = 1$ are exceptions. As observed in Chapter III, the kinks are caused by the existence of sharp setback (i.e. small c). The kink in the purely torsional modes (i.e. in the R modes at $e_2' = 0$) is usually somewhat sharper than in the corresponding purely translational modes. This is to be expected since the effect of setback felt on the torsional modes is proportional to c^2 (assuming α_b and α_t to remain constant), whereas in the case of translational mode it is proportional to $c(0 < c \leq 1)$.

Coupling

In a torsional (R) mode, the ratio $\phi_{1k}(z)/\phi_{3k}'(z)$, or its inverse in a translational mode, may be termed the degree of coupling at height z. The value of this ratio varies with z unless $\sigma_b^2 = q_3/q_1 = \sigma_t^2 = s_3/s_1 = 1$, see Equation (4.15). The mode shapes in Figures 4.4 and 4.5 show indirectly the degree of coupling, and the effect of e_2' on it, over the entire height of the beam. More direct and quantitative information about the effect of e_2' on the degree of coupling may be obtained by plotting the value of the ratio $\phi_{1k}(z)/\phi_{3k}'(z)$, or its inverse, for a constant z as a function of e_2'. Figure 4.6 shows the effect of e_2' on the ratios $\phi_1(\ell)/\phi_3'(\ell)$ for the modes R:1 through R:4 and on the ratios $\phi_3'(\ell)/\phi_1(\ell)$ for the modes T:1 through T:4. As noted earlier, these modes constitute the first eight modes except for the cases $\gamma^2 = .36$ and 2.78. The following observations may be made from Figure 4.6.

The ratios of modal rotations and displacements at the top of the beam invariably increase (numerically) with e_2' starting from zero at $e_2' = 0$. Generally, this increase is either linear or is such that

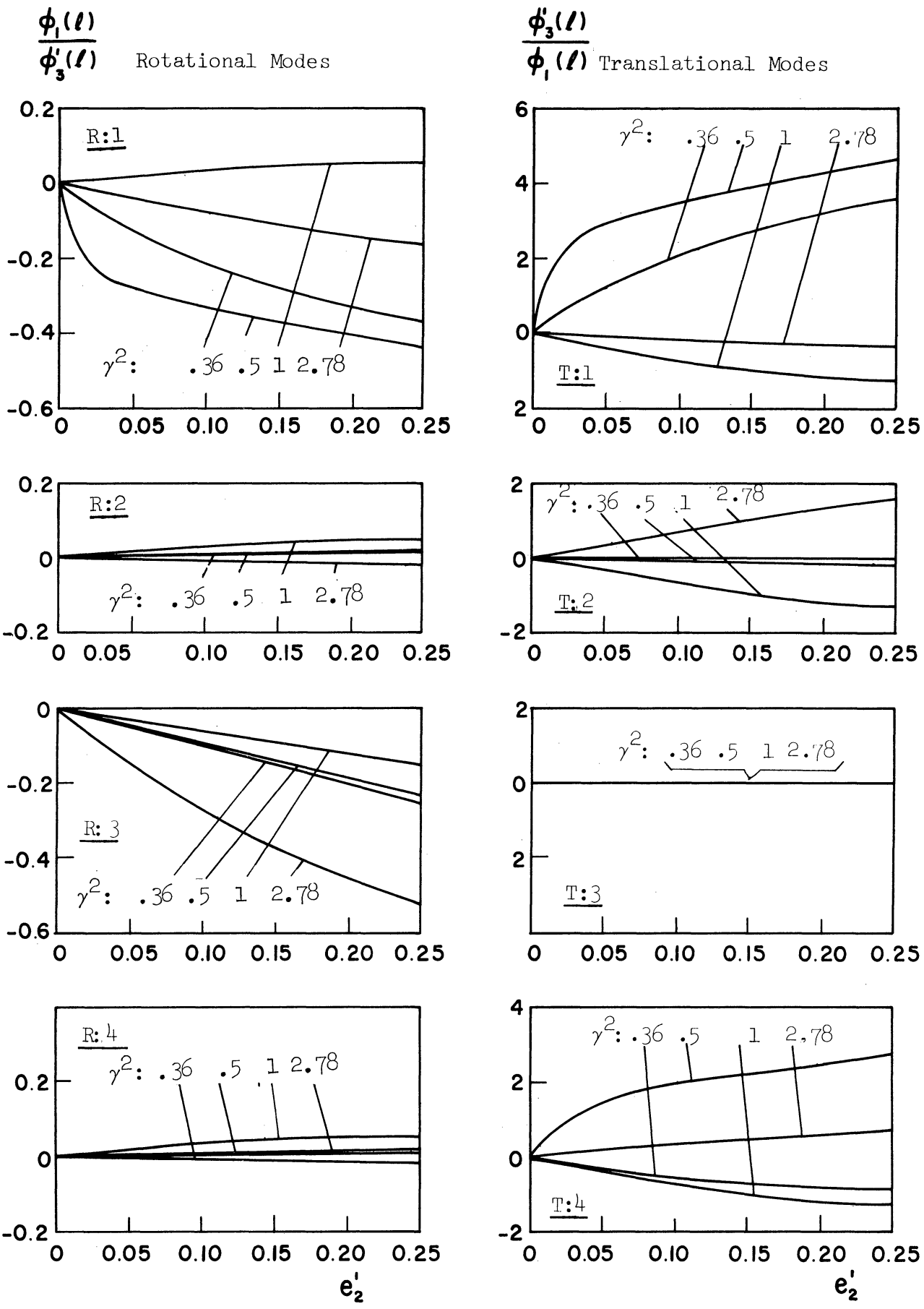

Figure 4.6. Coupling, Shear Beam.

the rate of increase decreases with increasing e_2' . The effect of change in γ^2 (or σ^2) is not uniform. However, for those pairs (consisting of one R and one T modes) having equal or almost equal periods at $e_2' = 0$, there is a sharp rise in the numerical value of the ratio for very small values of e_2' and then a slow increase in the rest of the range of e_2' . Examples are the T:1 and R:1 modes for $\gamma^2 = .5$, the T:4 and R:5 (not shown here) modes also for $\gamma^2 = .5$. In general, the closer the periods of such pairs of modes the sharper the increase in the value of the ratio for very small values of e_2' . For modes with sufficiently close periods a decrease in the ratio value may possibly be observed beyond small values of e_2' .

The T:3 mode in which the torsional component remains zero and in which, as observed earlier, the period does not change for all values of γ^2 , is an exception. Any torsional mode having a period close or equal to that of T:3, at $e_2' = 0$ (e.g. R:3 mode of $\gamma^2 = 1$), shows virtually no variation in period (no variation in the case of $\gamma^2 = 1$, see Figure 4.3), and the coupling in this mode, though it exists, proves also to be an exception to the observation made above.

In general, if similar ratios of displacements and rotations at other points (of height) of the beam were drawn a similar behavior would be observed.

Base Shear and Base Torque

Next, the effect of unsymmetric setback on two modal quantities which are more directly connected to the earthquake responses used for design purposes will be examined. These are the modal base shear and base torque coefficients when the beam is subjected to a static one g translational acceleration. When these quantities are multiplied by the maximum

absolute acceleration (in g units) attained by a single-degree-of-freedom system with the same frequency and damping when subjected to a ground acceleration, they will give the corresponding modal responses of the structure to that ground acceleration.

The effect of symmetric setback on base shear in the uncoupled translational mode was examined in a similar manner in Chapter III.

When the beam is subjected to ground excitation, the kth modal base shear coefficient (in the x direction) is given by

$$C_{1Bk} = \frac{\int_0^{\ell} m_1 \phi_{1k} dz}{\int_0^{\ell} m_1 dz} \cdot (\ddot{\eta}_k + \lambda_{1k} \ddot{x}_{01} + \lambda_{2k} \ddot{x}_{02})/g \quad . \qquad (4.50)$$

Since the y-translational vibrations are not coupled with the x-translational and the rotational vibrations, in the latter coupled modes the modal participation factor in the y direction λ_{2k} will be equal to zero, see Equation (4.11). Then, the modal displacement η_k will be given by

$$\ddot{\eta}_k + 2\beta_k \omega_k \dot{\eta}_k + \omega_k^2 \eta_k = - \lambda_{1k} \ddot{x}_{01} \quad . \qquad (4.51)$$

Equation (4.50) may then be rewritten as

$$C_{1Bk} = \lambda_{1k} \frac{\int_0^{\ell} m_1 \phi_{1k} \, dz}{\int_0^{\ell} m_1 dz} \cdot (\ddot{\xi}_k + \ddot{x}_o)/g \qquad (4.52)$$

where ξ_k is given by

$$\ddot{\xi}_k + 2\beta_k \omega_k \dot{\xi}_k + \omega_k^2 \xi_k = - \ddot{x}_{01} \quad . \qquad (4.53)$$

Because of the linearity of the systems (4.51) and (4.53)

$$\eta_k = \lambda_{1k} \xi_k \quad . \tag{4.54}$$

The quantity ξ_k is also the response of a linear single degree-of-freedom oscillator having the same frequency and damping as the kth coupled mode of the shear beam to a ground acceleration of $\ddot{x}_{01}$.

Base torque in the kth mode may be similarly shown to be

$$T_{Bk} = \lambda_{1k} \left(\int_0^{\ell} m_3 \phi_{3k} \, dz - e_2 \int_k^{\ell} m_1 \phi_{1k} \, dz\right) \cdot (\ddot{\xi}_k + \ddot{x}_{01}) \quad . \tag{4.55}$$

It may be noted that the torque produced by the inertial lateral forces (in the x direction) of the tower portion is accounted for in Equation (4.55).

To obtain a non-dimensional quantity corresponding to the base torque, which may be termed "base torque coefficient", several different alternatives are possible, e.g.:

$$\begin{aligned} &\text{a)} \quad T_B \Big/ \int_0^{\ell} m_1 g \, r \, dz \\ &\text{b)} \quad T_B \Big/ \left(\int_0^{\ell} m_1 g \, dz \cdot \sqrt{A_B}\right) \\ &\text{c)} \quad T_B \cdot \sqrt{A_B} \Big/ \int_0^{\ell} m_3 g \, dz \end{aligned} \tag{4.56}$$

in which r is the radius of gyration of the cross-section and has different values in the base and the tower portion; and $A_B = b_1 b_2$ is the cross-sectional area in the base portion.

Non-dimensionalisation of the type a.) was used by Skinner *et al* in their paper on unbalanced (i.e. dynamically unsymmetric) one-story building under earthquake forces.(7) However, due to its direct similarity with the non-dimensionalisation used for base shear, type c) is used here.

Thus the base torque coefficient is defined as

$$C_{3Bk} = \lambda_{1k} \frac{\int_0^{\ell} m_3 \phi_{3k} dz - e_2 \int_h^{\ell} m_1 \phi_{1k} dz}{\frac{1}{\sqrt{A_B}} \int_0^{\ell} m_3 dz} \cdot (\ddot{\xi}_k + \ddot{x}_{01})/g \quad . \qquad (4.57)$$

The non-dimensional parts of the base shear and base torque coefficients on the right hand side in Equations (4.52) and (4.57), that are independent of ground acceleration are:

$$C'_{1Bk} = \lambda_{1k} \cdot \frac{\int_0^{\ell} m_1 \phi_{1k} dz}{\int_0^{\ell} m_1 dz} \qquad (4.58)$$

and

$$C'_{3Bk} = \lambda_{1k} \frac{\int_0^{\ell} m_3 \phi_{3k} dz - e_2 \int_h^{\ell} m_1 \phi_{1k} dz}{\frac{1}{\sqrt{A_B}} \int_0^{\ell} m_3 dz} \quad . \qquad (4.59)$$

C'_{1Bk} and C'_{3Bk} are the base shear and torque coefficients in the kth mode of the shear beam subjected to static one g translational acceleration.(26)

Formulae for λ_1, which is given by Equation (4.11) with $\phi_2 \equiv 0$, and C'_{1B} and C'_{3B}, may be derived in terms of C_{ij} by using Equations (4.15) for i = 1, 3:

$$\lambda_{1k} = \frac{C_{11k}}{\frac{1}{2}\omega' [C_{11k}^2 \cdot P + (C_{12k}^2 + C_{13k}^2) \cdot c \cdot (1-p)} \qquad (4.60)$$

$$+ C_{31k}'^2 \cdot \frac{d_b}{\sigma_b} \cdot p + (C_{32k}'^2 + C_{33k}'^2) \cdot \frac{d_t}{\sigma_t} \cdot (1-p)]$$

$$C'_{1Bk} = \lambda_{1k} \frac{C_{11k}}{\omega' [p + (1-p)c]} \tag{4.61}$$

and

$$C'_{3Bk} = \lambda_{1k} \cdot \frac{\sigma_b \cdot C'_{31k}}{\omega' [p + (1-p)c_\theta^2]} \tag{4.62}$$

where

$$c_\theta^2 = \frac{c^2(\alpha_t + 1/\alpha_t)}{(\alpha_b + 1/\alpha_b)} = \frac{m_3(h < z < \ell)}{m_3(0 < z < h)} \quad . \tag{4.63}$$

It is interesting to note that e_2 does not appear explicitly in Equation (4.62) although it does in Equation (4.59). It should be noted that although the value of λ_1, as given by Equation (4.60), will depend on the manner in which the mode shape is normalised, the values of C'_{1B} and C'_{3B} as given by Equations (4.61) and (4.62) do not depend on it.

The base shears C'_{1Bk} and base torque C'_{3Bk} are given in Figures 4.7 and 4.8, respectively, as functions of e'_2 for the chosen values of γ^2. This is done for the eight modes: R:1 through R:4 and T:1 through T:4. Again, as noted earlier these modes constitute the first eight modes except for the cases $\gamma^2 = .36$ and $\gamma^2 = 2.78$.

In the torsional (R) modes the base shears increase from zero to some finite value as e'_2 varies from zero to its maximum possible value (i.e. $e'_2 = .25$). In the translational mode base shear decreases from some finite value at $e'_2 = 0$ (values which are obtainable from Figure 3.5 in Chapter III for $p = .6$ and $c = .25$), to some other finite value as e'_2 increases. The sign of C'_{1Bk} is the same in all modes.

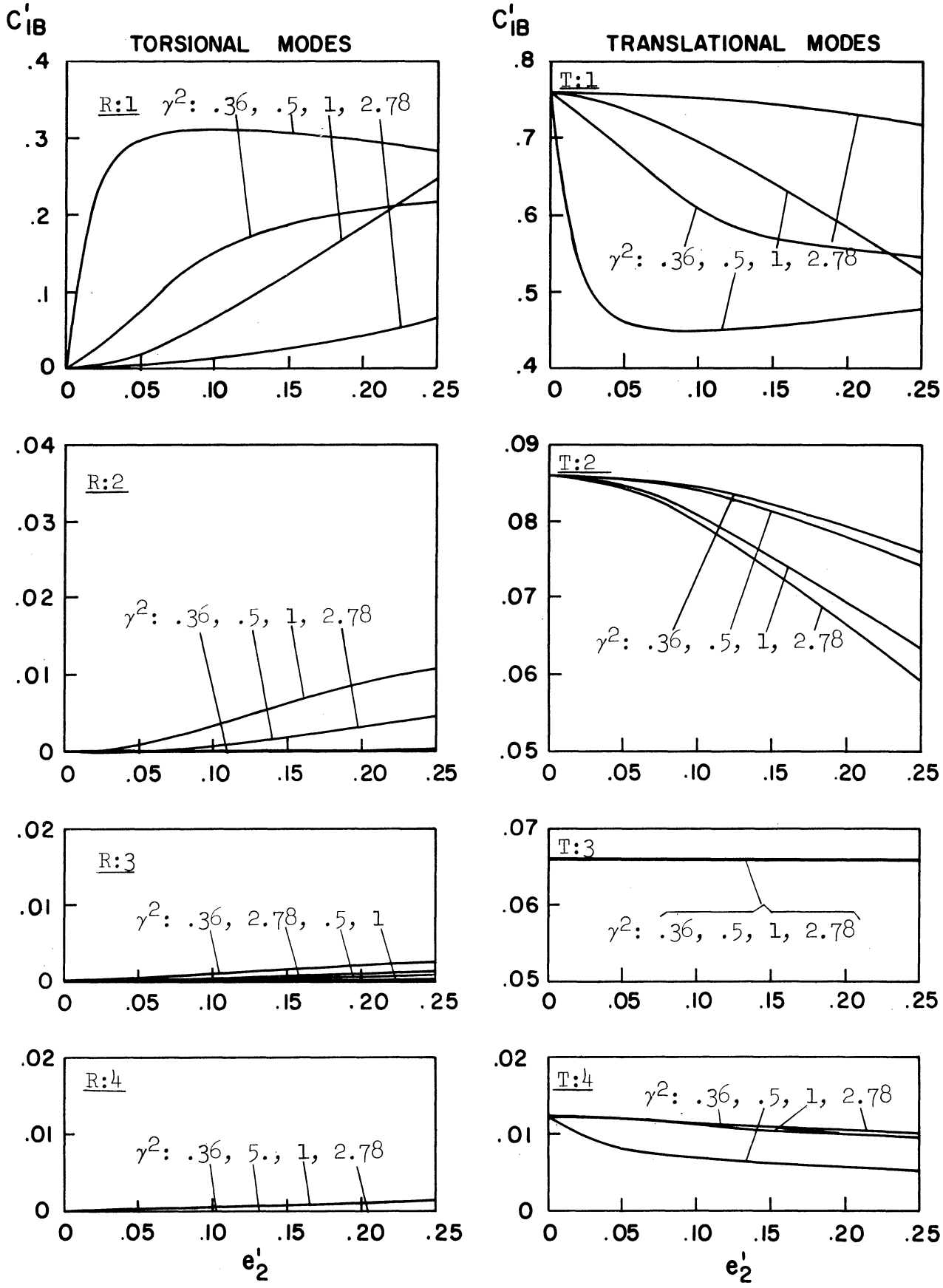

Figure 4.7. Modal Base Shear Coefficient, Shear Beam.

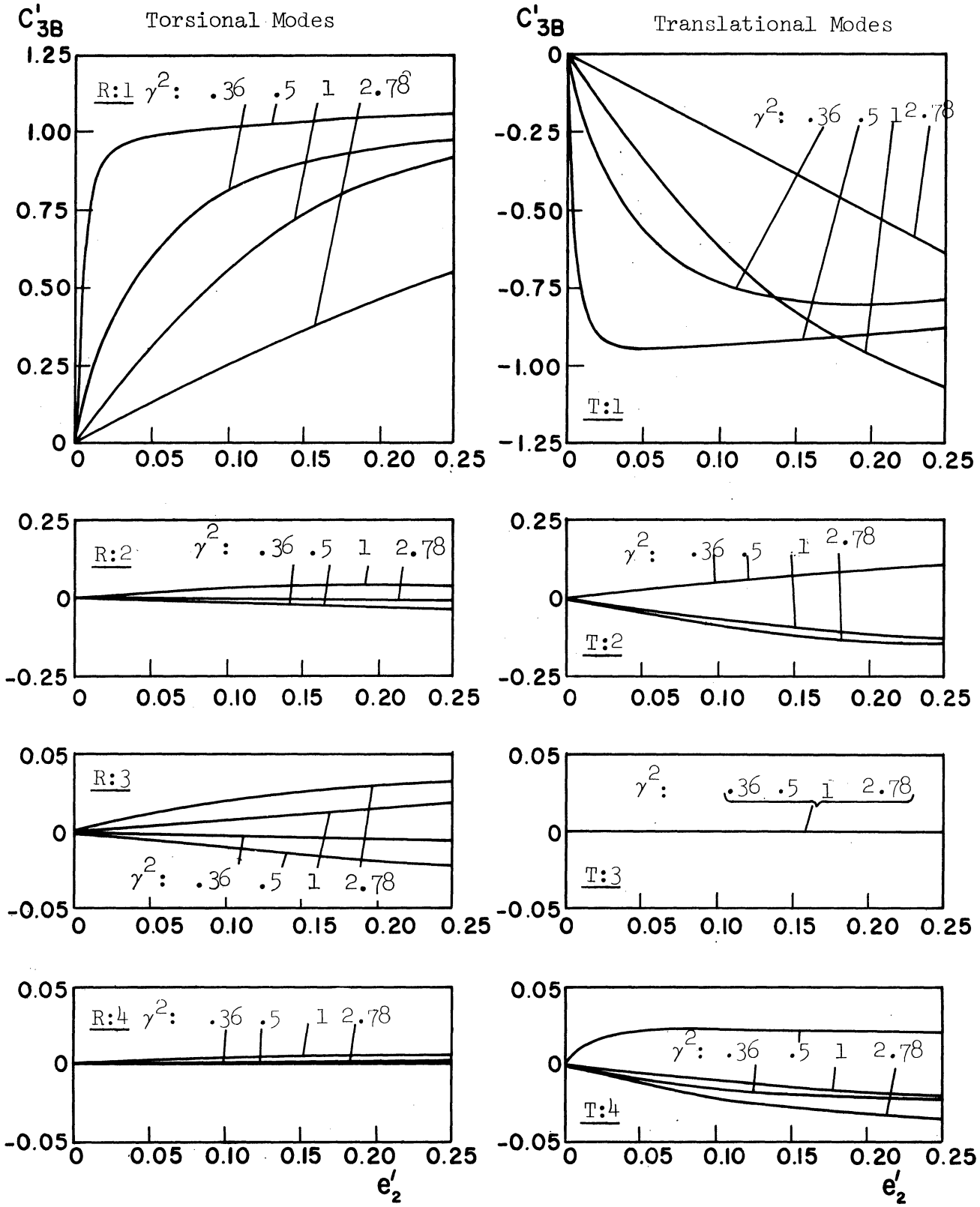

Figure 4.8. Modal Base Torque Coefficients, Shear Beam.

The antisymmetry between the increase in base shear in the R:1 mode and its decrease in the T:1 mode, especially for the cases $\gamma^2 = .36$, .5 and 1, is striking. For these cases, the sum of the C'_{1Bk} in the two modes remains almost constant (equal to C'_{1B} $(e'_2 = 0)$ value of T:1 mode) for all values of e'_2 ; the closer the periods of T:1 and R:1 modes at $e'_2 = 0$ the closer the sum remains to the original.

In the higher modes the base shears are considerably smaller. The change in the ordinate (C'_{1Bk}) scale for these modes in Figure 4.7 should be noted. The behavior noted above in the T:1 and R:1 modes does not seem to hold well in the higher modes.

In Chapter III it was found that for beams with $p < .5$ and small values of c, higher modes contribute significantly to the total base shear. Here of course the values in Figure 4.7 are for a beam with $p = .6$ and $c = .25$. For beams with $p < .5$ and c quite small, base shear in some of the higher modes can be expected to be as high or higher than in the first two (T:1 and R:1) modes. The behavior of such higher modes in such cases may be expected to be similar to the behavior of T:1 and R:1 modes observed for the beam considered here.

There is no change in base shear in the T:3 mode which, as noted before, remains purely translational with no change in period.

For the case $\gamma^2 = .5$, whose T:1 and R:1 mode periods at $e'_2 = 0$ are almost equal, the base shear increases sharply for small values of e'_2 (say $e'_2 < .05$) in the R:1 mode and decreases sharply by almost equivalent amounts in the T:1 mode. With further increase in e'_2 it decreases slowly in the R:1 mode and increases by almost equal amounts in the T:1 mode.

The kth mode base shear coefficient in a beam subjected to ground acceleration is given by Equation (4.52), i.e.

$$C_{1Bk} = C'_{1Bk} \cdot (\ddot{\xi}_k + \ddot{x}_{01})/g \quad . \tag{4.64}$$

At small values of e'_2 the periods of the T:1 and R:1 modes forthe case γ^2=.5 are still quite close. The modal accelerations in the two modes in response to ground acceleration $\ddot{x}_{01}$ will have almost equal maximum values and will reach these values at almost the same time if damping is not very low.(7) The maximum value of the combined base shear of the two modes will therefore be almost equal to the algebraic sum of the maximum value of base shear in each mode (obtained by using Equation (4.52)). Now it may be assumed that the maximum value of acceleration $(\ddot{\xi}_k + \ddot{x}_{01})$ achieved by system (4.53) responding to a given ground acceleration $\ddot{x}_{01}$ does not change much with small changes in periods. If the contributions to the total base shear of the higher modes are neglected it may be concluded that the base shear of the beam under consideration (with $\gamma^2 = .5$) will not change much, from its value in the symmetric case, with the introduction of small asymmetry when subjected to the same ground acceleration.

At $e'_2 = 0$, base torque in both the torsional and translational modes is zero; in the case of former because $\lambda_1 = 0$ and in the case of latter bacause $\phi_3 \equiv 0$. As e'_2 increases base torque increases in all modes, in magnitude (Figure 4.5).

The signs of C'_{3Bk} in the R:1 and T:1 modes are opposite to each other. In higher modes such pairing of consecutive modes in terms of opposite signs for base torque is not always possible.

As in the case of base shear, there is some antisymmetric similarity of the plots of base torque in the R:1 and T:1 modes. However this is not as precise as in the case of base shear. Only for $\gamma^2 = .5$ for very small values of e_2' (say $e_2' < .05$) does the (algebraic) sum of C'_{3Bk} in R:1 and T:1 add up to that at $e_2' = 0$ (which is zero).

The increase in C'_{3Bk} with increasing e_2' is either linear or it is such that the rate of increase diminishes with increasing e_2'. The T:1 mode is an exception where C'_{3B} actually decreases with e_2' beyond (roughly) $e_2' = .05$.

Base torque in higher modes (T:j , R:j , $j \geq 2$) is quite small compared to that in the first two modes (T:1 and R:1) for the beam considered here, i.e., for $p = .6$ and $c = .25$. For beams with other values of p and c (as well as α_b and α_t) some of the higher modes may be as important or more so. By analogy with the behavior of base shear C'_{1B} this may be expected to happen for beams with $p < .5$ and small c.

For the case $\gamma^2 = .5$ periods of T:1 and R:1 modes are very close to each other for small values of e_2' (say $e_2' < .05$). C'_{3B} in the two modes increase (numerically) very sharply for small values of e_2'. However, the values of C'_{3B} in the two modes are then almost equal and opposite. The kth mode base torque coefficient in the beam subjected to ground acceleration is given by Equation (4.57), viz.

$$C_{3Bk} = C'_{3Bk} \cdot (\ddot{\xi}_k + \ddot{x}_0)/g \quad . \tag{4.65}$$

Since the periods of the two modes are close the maximum base torque due to the two modes combined will be very nearly equal to the algebraic sum of maximum base torque C'_{3B} in the two modes, which is to say that it will be very small numerically.

The overall impression one may gather from Figure 4.8 is that when the beam is subjected to some ground acceleration the base torque will increase with increasing e'_2 and probably its rate of increase will itself diminish with increasing e'_2 .

SHEAR BUILDING

The effect of unsymmetric setbacks on the dynamic behavior of a shear beam was studied in the previous section. As in the case of Chapter III on the effect of symmetric setbacks, a similar study with the multi-mass shear building model will be presented in this section.

Equations of motions of a multi-story building using a multi-mass model and their solution were developed and presented in Chapter II. Mass is assumed to be concentrated at floor levels with massless springs connecting them with each other and with the ground. Further as in Chapter III, buildings are assumed to be simply coupled in stiffness, i.e., they are "shear buildings". This assumption was discussed in Chapter III.

Some Further Assumptions

Principal directions of structures are assumed to exist as mentioned in Chapter II. Furthermore, it is assumed here that in each part of the structure (i.e. the tower and the base portions) separately

the stiffness and mass are distributed symmetrically about two mutually perpendicular planes; i.e., the tower and the base portions are each assumed to be dynamically symmetric in themselves.

The building is assumed to be rectangular in plan in both portions and the plane of dynamic symmetry in each portion is assumed to be coincidental with the corresponding plane of geometric symmetry.

Putting it simply, the centers of mass and the centers of resistance above the setback level are assumed to fall on a single vertical axis through the geometric centroid; and the same is true for the centers of mass and centers of resistance below the setback level.

It should be observed here that such an assumption presumes simple coupling in stiffness. The statement about centers of resistance above or below some level would otherwise be meaningless.

With the above assumption, the structure is dynamically unsymmetric due only to the geometric asymmetry of setback. Thus, as in the case of the shear beam, the parameters representing dynamic asymmetry are e_1 and e_2, the offsets between the tower and base centroids along the x and y directions respectively. The x and y directions are of course chosen to be parallel to the planes of dynamic symmetry in each part of the structure.

Idealised Structural Properties

The distributions of mass m_i and lateral stiffness (in the x direction) kx_i over the height for an N-story building with a setback of degree c above the Pth story were idealised in Chapter III, Equations (3.61) and (3.62). This idealization is assumed to hold here also. Further, the distribution of lateral stiffness in the y direction,

ky_i , over the height is assumed to be similar to that of kx_i . This can be expressed simply as

$$ky_i = \gamma^2 kx_i \tag{4.66}$$

by analogy to a similar assumption in the case of the shear beam, see Equation (A.4) in the Appendix.

The torsional stiffness of ith story, $k\Theta_i$, is defined here as the second moment of the lateral stiffnesses (in both x and y directions) in the ith story about the vertical axis through the center of resistance of that story. The lateral stiffnesses in the case of the shear beam was assumed to be uniformly distributed over the plan area. In buildings, the lateral stiffnesses are provided by such items as columns and shear walls and are thus concentrated in points or lines in the horizontal plane. Let μ be the ratio of the second moment of stiffness about the vertical as obtained from its actual distribution (in plan) to that obtained by assuming it to be uniformly distributed (in plan) over the story cross-section.

The torsional stiffness is also equal to the sum of the second moment of lateral stiffnesses in the x direction about the x axis and that of lateral stiffnesses in y direction about y axis. The ratio μ may have different values for the second moments of stiffnesses in the two directions, say μ_x and μ_y . These ratios are assumed to have constant values (μ_{bx} , μ_{by} , μ_{tx} , μ_{ty}) for all stories in each of the two parts of structure. The subscripts b and t refer to base and tower portions, respectively. With this assumption

the torsional stiffnesses are given by:

$$\text{for} \quad 1 \leq i \leq P$$

$$k\theta_i = (\mu_{bx}\alpha_b + \mu_{by}\gamma^2/\alpha_b) \cdot \frac{A_B}{12} \cdot kx_i$$

$$\text{and for} \quad P+1 \leq i \leq N \tag{4.67}$$

$$k\theta_i = (\mu_{tx}\alpha_t + \mu_{ty}\gamma^2/\alpha_t) \cdot \frac{A_T}{12} \cdot kx_i \quad .$$

In Equation (4.67), $A_B = b_1 b_2$ is the plan area of the base portion of the building, and $A_T = a_1 a_2$ that of the tower portion. As with the shear beam, α_b and α_t are defined as the ratios of the plan dimensions:

$$\alpha_b = b_2/b_1$$
$$\alpha_t = a_2/a_1 \quad . \tag{4.68}$$

In Chapter III, the values of the lumped masses were assumed to be constant in each part of the structure, m_t and m_b in tower and base portion respectively, and their ratio $c = m_t/m_b$ (Equation (3.17)) was termed the degree of setback. In the case of the shear beam, c also is the ratio of tower cross-sectional area to base cross-sectional area (as well as that of lateral stiffness in tower to that in base), see Equation (3.24). Here also it is assumed that

$$c = \frac{a_1 a_2}{b_1 b_2} = \frac{A_T}{A_B} \quad . \tag{4.69}$$

This assumption along with the definition $c = m_t/m_b$ implies the assumption that the value of the lumped mass at a given floor level is proportional to the floor plan area.

Using Equation (4.4), Equation (4.2) may be rewritten as

for $1 \leq i \leq P$

$$k\Theta_i = (\mu_{bx}\,\alpha_b + \mu_{by}\,\gamma^2/\alpha_b) \cdot \frac{A_B}{12} \cdot kx_i \qquad (4.70)$$

and for $P + 1 \leq i \leq N$

$$k\Theta_i = (\mu_{tx}\,\alpha_t + \mu_{ty}\,\gamma^2/\alpha_t) \cdot \frac{cA_B}{12} \cdot kx_i \quad .$$

The (lumped) mass at floor levels is assumed to be uniformly distributed over the floor plan area. Although the walls, columns, partitions, etc., in the adjoining stories contribute to the value of lumped mass, it consists substantially of the floor mass itself, for which the above assumption may be approximately true. In any case, by adjusting the values of the ratio μ introduced in computation of torsional stiffness, provision may be made for any significant variation from the above assumption of uniform distribution of mass. Thus,

for $1 \leq i \leq P$

$$m\Theta_i = (\alpha_b + 1/\alpha_b) \cdot \frac{A_B}{12} \cdot m_i$$

and for $P + 1 \leq i \leq N$ (4.71)

$$m\Theta_i = (\alpha_t + 1/\alpha_t) \cdot \frac{cA_B}{12} \cdot m_i$$

where $m\Theta_i$ is the mass moment of inertia of the ith mass about the vertical axis through its centroid.

Equations of Motion

The equations of motion of an undamped N-story structure with 3N degrees of freedom, Equations (2.21) through (2.23), are derived in Chapter II. Since principal directions are assumed to exist, direct coupling between the two translational components vanishes and Equation (2.24) follows. The equations of motion of the N-story structure then become

$$\begin{aligned}
[M_u]\{\ddot{u}\} + [K_u]\{u\} + [K_{u\theta}]\{\theta\} &= \{f_u(t)\} \\
[M_v]\{\ddot{v}\} + [K_v]\{v\} + [K_{v\theta}]\{\theta\} &= \{f_v(t)\} \\
[M_\theta]\{\ddot{\theta}\} + [K_{\theta u}]\{\theta\} + [K_{\theta v}]\{v\} + [K_\theta]\{\theta\} &= \{f_\theta(t)\}
\end{aligned} \tag{4.72}$$

By introducing the following changes, Equation (4.72) is made dimensionally homogeneous. Let

$$\{w\} = \{\theta\} \cdot \sqrt{A_B} \tag{4.73}$$

$$e'_j = e_j \sqrt{A_B} \quad , \quad j = 1, 2 \tag{4.74}$$

$$[M_w] = [M_\theta] \cdot \frac{1}{A_B} \tag{4.75}$$

$$[K_w] = [K_w] \cdot \frac{1}{A_B} \tag{4.76}$$

$$[K_{uw}] = [K_{wu}]^T = [K_{\theta u}] \cdot \frac{1}{\sqrt{A_B}} \tag{4.77}$$

$$[K_{vw}] = [K_{wv}]^T = [K_{\theta v}] \cdot \frac{1}{\sqrt{A_B}} \, . \tag{4.78}$$

Introducing these changes in Equation (4.22), they may be rewritten as

$$\begin{aligned}
[M_u]\{\ddot{u}\} + [K_u]\{u\} + [K_{uw}]\{w\} &= \{f_u(t)\} \\
[M_v]\{\ddot{v}\} + [K_v]\{v\} + [K_{vw}]\{w\} &= \{f_v(t)\} \\
[M_w]\{\ddot{w}\} + [K_{wu}]\{u\} + [K_{wv}]\{v\} + [K_w]\{w\} &= \{f_w(t)\}
\end{aligned} \tag{4.79}$$

Evaluation of Stiffness and Inertia Matrices

The inertia matrices $[M_u]$ and $[M_v]$ are constructed from m_i values as per Equation (2.12). Equation (2.13) shows the relation between the matrix $[M_\theta]$ and the $m\theta_i$ values given by Equation (4.71). From Equation (4.75) it follows that

$$\begin{aligned} M_{wi,i} &= m\theta'_i \\ M_{wi,j} &= 0 \qquad i \neq j \end{aligned} \tag{4.80a}$$

where

$$m\theta'_i = m\theta_i / A_B \quad . \tag{4.80b}$$

The building is assumed to be simply coupled in stiffness. Hence as in Chapter III, Equation (3.66), the matrix $[K_u]$ is given by:

$$\begin{aligned} Ku_{i,i+1} &= -kx_i \\ Ku_{i,i} &= kx_i + kx_{i+1} \\ Ku_{i,i+1} &= -kx_{i+1} \\ Ku_{i,j} &= 0 \quad j > i+1, \text{ or } j < i+1 \end{aligned} \qquad i,j=1,2,\ldots N. \tag{4.81}$$

Similarly,

$$\begin{aligned} Kv_{i,i-1} &= -ky_i \\ Kv_{i,i} &= ky_i + ky_{i+1} \\ Kv_{i,i+1} &= -ky_{i+1} \\ Kv_{i,j} &= 0 \quad j > i+1, \text{ or } j < i+1 \end{aligned} \qquad i,j=1,2,..N. \tag{4.82}$$

and

$$Kw_{i,i-1} = -k\theta'_i$$

$$Kw_{i,i} = k\theta'_i + k\theta'_{i+1}$$

except $Kw_{p,p} = k\theta'_p + k\theta'_{p+1} + kx_{p+1}\, e_2'^2 + ky_{P+1}\, e_1'^2$ $\quad i,j=1,2..,N.$ (4.85)

$$Kw_{i,i+1} = -k\theta'_{i+1}$$

$$Kw_{i,j} = 0 \quad j > i+1 \text{ or } j < i-1$$

where $$k\theta'_i = k\theta_i / A_B$$

Finally, due to the assumptions made previously with regards to the location of centers of mass, resistance, and geometry of the building the coupling matrices $[K_{uw}]$ and $[K_{vw}]$ may be shown to be given as follows

$$Kuw_{i,j} = 0$$

$$Kvw_{i,j} = 0$$

except for $i,j = 1,2,...N$ (4.84)

$$Kuw_{p,p} = -Kuw_{p,p+1} = -e'_2\, kx_{p+1}$$

$$Kvw_{p,p} = -Kvw_{p,p+1} = e'_1\, ky_{p+1}$$

The matrices [Kwu] , [Kwv] are transpose of [Kuw] and [Kvw] , respectively.

Parameters of the Problem

As in Chapter III, the study here will be restricted to buildings with N=15 as a typical case. The quantities kx_i and m_i are computed from Equations (3.61) and (3.62). They depend on the values chosen for Δkx , kx'_N and m . In Chapter III, the values of $\Delta kx/kx'_N$ and kx'_N/m were chosen, respectively, to be 1/3 and 1.5g where g

is the acceleration due to gravity. These same values for the two quantities will be used in this chapter also.

Among the other parameters, then, are $p(= P/N)$, c, α_b, α_t, γ^2 e_1' , e_2' as well as μ_{bx} , μ_{by} , μ_{tx} , μ_{ty} . The former group of parameters are identical to those obtained for shear beams. The remarks made about them in the section on the shear beam applies equally here except that p can take on only finite number of values within its range.

The term μ was defined earlier as the ratio of the second moment of stiffness about the vertical axis through its centre of resistance as obtained from actual distribution to that obtained with the assumption of uniform distribution over the story cross-section. Since torsional stiffness may be divided into two parts, one obtained from lateral stiffness in the x direction and the other from lateral stiffness in the y direction, one may alternately define μ_x and μ_y , respectively, referring to the two parts.

The range of μ_x and μ_y may be easily shown to be

$$0 \leq \mu \leq 3 \quad . \tag{4.85}$$

When the stiffness is all lumped at the center of resistance there will be zero (actual) torsional stiffness and μ will be zero. When all the stiffness is distributed at the extremeties of the floor plan the value of μ will be 3.

The term σ^2 was defined in the previous section as the ratio $\frac{k_3}{m_3} / \frac{k_1}{m_1}$; in general it has different values in the two portions of the beam. For shear building, a similar quantity may be defined:

$$\sigma_i^2 = \frac{k\theta_i}{m\theta_i} / \frac{kx_i}{m\theta_i} \tag{4.86}$$

Noting the definitions of $k\theta_i$ and $m\theta_i$, from Equations (4.70) and (4.71), it is apparent that σ_i^2 has a constant value for each of the two parts of the structure. One may then write:

$$\sigma_b^2 = \frac{(\mu_{bx}\alpha_b + \mu_{by}\gamma^2/\alpha_b)}{(\alpha_b + 1/\alpha_b)}$$

and (4.87)

$$\sigma_t^2 = \frac{(\mu_{tx}\alpha_t + \mu_{ty}\gamma^2/\alpha_t)}{(\alpha_t + 1/\alpha_t)}$$

where the subscripts b and t stand for the base portion and the tower portion respectively.

The similarity between Equations (4.18) and (4.87) may be noted. The only difference between the two equations is the addition of the μ terms in Equation (4.87) to provide for the non-uniform distribution of stiffness in the case of shear building.

σ_b^2 and σ_t^2 may be conveniently considered to be the parameters in place of α_b, α_t, μ_{bx}, μ_{by}, μ_{tx}, and μ_{ty}. The advantage in considering the latter group of parameters, however, is that they provide a more direct applicability to real problems.

The range of σ^2 for a given value of γ^2 is

$$\begin{aligned} 0 < \sigma^2 < 3\gamma^2 \quad & \gamma^2 \leq 1 \\ 0 > \sigma^2 > 3\gamma^2 \quad & \gamma^2 \geq 1 \end{aligned} \qquad (4.88)$$

For a given γ^2, the value of σ^2 depends on the values of μ_x and μ_y as well as α. The difference between the range of σ^2 shown by Equation (4.39) and (4.88) should be noted. It is due to introduction of the terms μ_x and μ_y in Equation (4.87).

Shear Building With Setback Symmetric About One Axis

As in the case of shear beam in previous section the investigation will be restricted mainly to coupled vibrations of buildings with setback unsymmetric about one axis only. To this end the setback will be assumed to be symmetric about the y axis, i.e. $e_1' = 0$. The translational vibration in the y direction will then be uncoupled from the translational vibration in the x direction and the torsional vibration about the vertical. The latter two vibrations will be coupled to each other except when $e_2' = 0$, and these coupled vibrations only will be investigated.

Equation of Motion and Solution

From Equation (4.84) when $e_1' = e_1/\sqrt{A_B} = 0$

$$[K_{vw}] = 0 \tag{4.89}$$

Thus the equations of motion, Equation (4.79), are reduced to

$$\begin{aligned} [M_u]\{\ddot{u}\} + [K_u]\{u\} + [K_{uw}]\{w\} &= \{f_u(t)\} \\ [M_w]\{\ddot{w}\} + [K_{wu}]\{w\} + [K_w]\{w\} &= \{f_w(t)\} \end{aligned} \tag{4.90}$$

and

$$[M_v]\{\ddot{v}\} + [K_v]\{v\} = \{f_v(t)\} \tag{4.91}$$

It is the former set of coupled equations, Equation (4.90), that are of interest here. Equation (4.91) represents the translational vibrations in the y direction.

In the following the phrase "translational vibrations", unless otherwise qualified, will be used to mean the translational vibrations in the x direction.

Equation (4.90) may be written in the general form (2.42) of Chapter II with appropriate definitions of the matrices [M] and [K] and vectors $\{r\}$ and $\{f(t)\}$. The general solution of Equation (2.42) is given by Equations (2.61), (2.67) and (2.68) from which the solution of (4.90) may be written as follows

$$\left\{ \begin{matrix} u \\ w \end{matrix} \right\} = [\Phi] \{\eta\} \tag{4.92}$$

In Equation (4.92) $[\Phi]$ is the modal matrix, the columns $\{\phi^k\}$ (k=1,2,..,2N) of which are the modes of the related homogeneous system of Equation (4.90). The elements η_k of vector $\{\eta\}$ is given by

$$\ddot{\eta}_k + 2\beta_k\omega_k\dot{\eta}_k + \omega_k^2 \eta_k = g_k(t) \tag{4.93}$$

in which $\omega_k (k = 1,2,\ldots,2N)$ are the frequencies of the related homogeneous system of Equation (4.90) and β_k are the fraction of critical damping. The term containing β_k is added on the assumption that damping in buildings is viscous and that it does not affect the natural frequencies and modes of the corresponding undamped system (Equation (4.90)).

Also

$$g_k(t) = \frac{\{\phi^k\}^T \left\{ \begin{matrix} f_u(t) \\ f_w(t) \end{matrix} \right\}}{\{\phi^k\}^T [M] \{\phi^k\}} \tag{4.94}$$

When the structure is subjected to ground acceleration

$$\begin{aligned} f_u(t) &= - [M_u] \left\{ \begin{matrix} 1 \\ 1 \end{matrix} \right\} \ddot{x}_{01} \\ f_w(t) &= - [M_w] \left\{ \begin{matrix} 1 \\ 1 \end{matrix} \right\} \ddot{x}_{03} \cdot \sqrt{A_b} \end{aligned} \tag{4.95}$$

where $\ddot{x}_{01}$ is the translational component of the base acceleration in the x direction and $\ddot{x}_{03}$ is its rotational component about the vertical axis. The latter is generally assumed to be negligible in earthquake ground acceleration and will be neglected here. Then, $g_k(t)$ may be written as

$$g_k(t) = \lambda_{1k} \ddot{x}_{01} \tag{4.96}$$

where

$$\lambda_{1k} = \frac{\{\phi^{1k}\}^T [M_u] \{\begin{matrix}1\\1\\\vdots\end{matrix}\}}{\{\phi^k\}^T [M] \{\phi^k\}} \tag{4.97}$$

in which $\{\phi^{1k}\}$ is the translational component of the mode $\{\phi^k\}$.

A method of obtaining the modes $\{\phi^k\}$ and the frequencies ω_k, $k = 1,2,\ldots,2N$, pertaining to the equations of motion in general form, Equation (2.42), is described in Chapter II and can be used for the particular set of equations of interest here, viz. Equations (4.90).

Parameters Held Constant

Attention will be restricted further to the study of the effect of e_2', and to some extent of σ^2 (Equations (4.87) and (4.88)) on the dynamic behavior of a building with given level and degree of setback. As in Chapter III, 15-story building will be investigated as a typical case. As in the case of shear beam, the following level and degree of setback are assumed:

$$p = .6 \quad \text{or} \quad P = 9$$

and (4.98a)

$$c = .25$$

Further, α_b and α_t are also assumed to be fixed and are given by the same values as for the shear beam, viz.

$$\alpha_b = \alpha_t = 1 \tag{4.98b}$$

the values of μ_{bx} , μ_{by} , μ_{yx} , μ_{ty} will also be assumed to be fixed. These values are chosen from the following considerations.

Consider a story in a structure in which n lateral stiffness elements s_1, s_2,...s_n in one direction, say x, equally spaced in plan along a line y perpendicular to that direction. Suppose these stiffness elements are all identical, $s_1 = s_2 = \ldots s_n = 1$ (say). Then, the principal elastic axis (refer to Chapter II for definition) is midway between the end stiffness elements s_1 and s_n . It can be shown that the second moment of the stiffness elements s_1, s_2, ... s_n about the principal axis is

$$I_a = \frac{n(n+1)(n-1)}{12} \cdot \ell^2 \tag{4.99}$$

where ℓ is the spacing between consecutive stiffness elements.

If the same total stiffness $(s_1 + s_2 + \ldots + s_n)$ were distributed uniformly about the principal elastic (x) axis then the second moment of the lateral stiffness about the principal elastic axis will be

$$I_u = n \cdot \frac{(n-1)^2}{12} \cdot \ell^2 \tag{4.100}$$

The term μ is defined as the ratio

$$\mu = \frac{I_a}{I_u} \tag{4.101}$$

so that from Equations (4.99) and (4.100)

$$\mu = \frac{n + 1}{n - 1} \tag{4.102}$$

Table IV.2 gives the values of μ for various values of n. Also from Equation (4.102) it is seen that as $n \to \infty$, $\mu \to 1$.

TABLE IV.2

VALUES OF μ FOR SEVERAL VALUES OF n AS OBTAINED FROM EQUATION (4.102)

n	2	3	4	5	6	7	8	9	10
μ	3	2	1.67	1.50	1.40	1.33	1.29	1.25	1.22

In actual structures the conditions may very considerably from those assumed above (viz., equal spacing of equal valued stiffness elements). Table IV.2 provides only an indication of the possible values of μ . As was noted earlier the value of μ may range between 0 and 3.

Since the tower and the base portions of the building are assumed to be square (i.e. $\alpha_b = \alpha_t = 1$), it is reasonable to assume that

$$\begin{aligned} \mu_{bx} &= \mu_{by} \\ \mu_{tx} &= \mu_{ty} \quad . \end{aligned} \tag{4.103}$$

Further, since the tower is smaller than the base in plan area, the value of n for tower will be less than that of base and therefore $\mu_t > \mu_b$ (see Table IV.2). The following values

$$\begin{aligned} \mu_{bx} &= \mu_{by} = 1.2 \\ \mu_{tx} &= \mu_{ty} = 1.45 \end{aligned} \tag{4.104}$$

were chosen for computations. It may be noted from Equations (4.87) that increase or decrease in μ values would increase or decrease the

values of σ^2, and a relative increase or decrease in μ_b with respect to μ_t would increase or decrease the value of σ_b^2 with respect to σ_t^2.

With the values of the μ's, α_b and α_t chosen and fixed as above, the values of σ_b^2 and σ_t^2 will be varied by varying the value of γ^2, see Equation (4.87). Having chosen $\mu_{bx} = \mu_{by} = 1.2$ and $\mu_{tx} = \mu_{ty} = 1.45$ as well as $\alpha_b = \alpha_t$, it is not difficult to see from Equation (4.87) that

$$\sigma_t^2 = \frac{1.45}{1.2} \sigma_b^2 \tag{4.105}$$

and this relation holds regardless of the value of γ^2.

Uncoupled Translation and Torsional Mode Periods

When $e_2' = 0$, the translational vibration in the x direction and the torsional vibration will also uncouple from each other, since from Equation (4.84)

$$[K_{wu}] = [K_{uw}]^T = [0] . \tag{4.106}$$

The two equations referring to the translational and torsional vibration in Equation (4.90) then uncouple from each other.

The natural periods of the uncoupled translational vibrations are independent of σ_b^2 and σ_t^2. The natural periods of the uncoupled torsional vibration are however dependent on them. For a given p and c, due to the particular choice of values for α_b, α_t, μ_{bx}, μ_{by}, μ_{tx} and μ_{ty}, such that $\alpha_b = \alpha_t$, $\mu_{bx} = \mu_{by}$, and $\mu_{tx} = \mu_{ty}$, which leads to relation (4.105) between σ_b^2 and σ_t^2, the periods of torsional vibration will be linearly proportional to $1/\sigma_b$ or $1/\sigma_t$. This is illustrated in Figure 4.9 for first few mode periods of the shear building

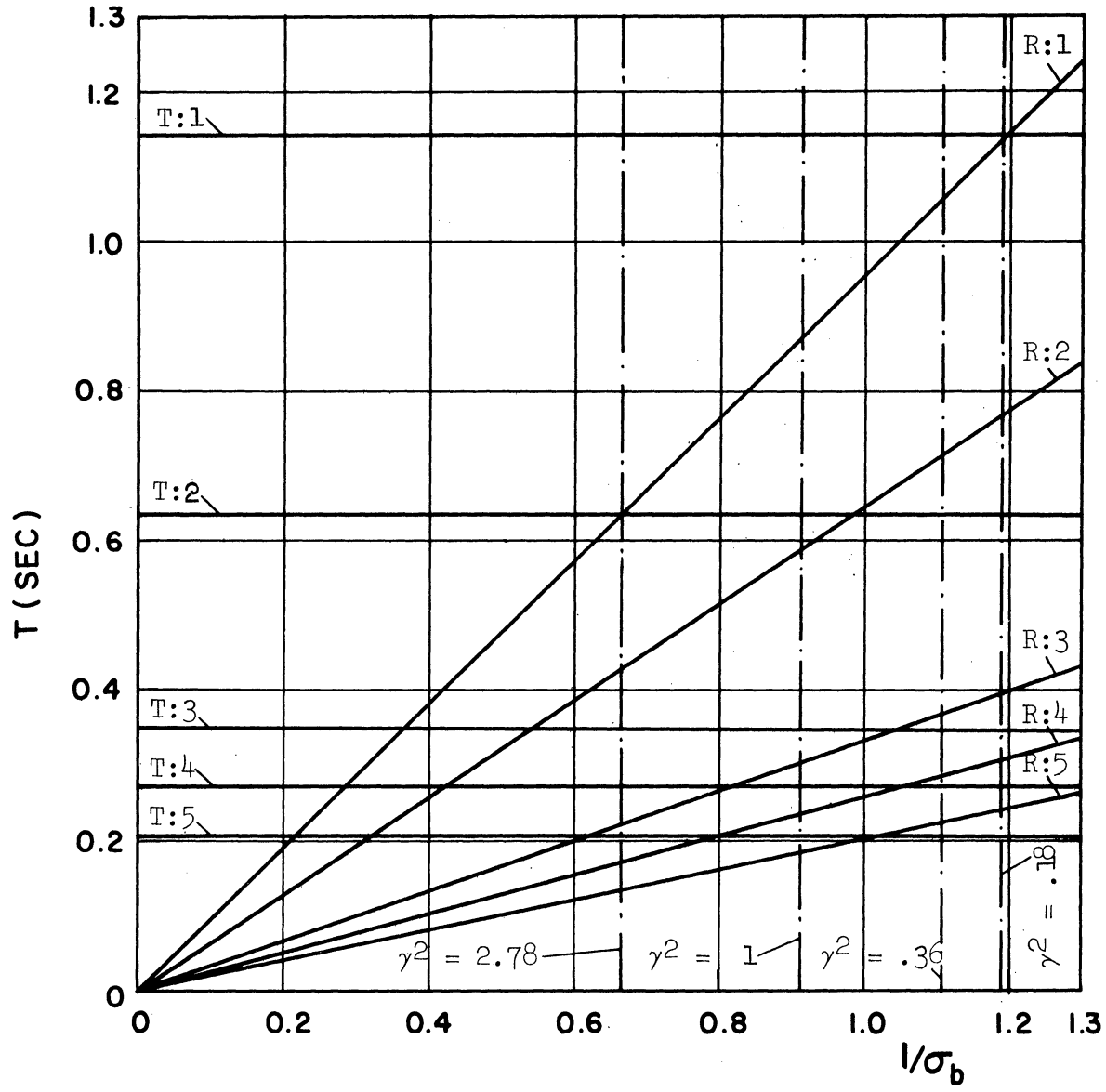

Figure 4.9. Uncoupled Translational and Torsional Mode Periods, Shear Building.

with properties already chosen, Equations (4.98), (4.104). The notation for modes introduced in the section on shear beam is used here.

From Figure 4.9 the following observation may be made. As was the case with shear beam, there are several values of σ_b for which a translational mode period and a torsional mode period have identical values. Also if the two groups of modes are combined together and ordered in the ascending order of their frequencies, the same torsional (or translational) mode will be ranked or numbered differently for different values of σ_b .

Next, the effect of varying e_2' on the various modal quantities will be examined for a few values of σ^2 . As mentioned earlier, the value of σ^2 will be controlled by varying γ^2 . The values of γ^2 for which the computations are made are: .36, 1., and 2.78. These same values of γ^2 were used in the case of the shear beam and their significance was discussed there.

Another value, $\gamma^2 = .5$, for which the T:1 and R:1 mode periods at $e_2' = 0$ were almost equal, was also used. Here the T:1 and R:1 mode periods of the uncoupled case are almost equal at $\gamma^2 = .18$ (see Figure 4.9). Computations will also be made for this value of γ^2 although it probably lies outside the normal range of values of γ^2 . Also it may be noted from Figure 4.9 that at $\gamma^2 = 2.78$ the R:1 and T:2 mode periods for the uncoupled case are almost equal.

The values of $1/\sigma_b$ corresponding to the above values of γ^2 are shown by vertical lines in Figure 4.9. In Table IV.3 are given the above values of γ^2 with the corresponding values of σ_b^2 and σ_t^2 . The difference between these values of σ_b^2 and σ_t^2 and those for the

shear beam, Table IV.1, should be noted; this difference is of course because of the μ values being taken different than 1 for shear buildings.

TABLE IV.3

EQUIVALENT VALUES OF σ_b^2 , σ_t^2 AND γ^2

γ^2	σ_b^2	σ_t^2
.18	.708	.740
.36	.816	.986
1.00	1.200	1.450
2.78	2.268	2.740

Periods

Periods vs. e_2' plots for R:1 through R:4 and T:1 through T:4 modes are given in Figure 4.10. The convention used for denoting the modes is explained in the section on the shear beam. Except for the case $\gamma^2 = 2.78$, the T:1 through T:4 and R:1 through R:4 modes constitute the first eight coupled modes (arranged in ascending order of their frequencies). For $\gamma^2 = 2.78$, the 8th and 9th modes are the T:5 and T:6 modes and the 10th mode is the R:4 mode (see Figure 4.9).

The first mode period (T:1 for all values of γ^2) always increases with increasing e_2' . The changes in the higher mode (T:j, R:j, $j \geq 2$) periods are generally very small. The T:2 mode period for the case $\gamma^2 = 2.78$ is an exception. There is a significantly greater change with e_2' in the T:2 mode for this case than for other values of γ^2 . As noted earlier, the R:1 and T:2 mode periods for $\gamma^2 = 2.78$ at $e_2' = 0$ are almost equal to each other (see Figure 4.9).

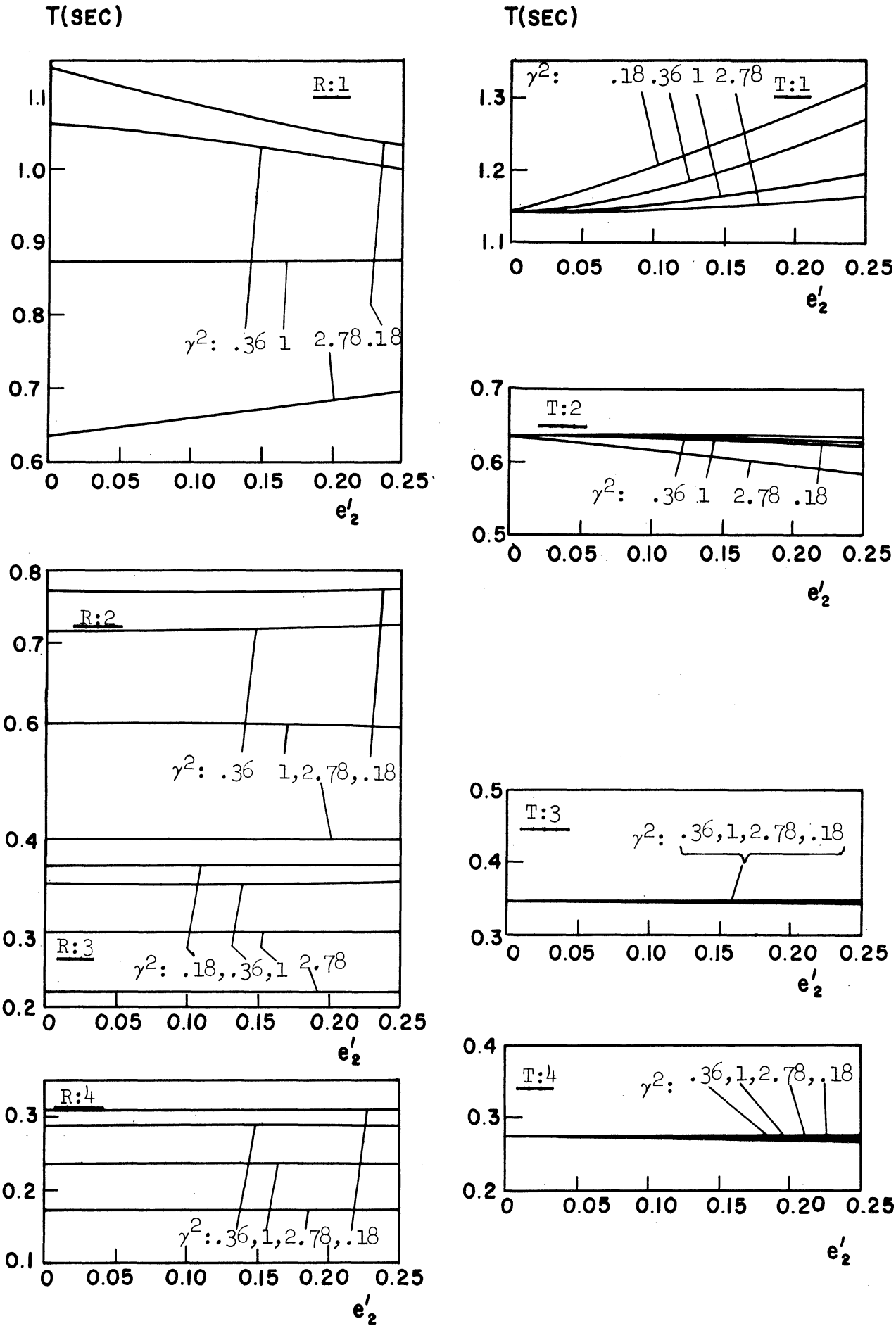

Figure 4.10. Coupled Mode Periods, Shear Building.

In the R:1 and T:1 modes the maximum change in period occurs for the case $\gamma^2 = .18$. For this case the T:1 and R:1 mode periods at $e_2' = 0$ are almost equal to each other. As the difference between the mode periods at $e_2' = 0$ increases with increasing γ^2, the extent of change in periods with increasing e_2' decreases. Thus, for the case $\gamma^2 = .36$, there is still a significant amount of change in the T:1 and R:1 periods as e_2' increases from zero to .25, although it is less than for the case $\gamma^2 = .18$. For $\gamma^2 = 1$ there is almost no change in the R:1 period. For $\gamma^2 = 2.78$ the change in T:1 period is very small but there is a noticeably more change in the R:1 period. This ties in with the observation made above that R:1 and T:2 modes are almost equal at $e_2' = 0$ for the case $\gamma^2 = 2.78$.

Mode Shapes

The two components of the R:1 and R:2, and T:1 and T:2 mode for the case $\gamma^2 = 1$ is given in Figure 4.11. The translational component $\{\phi^{1k}\}$ of the mode vector $\{\phi^k\} = \left\{\begin{matrix}\phi^{1k} \\ \hline \phi^{3k}\end{matrix}\right\}$ represents the displacements of the centroids of the floor. Since such centroids in the tower portion are on a different vertical line than those of the base portion, (except when $e_2' = 0$), the vector $\{\phi^{1k}\}$ does not represent the translations along a single vertical line in the building. This leads to some difficulty in representing the translational component by a planar figure. The same difficulty is also encountered in the case of shear beam for the same reasons. The translation component of the mode as drawn in Figure 4.11 represents the translations along a vertical line through the tower centroids (extended into the base portion) for the entire hieght of the structure. It should be noted that

the elements of $\{\phi^{3k}\}$ are the rotations of the floors times the constant $\sqrt{A_B}$, see Equation (4.92).

The modeshapes are normalised by making either ϕ_N^{1k} or ϕ_N^{3k} (the Nth element of vectors $\{\phi^{1k}\}$ and $\{\phi^{3k}\}$, respectively, representing the translation of the centroid of the top floor and rotation of the top floor about the vertical axis time $\sqrt{A_B}$), depending on whether it is a translational (T) mode or a torsional (R) mode, respectively.

The effect of increasing e_2' on the mode shapes is to increase the component (numerically) which is absent at $e_2' = 0$ relative to the other component. The shape of the component originally (i.e. at $e_2' = 0$) present is only slightly affected by the introduction and increase of the eccentricity e_2'. In general, similar effects are observed in the higher modes (of the case $\gamma^2 = 1$) and also the modes for the cases $\gamma^2 = .18$, $.36$ and 2.78 which have not been presented.

It may be observed from Figure 4.11 that the two components of the same mode do not necessarily have the same number of nodes. As stated above, the translational components in Figure 4.11 represent the translations along a vertical line passing through the tower centroid. If translations along some other vertical line (for example, the one passing through the base centroid) is taken as the translational component of the mode shape, it may show a different number of modes then there are for the translation component as given in Figure 4.11. It seems that this difference in the number of modes between any two representations of the translational component may be at most 1.

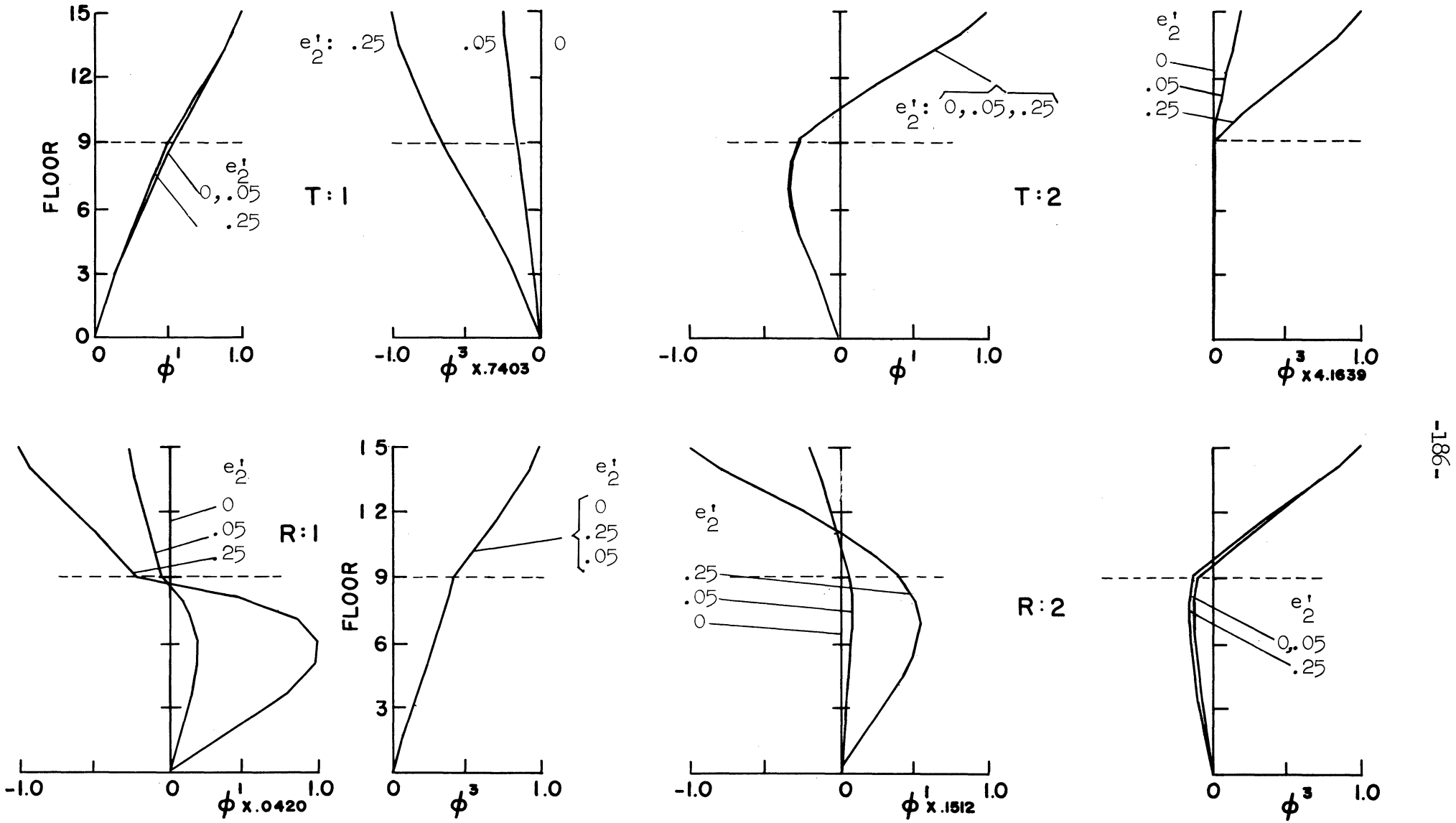

Figure 4.11. Coupled Mode Shapes, Shear Building.

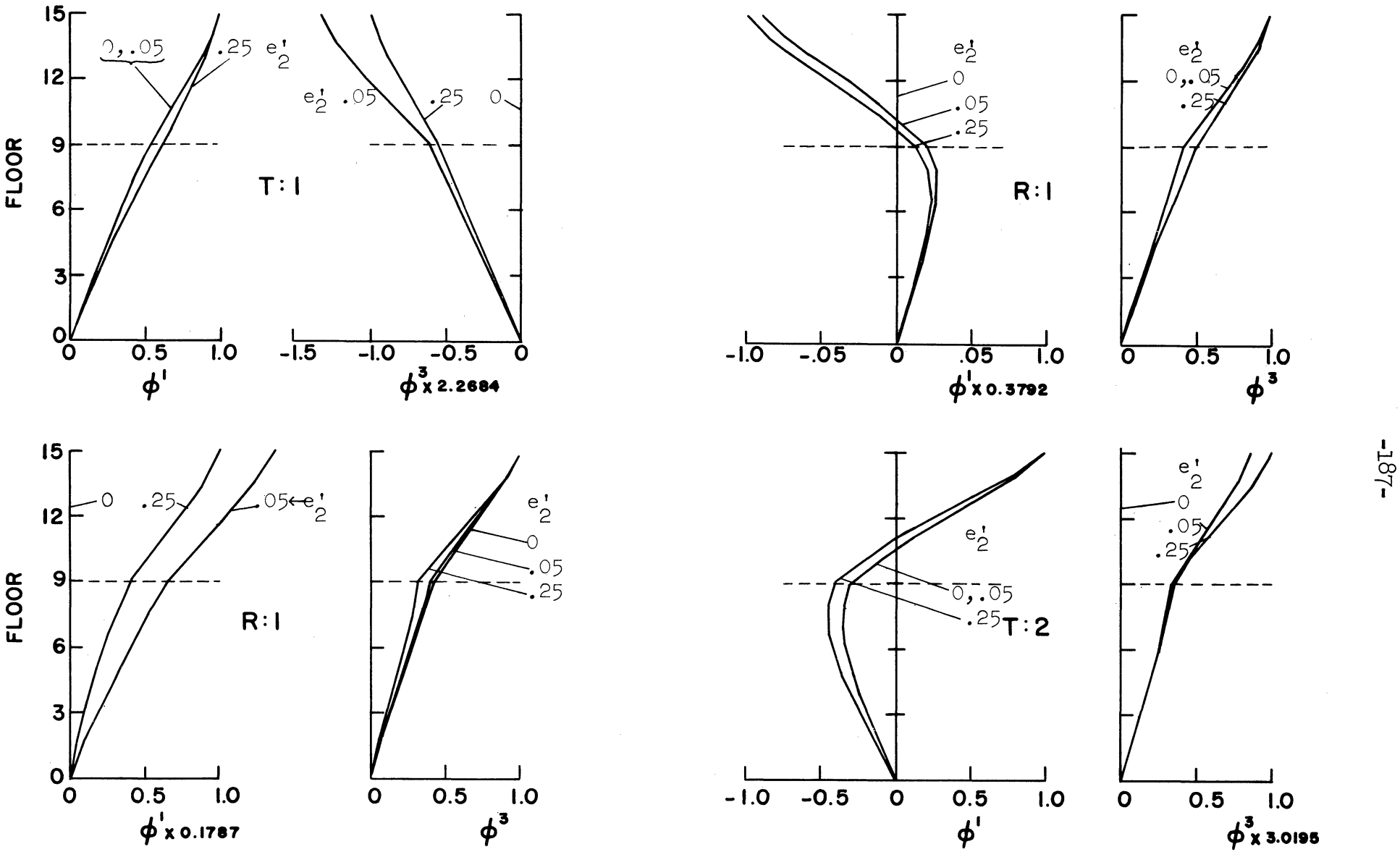

Figure 4.12. Coupled Mode Shapes, Shear Building.

The T:1 and R:1 mode shapes for the case $\gamma^2 = .18$ are given in Figure 4.12. The figure shows how in both modes the component of the mode originally (i.e. $e_2' = 0$) absent increases very sharply for small values of e_2' and then decreases with further increase in e_2'. A similar effect is seen in the T:2 and R:1 modes for the case $\gamma^2 = 2.78$, also given in Figure 4.12. As in the case of shear beam (T:1 and R:1 modes for $\gamma^2 = .5$, see Figure 4.5), this particular effect showing a high degree of coupling for small eccentricities seems to be due to the closeness of the periods of the pair of modes at $e_2' = 0$.

Kinks at setback level are present in both the components of all modes presented in Figures 4.11 and 4.12. They are due to the presence of setback which causes (as has been assumed) a sharp change at the setback level in the stiffness, mass, torsional stiffness, and mass-moment-of-inertia distribution. The presence of setback of degree $c = A_T/A_B$ has a sharper effect on the quantities related to the torsional vibration than those related to the translational vibration. This is because the former set of quantities are proportional to the square of plan area (and therefore to c^2) while the latter are proportional only to the first power of the plan (and therefore to c). This fact explains the sharper kinks generally observed in the rotational modes.

Coupling

The ratios ϕ_i^{1k}/ϕ_i^{3k} $(i = 1,2,\ldots,N)$ may be called the degree of coupling or simply coupling for the ith floor in the kth mode, if the kth mode is a torsional (R) mode. If the kth mode is a translational (T) mode, ϕ_i^{3k}/ϕ_i^{1k} may be termed the degree of coupling. The mode shapes as presented

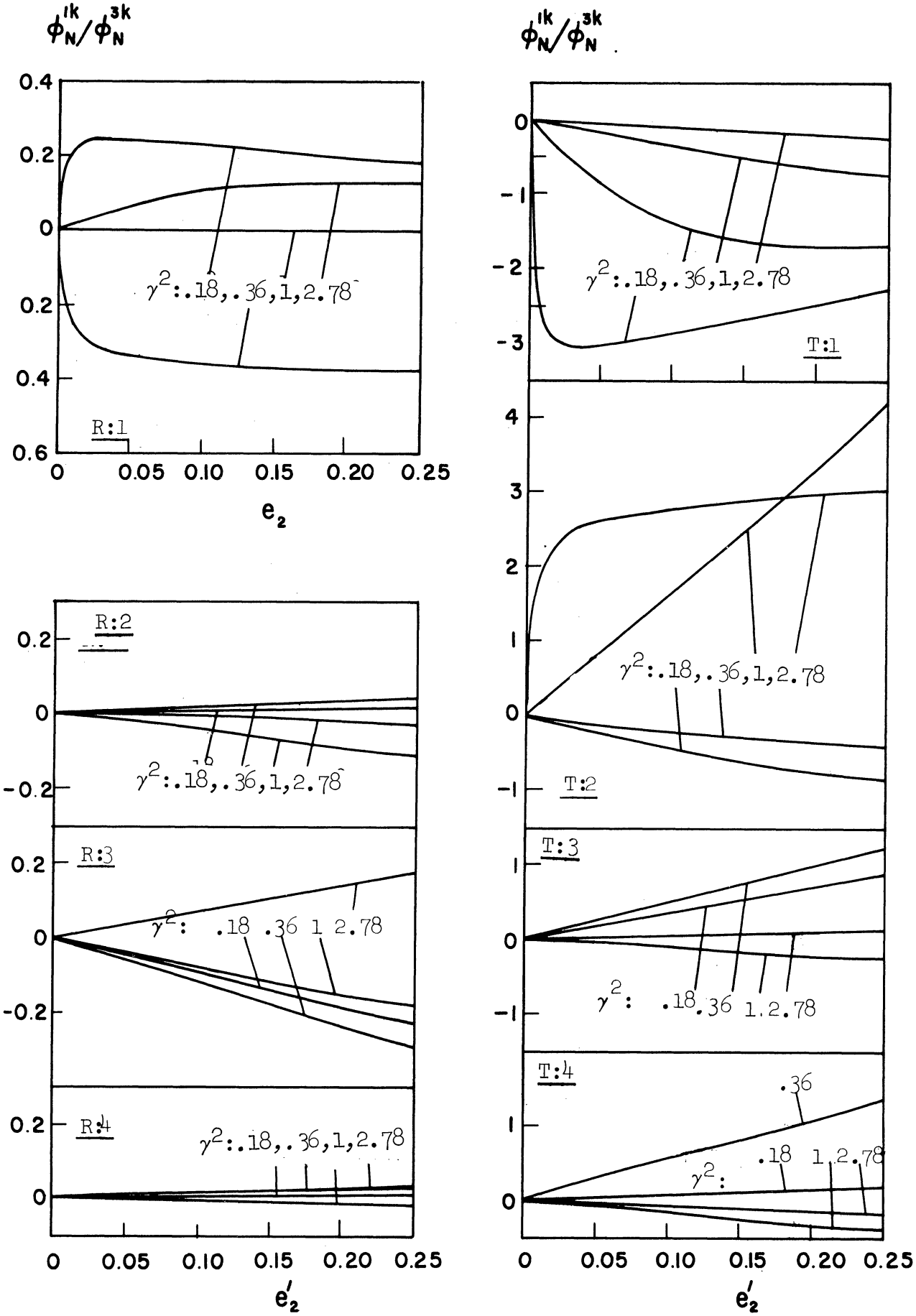

Figure 4.13. Coupling, Shear Building.

in Figures 4.11 and 4.12 show in a qualitive manner coupling at carious floor levels in these modes. As is apparent from these figures, the coupling (i.e., the ratio ϕ_i^{1k}/ϕ_i^{3k} or its inverse) will in general have different values for different floors in the same mode.

In order to obtain a quantitative idea about the effect of e_2' on coupling in various modes for various values of γ^2, coupling for a particular floor may be plotted against e_2'. This is done in Figure 4.13 for the (topmost) Nth floor. The ratios ϕ_N^{1k}/ϕ_N^{3k} are plotted on the first four torsional modes (R:1 through R:4) and the ratios ϕ_N^{3k}/ϕ_N^{1k} are plotted for the first four translational modes (T:1 through T:4). As mentioned earlier these modes constitute the first eight modes except for the case $\gamma^2 = 2.78$, in which R:4 is the tenth mode.

Coupling in general increases from zero at zero eccentricity of the tower to some finite value as the tower as shifted to its maximum eccentricity. The increase seems to be linear in most cases. Coupling seems to increase sharply for small eccentricities and then increase slowly on further increase in eccentricity in the T:2 and R:1 modes of the case $\gamma^2 = 2.78$ and in the T:1 and R:1 modes for the cases $\gamma^2 = .18$ and, to a lesser extent, $\gamma^2 = .36$. The coupling has opposite signs in each of these pairs of modes.

Base Shear and Base Torque

Next, the effect of tower eccentricity on the modal counterparts of base shear coefficient and base torque coefficient will be examined. Base shear coefficient has already been established as an important quantity in earthquake resistant design. Since dynamic unsymmetry induces rotational vibration in structures torques (or torsional

forces) will be generated throughout the height of the structure simultaneously with the shear forces. Thus in a manner similar to base shear coefficient one may define and use base torque coefficient.

Modal base shear and base torque are here defined as the responses of the structure subjected to a one g static acceleration. When these quantities are multiplied by the maximum absolute acceleration (in g units) attained by a single degree of freedom system with the same frequency and damping as the mode being considered when subjected to a ground acceleration, they will give the corresponding maximum modal responses of the structure to that ground acceleration.

The kth mode base shear coefficient is given by

$$C'_{1Bk} = \lambda_{1k} \frac{\{\phi^{1k}\}^T [M_u] \{1\}}{\{1\} [M_u] \{1\}} \tag{4.107}$$

where λ_{1k} is the modal participation coefficient given by Equation (4.97). The base shear coefficient response in the kth mode when subjected a ground acceleration $x_{01}(t)$ would then be

$$C_{1Bk}(t) = C'_{1Bk} [\ddot{\xi}_k(t) + \ddot{x}_{01}(t)]/g \tag{4.108}$$

where

$$\eta_k = \lambda_{1k} \xi_k \tag{4.109}$$

From Equation (4.93) it follows that ξ_k is given by

$$\ddot{\xi}_k + 2\beta_k\omega_k\dot{\xi}_k + \omega_k^2 \xi_k = - \ddot{x}_{01} \tag{4.110}$$

Base torque in the kth mode is given by

$$T_{Bk} = \lambda_{1k} \left[\sum_{i=1}^{N} m\theta'_i \phi_i^{3k} - e'_2 \sum_{i=P+1}^{N} m_i \phi_i^{1k} \right] \sqrt{A_B} \ (\ddot{\xi}_k + \ddot{x}_{01}) \ . \qquad (4.111)$$

The second term in the square bracket represents the torque produced by the shear at the base of tower about the base portion centroid.

Base torque is non-dimensionalized to obtain base torque coefficient in a similar manner as used in the case of shear beam, viz.

$$C'_{3Bk} = \lambda_{1k} \cdot \frac{\left[\sum_{i=1}^{N} m\theta'_i \phi_i^{3k} - e'_2 \sum_{i=P+1}^{N} m_i \phi_i^{1k} \right]}{\sum_{i=1}^{N} m\theta'_i} \ . \qquad (4.112)$$

The relation between $m\theta'_i$ and the mass moment of inertia $m\theta_i$ given by Equation (4.80b) may be noted.

The base torque coefficient response in the kth mode when subjected to a ground acceleration $\ddot{x}_{01}$ would then be

$$C_{3Bk}(t) = C'_{3Bk} \cdot [\ddot{\xi}_k(t) + \ddot{x}_{01}(t)]/g \qquad (4.113)$$

C'_{1Bk} and C'_{3Bk} values for R:1 through R:4 and T:1 through T:4 modes are plotted against e'_2 in Figures 4.14 and 4.15 for several values of γ^2 . R:1 through R:4 and T:1 through T:4 modes constitute the first eight modes except for the case $\gamma^2 = 2.78$ for which R:4 is the tenth mode.

In the torsional modes the base shear coefficient increases from zero at $e'_2 = 0$ to some finite value as e'_2 increases to its maximum value. In the translational modes C'_{1Bk} decreases from some finite

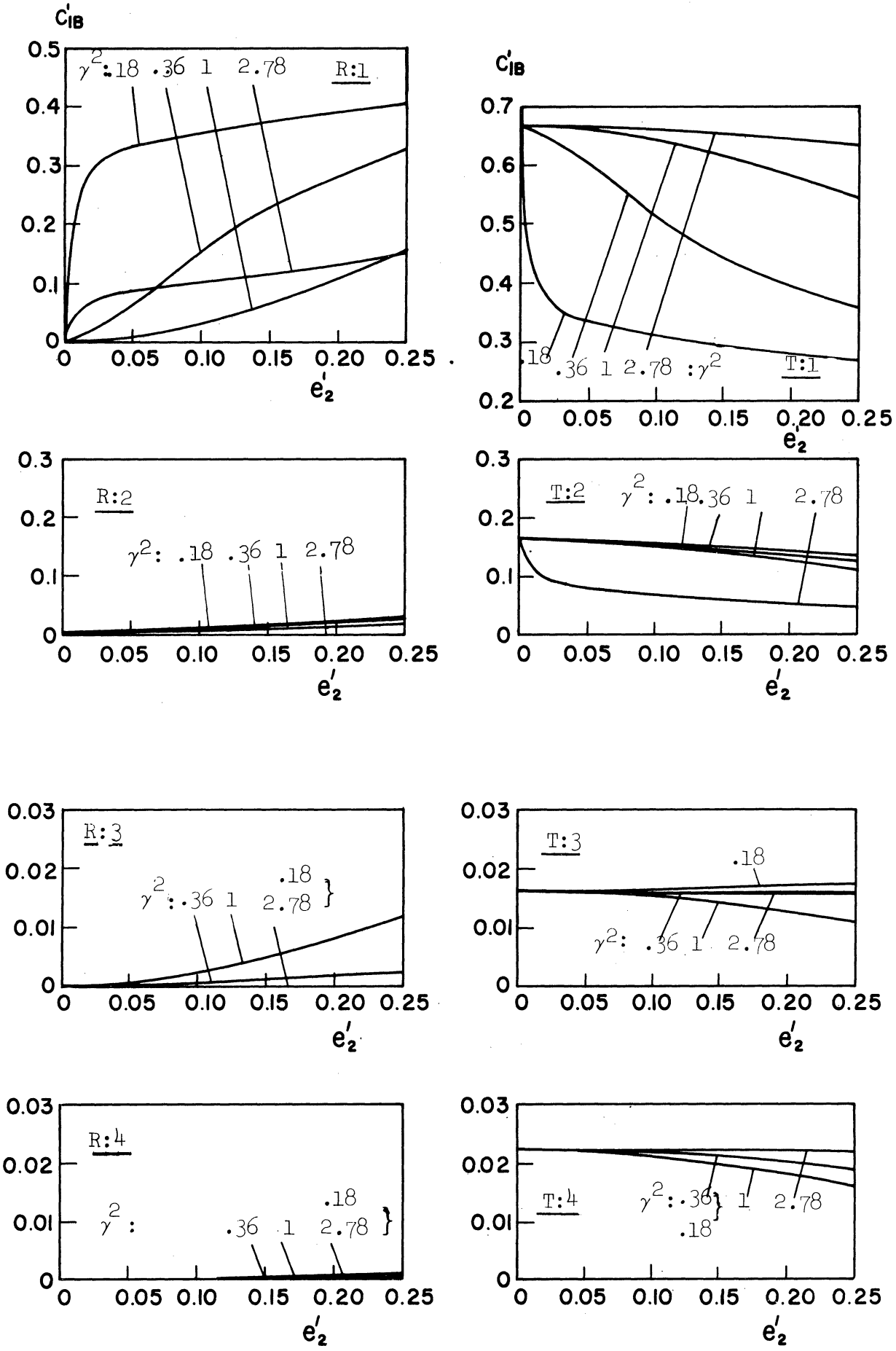

Figure 4.14. Modal Base Shear Coefficients, Shear Building.

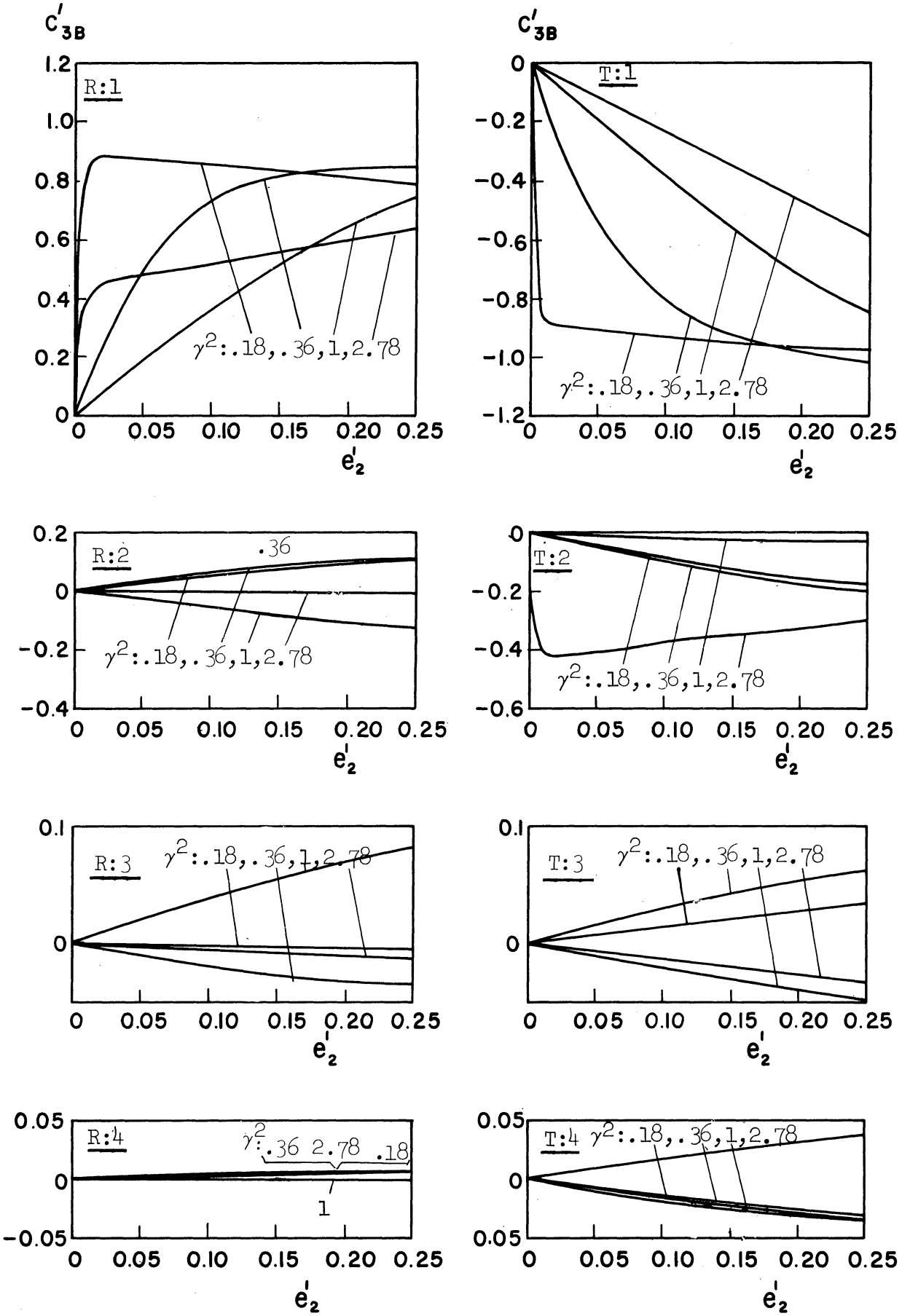

Figure 4.15. Modal Base Torque Coefficients, Shear Building.

value at $e_2' = 0$, which is obtainable from Figure 3.2 (with P = 9 or p = .6 and c = .25), and decreases to some finite values as e_2' increases to its maximum value. C'_{1Bk} has the same sign in all modes.

The antisymmetry between the increase and decrease of C_{1Bk} in the R:1 and T:1 modes, respectively, for the cases $\gamma^2 = .18$, .36 and 1, is quite remarkable; i.e., for these cases the sum of C'_{1Bk} in the R:1 and T:1 modes remains almost constant for all values of e_2'. This behavior is best for $\gamma^2 = .18$ and then worsens slightly for $\gamma^2 = .36$ and further for $\gamma^2 = 1$.

For the case $\gamma^2 = 2.78$ somewhat similar antisymmetry seems to exist between the R:1 and T:2 modes although it is not as pronounced as in the above cases. In fact for this case it seems that the sum of C'_{1Bk} in the R:1, T:1, and T:2 modes seems to be much closer at being constant for all values of e_2' than the sum of C'_{1Bk} in the T:1 and R:2 modes alone.

In the higher modes base shear is quite small compared to the R:1 and T:1 modes. It was observed in Chapter III that for setback levels below midheight, base shear might be largerin one of the higher (T:j $j \geq 2$) modes that in the first mode (T:1) in a building with symmetric setback. For a building with unsymmetric setback level below midheight and small c, large base shear may similarly be expected in higher modes.

As mentioned earlier the maximum base shear coefficient response in the kth mode to a given earthquake excitation is $C'_{1Bk} \cdot S_a(\omega_k, \beta_k)/g$, where $S_a(\omega_k, \beta_k)$ is the acceleration response spectrum value for that earthquake excitation. Unless the frequencies of some of the modes are very close, the maximum total base shear

coefficient response may be approximately given by the square root of the sum of squares (RSS) of the modal maximum base shear coefficient responses. In case two of the modes have close periods (as is the case of R:1 and T:1 modes when $\gamma^2 = .18$ for small values of e_2') and damping in the two modes is not very low[7], the responses in these modes may be added algebraicly first and then the above rule of the sum of squares may be applied to obtain a good approximation for the maximum total base shear coefficient.

The sum of C'_{1Bk} in all 2N modes is equal to one. This is proved in Appendix B. Further, C'_{1Bk} is always positive in all modes, see Equations (4.107) and (4.97). Now at $e_2' = 0$ the value of C'_{1Bk} in the N torsional modes is zero and it has non-zero values only in N translational modes. However when $e_2' \neq 0$, C'_{1Bk} is, in general, non-zero and positive in all the 2N modes.

Consider, now, two buildings which are exactly similar except that the setback in one is symmetric $(e_2' = 0)$ and in the other is unsymmetric about x axis $(e_2' \neq 0)$. As was observed previously, the introduction of asymmetry of setback changes the period of some extent especially in the lower modes, see Figure 4.10.

Let us assume that the mode periods of each of the two buildings are well separated so that the RSS combination of modal maximum responses is a good approximation of the true combined response. Let us also assume that the S_a (absolute acceleration response spectrum) value does not change significantly with the small differences between the corresponding mode periods of the two buildings. Then, with these assumptions, the properties of C'_{1Bk} stated above suggest that the

base shear coefficient response of a building with setback unsymmetric about one principal direction subjected to a given earthquake will, in general, be smaller than that of the corresponding building with symmetric setback.

When the setback is symmetric (i.e. $e_2' = 0$), base torque (and for that matter all torsional motion) is zero in the uncoupled translational modes and torsional modes. This is because there is no coupling between the rotational and translational vibration and external rotational exciting forces are assumed to be zero.

As the setback becomes unsymmetric the base torque coefficient (C'_{3Bk}) begins to increase numerically. As e_2' increases the rate of increase in C'_{3Bk} either decreases or remains nearly constant. In some cases like the R:1 mode of $\gamma^2 = .18$ and T:2 mode of $\gamma^2 = 2.78$ after a sharp increase for small values of e_2', C'_{3Bk} decreases slightly with further increase in e_2' (Figure 4.15).

The base torque coefficient in the R:1 and T:1 modes are opposite in sign and some antisymmetry is apparent in the variation of C'_{3Bk} in the two modes for the case $\gamma^2 = .18, .36$ and 1. for small values of e_2'. Pairing of higher modes in terms of opposite signs of C'_{3Bk} is not always possible.

Base torque coefficient (BTC) is, in general, progressively smaller (in numerical value) in the higher modes. But, as observed earlier in the case of base shear coefficient, for structures with setback level below midheight and with small c, base torque coefficient may be larger (in numerical value) in some of the higher modes than in the T:1 and R:1 modes.

The maximum modal BTC response in the kth mode to an earthquake acceleration is $C'_{3Bk} \cdot S_a(\omega_k, \beta_k)/g$ where $S_a(\omega_k, \beta_k)$ is the acceleration response spectrum value for that earthquake acceleration. Unless the periods of some of the modes are very close to each other, the maximum total BTC response to that earthquake will be approximately equal to the square root of the sum of squares (RSS) of the maximum modal responses. For such cases, assuming that S_a is not much affected by the change in periods as e'_2 changes, the behavior of C'_{3Bk} observed in Figure 4.15 suggests that maximum BTC response to an earthquake would generally increase with increase in eccentricity e'_2. Further, the rate of increase in the BTC response will generally diminish with increasing e'_2.

If the above rule of adding the modal maximum responses to obtain the total maximum response were applied to the cases of $\gamma^2 = .18$ or $\gamma^2 = 2.78$, it would lead to very high BTC response (in comparison with the other two cases) for very small values of e'_2 ($e'_2 < .05$ say). This is because, as seen in Figure 4.15, the C'_{3Bk} values increase sharply for very small values of e'_2 in the T:1 and R:1 modes for the case $\gamma^2 = .18$ and in the T:2 and R:1 modes for the case $\gamma^2 = 2.78$.

However, from Figure 4.9 and 4.10 it is also obvious that for very small values of e'_2 the periods in the pairs of modes mentioned above are quite close to each other. For this reason, and if the damping in the two modes is not too low,(7) algebraic addition of modal maximum BTC responses will be much closer to the combined maximum BTC response of the two modes in such cases. Since C'_{3Bk} values in such pairs of modes are almost equal to each other but opposite in sign (see Figure 4.15), the maximum BTC response of the

of the two modes combined, and hence also the total maximum BTC response, will be much smaller than the one obtained by the method of adding modal responses described earlier. Thus the conclusion made above about the BTC response may be said to hold in general.

Responses to Recorded Earthquake Excitations

Responses of the 15-story building with setback level P = 9 and degree of setback c = .25 , examined in the preceding modal study, to two recorded earthquake excitations have been computed. The earthquake excitations used here are the S component of the El Centro, May 18, 1940, and the N69°W component of the Taft, July 21, 1952 earthquake records. The same records were used in the response studies for buildings with symmetric setbacks in Chapter III.

First eight modes were used in computing the total responses. In the responses computed (displacements, rotations, shears, and torques) the contribution of higher modes, including some within the first eight modes, is negligible compared to that of the first few (say four) modes. In Chapter III, where only the uncoupled translational modes were used to compute the translational responses, only the first four modes were considered for similar reasons.

Damping was assumed to be 4% of critical in the first four modes and 6% of cirtical in the next four modes. At $e_2' = 0$, the first four modes consist of first two translational modes and first two rotational modes. The next four modes are made up of higher translational and rotational modes. In Chapter III, where first four uncoupled translational modes were used in computing responses, damping was assumed to be 4% of critical in the first two modes and

6% of critical in the next two. Higher damping coefficients assumed in the two higher (third and fourth) modes were justified on the basis of results obtained from recent vibration tests.[36,37] The same vibration test[37] results also indicate that damping in the torsional modes is about the same (in terms of fraction of critical damping) as in the translational modes.

The procedure used in computing the responses is the same as described in Chapter III. The absolute maximum values attained during the response by the displacements u_i, rotations θ_i, relative story displacements $\Delta u_i = u_i - u_{i-1}$, and relative story rotations $\Delta\theta_i = \theta_i - \theta_{i-1}$ $(i = 1,2,\ldots,N)$ were recorded. Since the structure is assumed to be simply coupled in stiffness, the shear and torque in a story are proportional to the relative story displacement and the relative story rotation, respectively, of that story. It should be noted here that due to the manner in which $\{\theta\}$, $[M_\theta]$, $[K_\theta]$, etc., have been normalised (Equations (4.73) through (4.78)), all the torsional responses will be in terms A_B.

Comparison of Actual and Approximate (RSS) Responses

The square root of the sum of squares (RSS sum) of the modal maxima of the above mentioned responses were also computed. The square root of the sum of square combination for rotations and displacements of the top floor are compared with the actual maximum values in Tables IV.4 and IV.5 for all four values of γ^2. The comparison is made for $e_2' = .05$ and .25 in the case of rotations, and $e_2' = 0$ (from results obtained for Chapter III) and $e_2' = .25$ in the case of displacements.

TABLE IV.4

COMPARISON OF ACTUAL MAXIMUM AND RSS COMBINATION OF MODAL MAXIMUM RESPONSES, ROTATIONS $\theta_N \cdot \sqrt{A_B}$, ft.

e_2'	Combination of Modal Responses	γ^2 .18	.36	1.00	2.78
		El Centro			
.05	Actual	.633	.685	.354	.181
	RSS	1.775	1.039	.430	.600
.25	Actual	1.877	1.898	1.414	.630
	RSS	2.202	2.074	1.605	.605
		Taft			
.05	Actual	.298	.197	.193	.107
	RSS	.833	.377	.195	.253
.25	Actual	.783	.689	.799	.252
	RSS	.802	.671	.739	.252

TABLE IV.5

COMPARISON OF ACTUAL MAXIMUM RESPONSES AND RSS COMBINATION OF MODAL MAXIMUM RESPONSES, DISPLACEMENTS u_N, ins.

e'_2	Combination of Modal Responses	γ^2 .18	.36	1.00	2.78
		El Centro			
0	Actual	8.362	8.362	8.362	8.362
	RSS	9.218	9.218	9.218	9.218
.05	Actual	8.153	8.151	8.280	8.235
	RSS	6.965	8.483	9.104	8.818
.25	Actual	6.032	8.135	7.996	8.077
	RSS	6.974	7.150	7.817	8.210
		Taft			
0	Actual	4.741	4.741	4.741	4.741
	RSS	4.393	4.393	4.393	4.393
.05	Actual	4.607	4.655	4.717	4.668
	RSS	3.287	4.189	4.391	4.259
.25	Actual	3.626	4.142	4.427	4.403
	RSS	3.146	3.112	4.160	4.367

Rotations and Displacements

The maximum rotations of the Nth floor, $\theta_N \cdot \sqrt{A_B}$, are shown in Figure 4.16. The maximum displacements of Nth floor centroids, u_N, are shown in Figure 4.17 The maximum rotations and displacements (centroidal) of a floor do not occur simultaneously. A simple combination of the two maximum responses in order to obtain maximum displacements at other points of the floor (on the assumption that they occur simultaneously) will give an upper bound to the maximum displacements of such points that may actually occur during the response. The actual maximum displacements that occur at either of the edges of the Nth floor parallel to the x axis, $u_N(E)$, during the response were also recorded. These responses are shown by dotted lines in Figure 4.17.

Maximum rotations increase with increasing eccentricity e_2' for all values of γ^2. Generally, the smaller the value of γ^2 the larger the rotations. The El Centro responses for the cases $\gamma^2 = .18$ and .36 and the Taft responses for the cases $\gamma^2 = .36$ and 1 are exceptions. Increasing values of γ^2, and therefore of σ^2 (see Equation (4.87)), remembering that the α's and the μ's are kept constant, means increasing rotational stiffnesses $(k\theta_i)$ relative to the lateral stiffness in the x direction (kx_i). This is seen from Equation (4.70). The stiffnesses kx_i are kept constant so that increased rotational stiffness can be expected to result in decreasing rotations.

Maximum centroidal displacements of the top floor are smaller for buildings with unsymmetric setback than those of the identical building with symmetric setback (i.e. with $e_2' = 0$). In the Taft responses the centroidal displacements generally seem to decrease with

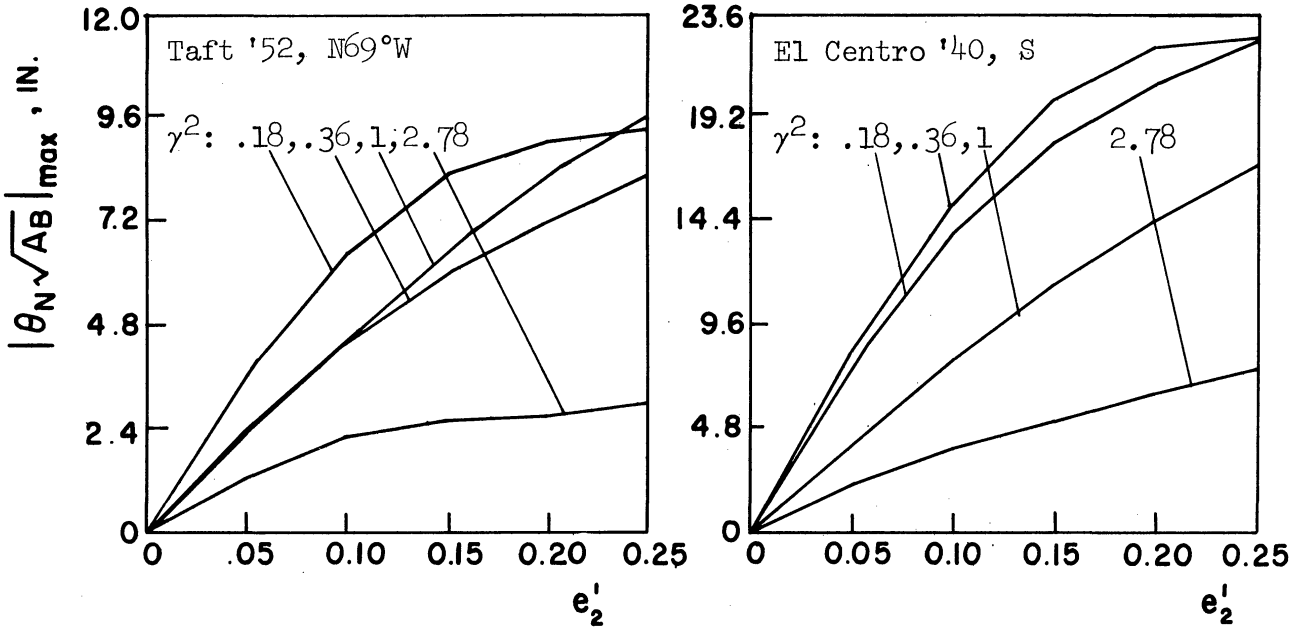

Figure 4.16. Maximum Rotation Response of Top Story.

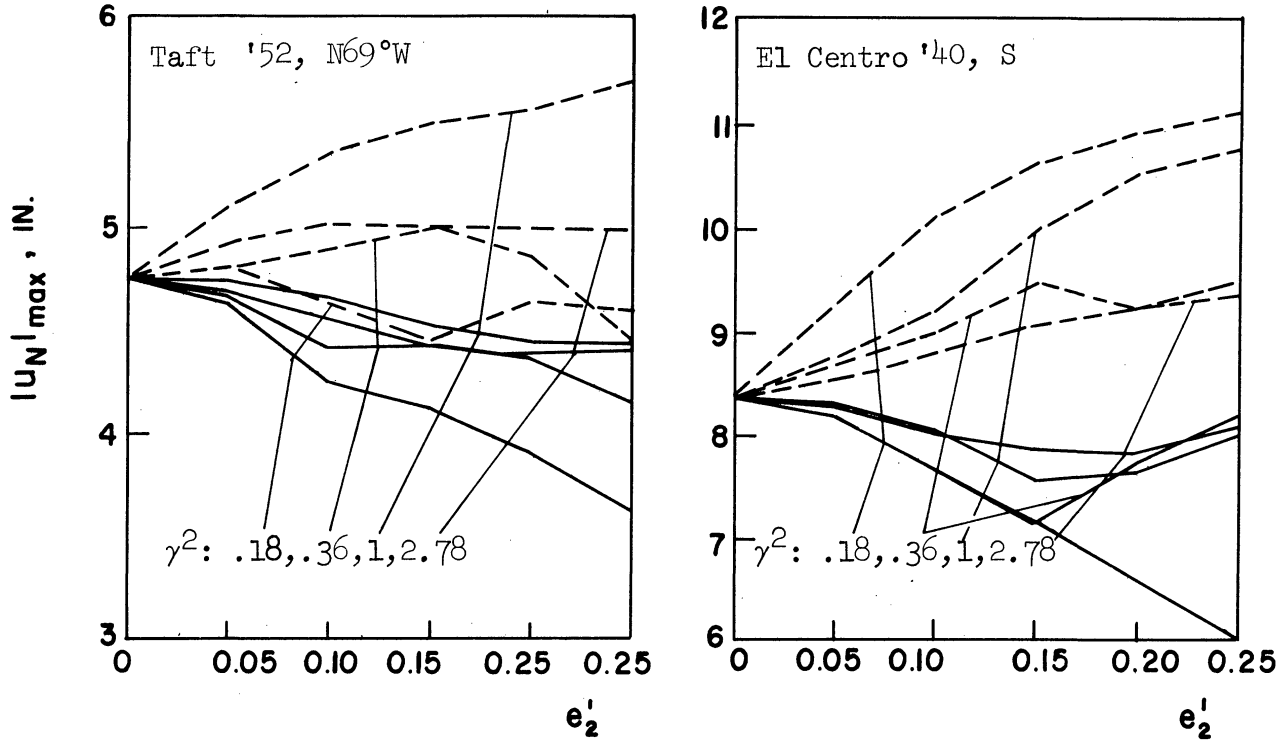

Figure 4.17. Maximum Displacement Response of Top Story.

increasing e_2' , but this is not the case in the El Centro responses for $e_2' > .15$. The maximum decrease in both sets of responses (which occurs for the case $\gamma^2 = .18$, the reason for which is not quite clear) at $e_2' = .25$ are 24% for the Taft responses and 30% for the El Centro responses.

The effects of the eccentricity of the setback e_2' and of γ^2 on maximum rotation and displacement responses of the top floor is representative of the effects on such responses of all the floors. This is shown to some extent in Figure 4.18 in which are given the plots of the maximum rotation and displacement responses of all floors to the El Centro '40 S excitation for the case $\gamma^2 = 1$. The rotation plots are given for $e_2' = .05$ and $.25$, and the displacement plots are given for $e_2' = 0$ and $.25$. Plots of relative story rotations and displacement responses, of all the N stories, to the El Centro '40 S excitation for the above cases are also given in Figure 4.18.

It was observed in Chapter III that the maximum relative story displacements (MRSD) are considerably large in the tower portion than those in the base portion in buildings having setbacks with small c , see Figures 3.15 and 3.17. The same is seen to be true about the maximum relative story rotations from Figure 4.18.

Base Shear and Base Torque Coefficients

The maximum base torque coefficient (BTC) and base shear coefficient (BSC) responses are plotted in Figures 4.19 and 4.20, respectively Base shear coefficient is the ratio of base shear to the weight of the structure. Base torque coefficient is similarly defined as the ratio

$$C_{3B} = \frac{T_B}{\sum_{i=1}^{N} m\Theta_i} \cdot \sqrt{A_B}$$

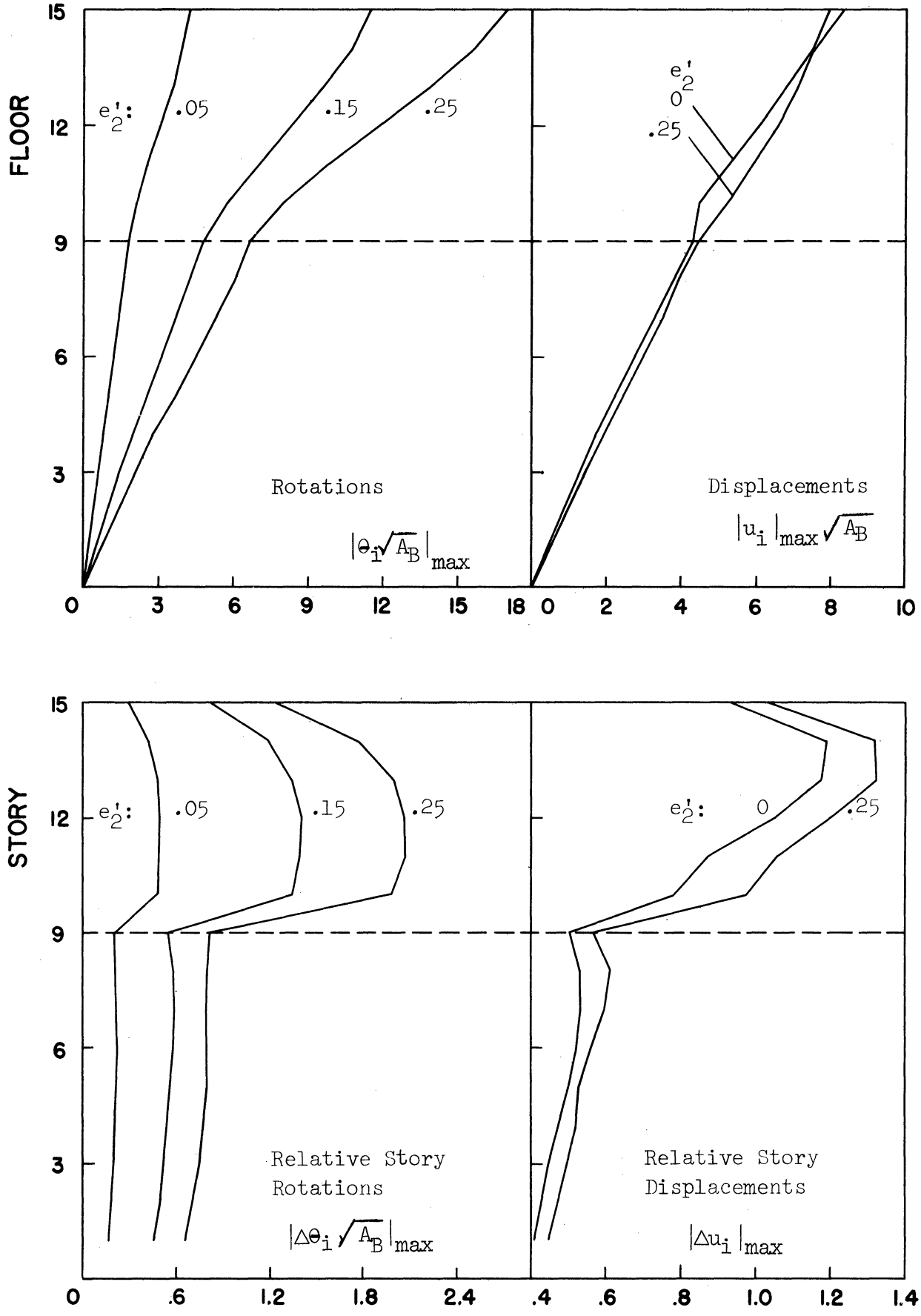

Figure 4.18. Typical Maximum Response Envelopes, El Centro '40, S. $\gamma^2 = 1$.

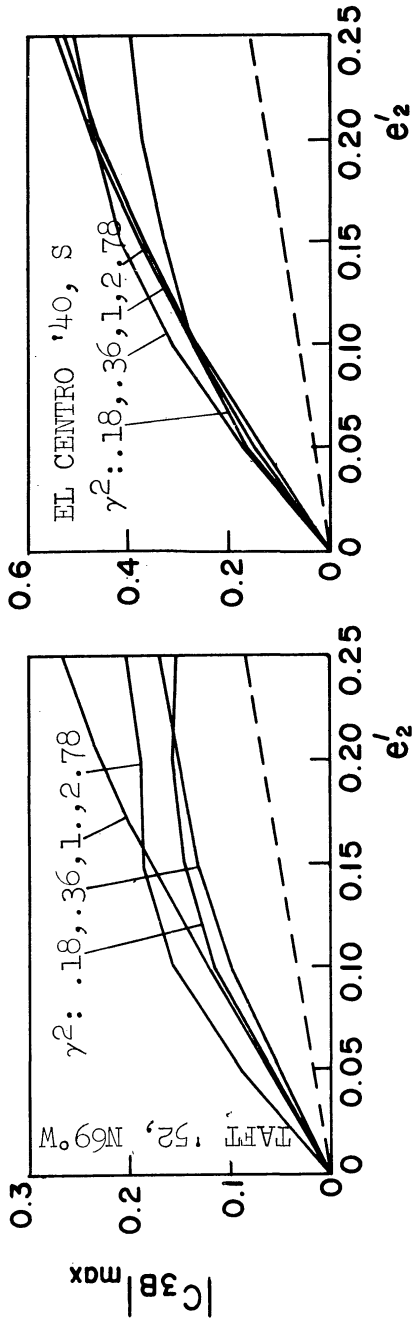

Figure 4.19. Maximum Base Torque Coefficient Responses.

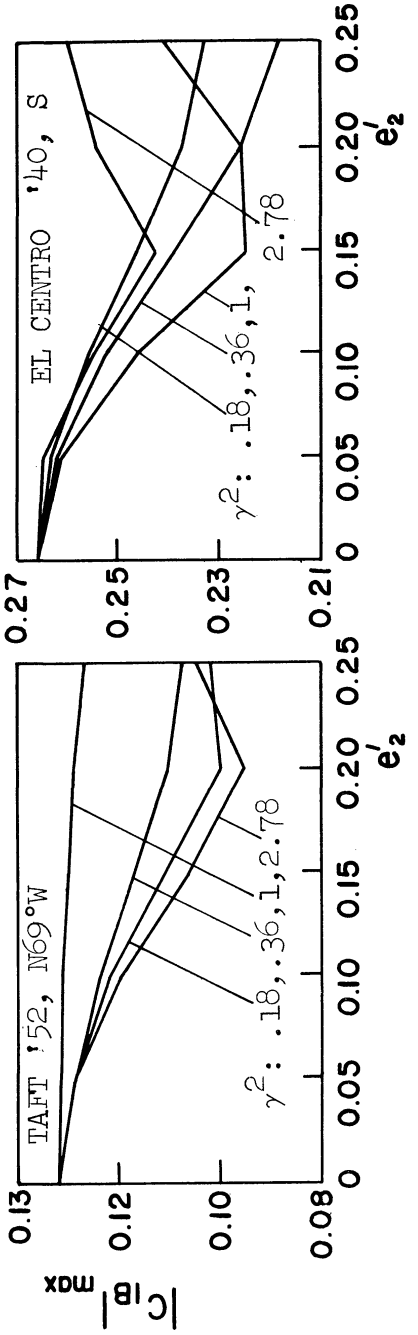

Figure 4.20. Maximum Base Shear Coefficient Responses.

In the case of uncoupled translation vibrations of buildings with setbacks studied in Chapter III, it was found that the RSS combination of modal maximum responses gave a good approximation for the actual responses. In Table IV.2, it is seen that for $e_2' = .05$ the difference between the two responses in the case of rotations is considerable for the cases $\gamma^2 = .18$, 2.78 and $.36$. For $e_2' = .25$, however, the RSS combination maximum modal rotations approximates the actual maximum rotations very well.

The RSS combination of displacements generally approximates the actual maximum displacements quite well (within $\pm$ 25%) for all cases.

The reason for the large difference between the RSS combination and the actual maximum of the rotation response for small e_2' is a pair of lower modes with close periods in the cases of $\gamma^2 = .18$ and 2.78 and, to some extent, of $\gamma^2 = .36$. This violates the condition of well separated mode periods on which the RSS combination of the modal maxima is supposed to be the "probable" value of the total maximum response.(31)

In the pair of modes with close periods the rotation responses are of opposite sign, i.e. out of phase by almost 180°. The maximum rotation response of the two modes combined is nearly equal to the difference of the maximum rotations in each mode. The displacements response in the two modes are of the same sign and the maximum displacement response of the two modes combined is nearly equal to the sum of the maximum displacements in each mode. By its very nature, therefore, the RSS combination of the two modal maximum responses will be much different from the actual maximum response in the case of the rotations and less so in the case of displacements.

where T_B is the base torque, $m\theta_i$ is the mass moment of inertia of the ith mass, and A_B is the base plan area. The term $\sqrt{A_B}$ is introduced to make C_{3B} nondimensional as T_B is of $[ML^{-1}T]$ units and $m\theta_i$ is of $[MT]$ units in the standard notation.

The base torque increases with increasing eccentricity e_2' of the setback for all values of γ^2, the rate of increase diminishing with increasing e_2'. The effect of change in γ^2 on the BTC values does not show much consistency.

Present day (1966) seismic building codes specify that any lack of symmetry in structures be accounted for statically. That is, the static torque produced by the application of the lateral forces computed on the assumption of uncoupled lateral (translational) vibrations should be taken into account, along with the lateral forces, for design purposes.

The dotted line in Figure 4.19 shows the base torque coefficient resulting from the shear at the base of tower obtained for the building with $e_2' = 0$ in Chapter III. The BTC values thus obtained are 1/5 to 1/2 times the actual base torque coefficients (as obtained here by taking the dynamic coupling into account).

The maximum base shear coefficients are somewhat smaller for the buildings with unsymmetric setback compared to that for the corresponding building with symmetric setback (i.e. with, $e_2' = 0$). The BSC decreases at first with increasing e_2' for all values of γ^2 in both, the Taft and the El Centro responses but beyond $e_2' = .15$ its behavior is not regular. The maximum decrease in BSC due to the introduction of asymmetry of the setback below the BSC at $e_2' = 0$ is about 28% in the case of Taft responses and about 18% in the case of El Centro responses.

The maximum shear and the maximum torque in a story do not, generally, occur simultaneously during the response. Forces in the resisting elements of the story computed on the assumption that they do occur simultaneously will overestimate the actual maximum forces. All the same, it is much more convenient to keep track of a few resultant forces per story in a structure rather than the forces in the innumerable resisting elements of the structure. The latter course is also impossible here because of the manner in which the properties of the structures have been idealised.

A rough idea about the extent of overestimation of the forces in resisting elements located at the edges (in plan) of the story has been obtained as follows. The structure has been assumed to be simply coupled in stiffness. The forces in the story, and therefore also in the individual resisting elements, are, then, proprotional to the relative story displacement. The actual maximum relative displacement between the edges of the two floors adjacent to the story,

$$|\Delta u_i(E)|_{max} = \begin{cases} |\Delta u_i + \Delta\theta_i \cdot \frac{b_2}{2}|_{max}, & i = 1, 2, \ldots, P \\ |\Delta u_i + \Delta\theta_i \cdot \frac{a_2}{2}|_{max}, & i = P+1, \ldots N \end{cases} \tag{4.114}$$

may be compared with the value

$$|\Delta u_i'(E)|_{max} = \begin{cases} |\Delta u_i|_{max} + |\Delta\theta_i|_{max} \cdot \frac{b_2}{2} & i = 1, 2, \ldots, P \\ |\Delta u_i|_{max} + |\Delta\theta_i|_{max} \cdot \frac{a_2}{2} & i = P+1, \ldots, N \end{cases} \tag{4.115}$$

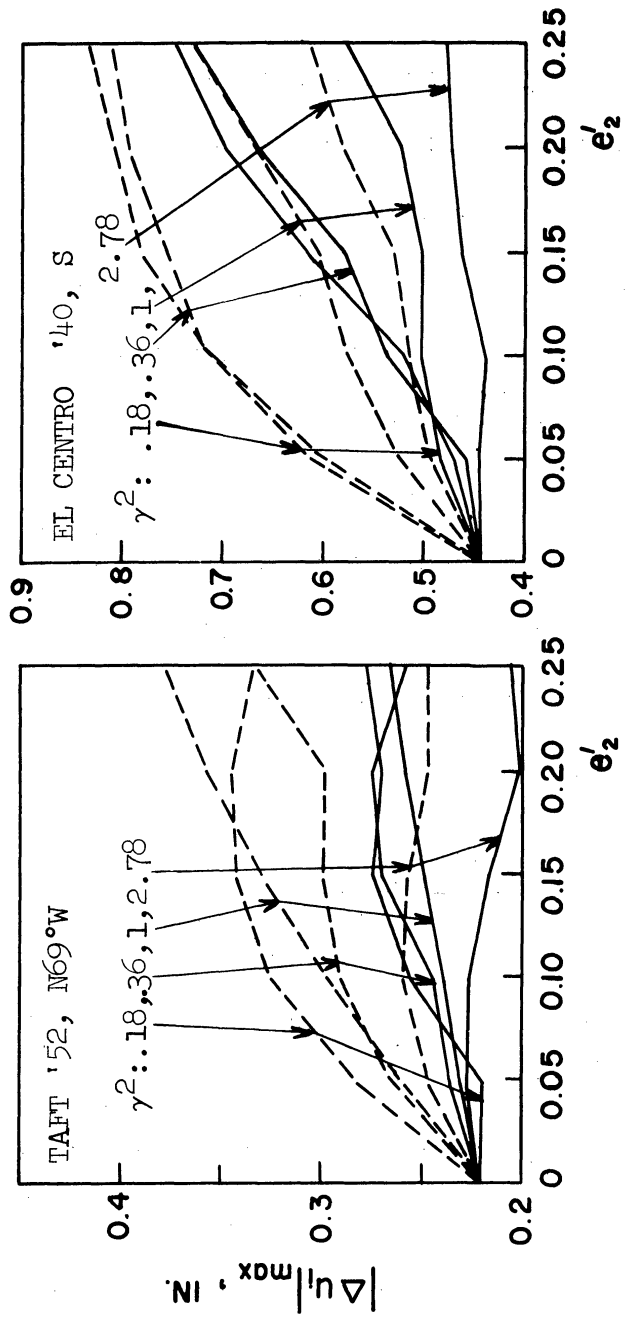

Figure 4.21. Comparison of $|\Delta u_1(E)|_{max}$ (full lines) and $|\Delta u_1'(E)|_{max}$ (dotted lines).

obtained on the assumption that the relative displacements between the centroids of the two floors and the relative story rotations both occur simultaneously.

The values $|\Delta u_i(E)|_{max}$ and $|\Delta u_i'(E)|_{max}$ were obtained for the first story during the response computations and are shown in Figure 4.21. No definite trend about the effect of either e_2' or γ^2 on the difference between the two quantities seems to emerge in Figure 4.21. The overestimation of $|\Delta u_i(E)|_{max}$ by $|\Delta u_i'(E)|_{max}$ ranges from 5% to as high as 40% in both the Taft and the El Centro responses, not showing any definite trend with respect to variation in e_2' or γ^2 .

The upper limit of the range of overestimation observed here is quite high. The lower limit of this range suggests, however, that it may be safer to design structures on the assumption that they are subjected to the maximum seismic shear and torque simultaneously, which is also much more convenient.

Effect of Damping in Cases of Close Periods

When examining the modal properties, a high degree of coupling was observed for very small values of e_2' in the T:1 and R:1 modes for the case $\gamma^2 = .18$ and also in the T:2 and R:1 modes for the case $\gamma^2 = 2.78$. These results suggest that there would be severe twisting in these modes of the building when subjected to earthquakes. The RSS combination of the modal maximum responses would then indicate very high rotations and torque in such building. However, no such special effects are apparent in actual combined maximum responses, see Figure 4.16 and 4.19.

It may be recalled that in computing the responses damping has been assumed to be 4% of critical in the first four modes and 6% of critical in the next four modes. If the damping is assumed to be very small or absent then the actual combined responses will also indicate that a building with close (uncoupled) translational and torsional mode periods is subjected to severe torsional forces even when the eccentricity of the setback is very small. This is shown in Table IV.6 in which the maximum rotation responses of the top story for the damped and the undamped cases are given for $\gamma^2 = .18$ for which case the uncoupled R:1 and T:1 mode periods are almost equal. Similar results for the case $\gamma^2 = 1$, which does not have modes with close periods, are also given in Table IV.6 for the sake of comparison.

Table IV.6

COMPARISON OF EFFECT OF CLOSE PERIODS ON ROTATION RESPONSES ($\Theta_N\sqrt{A_B}$) IN DAMPED AND UNDAMPED CASES

γ^2	$e_2' \rightarrow$	$\Theta_N \cdot \sqrt{A_B}$, ins.			
		.01	.05	.15	.25
.18	no damp.	11.54	36.84	41.50	35.11
	damp. incl.	1.61	7.60	18.00	22.52
1	no damp.	-----	12.11	30.89	43.52
	damp. incl.	-----	4.25	11.54	16.97

Torque Distribution

In Figure 4.22 are given the torque distributions for buildings with eccentricities $e_2' = .05$ and .25. The torque distribution is an envelope of the values $|T_i|_{max}/|T_B|_{max}$ plotted against i, where $|T_i|_{max}$ is the maximum torque obtained in the ith story during the response history and $|T_B|_{max} = |T_1|_{max}$.

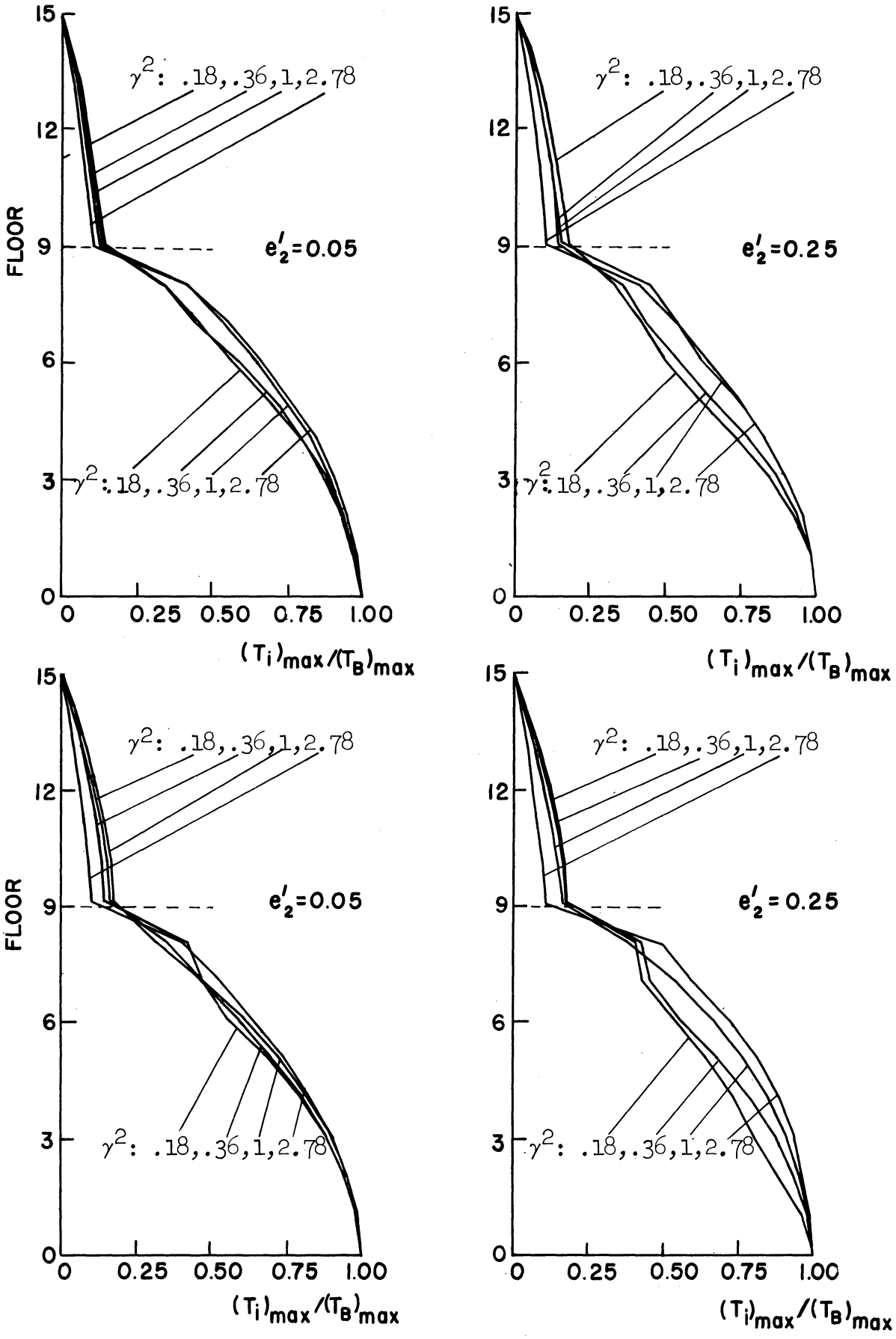

Figure 4.22. Torque Distributions.
Above: El Centro '40, S.
Below: Taft. '52, N69°W.

The plots of torque distributions in Figure 4.22 are quite similar in shape to the plots of shear distributions of buildings with setback given in Figure 3.20 in Chapter III, and in Figure 4.23 to be introudced later.

The variation in the value of e_2' and γ^2 affects the torque distribution (i.e. the $|T_i|_{max}/|T_B|_{max}$ values) in buildings with otherwise identical properties and subjected to the same excitation. However these effects on the torque distributions of variation in e_2' or γ^2 do not seem to be much more than the differences between the torque distributions obtained for the same structure subjected to the two different excitations (viz. the El Centro and the Taft earthquake components).

It may therefore be expected that the torque distributions in buildings with the type of unsymmetry assumed here, is mainly dependent on two quantities: first, the level of setback and, second, a quantity playing a role similar to the one played by degree of setback c in the case of shear distributions in buildings with setbacks. Noting that $c = m_t/m_b$, this second quantity may be defined as $c\Theta = (m_t r_t)/(m_b r_b)$ where m_t, m_b are the lumped mass values in the tower and the base portions of the building, respectively, and r_t and r_b are the radii of gyrations of the lumped masses in the two parts of the structure. (Alternately one may define $c\Theta$ as $c\Theta = (m\Theta_t/\sqrt{A_T})/m\Theta_b/\sqrt{A_B})$.

Shear Distribution

The shear distributions $|V_i|_{max}/|V_B|_{max}$ obtained in the two responses for buildings with setback eccentricities $e_2' = .05$ and $.25$ are plotted in Figure 4.23. For comparison, the shear distributions

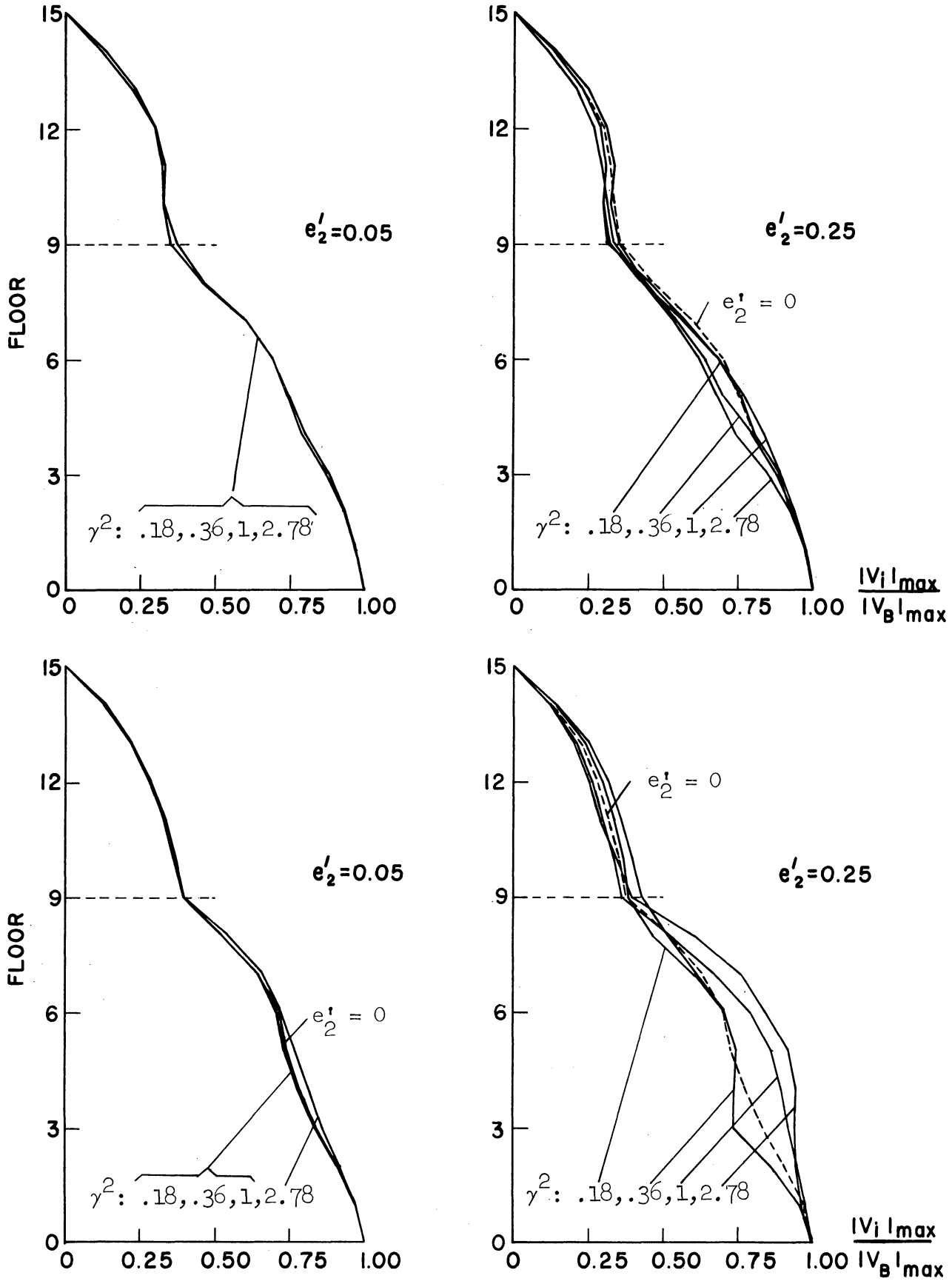

Figure 4.23. Shear Distributions.
Above: El Centro '40, S.
Below: Taft '52, N69°W.

obtained for the same building with symmetric setback ($e_2' = 0$) responding to the two excitations in Chapter III are shown by dotted lines in Figure 4.23.

The shear distributions for $e_2' = .05$ are almost identical for all four values of γ^2. They are also almost identical to the shear distribution for the same building with symmetric setback. This is true in the case of both, the Taft and the El Centro, responses.

As the setback eccentricity e_2' increases, the shear distributions are affected noticeably by changes in γ^2 as well as by the eccentricity itself. This shows up in the shear distribution plots for $e_2' = .25$ in Figure 4.23.

Keeping in mind the approximations and uncertainties involved in the present day (1966) earthquake resistant design practices it is reasonable to conclude the following (for design purposes) from the above observations. In a building with setback with the type of asymmetry considered here, the distribution of shear in the direction in which the lateral vibrations are coupled with the torsional vibrations remains approximately the same as for an identical building with coupling neglected.

CHAPTER V

SUMMARY AND CONCLUSIONS

A study of the effects of a setback on the dynamic behavior of a tall building when subjected to earthquake ground motion has been presented. As a first step in the study of this problem, the stiffness in structures is assumed to be linearly elastic and damping is assumed to be of the viscious type.

In Chapter II, the equations of motion of multi-story buildings treated as lumped mass systems has been presented. In these equations, the translations and rotations of each floor (mass) in the horizontal plane, as a rigid body, is taken into account. Conditions are set forth under which one or more of the three subsets of these equations representing the translations of the floors in two mutually perpendicular directions and their rotations uncouple from the remaining equations. Finally, the usual superposition-of-modes method of solution of these equations and a method of obtaining the frequencies and modes of the system is described.

In Chapter III, a study of the effects of setback on the uncoupled translational vibrations of two models of buildings, a shear beam and a lumped mass system with idealized mass and stiffness properties, was presented. A 15-story "shear building" was used as the lumped mass model in this study. The setback was represented by two parameters, the level and the degree of setback. The effects of these parameters on the modal properties of the two models and the responses of the lumped mass model to recorded earthquakes, as well as the

approximate responses of the shear beam model, were examined. The responses were compared with the specifications for dealing with setbacks in buildings from one of the current seismic building codes.(3)

The coupled lateral-torsional vibrations of buildings with unsymmetric setbacks were examined in Chapter IV. Again, two models were used, a shear beam and a 15-story (lumped mass) "shear building". Results were presented for a building with given level and degree of setback and having a square cross-section in both base and tower portions. The setback was assumed to be unsymmetric about one principal direction only. The effect of varying the eccentricity of the setback on the modal properties of both the models and on the responses of the lumped mass model to recorded earthquakes were examined for several values of σ^2 the ratio of dynamic torsional stiffness to dynamic lateral stiffness.

The following conclusions may be drawn from the study reported here. The conclusions dealing with various response parameters refer to the maximum values of the corresponding response parameters.

1. The fundamental translational mode period of a building with setback is smaller than that of a comparable* uniform building; the more slender the tower (relative to the base portion) or the nearer the level of setback to the midheight of the building, the greater the decrease in fundamental period from that of a comparable uniform building.

2. If a building with setback is subjected to an earthquake, the displacements of the floors in its tower portion will, in general,

---

* A definition of the "comparable" uniform building is given in Chapter III, page 80.

be larger than those at similar levels in a comparable uniform building subjected to the same earthquake. The same is true about the relative story displacements in the tower portion of a building with setback. The slimmer the tower, the larger is the increase in these floor and relative story displacements. The increase, in percentage terms, is greater in the case of relative story displacements than in the case of floor displacements.

3. The tower-base shear coefficient (defined as the ratio of shear at the base of tower to weight of tower) in a building with setback is, in general, greater than the seismic coefficient at the same level (defined as the ratio of shear at the given level to the weight of building above that level) in a comparable uniform building, if both are subjected to the same earthquake. The more slender the tower or the higher the level of setback, the greater is the increase in the tower-base shear coefficient. When compared with the response results, the code specifications for buildings with setback seem to provide for a sufficient increase in the tower-base shear coefficient when the setback level is below midheight. In the case of buildings with setback level above midheight, however, the increase provided in the code is smaller than that indicated by the response results.

4. When the tower is very slender (say $c < .05$) compared to the base portion and a lower mode period of the tower acting alone is close or equal to a lower mode period of the base portion acting alone, very high tower-base shear coefficients can be expected.

5. In uniform buildings the contribution of the fundamental mode to the total base shear coefficient is normally much larger than

that of any of the higher modes. However, in a building with setback level below midheight if the tower is very slim, the contribution of one of the higher modes to the total base shear coefficient may be as much or more than that of the fundamental mode.

6. Whether the base shear coefficient in a building with setback will be greater or smaller than that in a comparable uniform building when both are subjected to the same earthquake, will depend very much on the nature of the earthquake, as represented (roughly) by its response spectra, and on the range of the lower mode periods of the building.

The following conclusions are primarily applicable to buildings with setback unsymmetric about one axis only. Some of these conclusions may, however, be also applicable to buildings with setbacks unsymmetric about both axes and to buildings that are dynamically unsymmetric due to reasons other than those considered in this study such as eccentricity between centers of mass and centers of resistance in one or more stories.

7. A dynamically unsymmetric building when subjected to translational ground motion will be subjected to lateral as well as torsional inertial forces. The actual torsional forces in such buildings are much larger than the static torsional forces obtained by neglecting the dynamic lateral-torsional coupling. In the case of buildings with setback unsymmetric about one axis for which computations were made, the base torque responses are as much as two to five times larger than the static torque values. The maximum resultant shear and torsional forces do not, in general, occur simultaneously in dynamically unsymmetric buildings subjected to earthquakes. However, it seems reasonable and convenient to design buildings on the assumption that they do occur simultaneously.

8. The rotations and torques in a building with unsymmetric setback subjected to an earthquake, in general, increase with increasing eccentricity of the setback. Close translational and torsional mode periods do not result in very high rotations or torques in a building with very small eccentricity of the setback unless damping is quite low in the modes involved.

9. The torque distribution plot for a building with unsymmetric setback subjected to earthquakes is found to be quite similar in shape to the shear distribution plot, except that the kink at the setback level is sharper in the case of torque distribution.

10. In a building with setback unsymmetric about one principal direction, the base shear coefficient in that direction will be slightly less than that for an identical building with symmetric setback when both are subjected to the same earthquake. Among the cases for which response computations were made, the maximum decrease was found to be around 30%. The shear distribution in a building with unsymmetric setback does not change much from that corresponding to an identical building with symmetric setback.

APPENDIX A.

THE STEPPED CANTILEVER SHEAR BEAM: EQUATIONS OF MOTION AND THEIR SOLUTION[5]

The beam under consideration here is a vertical cantilever shear beam of rectangular cross section, stepped at one location along its height. The shear beam is a hypothetical ideal beam in which all deformations result from shearing strains, and extensional strains are zero. This provides a mathematical model which behaves in a manner roughly comparable with a tall building, in which horizontal shearing deformation (due to flexure of the columns) predominates and bending deformation (due to lengthening and shortening of the columns) is small. The cross section of the beam is uniform above and below the step and the upper section may be set back from any or all sides of the base section. The rigidity per unit area and the density are uniform throughout the beam but the rigidity need not be the same in both directions.

The stepped beam is shown in Figure A.1. Let

b_1, b_2 = base width in x and y directions

a_1, a_2 = top width in x and y directions

e_1, e_2 = offsets from centroid of base section to centroid of top section in x and y directions

h = height to step

ℓ = overall height

G = rigidity per unit area in x direction

ρ = mass per unit volume

$\gamma^2 G$ = rigidity per unit area in y direction

z = vertical coordinate axis

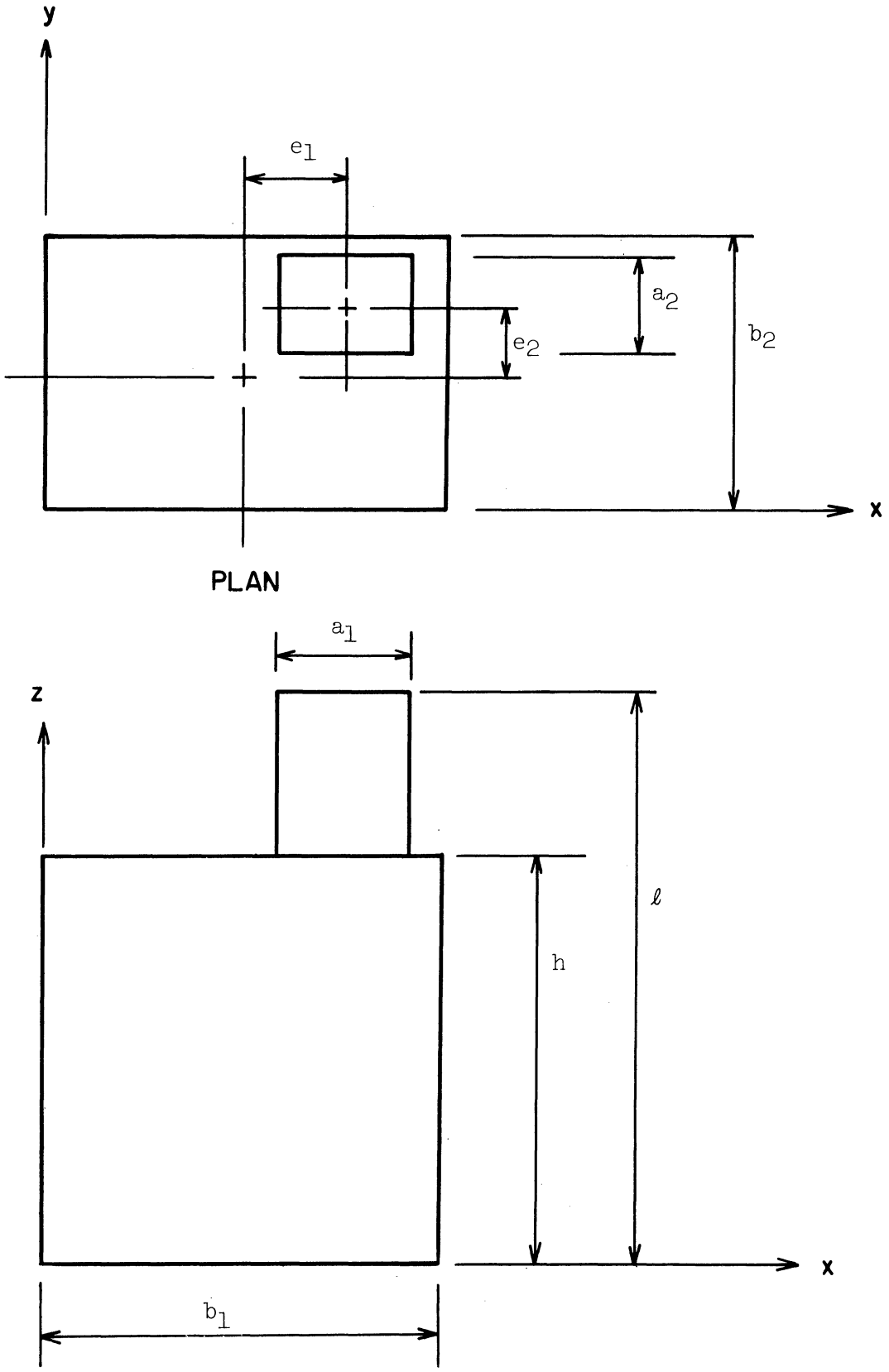

Figure A.1. Stepped Shear Beam.

t = time coordinate

u,v = lateral displacements of centroid of section, relative to base, from equilibrium position, in x and y directions

θ = rotation of section about vertical axis through centroid, relative to base, positive counter-clockwise

V_1, V_2 = resultant shear forces on horizontal cross section

V_3 = resulting twisting moment on horizontal cross section

A = cross-sectional area

I_1, I_2 = moments of inertia of cross-sectional area about x and y axes

J = polar moment of inertia of cross-sectional area about vertical centroidal axis

f_1, f_2 = driving force per unit length in x and y directions

f_3 = driving moment per unit length about vertical centroidal axis.

Referring to Figure A.2, the three equations of motion for the element are

$$\begin{aligned} V_{1,z} + f_1 &= \rho A u_{,tt} \\ V_{2,z} + f_2 &= \rho A v_{,tt} \\ V_{3,z} + f_3 &= \rho J \theta_{,tt} \end{aligned} \qquad \text{(A.1)}$$

where the subscripts following the commas denote differentiation with respect to the indicated variables.

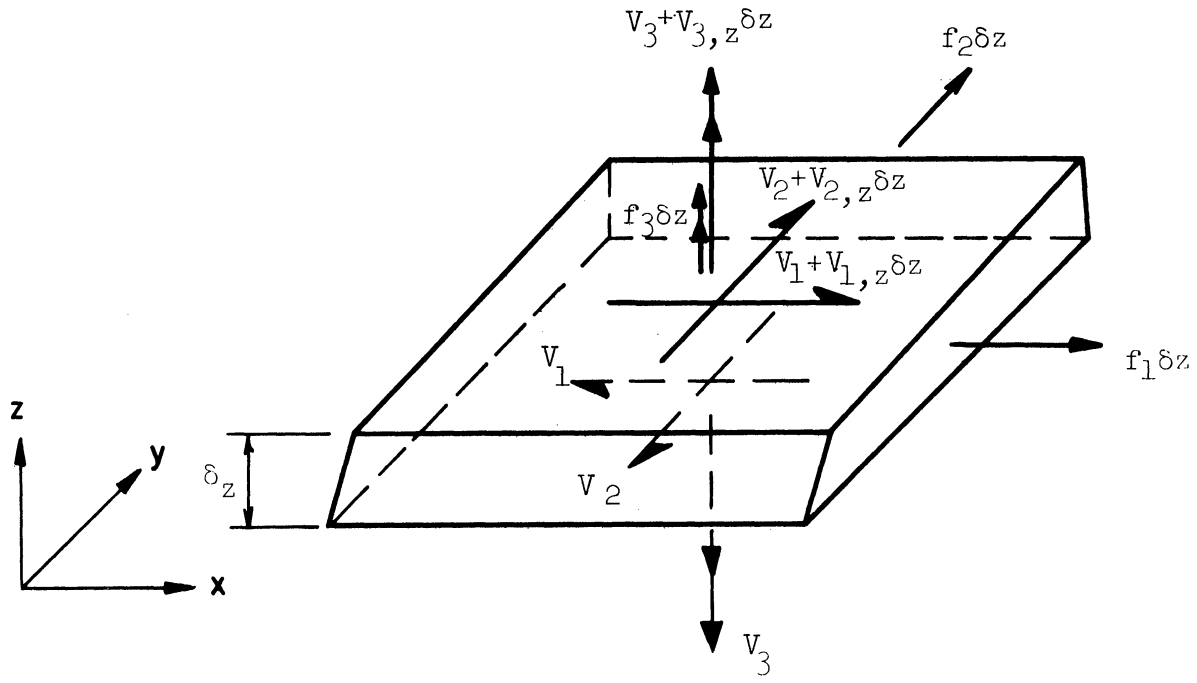

Figure A.2. Forces on Element of Shear Beam.

The force-displacement relations are

$$\begin{aligned} V_1 &= G\,A\,u_{,z} \\ V_2 &= \gamma^2 G\,A\,u_{,z} \\ V_3 &= G(I_1 + \gamma^2 I_2)\,\theta_{,z}\ . \end{aligned} \tag{A.2}$$

Define the inertia coefficients in Equation (A.1).

$$\begin{aligned} m_1 &= \rho A \\ m_2 &= \rho A \\ m_3 &= \rho J \end{aligned} \tag{A.3}$$

and the stiffness coefficients in Equation (A.2)

$$\begin{aligned} k_1 &= G\,A \\ k_2 &= \gamma^2 G\,A \\ k_3 &= G(I_1 + \gamma^2 I_2)\ . \end{aligned} \tag{A.4}$$

The values of m_i and k_i are discontinuous at the step. In terms of the beam dimensions

(in $0 < z < h$)

$$\begin{aligned} m_1 &= \rho\, b_1 b_2 \\ m_2 &= \rho\, b_1 b_2 \\ m_3 &= \rho\, \frac{b_1 b_2}{12}\,(b_1^2 + b_2^2) \end{aligned}$$

$$\begin{aligned} k_1 &= G\, b_1 b_2 \\ k_2 &= \gamma^2 G\, b_1 b_2 \\ k_3 &= G\, \frac{b_1 b_2}{12}\,(\gamma^2 b_1^2 + b_2^2) \end{aligned} \tag{A.5}$$

and

$$
\begin{aligned}
&(\text{in} \quad h < z < \ell) \\
m_1 &= \rho\, a_1 a_2 \\
m_2 &= \rho\, a_1 a_2 \\
m_3 &= \rho\, \frac{a_1 a_2}{12}\,(a_1^{\,2} + a_2^{\,2}) \\
k_1 &= G\, a_1 a_2 \\
k_2 &= \gamma^2 G\, a_1 a_2 \\
k_3 &= G\, \frac{a_1 a_2}{12}\,(\gamma^2\, a_1^{\,2} + a_2) \quad .
\end{aligned}
\tag{A.6}
$$

Then Equations (A.1) through (A.4) may be combined to get the partial differential equations of motion

$$
m_i\, x_{i,tt} - k_i\, x_{i,zz} = f_i\,(z, t) \tag{A.7}
$$

in which the following notations are introduced for convenience in writing the equations

$$
\begin{aligned}
x_1 &= u \\
x_2 &= v \\
x_3 &= \theta
\end{aligned}
\tag{A.8}
$$

The boundary conditions are

$$
x_i(0,t) = 0 \tag{A.9}
$$

and

$$
V_i(\ell,t) = 0 \tag{A.10}
$$

The conditions at the step are:

for equilibrium

$$\begin{aligned} [V_1]_{(h-0,t)} &= [V_1]_{(h+0,t)} \\ [V_2]_{(h-0,t)} &= [V_2]_{(h+0,t)} \\ [V_3 - e_1 V_2 + e_2 V_1]_{(h-0,t)} &= [V_3]_{(h+0,t)} \end{aligned} \tag{A.11}$$

and for continuity

$$\begin{aligned} [x_1 - e_2 x_3]_{(h-0,t)} &= [x_1]_{(h+0,t)} \\ [x_2 + e_1 x_3]_{(h-0,t)} &= [x_2]_{(h+0,t)} \\ [x_3]_{(h-0,t)} &= [x_3]_{(h+0,t)} \end{aligned} \tag{A.12}$$

Assume that the beam is in free vibration. The term $f_i(z,t)$ in Equation (A.7) is then zero, leaving

$$k_i x_{i,zz} = m_i x_{i,tt} \tag{A.13}$$

In the customary manner we express the solution in product form

$$x_i(z,t) = Z_i(z) \cdot T(t) \tag{A.14}$$

This, substituted in Equation (A.13), gives

$$k_i Z_i'' T = m_i Z_i T'' \tag{A.15}$$

Separation of variables leads to the equation of free vibration

$$T'' + \omega^2 T = 0 \tag{A.16}$$

and the equation determining the mode shape

$$Z_i'' + \frac{m_i}{k_i}\omega^2 Z_i = 0 \qquad \text{(A.17)}$$

where ω, the natural frequency, is yet undetermined. The values of k_i and m_i are constant in $0 < z < h$ and in $h < z < \ell$.

Let

$$q_i^2 = \frac{k_i}{m_i} \qquad \text{in} \qquad 0 < z < h$$

and (A.18)

$$s_i^2 = \frac{k_i}{m_i} \qquad \text{in} \qquad 0 < z < \ell$$

Then Equation (A.17) becomes

$$Z_i'' + \frac{\omega^2}{q_i} Z_i = 0 \qquad \text{in} \qquad 0 < z < h$$

and (A.19)

$$Z_i'' + \frac{\omega^2}{s_i^2} Z_i = 0 \qquad \text{in} \qquad h < z < \ell$$

The general solution of Equation (A.19) is

$$\begin{aligned} Z_i &= C_{i0} \cos \frac{\omega z}{q_i} + C_{i1} \sin \frac{\omega z}{q_i}, \quad 0 < z < h \\ Z_i &= C_{i2} \cos \frac{\omega z}{s_i} + C_{i3} \sin \frac{\omega z}{s_i}, \quad h < z < \ell \end{aligned} \qquad \text{(A.20)}$$

where the coefficients C_{ij} are undetermined constants. Equation (A.9) requires that

$$C_{i0} = 0 \qquad \text{(A.21)}$$

$$
\left[\begin{array}{ccc|ccc|ccc}
0 & -\sin\frac{\omega\ell}{s_1} & \cos\frac{\omega\ell}{s_1} & 0 & 0 & 0 & 0 & 0 & 0 \\
-\sin\frac{\omega h}{q_1} & \cos\frac{\omega h}{s_1} & \sin\frac{\omega h}{s_1} & 0 & 0 & 0 & e_2\sin\frac{\omega h}{q_3} & 0 & 0 \\
b_1b_2\cos\frac{\omega h}{q_1} & a_1a_2\sin\frac{\omega h}{s_1} & -a_1a_2\cos\frac{\omega h}{s_1} & 0 & 0 & 0 & 0 & 0 & 0 \\
\hline
0 & 0 & 0 & 0 & -\sin\frac{\omega\ell}{s_2} & \cos\frac{\omega\ell}{s_2} & 0 & 0 & 0 \\
0 & 0 & 0 & -\sin\frac{\omega h}{q_2} & \cos\frac{\omega h}{s_2} & \sin\frac{\omega h}{s_2} & -e_1\sin\frac{\omega h}{q_3} & 0 & 0 \\
0 & 0 & 0 & b_1b_2\cos\frac{\omega h}{q_2} & a_1a_2\sin\frac{\omega h}{s_2} & -a_1a_2\cos\frac{\omega h}{s_2} & 0 & 0 & 0 \\
\hline
0 & 0 & 0 & 0 & 0 & 0 & 0 & -\sin\frac{\omega\ell}{s_3} & \cos\frac{\omega\ell}{s_3} \\
0 & 0 & 0 & 0 & 0 & 0 & -\sin\frac{\omega h}{q_3} & \cos\frac{\omega h}{s_3} & \sin\frac{\omega h}{s_3} \\
e_2\,b_1b_2\cos\frac{\omega h}{q_1} & 0 & 0 & -e_1\frac{q_2}{q_1}b_1b_2\sin\frac{\omega h}{q_2} & 0 & 0 & \frac{q_3}{q_1}J_b\cos\frac{\omega h}{q_3} & \frac{s_3}{s_1}J_t\sin\frac{\omega h}{s_3} & -\frac{s_3}{s_1}J_t\cos\frac{\omega h}{s_3}
\end{array}\right]
\left\{\begin{array}{c} c_{11} \\ c_{12} \\ c_{13} \\ c_{21} \\ c_{22} \\ c_{23} \\ c_{31} \\ c_{32} \\ c_{33} \end{array}\right\}_{2=2}
\left\{\begin{array}{c} 0 \\ 0 \\ 0 \\ 0 \\ 0 \\ 0 \\ 0 \\ 0 \\ 0 \end{array}\right\}
\qquad \text{(A.22)}
$$

The equilibrium conditions at the free end (A.10) and the equilibrium and continuity conditions at the step, (A.11) and (A.12), may then be reduced to the matrix equation (A.22).

The natural frequencies of the system are the values of ω which make the matrix singular, i.e., which make the determinant of the matrix zero. Equation (A.22) can be solved for the coefficients C_{ij} to within an arbitrary constant when ω is equal to a natural frequency of the system. A closed expression has been derived for the determinant of the matrix as a function of ω.

Some properties of the system may be observed from Equation (A.22) without recourse to numerical calculation. If one partitions the matrix into 3 x 3 submatrices, the diagonal submatrices are associated with vibrations in the x, y and Θ directions and the off-diagonal submatrices are associated with the coupling of these vibrations.

If the beam is symmetric about both the x and y axes, then $e_1 = e_2 = 0$ and all the coupling terms vanish. The modes then appear as translational modes in the x and y directions and torsional modes, all of which are uncoupled.

If the beam has one plane of symmetry, the modes involving translation in that plane will be uncoupled from translation in the other direction and from torsion.

Except for special cases, translation in the direction of one axis of asymmetry will be coupled with torsion. In a unsymmetric isotropic ($\gamma^2 = 1$) beam, the vertical plane through the centroids of the upper and lower sections is a plane of dynamic symmetry, and there are modes in this case which involve only translation in the plane of dynamic symmetry, uncoupled from torsion.

Orthogonality of the modes may be established in the following manner. Equation (A.17), for the kth mode of vibration, says (substituting ϕ for Z)

$$k_i \phi''_{ik} + m_i \omega_k^2 \phi_{ik} = 0 \qquad (A.23)$$

where the subscript k denotes the kth mode. Multiplying by ϕ_{ij} and integrating from 0 to ℓ, one gets

$$\int_0^{\ell} k_i \phi''_{ik} \phi_{ij} \, dz + \omega_k^2 \int_0^{\ell} m_i \phi_{ik} \phi_{ij} \, dz = 0 . \qquad (A.24)$$

If one integrates the first term by parts taking into account the discontinuities at h, Equation (A.24) becomes

$$\left[k_i \phi_{ik} \phi_{ij} - k_i \phi_{ik} \phi'_{ij}\right]_0^{h-0} + \left[k_i \phi'_{ik} \phi_{ij} - k_i \phi_{ik} \phi_{ij}\right]_{h+0}^{\ell} + \int_0^{\ell} k_i \phi_{ik} \phi_{ij} \, dz + \omega_k^2 \int_0^{\ell} m_i \phi_{ik} \phi_{ij} \, dz = 0 . \qquad (A.25)$$

The bracketed expression vanishes at $z = 0$ and $z = \ell$ because of the boundary conditions. From the conditions of continuity and equilibrium at $z = h$, it is readily shown that

$$\sum_{i=1}^{3} \left\{ \left[k_i \phi_{ik} \phi_{ij}\right]_{h+0} - \left[k_i \phi_{ik} \phi'_{ij}\right]_{h-0} \right\} = 0 . \qquad (A.26)$$

By virtue of these relations and Equation (A.24), Equation (A.25) yields

$$(\omega_k^2 - \omega_j^2) \sum_{i=1}^{3} \int_0^{\ell} m_i \phi_{ik} \phi_{ij} \, dz = 0 , \qquad (A.27)$$

and therefore if $\omega_k^2 \neq \omega_j^2$

$$\sum_{i=1}^{3} \int_0^{\ell} m_i \phi_{ik} \phi_{ij} \, dz = 0 . \qquad (A.28)$$

Equation (A.28) is then the orthogonality relation of the modes.

The displacements of the beam can always be expressed in a modal series

$$x_i(z, t) = \sum_{k=1}^{\infty} \phi_{ik}(z)\, \eta_k(t) \tag{A.29}$$

where η is the r-th modal displacement. It follows that

$$\begin{aligned} x_{i,tt} &= \sum_{k=1}^{\infty} \phi_{ik}\, \eta_{k,tt} \\ x_{i,zz} &= \sum_{k=1}^{\infty} \phi_{ik,zz}\, \eta_k \end{aligned} \tag{A.30}$$

and the equation of forced vibration, Equation (A.7), can be written

$$m_i \sum_{k=1}^{\infty} \phi_{ik}\, \eta_{k,tt} - k_i \sum_{k=1}^{\infty} \phi_{ik,zz}\, \eta_k = f_i(z,t) \quad . \tag{A.31}$$

With Equation (A.17), substituting ϕ for Z, this can be converted into

$$\sum_{k=1}^{\infty} \phi_{ik}\, \eta_{k,tt} + \sum_{k=1}^{\infty} \omega_k^2\, \phi_{ik}\, \eta_k = \frac{f_i(z, t)}{m_i(z)} \quad . \tag{A.32}$$

Multiplying by $m_i \phi_{ij}$, integrating from 0 to ℓ under the summation, and summing over i, one gets

$$\sum_{k=1}^{\infty} \left\{ \eta_{k,tt} \sum_{i=1}^{3} \int_0^{\ell} m_i \phi_{ik}\, \phi_{ij}\, dz \right\} + \sum_{k=1}^{\infty} \left\{ \omega_k^2 \eta_k \sum_{i=1}^{3} \int_0^{\ell} m_i \phi_{ik}\, \phi_{ij}\, dz \right\} \tag{A.33}$$

$$= \sum_{i=1}^{3} \int_0^{\ell} f_i\, \phi_{ij}\, dz \quad .$$

By virtue of the orthogonality property, all terms in the summation on k vanish except the ones for which $j = k$, leaving

$$\eta_{k,tt} + \omega_k^2\, \eta_k = g_k(t) \tag{A.34}$$

where

$$g_k(t) = \frac{\sum_{i=1}^{3} \int_0^{\ell} f_i \phi_{ik} \, dz}{\sum_{i=1}^{3} \int_0^{\ell} m_i \phi_{ik}^2 \, dz} \tag{A.35}$$

Damping has thus far been neglected. Assuming that viscous damping exists and that the undamped modes remain valid for the damped case as well, we get for the equation of motion for the k-th damped mode

$$\eta_{k,tt} + 2\beta_k \omega_k \eta_{k,t} + \omega_k^2 \eta_k = g_k(t) \tag{A.36}$$

where β_k is the fraction of critical damping in the k-th mode.

APPENDIX B

PROOF OF $\sum_{k=1}^{2N} C'_{1Bk}{}^{*} = 1$**

Consider a N-story building in which principal directions exist (see Chapter II) and in which the translations in one principal direction are coupled with torsion. A building with setback unsymmetric about one principal direction, the behavior of which was examined in Chapter IV, is an example.

Let the translations in the x direction (assumed to be one of the principal directions) be coupled with torsion. The equation of motion of the coupled lateral-torsional vibrations are then given by Equations (2.31) and (2.32), (or by Equation (4.90) if viscous damping is included and relations (4.73)-(4.78) between the various quantities in the two sets of equations are taken into account).

Noting that the matrices $[M_u]$ and $[M_\theta]$ are diagonal as shown in Equations (2.12) and (2.13), Equations (2.21) and (2.32) may be rewritte as

$$m_i\ddot{u}_i + \sum_{j=1}^{N} K_{uij}u_j + \sum_{j=1}^{N} K_{u\theta ij}\theta_j = - m_i\ddot{x}_{01} \ , \ i = 1,2,\ldots,N \quad (B.1)$$

and

$$m\theta_i\ddot{\theta}_i + \sum_{j=1}^{N} K_{\theta uij}u_j + \sum_{j=1}^{N} K_{\theta ij}\theta_j = 0 \ , \ i = 1,2,\ldots,N. \quad (B.2)$$

---

* C'_{1Bk} is defined in Chapter IV, Equation (4.107), page

** The proof presented here was suggested by Professor G. V. Berg.

In writing Equations (B.1) and (B.2) it is assumed that the structure is subjected to only a translational ground acceleration $\ddot{x}_{01}$ in the x direction. The solution of these equations may be written as (Equations (2.61), (4.29))

$$u_i = \sum_{k=1}^{2N} \phi_i^{1k} \eta_k , \quad i = 1,2,\ldots,N \tag{B.3}$$

$$\theta_i = \sum_{k=1}^{2N} \phi_i^{3k} \eta_k , \quad i = 1,2,\ldots N. \tag{B.4}$$

where ϕ_i^{1k} and ϕ_i^{3k} are the ith elements of the translational and torsional components, respectively, of the kth mode. The kth modal displacement η_k is given by (Equation (2.67), (4.93)-(4.96))

$$\ddot{\eta}_k + \omega_k^2 \eta_k = - \lambda_{1k} \ddot{x}_{01} , \quad k = 1,2,\ldots,2N. \tag{B.5}$$

where λ_{1k} is the kth modal participation factor, Equation (4.97). Damping is ignored.

$$m_i \sum_k \phi_i^{1k} \ddot{\eta}_k + \sum_j K_{uij} \sum_k \phi_j^{1k} \eta_k + \sum_j K_{u\theta ij} \sum_k \phi_j^{3k} \eta_k = - m_i \ddot{x}_{01} , \quad i = 1,2,\ldots,N. \tag{B.6}$$

where the summation over the indices j and k extends from 1 to N and 1 to 2N, respectively. Using Equation (B.5) for η_k and interchanging the order of summation

$$m_i \sum_k \phi_i^{1k} (-\omega_k^2 \eta_k - \lambda_{1k} \ddot{x}_{01}) + \sum_k \eta_k \sum_j K_{uij} \phi_k^{1k} + \sum_k \eta_k \sum_j K_{u\theta ij} \phi_j^{3k} = - m_i \ddot{x}_{01} , \quad i = 1,2,\ldots,N. \tag{B.7}$$

Now it is the property of the natural modes (Equation (2.47)) that

$$- m_i \omega_k^2 \phi_i^{1k} + \sum_j K_{u_{ij}} \phi_i^{1k} + \sum_j K_{u\theta ij} \phi^{3k} = 0, \quad i = 1,2,\ldots,N. \tag{B.8}$$

Using this relation in (B.7), one gets

$$m_i \sum_k \lambda_{1k} \phi_i^{1k} = m_i , \quad i = 1,2,\ldots,N. \tag{B.9}$$

Summing over i, interchanging the order of summation, and rearranging, one gets

$$\sum_{k=1}^{2N} \lambda_{1k} \frac{\sum_{i=1}^{N} m_i \phi_i^{1k}}{\sum m_i} = 1 . \tag{B.10}$$

The kth term in the summation on the left hand side in Equation (B.10) is defined as C'_{1Bk} in Chapter IV, see Equation (4.107). Thus, it follows that

$$\sum_{k=1}^{2N} C'_{1Bk} = 1 . \tag{B.11}$$

REFERENCES

1. San Francisco City Building Code, 1956.

2. Los Angeles City Building Code, 1959.

3. Uniform Building Code, International Conference of Building Officials, 1966.

4. Martel, R. R., Housner, G. W., and Alford, J. L., Discussion on "Lateral Forces of Earthquake and Wind", Trans. A.S.C.E., 117, 1952.

5. Berg, G. V., "Earthquake Stresses in Tall Buildings with Setbacks", Proceedings of Second Symposium on Earthquake Engineering, University of Roorkee, India, November 1962.

6. Penzien, J., and Chopra, A. K., "Earthquake Response of Appendage on a Multi-story Building," Proceedings of Third World Conference on Earthquake Engineering, New Zealand, January-February 1965.

7. Skinner, R. I., Skilton, D. W. C., and Laws, D. A., "Unbalanced Buildings with Light Towers, under Earthquake Forces," Proceedings of Third World Conference on Earthquake Engineering, New Zealand, January-February 1965.

8. Ayre, R. S., "Interconnection of Translational and Torsional Vibration in Buildings", Bulletin, Seismological Society of America, 28, 1938.

9. Ayre, R. S., "Experimental Response of Asymmetric One-Story Building Model to an Idealized Transient Ground Motion", Bulletin, Seismological Society of America, 33, 1943.

10. Ayre, R. S., "Methods of Calculating the Earthquake Response of 'Shear' Buildings", Proceedings of World Conference on Earthquake Engineering, Berkley, Calif., June 1956.

11. Housner, G. W., and Outinen, H., "The Effect of Torsional Oscillations on Earthquake Stresses", Bulletin, Seismological Society of America, 48, 1958.

12. Bustamante, J. I., and Rosenbleuth, E., "Building Code Provisions on Torsional Oscillations", Proceedings of Second World Conference on Earthquake Engineering, Vol. II, Tokyo, Japan, July 1960.

13. Bustamante, J. I., "Torsion Dinamica en Estructuras Edificians", University of Mexico, Publication No. 44, 1961.

14. Shiga, Toshio, "Torsional Vibration of Multi-storied Buildings", Proceedings of Third World Conference on Earthquake Engineering, New Zealand, January-February 1965.

15. Medearis, K., "Coupled Bending on Torsional Oscillations of a Modern Skyscraper", Bulletin, Seismological Society of America, 56, August 1966.

16. Gere, J. M., and Lin, Y. K., "Coupled Vibrations of Thin-Walled Beams of Open Cross Section", Journal of Applied Mechanics, 25, September 1958.

17. Lin, Y. K., "Coupled Bending and Torsional Vibrations of Restrained Thin-Walled Beams", Brief Note, Journal of Applied Mechanics, 27, December 1960.

18. Tso, W. K., "Coupled Vibrations of Thin-Walled Elastic Bars", Journal of Engineering Mechanics Division, Proc. A.S.C.E., 91, June 1965.

19. Masur, E. F., "On the Fundamental Frequencies of Vibration of Rigid Frames", Proceedings of the First Midwestern Conference on Solid Mechanics, Urbana, Illinois, April, 1953.

20. Caughey, T. K., "Classical Normal Modes in Damped Linear Systems", Journal of Applied Mechanics, 27, June 1960.

21. O'Kelly, M. E. J., Vibrations of Viscously Damped Linear Dynamic Systems , Ph.D. Thesis, California Institute of Technology, 1964.

22. Frazer, R. A., Duncan, W. J., Collar, A. R., Elementary Matrices, Cambridge University Press, Cambridge (1955).

23. Foss, K. A., "Co-ordinates Which Uncouple the Equations of Motions of Damped Linear Systems", Journal of Applied Mechanics, 25, September 1958.

24. Bodewig, E., Matrix Calculus, Nordhoff, Amsterdam, Netherlands (1959).

25. Givens, W. C., "A Method of Computing Eigenvalues and Eigenvectors Suggested by Classical Results on Symmetric Matrices", Simultaneous Linear Equations and the Determination of Eigenvalues, L. J. Paige, Olga Taussky, editors, National Bureau of Standards, Applied Mathematics Series 29, 1953.

26. Skinner, R. I., et al, "Earthquake Response of Bending Structures Derived from a Mixed Mechanical-Electrical Analogue", Proceedings of Second World Conference of Earthquake Engineering, Vol. II, Tokyo, Japan, July 1960.

27. Hudson, D. E., "The Response Spectrum Technique", Proceedings of First World Conference on Earthquake Engineering, Berkeley, California, June 1956.

28. Blume, J. A., Newmark, N. M., Corning, L. H., Design of Multi-story Reinforced Concrete Buildings for Earthquake Motion, Portland Cement Association, Chicago, Illinois (1961).

29. Merchant, H. C., and Hudson, D. E., "Mode Superposition in Multi-degree of Freedom Systems Using Earthquake Response Spectrum Data", Bulletin, Seismological Society of America, 52, April, 1962.

30. Clough, R. W., "Earthquake Analysis by Spectrum Superposition", Bulletin, Seismological Society of America, 52, July 1962.

31. Goodman, L. E., Rosenbleuth, E., and Newmark, N. M., "Aseismic Design of Firmly Founded Elastic Structures", Trans. ASCE, 120, 1955.

32. Housner, G. W., "Behavior of Structures During Earthquakes," Journal of Engineering Mechanics Division Proc, ASCE, 85, October 1959.

33. Rubinstein, M. F., and Hurty, W. C., "Effect of Joint Rotation on Dynamics of Structures", Journal of Engineering Mechanics Division, Proc. ASCE, 87, December, 1961.

34. Housner, G. W., and Brady, A. G., "Natural Periods of Vibration of Buildings", Journal of Engineering Mechanics Division, Proc. ASCE, 89, August, 1963.

35. Berg, G. V., and Thomaides, S. S., "Punched Card Accelerograms of Strong Motion Earthquakes", The University of Michigan Research Institute, Report No. 2881-1-P, September, 1959.

36. Hudson, D. E., "A Comparison of Theoretical and Experimental Determinations of Building Response to Earthquakes", Proceedings of the Second World Conference on Earthquake Engineering, Vol. II, Tokyo, Japan, July, 1960.

37. Nielsen, N. Norby, "Vibration Tests of a Nine-Story Steel Frame Building", Journal of Engineering Mechanics Division, Proc. ASCE., 92, February, 1966.

38. Aitken, A. C., Determinants and Matrices, Interscience Publishers, New York (1939).